CLAUDIO BRÁNDOLI

Universidad Politécnica de Cartagena

PhD THESIS 2020

ESCUELA INTERNACIONAL DE DOCTORADO

Universidad Politécnica de Cartagena | Campus de Excelencia Internacional

Comparative genetic analysis of GIGANTEA, a gene involved in the control of circadian rhythm in Solanaceae.

Official PhD Program in Técnicas Avanzadas en Investigación y Desarrollo Agrario y Alimentario

Claudio Brándoli

Dr. Julia Weiss
Dr. César Petri Serrano
Dr. Marcos Egea Gutiérrez-Cortines

Cartagena (2020)

DEPARTAMENTO DE CIENCIA Y TECNOLOGÍA AGRARIA
INSTITUTO DE BIOTECNOLOGÍA VEGETAL

Comparative genetic analysis of GIGANTEA, a gene involved in the control of circadian rhythm in Solanaceae.

Claudio Brándoli

Universidad Politécnica de Cartagena
2020

Supervisors

Julia Weiss, Ph.D., Universidad Politécnica de Cartagena

Marcos Egea-Cortines, Ph.D., Universidad Politécnica de Cartagena

César Petri Serrano, Ph.D., IHSM-UMA-CSIC, Dpto. Fruticultura Subtropical y Mediterránea

Contact information

Institute of Plant Biotechnology - Genetics
Department of Agrarian Science and Technology
I+D+i Building
Plaza del Hospital, s/n
30202 Cartagena, Spain
Email address: ibv@upct.es
URL: http://www.upct.es/~ibvupct/
URL: http://www.upct.es/~genetica

Universidad Politécnica de Cartagena

DT-16

CONFORMIDAD DE SOLICITUD DEAUTORIZACIÓN DE DEPÓSITO DE TESIS DOCTORAL POR EL/LA DIRECTOR/A DE LA TESIS

D/Dª. Jiulia Weiss Director/a de la Tesis doctoral Comparative genetic analysis of GIGANTEA, a gene involved in the control of circadian rhythm in Solanaceae.

INFORMA:

Que la referida Tesis Doctoral, ha sido realizada por D/Dª. Claudio Brándoli , dentro del Programa de Doctorado en Técnicas Avanzadas en Investigación y Desarrollo Agrario y Alimentario , dando mi conformidad para que sea presentada ante el Comité de Dirección de la Escuela Internacional de Doctorado para ser autorizado su depósito.

X Informe positivo sobre el plan de investigación y documento de actividades del doctorando/a emitido por el Director/ Tutor (**RAPI**).

La rama de conocimiento en la que esta tesis ha sido desarrollada es:

- X Ciencias
- ☐ Ciencias Sociales y Jurídicas
- ☐ Ingeniería y Arquitectura

En Cartagena, a 7 de _mayo de 2020

EL/LA DIRECTOR/A DE LA TESIS

JULIA ROSL| WEISS

Firmado digitalmente por JULIA ROSL|WEISS
Fecha: 2020.05.07 14:18:36 +02'00'

Fdo.: _____

COMITÉ DE DIRECCIÓN ESCUELA INTERNACIONAL DE DOCTORADO

DT-17

CONFORMIDAD DE DEPÓSITO DE TESIS DOCTORAL POR LA COMISIÓN ACADÉMICA DEL PROGRAMA

D/Dª. Francisco Artes Hernandez , Presidente/a de la Comisión Académica del Programa de Doctorado en Técnicas Avanzadas en Investigación y Desarrollo Agrario y Alimentario

INFORMA:

Que la Tesis Doctoral titulada, " Comparative genetic analysis of GIGANTEA, a gene involved in the control of circadian rhythm in Solanaceae", ha sido realizada, dentro del mencionado Programa de Doctorado, por D/Dª. Claudio Brándoli , bajo la dirección y supervisión del Dr./ Dra. Julia Weiss .

En reunión de la Comisión Académica, visto que en la misma se acreditan los indicios de calidad correspondientes y la autorización del Director/a de la misma, se acordó dar la conformidad, con la finalidad de que sea autorizado su depósito por el Comité de Dirección de la Escuela Internacional de Doctorado.

☐ Evaluación positiva del plan de investigación y documento de actividades por el Presidente de la Comisión Académica del programa (**RAPI**).

La Rama de conocimiento por la que esta tesis ha sido desarrollada es:

- ☒ Ciencias
- ☐ Ciencias Sociales y Jurídicas
- ☐ Ingeniería y Arquitectura

En Cartagena, a ____ de _____ de _____

EL PRESIDENTE DE LA COMISIÓN ACADÉMICA

[redacted]

FRANCISCO DE ASIS|ARTES|HERNANDEZ
2020.05.07 17:14:48 +02'00'

COMITÉ DE DIRECCIÓN ESCUELA INTERNACIONAL DE DOCTORADO

Acknowledgments

I would like to thank those people without whom this PhD thesis could not have been completed.

First of all, I would like to express my gratitude to my thesis directors Julia Weiss, César Petri and Marcos Egea-Cortines. With them I took my first steps in the lab and everything I know about lab work I owe to them. Thank you for your invaluable help during this last five years, your trust and for sharing with me your knowledge.

I would also like to thank my colleagues in the Genetics group, doctors and PhD students: Victoria Ruiz-Hernández, Marina Martos Fuentes and Marta Terry López, the "Brend angels", for all your help during my first doctoral years and your friendship. Raquel Alcantud Rodríguez for your kindness, for all the times you took me to the greenhouse and for taking care of my three mango trees every summer. Julia Muñoz for your valuable contribution during the work in the lab and the support when the experiments didn't work out. Sara Bautista for all the times you put up with me when I needed to talk and for your precious friendship. Thanks to you, Maricarmen, Victoria, Onurçan, Fernándo, Maria, Pedro and Paqui.

I wish to acknowledge Perla Gómez Di Marco and Mariano Otón Alcaraz from the Institute of Plant Biotechnology for your openness, friendliness and technical support and María José Roca Hernández and Vicente Muñoz Martínez from the SAIT for your help and your joy every time I went down to your lab.

Thanks to Javier Fernando Palatnik for giving me the opportunity to stay in his research group at the Institute of Molecular and Cellular

Biology of Rosario - CONICET (Argentina) and to all his team with whom I worked during my stay.

I'm very grateful to have met on my way Kristyna Sebkova for teaching me so much during her language classes during my P.hD.

I would like to thank all the friends who supported me from Italy: Ennio for cheering me up with his jokes, Angelo, Manu and Michele for all the group video calls during the lock down period, Mazz and Peppy for the beers every time I went back to Bologna and Sonia Scaramagli for the help she always gave me and for being a friend in the years after the Master. The new friends I met during these last unforgettable five years: Asia, Alicia, Jenny, Sara, Leonor, Laura, Luiza, Sonia, Rocio, Emma, Lucy, Nuria, Pedro, Bryan, Diego, Adrian, Jeronimo and Mariano.

Finally, my special thanks to my Mother and Father for your support, love and infinite patience during my stay in Spain.

RESUMEN

Las Solanáceas son una familia de plantas que van desde hierbas anuales hasta arbustos y árboles perennes. Incluyen muchas especies ornamentales apreciadas en todo el mundo, como el género *Petunia*, *Browallia* y *Lycianthes*, así como géneros de considerable impacto económico en el mercado mundial. Entre estos se encuentran la patata (*S. tuberosum*) tomate, (*S .lycopersicum)* y berenjena (*S. melongena*), tabaco (*Nicotiana tabaccum*) o pimiento (*C. annuum*) que incluye las variedades chili y pimiento dulce, dos de las más comercializadas en el mundo. El objetivo de esta tesis fue llevar a cabo un análisis genético comparativo del gen *GIGANTEA* (*GI*), para profundizar en el conocimiento de su expresión y regulación génica, así como el papel que desempeña en el control del desarrollo y ritmo circadiano en las Solanáceas.

Para lograr los objetivos que nos propusimos analizamos en el sistema modelo *Petunia x hybrida* los dos parálogos préviamente identificados *PhGI1* y *PhGI2*, a través de dos técnicas distintas: primero creando líneas de perdida de función, por cada uno de los dos parálogos, mediante técnica de ARN de interferencia y posteriormente mutantes knock-out mediante la técnica CRISPR/Cas9, para confirmar los resultados obtenidos. Se realizaron análisis de fenotipado de los caracteres vegetativos y reproductivos, genotipado y análisis de los componentes volátiles utilizando el método SPME desde el espacio de cabeza, seguido de GC/MS.

Dentro de los estudios realizados hemos podido observar cómo los parálogos comparten funciones comunes. Ambos tienen efectos

menores en el ritmo y la expresión de los genes del reloj. Esto es debido a que la función de *GI* ocurre a través de las interacciones proteína-proteína. *PhGI1* y *PhGI2* actúan como reguladores negativos del crecimiento vegetativo, controlando el tamaño y el contenido relativo de clorofila de las hojas, así como la longitud de entrenudos. Con respecto a los caracteres generativos, hemos identificado una nueva función aún no descrita hasta ahora. Líneas silenciadas para cada uno de los paralogos, presentaron flores abortadas caracterizadas por la senescencia temprana de los tejidos. Además, el número total y el tamaño de las flores fue menor en comparación con el fenotipo silvestre. Al mismo tiempo se observó como la cantidad y el perfil de los compuestos volátiles emitidos resultó afectado en las líneas silenciadas. La cantidad total de aromas emitidos durante 24 horas resultó inferior en comparación con el fenotipo silvestre y el perfil de aromas emitidos durante el día resultó alterado. Los resultados de está Tesis confirman que *PhGI1 y PhGI2* están involucrados en el desarrollo floral.

Observamos también diferentes fenotipos entre las líneas silenciadas para cada uno de los parálogos, particularmente en el control del tiempo de floración. Aunque el silenciamiento de *PhGI1* no mostró ninguna diferencia en comparación con el fenotipo silvestre, plantas silenciadas en *PhGI2* mostraron un retraso de entre dos/tres semanas más tarde en la floración, confirmándose como gen cuya pérdida de función provoca floración tardía, ya descrito en *Arabidopsis thaliana*. Estos datos confirmaron la hipótesis previa de que algunos genes duplicados podrían haber sufrido subfuncionalización o neofuncionalización.

ABSTRACT

Solanaceae are a family of plants ranging from annual grasses to evergreen shrubs and trees. They include many ornamental species appreciated around the world, such as the genus *Petunia*, *Browallia* and *Lycianthes*, as well as genera of considerable economic impact on the world trade such as potato (*S. tuberosum)*, tomato (*S .lycopersicum)*, eggplant (*S. melongena*), tobacco (*Nicotiana tabaccum*) and pepper (*Capsicum annuum*) that includes the chili pepper and bell pepper varieties, two of the most commercialized in the world. The objective of this thesis was to carry out a comparative genetic analysis of the *GIGANTEA* (*GI*) gene, to deepen the knowledge of its expression and gene regulation, as well as the role it plays in the control plant development and circadian rhythm in *Solanaceae*.

In order to achieve the objectives that we set, we analyzed in the model system *Petunia x hybrida* the two paralogs previously identified *PhGI1* and *PhGI2*, through two different techniques: first creating loss of function lines for each of the two paralogs, using the interference-RNA technique and subsequently knock-out mutants using the CRISPR/Cas9 technique to confirm the results obtained. Phenotypic analysis of vegetative and reproductive traits, genotyping and volatile components analysis were performed using the SPME method from the headspace, followed by GC/MS.

Among the studies carried out we have been able to observe how the paralogs share common functions. Both have minor effects on the timing and expression of clock genes, this could be because *GI* molecular function occurs through protein-protein interactions. *PhGI1*

and *PhGI2* act as negative regulators of vegetative growth, controlling the size and relative content of chlorophyll in the leaves, as well as the internode distance. Regarding generative characters, we have identified a new function non described so far. Both, *PhGI1* and *PhGI*2, silenced plants presented aborted flowers characterized by early tissue senescence. Furthermore, the size and total number of the flowers were reduced compared to the wild type phenotypes. At the same time, it was observed how the amount and the profile of the volatile compounds emitted were affected in the silenced lines. The total amount of aromas emitted during 24 hours was lower compared to wild type phenotypes and the profile of aromas emitted during the day was altered. Our results confirm that *PhGI1* and *PhGI*2 are involved in flower development.

We also observed different behaviors between the silencing of each paralog, particularly in the control of the flowering time. Although *PhGI1*-silenced plants did not show difference compared to wild type phenotypes, *PhGI2*-silenced plants flowered two to three weeks later, confirming itself as a late-flowering mutant, as already described in *Arabidopsis thaliana*. These data confirmed the previously hypothesized idea that some duplicate may undergo subfunctionalization or neofunctionalization.

Original Publications of the Thesis

Chapter 1: Claudio Brandoli, César Petri, Marcos Egea-Cortines & Julia Weiss (2020). The clock gene *Gigantea 1* from *Petunia hybrida* coordinates vegetative growth and inflorescence architecture. *Scientific Reports,* 10: 275. DOI: 10.1038/s41598-019-57145-9

Peer Reviewed Conferences:

- C. Brandoli, M. Egea-Cortines, C. Petri, J. Weiss (2019). The *GIGANTEA1* iRNA-silencing effects in Petunia, show new surprising floral buds growth and scent emission habits. Vth doctoral conferences of the University of Murcia. 29-31/05/2019
- C. Brandoli, M. Egea-Cortines, C. Petri, J. Weiss (2019). The *GIGANTEA1* iRNA-Silencing effects in Petunia, show new surprising vegetative and floral growth habits. Ith Congress of Young Researchers in Agri-Food Sciences. University of Almeria. 20/12/2018
- Marta I. Terry Lopez, Claudio Brandoli, Marta Carrera-Alesina, Marcos Egea-Cortines, Julia Weiss. Organ-specific evolution and subfunctionalization of circadian clock in Petunia. XIIIth Meeting of Plant Molecular Biology. University of Oviedo. 22-24/06/2016

Peer Reviewed Workshops:

- C. Brandoli, M. Egea-Cortines, C. Petri, J. Weiss (2019). 8th Agri-food Research Workshop (Workshop de Investigación Agroalimentaria - WIA 2019) of the Technical University of Cartagena (Spain) with

the presentation of an article entitled: Silencing of the *GIGANTEA 1* gene in *Petunia hybrid* affects the vegetative development. (27-28/05/2019)

- C. Brandoli, M. Egea-Cortines, C. Petri, J. Weiss (2018). 7th Agri-food Research Workshop (Workshop de Investigación Agroalimentaria - WIA 2018) of the Technical University of Cartagena (Spain) with the presentation of an article entitled: Design of guide RNA for gene editing of *Gigantea* in *Solanaceae*. (7-8/05/2018)
- C. Brandoli, M. Egea-Cortines, C. Petri, J. Weiss (2017). 6th Agri-food Research Workshop (Workshop de Investigación Agroalimentaria - WIA 2017) of the Technical University of Cartagena (Spain) with the presentation of an article entitled: Agrobacterium mediated genetic transformation of Petunia for gene silencing using Kanamycin as the selection agent. (8-9/05/2017)
- C. Brandoli, M. Egea-Cortines, J. Weiss (2016). 5th Agri-food Research Workshop (Workshop de Investigación Agroalimentaria - WIA 2016) of the Technical University of Cartagena (Spain) with the presentation of a poster titled: Genetic and molecular analysis of *Gigantea*, a gene involved in climate adaptation through regulation of the circadian clock in Solanáceas. (9-10/05/2016)

Manuscripts in progress:

- Phenotypic- and expression analysis of *GIGANTEA* paralog *GI2,* in *iRNA::PhGI2* silenced *Petunia x hybrida* plants, reveals both sub- and neofunctionalizations with respect to paralog *GI1.*
- Review about Gigantea gene

Index

List of Figures

List of Tables

Abbreviations and acronyms

AAA aromatic amino acid

AGO2 Argonaute2 protein

ALF *Aberrant Leaf and Flower*

aNHEJ alternative Non Homologous End Joining

AN2 *Antocianin2*

AP2 APETALA 2

Cas9 Crispr Associated Protein 9

CCA1 *Circadian Clock Associated 1*

cDNA Complementary Deoxyribonucleic Acid

CHL *Chanel*

cNHEJ classical Non Homologous End Joining

Cas CRISPR associated system

Cascade complex associated with CRISPR for antiviral defense

CDF1 CYCLING DOF FACTOR 1

CO CONSTANS

COR cold-regulated

cRdRP cellular RNA-dependent RNA polymerase

CRISPR Clustered Regularly Interspaced Short Palindromic Repeats

crRNA CRISPR-derived RNAs

DOT *Double Top*

DR Direct Repeats

DSBs double strand breaks

dsRNA double stranded RNA

ELF3 *Early Flowering 3*

ELF4 *Early Flowering 4*

ERD early dehydration-inducible

EVG *Evergreen*

FAD8 Arabidopsis Fatty Acid Desaturase 8

FKF1 Flavin-binding, Kelch repeat, F box protein 1

FT FLOWERING LOCUS T

GA gibberellic acid

GFP green florescent protein

GI GIGANTEA

GI1 GIGANTEA 1

GI2 GIGANTEA 2

HIR high-irradiance response

HR homologous recombination

iap apoptosis inhibitor

Ihp Intronhairpin

Indel insertion-deletion

KIN cold inducible

LDs Long Days

LFY *Leafy*

LHY *Late Elongated Hypocotyl*

LIG4 LIGASE 4

LUX Lux Arhythmo

LTI low temperature-induced

mRNA Messenger RNA

MMEJ Microhomology-Mediate End Joining

NHEJ Non Homologous End Joining

nptII neomycin phosphotransferase II enzyme

ODO1 ODORANT1

ORF Open Reading Frame

PAL phenylalanine ammonia lyase

PAM proto-spacer-adjacent motifs

PCR Polymerase Chain Reaction

PEB phenylethylbenzoate

PFG PETUNIA FLOWERING GENE

Phe Phenylalanine

PhEth 2-phenylethanol

Phy phytochromes

PRR1 PSEUDO RESPONSE REGULATOR 1

PRR5 PSEUDO RESPONSE REGULATOR 5

PRR7 PSEUDO RESPONSE REGULATOR 7

PRR9 PSEUDO RESPONSE REGULATOR 9

PTGS post-transcriptional gene silencing

Q-PCR Quantitative PCR

RD responsive to desiccation

REST Relative Expression Software Tool

RISC RNA-induced silencing complex

RNA Ribonucleic acid

RNAi RNA interference

RNase Ribonuclease

RPA REPLICATION PROTEIN A

RT-PCR Real Time PCR

SDs Short Says

siRNA small interfering RNA

SPY Spindly

SVP SHORT VEGETATIVE PHASE

T-DNA Transfer DNA

TEM1 TEMPRANILLO 1

TEM2 TEMPRANILLO 2

TEs transposable elements

TOC1 *Timing Of Cab1*

TOE1 TARGET OF EAT 1

tracrRNA transactivating CRISPR RNA

Trp Tryptophan

Tyr Tyrosine

UFO *Unusual Floral Organs*

VBP floral volatile benzenoids/phenylpropanoids

VLFR very-low-fluence response

VOCs Volatile Organic Compounds

vRdRP viral RNA-dependent RNA polymerase

W115 *P. hybrida* Mitchell diploid

WT Wild type

XRCC1 X-Ray Repair Cross-Complementing Protein 1

XRCC4 X-Ray Repair Cross-Complementing Protein 4

ZT Zeitgeber Time

ZTL *Zeitlupe*

General Introduction

Among the fields of sciences, developmental biology occupies a remarkable position in the study of the processes by which organisms grow and define their intrinsic characteristics during development. Those studies include organ identity, reproduction, symmetry, final size, floral phyllotaxis and the organization between environmental cues and morphogenesis (Bowman, 1997; Endress, 2006).

In all living beings, cellular movement is a need dictated by the organ's necessity to differentiate its tissues to achieve a more complete metabolic self-sufficiency and to reach nourishment sources. Plant tissues are composed of static cells, surrounded by a rigid and firmly cemented cell wall that limits their cellular mobility. This is why morphogenesis in plants takes place thanks to a combined formation process dependent on growth and differentiation (de Almeida *et al.*, 2015). Growth is that irreversible phenomenon characterized by the increase in tissue size due to cell division (mitosis), and cell expansion, the result of the absorption of water and metabolites for protoplasm formation. Differentiation is the result of all those processes that lead to an increase in the complexity of a tissue, thanks to a consequent cellular specialization. Both, work in synergy, coordinating environmental and internal signals to define organogenesis and plant structure (de Almeida *et al.*, 2015).

Vascular plants maintain two distinctive zones which retain a continued growth capacity. These regions are the apical meristems: the shoot apical meristem, which give rise to aerial organs; and the

root apical meristems, responsible of the enlargement of the root system. This ability to have an area in continuous proliferation is due to the fact that the growth of the vegetative meristems is uninterrupted and indeterminate.

The transition from the vegetative to the reproductive phase involves the formation of a floral meristem and therefore a highly precise organ-tissue specialization. Studies in *Arabidopsis thaliana* and other species, including *Petunia spp.*, have revealed that the intricate expression of the genes forming the oscillator, is closely related to internal and environmental factors. These include an interplay with hormone signaling (Bancos *et al.*, 2006; Nozue *et al.*, 2007; Thines and Harmon, 2011), cell division and expansion (Soy *et al.*, 2016; Fung-Uceda *et al.*, 2018), primary metabolism (Farré and Weise, 2012), abiotic stress response (Marcolino-Gomes *et al.*, 2014), biomass production (Ni *et al.*, 2009; Atamian *et al.*, 2016; Edwards *et al.*, 2018), flower orientation (Atamian *et al.*, 2016) and flower scent emission (Fenske *et al.*, 2015; Yon *et al.*, 2015; Terry, Pérez-Sanz, Díaz-Galián, *et al.*, 2019).

1. *Petunia*, a Model System for Genetics and Developmental Studies

1.1 Description

The genus *Petunia* belongs to the family of the *Solanaceae* and comprises around 30 subspecies. Widely diffused nowadays all over the world as an appreciated ornamental plant, it exhibits a wide range of floral colors (Ando *et al.*, 2001). It is endemic to South America with a subtropical distribution, typical of southern Brazil, Uruguay and Argentina, especially at the foothills of the Andes (Kulcheski *et al.*, 2006). It maintains the supremacy as one of the most used flower beds in the world and it is considered one of the preferred genera for the development of new varieties (Gerats and Vandenbussche, 2005) .

Considering the main emerging model systems for developmental studies, such as *Arabidopsis thaliana*, *Antirrhinum spp.*, *Oryza sativa* and *Nicotiana spp.*, it is impossible not to mention *Petunia*. This genus emerged in the last two decades as one of the main model systems for physiological, biochemical and genetic research, thanks to its relatively short generation time, easy culturing, generation of stable transgenic plants using leaf-disk transformation and also *Agrobacterium* infiltration (Gerats and Vandenbussche, 2005).

Petunia is characterized by a paleohexaplodization typical of the *Solanaceae* famil*y. H*owever, an early branching occurred in the clade moving away from *S. lycopersicon*, *S. tuberosum*, *Nicotiana* spp. and *Capsicum* spp., which have n=12 chromosome number, while *Petunia* has n=7 chromosomes.

Petunia taxa are herbs with non-woody stems, imbricated aestivation, usually annual. *Petunia x hybrida*, also called *Petunia hybrida*, derived from a cross between the white-flowered *P. axillaris* and the purple-flowered *P. integrifolia* (Figure 1) (Segatto *et al.*, 2014; Fenske *et al.*, 2015).

Figure 1| *P.axillaris* and *P.integrifolia* flower shape and syndromes.

P. axillaris on the left and *P. integrifolia* on the right (a). Changes of limbs, tube and calyces morphology as well as the pigmentation in the two species. (b) A hawkmoth hovers while using its long proboscis to reach the nectar. Photo from Alexandre Dell'Olivo/FLICKR (https://urly.it/3605x). (c) A bee on a red *Petunia*. Photo from labsafeharbor/PIXABAY (https://urly.it/3605z).

P. axillaris, with its colorless flowers, emits a characteristic mixture of aromas during the night hours in order to attract the hawkmoths during its hours of activity. It is characterized by white color with a long tube, similar in length to the proboscis of its nocturnal pollinators (Stuurman *et al.*, 2004) (Figure 1b). On the

other hand, *P. integrifolia* is pollinated by bees (Figure 1c), has a short and wide tube with purple and almost scentless flowers that close at night, a strategy to exclude nocturnal pollinators (Ando *et al.*, 2001). Studies have hypothesized that the genus *Petunia* derives from an ancestor similar to *P. integrifolia* (Gübitz *et al.*, 2009; Dell'Olivo *et al.*, 2011) and that the transformation to the white flowers of *P. axillaris* might be for the inactivation of *ANTOCIANIN2 (AN2*), a MYB transcription factor that regulates the biosynthesis of anthocyanins (Quattrocchio *et al.*, 1999). This fact favored new species of pollinators such as the hawkmoth that prefers UV-absorbing flowers (white flower) rather than UV-reflecting flowers (purple flower).

Petunia x hybrida shows a typical monopodial vegetative growth whereas the inflorescences are sympodial, both in the central as in the lateral branches, following a scorpioid pattern. Considering that most of the *Solanaceae* show a similar type of inflorescence, this characteristic also makes it an excellent point of reference for flower physiology and development studies in this family.

1.2 *Petunia* inflorescence, from vegetative growth to flowering

Angiosperms show an incredible variability in plant and inflorescence architecture, especially during the switch from vegetative growth to the reproductive phase. There are over 300,000 different species, each with a unique flower but with similar features and functions, evolved from the same common ancestor.

Although flowers share the same types of organs, these can change in number and position (Koes *et al.*, 2009). Considering only

the different patterns of inflorescence appearance, it is possible to classify the plants into four mayor classes: 1) Seasonal plants, which can flower in different stages of development or at different times during the year. 2) Annual plants, which bloom and complete their lifecycle in the same year or growing season, in which they first sprouted. Many of the food plants are annuals, such as the *Solanaceae,* the *Fabaceae* and the *Graminaceae.* 3) Biennial plants, which take two years to complete their biological lifecycle and flower only after a cold winter period. 4) Perennial plants, such as trees, which need several years to flower.

The reproductive phase that, in all the higher plants, takes place after an appropriate period during which leaves and axillary meristems are generated, is species-specific. Although there are several kinds of inflorescences, it is possible to distinguish three basic types: racemes, panicles and cymes (Figure 2) (Benlloch *et al.*, 2007). The two first are typical of species with monopodial growth, where the new inflorescence shoots appear at the flanks of the apical meristem, as in *Arabidopsis* and *Antirrhinum*. In cymose inflorescences, typical of plants with sympodial growth like *Petunia*, every axis terminates with a flower and the next one growth in a lateral position, perpetuating this pattern (Rebocho *et al.*, 2008).

Considering a few basic floral structures, it is possible to understand the texture and function of most flowers. For *Petunia*, the typical flower morphology consists of four organs: sepals, petals, stamens and pistils (including carpels and ovules). To maintain an ordinate and functional symmetric structure during life, plants have developed an organized organ direction initiation, commonly known as phyllotaxis. In plants there are two major types of flower pattern

arrangement: spiral and whorled. In spiral phyllotaxis, organs are initiated at constant time intervals, called plastochrons. In whorled phyllotaxis, initiation of organs is almost synchronous and appears organized inside a ring shaped geometry.

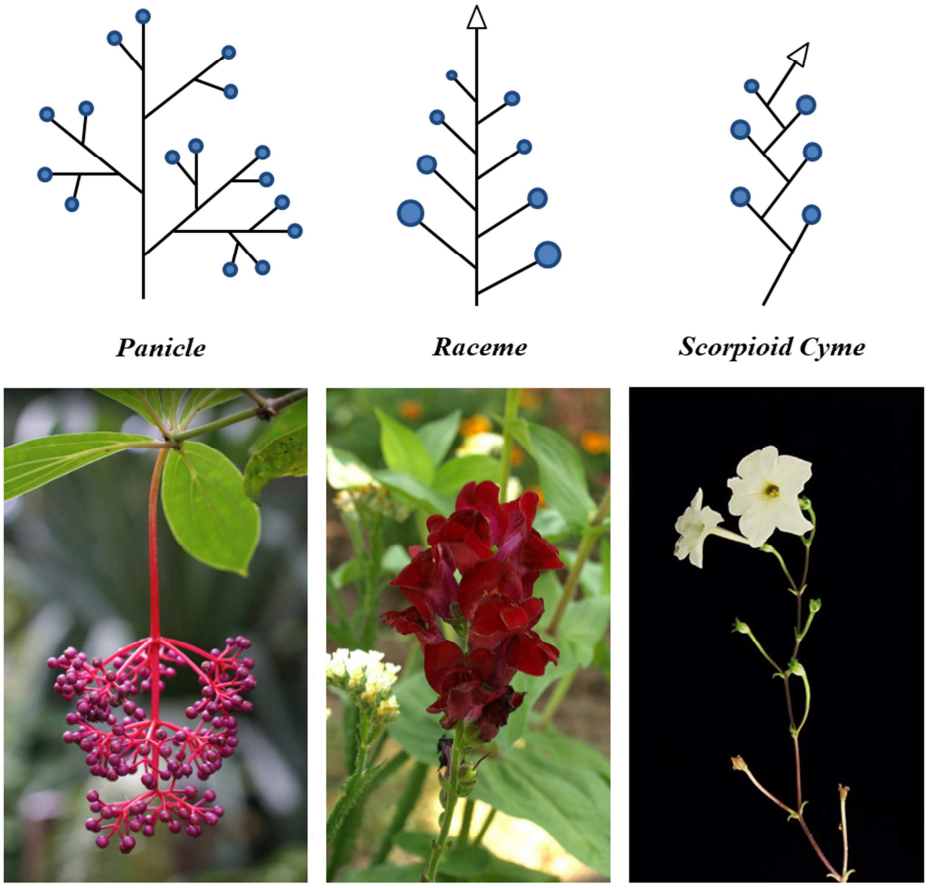

Figure 2| Example of inflorescence architecture.

From left to right, *Medinilla magnifica* panicle flower, the photo was taken by PXHERE . Red *Arabidopsis* raceme flower, the photo was taken by PXHERE (https://pxhere.com/en/photo/644035). White *Petunia* scorpioid cyme flower, own photo.

In the angiosperms, such as *Arabidopsis thaliana*, *Antirrhinum majus* (Snapdragon) and *Petunia hybrida*, flowers form concentric whorls of organs. In Petunia, what organ is formed and where, is determined by the ABCDE model (Figure I.3) (Coen and Meyerowitz,

1991; Rijpkema *et al.*, 2010). Basically, the classical ABCDE model determines the formation of four types of whorls according to an expression pattern of few genes (Figure 3). “A” genes, specify sepals; “A” plus “B” genes, specify petals; “B” plus “C” genes, stamens; and “C” genes alone, specify carpels. “D” and “E” genes are the latest group of genes added to the model. “D” genes are involved in the ovule formation and seed development. “E” genes, are required for all the floral organs specification.

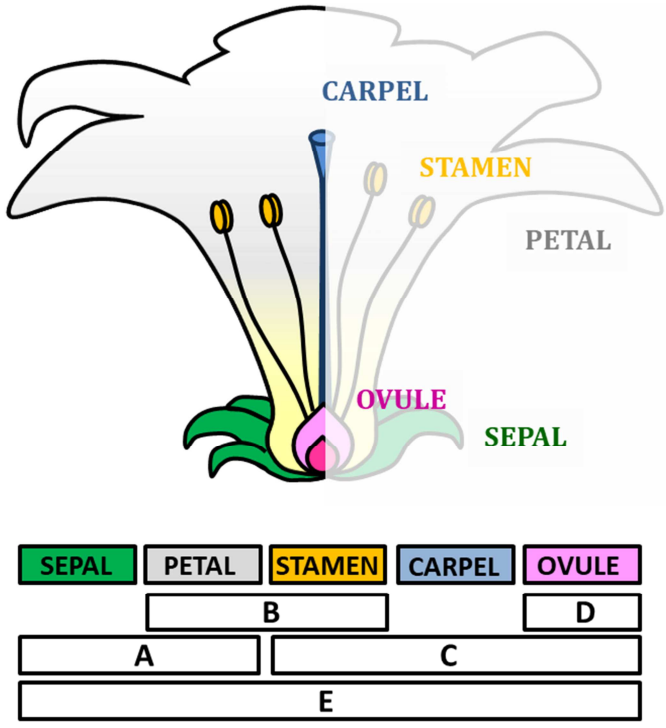

Figure 3| Diagram of the ABCDE model of flower development.

It is not surprising that the molecular mechanism that controls flowering has taken a prominent place in scientific research over the years. One of the most studied plants, used to better understand this intricate mechanism, has been *Arabidopsis* (Mouradov *et al.*, 2002; Simpson, 2002; Krizek and Fletcher, 2005; Blázquez *et al.*, 2006) in

which two main pathways of signaling were identified. The gibberellic acid (GA) pathway, that mediates hormonal and endogenous cues (Blázquez *et al.*, 1998); and the photoperiod pathway, responsible to mediate the environmental signals (Blázquez *et al.*, 2003). At the center of this system of flowering pathways, there are a series of genes called "floral pathway integrators" that converge all the distinct signals received (Koes *et al.*, 2009). Over the year, several molecular genetic experiments in Arabidopsis and Petunia have identified a pool of integrator genes involved in mediation, integration and perception of flowering signals. The Petunia floral formation of the apical meristem involves the activity of the genes *PETUNIA FLOWERING GENE (PFG),* a MADS box gene responsible of flower meristem identity (R., G., Immink *et al.*, 1999) and *ABERRANT LEAF AND FLOWER (ALF),* the orthologue of *LEAFY* (LFY) in *Arabidopsis* (Souer *et al.*, 1998). This last one needs the action of *DOUBLE TOP (DOT),* the homolog of *UNUSUAL FLORAL ORGANS (UFO),* to induce the floral meristem identity (Souer *et al.*, 1998).

The F-box of DOT interacts physically with ALF protein via the SCF-E3-ubiquitin ligase complex, which results in the post-transcriptional activation of ALF (Souer *et al.*, 1998). Indeed, it has been discovered, using a yeast two-hybrid assay, that UFO and DOT bind with SKP1-like proteins, which are components of the SCF complex (Samach *et al.*, 1999; Souer *et al.*, 2008).

Although flowering in Petunia and Arabidopsis are influenced by the same environmental signals, they appear to follow a different path of gene expression. In *Arabidopsis* the expression of *UFO* occurs already during the vegetative phase and the increasing activation of

LFY induces the floral transition. On the other hand, in Petunia, *ALF* only needs *DOT* to initiate the floral development induction (Figure 4).

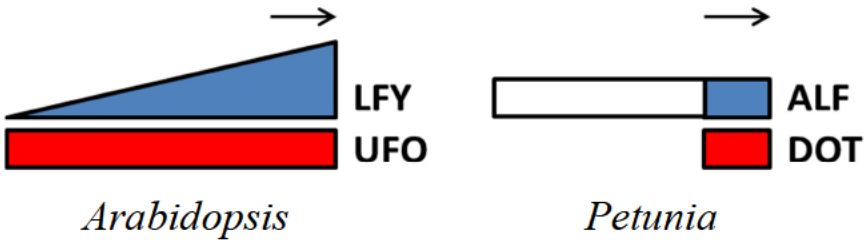

Figure 4| Schematic representation of ALF and DOT expression in Petunia.

ALF and *DOT* have different roles and expression patterns in floral induction in Petunia than their Arabidopsis's homologs, *LFY* and *UFO*. In Arabidopsis, the activation of *LFY* induces the floral transition while *UFO* is expressed throughout the vegetative phase. In Petunia, ALF production occurs early during the vegetative phase but requires the DOT function to induce the floral transition. Black arrows indicate the floral induction.

Another gene implicated in *Petunia* inflorescence's architecture is *EVERGREEN (EVG). EVG* is involved in the activation of *DOT* and the initiation of the floral identity in the apical meristem as well as in the lateral inflorescence shoot development (Rebocho *et al.*, 2008).

1.3 Petunia floral scent production

Plants, like many sessile organisms, have evolved specific mechanisms to face the environmental challenges. Biotic/abiotic stress responses, communication with pollinators, antagonist and other plants are just few examples. Among the main strategies that plants use to ensure entomophilic reproduction is the emission of scents. The Volatile organic compounds (VOCs) are mixtures of volatile lipophilic molecules of benzenoids/phenylpropanoids and

fatty acid derivatives with low molecular weight and high vapor pressure at ambient temperature, synthesized in all plant organs, from roots to flowers (Knudsen *et al.*, 1993; Pichersky and Gershenzon, 2002).

Over 1,700 volatile compounds have been identified in plants and although some of them are largely widespread among plants, others are exclusive to some specific taxa (Pichersky and Gershenzon, 2002; Pichersky *et al.*, 2006). Petunia emits a wide range of different VOCs during the day, especially in the late evening, making this species an excellent model system for studying the emission and composition of aromas.

Flowers are typically the main organs for the emission of volatile substances in plants, which occurs through the epidermal cells, ensuring rapid release into the atmosphere (Kolosova, Gorenstein, *et al.*, 2001). Floral VOCs act mainly as signal molecules for pollinators, with a maximal peak of emission when pollinators are seasonally active and flowers are mature. *P. axillaris* for instance, produces fragrant flowers, with an emission peak during the night, featured mainly by methyl benzoate, benzyl alcohol and benzaldehyde (Hoballah *et al.*, 2005). The highest emission coincides with the hawkmoth nocturnal activity. Briefly, different plant species produce different fragrances, reflecting the preferences of their pollinators. This olfactory sensitivity of insects, able to distinguish the different floral fragrances, makes the floral scent a character of fundamental importance for plant-insect interactions (Negre *et al.*, 2003). The species-specificity of the floral fragrance greatly improves the specificity of pollination, reducing the risk of useless interspecific pollination (Huang and Shi, 2013).

On the other hand, in vegetative organs, VOCs are part of the plant's defense system and are mainly synthesized in glandular trichomes (Tissier *et al.*, 2017), single specialized cells (Lewinsohn, 1998) or tubes (Franceschi *et al.*, 2005) from which they can sprout out in case of breakage. They generally act as a deterrent against herbivores and florivores (Klahre *et al.*, 2011), as an attractant for natural enemies of parasites and pests (Schnee *et al.*, 2006; Scala *et al.*, 2013), or directly function as antifeedant or have antimicrobial and antifungal roles (Dudareva *et al.*, 2006).

The availability of carbon, nitrogen, sulfur and energy from the primary metabolism of the plant are essential for the biosynthesis of VOCs (Schuurink *et al.*, 2006; Dudareva *et al.*, 2013), highlighting the high degree of dependence and communication between the secondary and primary metabolism in the plant kingdom (Dudareva *et al.*, 2013).

In Petunia, as in many Angiosperms, the quantity and composition of the VOCs can fluctuate during the day, mainly in relation with the age of the flower. This rhythmic release of scent is also closely related to the flower hormonal regulation, circadian clock, flower and plant development, nutrient availability, temperature, humidity and general environmental conditions (Colquhoun *et al.*, 2010; Cna'Ani *et al.*, 2015; Fenske *et al.*, 2015).

The synthesis and emission of VOCs begin after the opening of the flower bud (anthesis), from the epidermal cells of the corolla limb, following a rhythmic pattern. Thirteen main benzenoids/phenylpropanoids have been identified in Petunia including benzaldehyde, methyl benzoate, benzyl benzoate, benzyl

alcohol, benzyl acetate, phenylacetaldehyde, methyl-salicylate, phenylethyl benzoate, 2-phenylethyl acetate, phenylethyl alcohol, eugenol, isoeugenol and vanillin (Kolosova, Gorenstein, *et al.*, 2001; Verdonk *et al.*, 2003; Colquhoun *et al.*, 2010).

The plant VOCs are basically classified into different classes according to their biosynthetic origins, such as: terpenoids, benzenoids/phenylpropanoids, fatty acid derivates and amino acid derivates as well as few other genus-specific volatiles (Dudareva *et al.*, 2013). Among the most emitted volatile compounds by *Petunia* flowers there are undoubtedly the benzenoids/phenylpropanoids (Weiss *et al.*, 2016; Amrad *et al.*, 2016; Terry, Pérez-Sanz, Díaz-Galián, *et al.*, 2019) whose emission intensity decreases during the senescence induced after pollination (Negre *et al.*, 2003; van Schie *et al.*, 2006).

The Shikimate pathway converts the carbon of the primary metabolism into chorismate, the precursor of the aromatic amino acids (AAA) phenylalanine (Phe), tyrosine (Tyr) and tryptophan (Trp), through seven enzymatic reactions (Tzin and Galili, 2010; Dudareva *et al.*, 2013), which in turn are precursors of a large number of primary and secondary metabolites (Schuurink *et al.*, 2006). In the shikimate pathway, DAHP synthase is the first enzyme to be activated and is responsible for controlling the amount of carbon that enters in the pathway. Unlike what happens in bacteria, in which DAHP synthase protein is regulated both at transcriptional level and by an inhibition feedback reaction; in plants there is no evidence for an enzyme inhibition (Herrmann and Entus, 2001).

Chorismate is also a precursor of the plant defense hormone

salicylic acid and for vitamins K1 and B9 synthesis (Maeda and Dudareva, 2012). The phosphoenolpyruvate of the glycolysis pathway and the erytrose 4-phosphate of the pentose phosphate pathway, are both the first immediate precursors of this complicated pathway (Widhalm and Dudareva, 2015) (Figure 5).

The first steps for the biosynthesis of the main volatile benzenoid/phenylpropanoid compounds is catalyzed by the action of the enzyme phenylalanine ammonia lyase, that deaminates Phe in *trans*-cinnamic acid, the main intermediate in the VBP biosynthesis (Colquhoun *et al.*, 2010; Dudareva *et al.*, 2013). While the biosynthesis of AAs occurs in plastids, their further conversions to VBP occur outside in the cytosol (Maeda and Dudareva, 2012; Widhalm and Dudareva, 2015).

The synthesis of C_6-C_3 phenylpropanoids, which get their name from the six-carbon aromatic phenyl group and from the three carbons of the propene tail of CA, starts from the formation of para-coumaric acid by the cinnamate-4-hydroxylase enzyme. Among these, the monolignols, monomers used to generate various forms of lignin and suberin, are mainly used as a structural component of plant cell wall.

One of the monolignols is conifer alcohol, which is converted into coniferil acetate before its reduction into eugenol and isoeugenol by eugenol syntase and isogeugenol synthase, respectively (Dexter *et al.*, 2007; Dudareva *et al.*, 2013; Muhlemann *et al.*, 2014) (Figure 5).

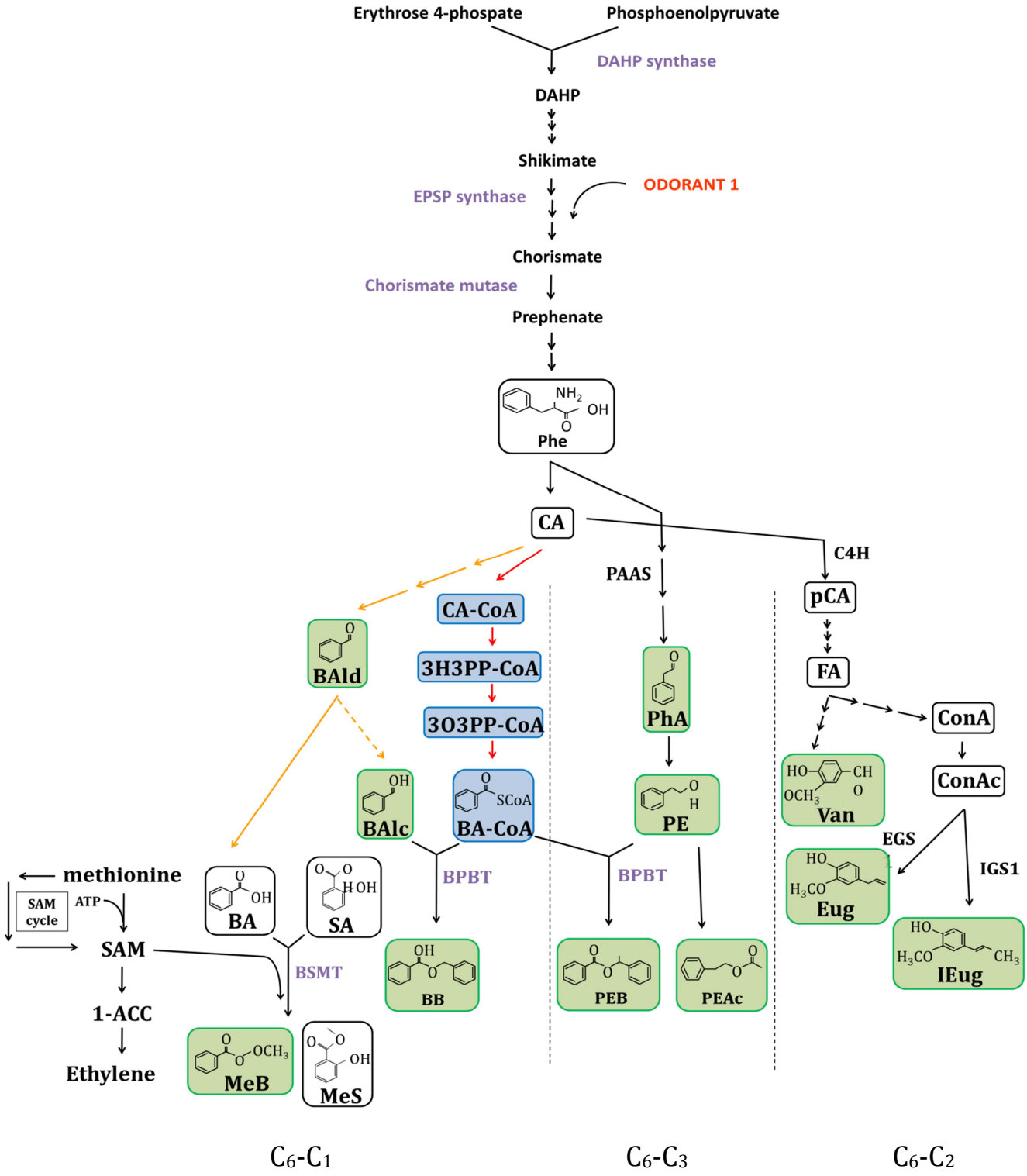

Figure 5| Schematic plant benzenoid/phenylpropanoid VOC synthesis.

Volatile benzenoid/phenylpropanoid C_6-C_1, C_6-C_2 and C_6-C_3 metabolic pathway in Petunia. Volatile compounds are highlighted with a green background. Red and yellow arrows indicate respectively the β-oxidative and non β-oxidative pathway. Plan arrows indicate reactions that are catalyzed by single enzymes. Dashed arrows indicate the involvement of multiple enzymatic reactions. Broken arrows indicate hypothetical

steps not yet described. Abbreviations: **3H3PPA**, 3-hydroxy-3-phenylpropanic acid; **3O3PPA**, 3-oxo-3-phenylpropanoyl acid; **BA**, benzoic acid; **BA-CoA**, benzoyl-Coa; **BAlc**, benzyl alcohol; **Bald**, benzaldehyde; **BALDH**, benzaldehyde dehydrogenase; **BB**, benzyl benzoate; **CA**, trans cinnamic acid; **CA-CoA**, Cinnamoil-CoA; **C4H**, cinnamate-4-hydroxylase; **ConA**, coniferil alcohol; **ConAc**, coniferil acetate; **EGS1**, eugenol synthase1; **Eug**, eugenol; **FA**, ferulic acid; **MB**, methylbenzoate; **PAAS**, phenilacetaldehyde synthase; **PAL**, phenylalanine ammonia lyase; **pCA**, para cumaric acid; **PEAc**, 2-phenylethyl acetate; **PEB**, phenylethylbenzoate; **PhA**, phenylacetaldeyde; **Phe**, phenylalanine; **PhEth**, 2-phenylethanol.

It has been shown that the formation of C_6-C_1 benzenoids proceeds through three routes: a β-oxidative, a non-β-oxidative and a combination of both. The β-oxidative pathway occurs in peroxisomes, in a similar way to the β-oxidation of fatty acids and branched-chains of amino acid (Dudareva *et al.*, 2013). The β-oxidative route starts with CA, which undergoes a series of hydrations and oxidations, leading to the formation of benzoyl-CoA, a key intermediate for the formation of benzylbenzoate and phenylethylbenzoate in the cytosol. Recent experiments, performed on *Nicotiana attenuata* plants, using stable isotope-labeled ($^{2}H_6$, ^{18}O)3-hydroxy-3-phenylpropanic acid, support β-oxidation as one of the possible pathways for the formation of benzoic acid in the cytoplasm. (Jarvis *et al.*, 2000; Widhalm and Dudareva, 2015). Benzaldehyde is the key intermediate for the non-β-oxidative pathway, which is oxidized to benzoic acid. The biochemical steps that lead to the Bald formation are still not entirely clear.

Unlike the C_6-C_1 benzenoids and the C_6-C_3 phenylpropnoids, the remaining VBP C_6-C_2 compounds do not derive directly from CA, but from Phe. The biosynthesis starts with phenylacetaldehyde synthase, that converts Phe to phenylacetaldehyde, this means that it must compete with the PAL enzyme for its use (Kaminaga *et al.*,

2006). 2-phenylethanol and BA-CoA are used by BTBP enzyme to form phenylethylbenzoate (Orlova *et al.*, 2006) (Figure 5). 2-phenylethyl acetate is also produced by PhEth, but the enzyme in Petunia has never been characterized.

2. GIGANTEA

GIGANTEA (GI) is a specific plant nuclear protein, identified for the first time in *Arabidopsis thaliana* as a late flowering mutant (Redei, 1962). Although six decades have passed since its discovery, its precise molecular function has not been clarified yet. Only at the end of the XXth century it was possible to obtain further information describing its chromosomal organization (Fowler *et al.*, 1999). The mapping identified the genomic locus on the chromosome 1, consisting of 14 exons and encoding for a protein of 1,173 amino acids (Park *et al.*, 1999; Fowler *et al.*, 1999).

The *GI* gene, which appeared early in land plants, is present in a single copy in most plants, such as *Arabidopsis thaliana* or rice (Izawa *et al.*, 2011), while in *Solanaceae* it is found in two or three copies (Bombarely *et al.*, 2016). Evolutionary phylogenetic analysis of the gene has shown that *GI* in Petunia and in general in *Solanaceae*, is grouped separately from the clade of *Brassicaceae*, *Rosaceae* and *Fabaceae* (Figure *6*). This indicates an evolutionary departure that appears to be specific to plant families. Further gene duplications have been found in the subclades of tomato, *Nicotiana benthamiana* and *Petunia inflata*.

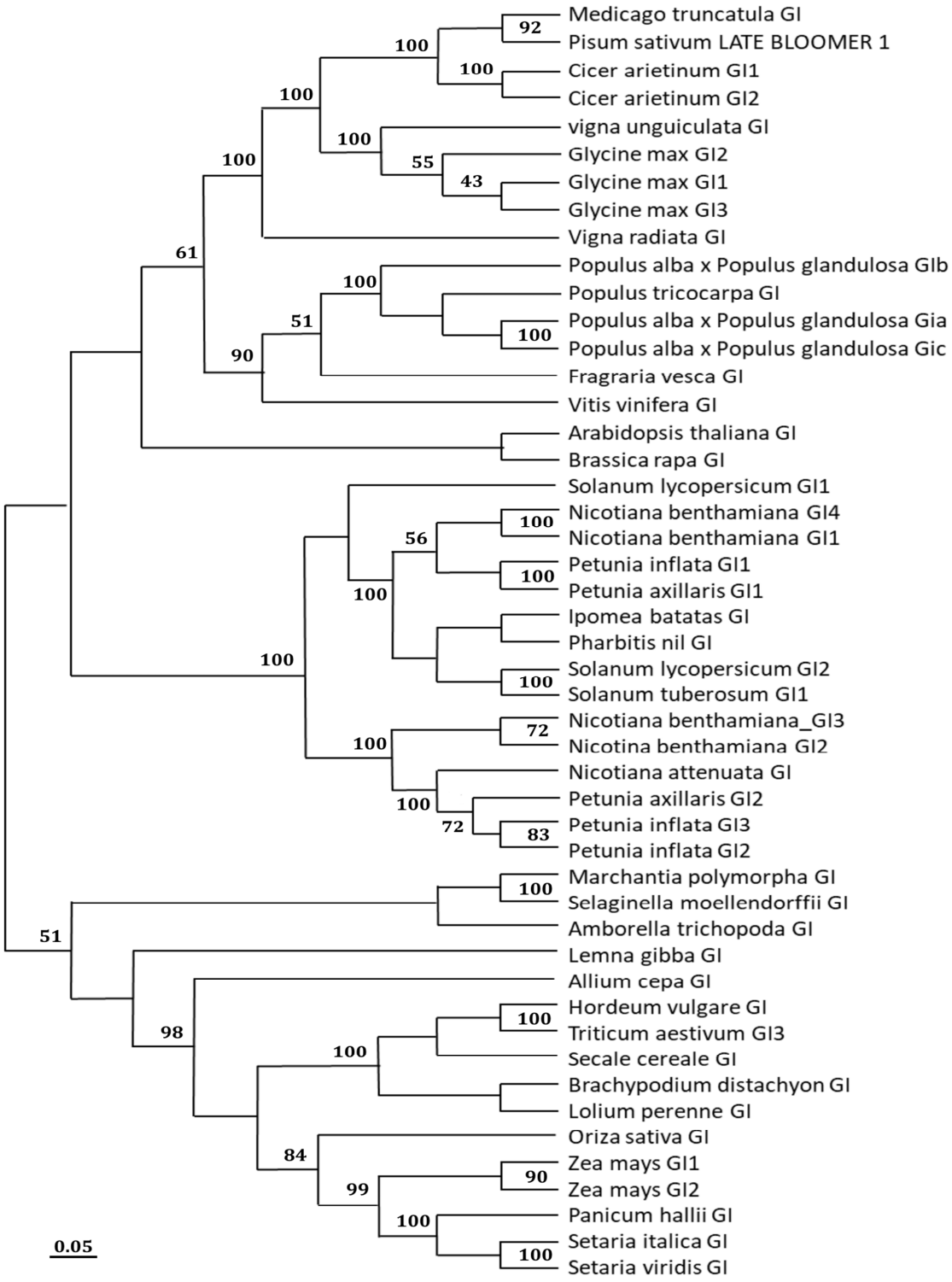

Figure 6| Phylogenetic analysis of GIGANTEA gene.

The phylogenetic tree was performed using MEGA-X software and constructed using the Neighbor-Joining method (NJ). This tree contains 47 sequences from 33 species The accession numbers of the protein sequences used are listed in Table S1.

Recent studies carried out by (Terry, Carrera-Alesina, *et al.*, 2019) supported the hypothesis that the structural evolution of the main circadian clock genes such as *GI*, occurred through changes in the number of paralogs, duplications and subfunctionalizations, changes in the gene structure and in the coding region. The proteins of *Petunia inflata* PinfS6GI1 and *Petunia axillaris* PaxiNGI1 share a conserved N-terminal with the Arabidopsis orthologue AtGI. This N-terminal region is absent in PaxiNGI2. PinfS6GI3 is, on the other hand, much shorter than the other paralogs, with the exception of *Nicotiana benthamiana* NbGI3, which shows the same characteristic. PaxiNGI2 has 41 supplementary amino acids not conserved in PinfS6GI2 or any other GI genes likewise PinfSGI1 that shows an additional C-terminal fragment of 105 amino acids, which is absent in other paralogs (Terry, Carrera-Alesina, *et al.*, 2019).

2.1 Cellular localization of Gigantea

Its sub-cellular localization was identified thanks to the use of the green fluorescent protein (GFP) fused to the GI protein. Fluorescent microscopy analysis on over-expressed GI:GFP transgenic *Arabidopsis* plants revealed that GI protein is predominantly present in the nucleus of some cell types, forming nuclear bodies (Huq *et al.*, 2000; Mizoguchi *et al.*, 2005). To better understand the nature of these formations, specific sub-nuclear marker-proteins of different compartments were used, directed specifically to nucleoli, spliceosomes, heterochromatin beams and Cajal bodies (Kim *et al.*, 2013). GI was not localized in any of the aforementioned nuclear compartments, showing that GI does not

play any role in the processes of protein degradation, pre-mRNA splicing and biogenesis of rRNA and snRNP (Kim *et al.*, 2013).

2.2 Main molecular function of Gigantea

2.2.1 Regulation of photoperiodic flowering

In land plants, the transition from the vegetative phase to flowering is regulated by the diurnal expression of *CONSTANS* (*CO*) (Paula *et al.*, 2001; Imaizumi and Kay, 2006). It has been observed that during LDs, light stabilizes CO protein and the expression of *CO* coincides with the period of light, leading to the activation of *FLOWERING LOCUS T* (*FT*) gene. On the other hand, in SD conditions the peak expression of *CO* occurs after sunset because the *CO* protein is not sufficiently stabilized by light (Valverde *et al.*, 2004). The transcription of *CO* is repressed during sunrise, thanks to the activity of the *CYCLING DOF FACTOR 1* (*CDF1*) transcription repressor bound to the CO promoter.

GIGANTEA plays a key role in growth phase transition. Thanks to a direct protein-protein interaction with FLAVIN-BINDING, KELCH REPEAT, F BOX protein 1 (FKF1), through its FKF1 LOV (Light, Oxygen or Voltage) domain, (Song et al., 2018), it forms an enzymatic complex that mediates the degradation of *CYCLING DOF FACTOR 1* (*CDF1*), a main *CO* repressor. This complex is strictly dependent on light, being the expression of *GI* under the control of the circadian clock. Therefore, towards the middle of the day, when the accumulation of GI along with FKF1 reaches the peak, the *DOF*-degradation complex leads to an increase in the transcription of *CO* and therefore to the transcription of *FT* (Imaizumi *et al.*, 2003; Sawa

General Introduction

Among the fields of sciences, developmental biology occupies a remarkable position in the study of the processes by which organisms grow and define their intrinsic characteristics during development. Those studies include organ identity, reproduction, symmetry, final size, floral phyllotaxis and the organization between environmental cues and morphogenesis (Bowman, 1997; Endress, 2006).

In all living beings, cellular movement is a need dictated by the organ's necessity to differentiate its tissues to achieve a more complete metabolic self-sufficiency and to reach nourishment sources. Plant tissues are composed of static cells, surrounded by a rigid and firmly cemented cell wall that limits their cellular mobility. This is why morphogenesis in plants takes place thanks to a combined formation process dependent on growth and differentiation (de Almeida *et al.*, 2015). Growth is that irreversible phenomenon characterized by the increase in tissue size due to cell division (mitosis), and cell expansion, the result of the absorption of water and metabolites for protoplasm formation. Differentiation is the result of all those processes that lead to an increase in the complexity of a tissue, thanks to a consequent cellular specialization. Both, work in synergy, coordinating environmental and internal signals to define organogenesis and plant structure (de Almeida *et al.*, 2015).

Vascular plants maintain two distinctive zones which retain a continued growth capacity. These regions are the apical meristems:

the shoot apical meristem, which give rise to aerial organs; and the root apical meristems, responsible of the enlargement of the root system. This ability to have an area in continuous proliferation is due to the fact that the growth of the vegetative meristems is uninterrupted and indeterminate.

The transition from the vegetative to the reproductive phase involves the formation of a floral meristem and therefore a highly precise organ-tissue specialization. Studies in *Arabidopsis thaliana* and other species, including *Petunia spp.*, have revealed that the intricate expression of the genes forming the oscillator, is closely related to internal and environmental factors. These include an interplay with hormone signaling (Bancos *et al.*, 2006; Nozue *et al.*, 2007; Thines and Harmon, 2011), cell division and expansion (Soy *et al.*, 2016; Fung-Uceda *et al.*, 2018), primary metabolism (Farré and Weise, 2012), abiotic stress response (Marcolino-Gomes *et al.*, 2014), biomass production (Ni *et al.*, 2009; Atamian *et al.*, 2016; Edwards *et al.*, 2018), flower orientation (Atamian *et al.*, 2016) and flower scent emission (Fenske *et al.*, 2015; Yon *et al.*, 2015; Terry, Pérez-Sanz, *et al.*, 2019).

1. *Petunia*, a Model System for Genetics and Developmental Studies

1.1 Description

The genus *Petunia* belongs to the family of the *Solanaceae* and comprises around 30 subspecies. Widely diffused nowadays all over the world as an appreciated ornamental plant, it exhibits a wide range of floral colors (Ando *et al.*, 2001). It is endemic to South America with a subtropical distribution, typical of southern Brazil, Uruguay and Argentina, especially at the foothills of the Andes (Kulcheski *et al.*, 2006). It maintains the supremacy as one of the most used flower beds in the world and it is considered one of the preferred genera for the development of new varieties (Gerats and Vandenbussche, 2005) .

Considering the main emerging model systems for developmental studies, such as *Arabidopsis thaliana*, *Antirrhinum spp.*, *Oryza sativa* and *Nicotiana spp.*, it is impossible not to mention *Petunia*. This genus emerged in the last two decades as one of the main model systems for physiological, biochemical and genetic research, thanks to its relatively short generation time, easy culturing, generation of stable transgenic plants using leaf-disk transformation and also *Agrobacterium* infiltration (Gerats and Vandenbussche, 2005).

Petunia is characterized by a paleohexaplodization typical of the *Solanaceae* famil*y. H*owever, an early branching occurred in the clade moving away from *S. lycopersicon*, *S. tuberosum*, *Nicotiana* spp. and *Capsicum* spp., which have n=12 chromosome number, while *Petunia* has n=7 chromosomes.

Petunia taxa are herbs with non-woody stems, imbricated aestivation, usually annual. *Petunia x hybrida*, also called *Petunia hybrida*, derived from a cross between the white-flowered *P. axillaris* and the purple-flowered *P. integrifolia* (Figure 1) (Segatto *et al.*, 2014; Fenske *et al.*, 2015).

Figure 1| *P.axillaris* and *P.integrifolia* flower shape and syndromes.

P. axillaris on the left and *P. integrifolia* on the right (a). Changes of limbs, tube and calyces morphology as well as the pigmentation in the two species. (b) A hawkmoth hovers while using its long proboscis to reach the nectar. Photo from Alexandre Dell'Olivo/FLICKR (https://urly.it/3605x). (c) A bee on a red *Petunia*. Photo from labsafeharbor/PIXABAY (https://urly.it/3605z).

P. axillaris, with its colorless flowers, emits a characteristic mixture of aromas during the night hours in order to attract the hawkmoths during its hours of activity. It is characterized by white color with a long tube, similar in length to the proboscis of its nocturnal pollinators (Stuurman *et al.*, 2004) (Figure 1b). On the

other hand, *P. integrifolia* is pollinated by bees (Figure 1c), has a short and wide tube with purple and almost scentless flowers that close at night, a strategy to exclude nocturnal pollinators (Ando *et al.*, 2001). Studies have hypothesized that the genus *Petunia* derives from an ancestor similar to *P. integrifolia* (Gübitz *et al.*, 2009; Dell'Olivo *et al.*, 2011) and that the transformation to the white flowers of *P. axillaris* might be for the inactivation of *ANTOCIANIN2 (AN2*), a MYB transcription factor that regulates the biosynthesis of anthocyanins (Quattrocchio *et al.*, 1999). This fact favored new species of pollinators such as the hawkmoth that prefers UV-absorbing flowers (white flower) rather than UV-reflecting flowers (purple flower).

Petunia x hybrida shows a typical monopodial vegetative growth whereas the inflorescences are sympodial, both in the central as in the lateral branches, following a scorpioid pattern. Considering that most of the *Solanaceae* show a similar type of inflorescence, this characteristic also makes it an excellent point of reference for flower physiology and development studies in this family.

1.2 *Petunia* inflorescence, from vegetative growth to flowering

Angiosperms show an incredible variability in plant and inflorescence architecture, especially during the switch from vegetative growth to the reproductive phase. There are over 300,000 different species, each with a unique flower but with similar features and functions, evolved from the same common ancestor.

Although flowers share the same types of organs, these can change in number and position (Koes *et al.*, 2009). Considering only

the different patterns of inflorescence appearance, it is possible to classify the plants into four mayor classes: 1) Seasonal plants, which can flower in different stages of development or at different times during the year. 2) Annual plants, which bloom and complete their lifecycle in the same year or growing season, in which they first sprouted. Many of the food plants are annuals, such as the *Solanaceae,* the *Fabaceae* and the *Graminaceae.* 3) Biennial plants, which take two years to complete their biological lifecycle and flower only after a cold winter period. 4) Perennial plants, such as trees, which need several years to flower.

The reproductive phase that, in all the higher plants, takes place after an appropriate period during which leaves and axillary meristems are generated, is species-specific. Although there are several kinds of inflorescences, it is possible to distinguish three basic types: racemes, panicles and cymes (Figure 2) (Benlloch *et al.*, 2007). The two first are typical of species with monopodial growth, where the new inflorescence shoots appear at the flanks of the apical meristem, as in *Arabidopsis* and *Antirrhinum*. In cymose inflorescences, typical of plants with sympodial growth like *Petunia*, every axis terminates with a flower and the next one growth in a lateral position, perpetuating this pattern (Rebocho *et al.*, 2008).

Considering a few basic floral structures, it is possible to understand the texture and function of most flowers. For *Petunia*, the typical flower morphology consists of four organs: sepals, petals, stamens and pistils (including carpels and ovules). To maintain an ordinate and functional symmetric structure during life, plants have developed an organized organ direction initiation, commonly known as phyllotaxis. In plants there are two major types of flower pattern

arrangement: spiral and whorled. In spiral phyllotaxis, organs are initiated at constant time intervals, called plastochrons. In whorled phyllotaxis, initiation of organs is almost synchronous and appears organized inside a ring shaped geometry.

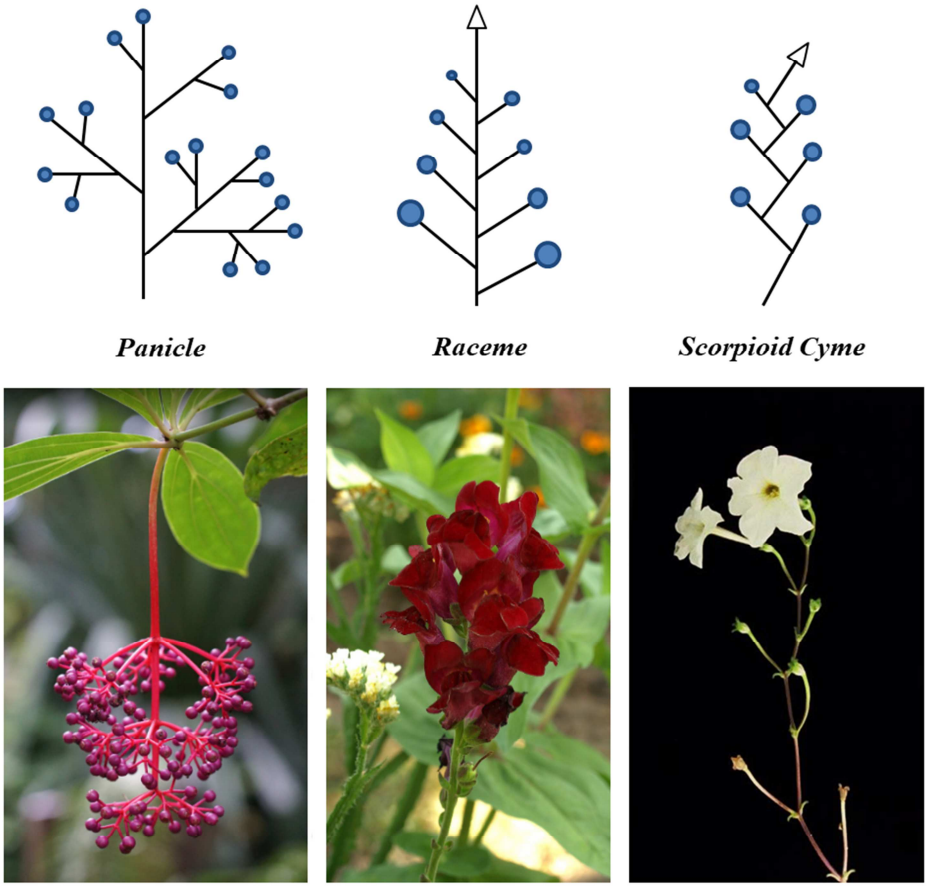

Figure 2| Example of inflorescence architecture.

From left to right, *Medinilla magnifica* panicle flower, the photo was taken by PXHERE . Red *Arabidopsis* raceme flower, the photo was taken by PXHERE (https://pxhere.com/en/photo/644035). White *Petunia* scorpioid cyme flower, own photo.

In the angiosperms, such as *Arabidopsis thaliana*, *Antirrhinum majus* (Snapdragon) and *Petunia hybrida*, flowers form concentric whorls of organs. In Petunia, what organ is formed and where, is determined by the ABCDE model (Figure I.3) (Coen and Meyerowitz,

1991; Rijpkema *et al.*, 2010). Basically, the classical ABCDE model determines the formation of four types of whorls according to an expression pattern of few genes (Figure 3). “A” genes, specify sepals; “A” plus “B” genes, specify petals; “B” plus “C” genes, stamens; and “C” genes alone, specify carpels. “D” and “E” genes are the latest group of genes added to the model. “D” genes are involved in the ovule formation and seed development. “E” genes, are required for all the floral organs specification.

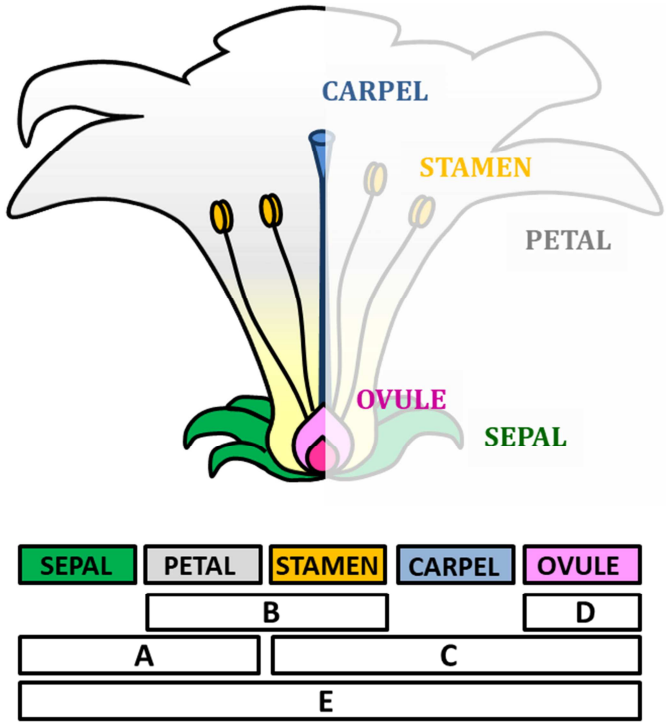

Figure 3| Diagram of the ABCDE model of flower development.

It is not surprising that the molecular mechanism that controls flowering has taken a prominent place in scientific research over the years. One of the most studied plants, used to better understand this intricate mechanism, has been *Arabidopsis* (Mouradov *et al.*, 2002; Simpson, 2002; Krizek and Fletcher, 2005; Blázquez *et al.*, 2006) in

which two main pathways of signaling were identified. The gibberellic acid (GA) pathway, that mediates hormonal and endogenous cues (Blázquez *et al.*, 1998); and the photoperiod pathway, responsible to mediate the environmental signals (Blázquez *et al.*, 2003). At the center of this system of flowering pathways, there are a series of genes called "floral pathway integrators" that converge all the distinct signals received (Koes *et al.*, 2009). Over the year, several molecular genetic experiments in Arabidopsis and Petunia have identified a pool of integrator genes involved in mediation, integration and perception of flowering signals. The Petunia floral formation of the apical meristem involves the activity of the genes *PETUNIA FLOWERING GENE (PFG),* a MADS box gene responsible of flower meristem identity (Immink *et al.*, 1999) and *ABERRANT LEAF AND FLOWER (ALF),* the orthologue of *LEAFY* (LFY) in *Arabidopsis* (Souer *et al.*, 1998). This last one needs the action of *DOUBLE TOP (DOT),* the homolog of *UNUSUAL FLORAL ORGANS (UFO),* to induce the floral meristem identity (Souer *et al.*, 1998).

The F-box of DOT interacts physically with ALF protein via the SCF-E3-ubiquitin ligase complex, which results in the post-transcriptional activation of ALF (Souer *et al.*, 1998). Indeed, it has been discovered, using a yeast two-hybrid assay, that UFO and DOT bind with SKP1-like proteins, which are components of the SCF complex (Samach *et al.*, 1999; Souer *et al.*, 2008).

Although flowering in Petunia and Arabidopsis are influenced by the same environmental signals, they appear to follow a different path of gene expression. In *Arabidopsis* the expression of *UFO* occurs already during the vegetative phase and the increasing activation of

LFY induces the floral transition. On the other hand, in Petunia, *ALF* only needs *DOT* to initiate the floral development induction (Figure 4).

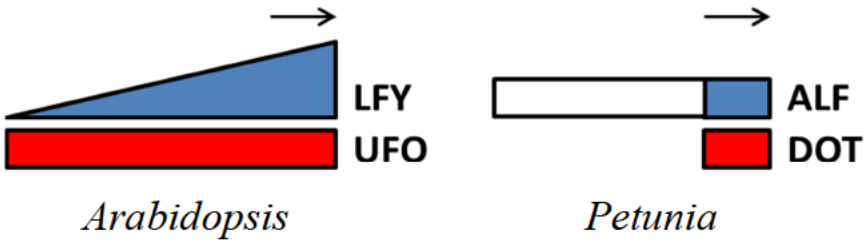

Figure 4| Schematic representation of ALF and DOT expression in Petunia.

ALF and *DOT* have different roles and expression patterns in floral induction in Petunia than their Arabidopsis's homologs, *LFY* and *UFO*. In Arabidopsis, the activation of *LFY* induces the floral transition while *UFO* is expressed throughout the vegetative phase. In Petunia, ALF production occurs early during the vegetative phase but requires the DOT function to induce the floral transition. Black arrows indicate the floral induction.

Another gene implicated in *Petunia* inflorescence's architecture is *EVERGREEN (EVG). EVG* is involved in the activation of *DOT* and the initiation of the floral identity in the apical meristem as well as in the lateral inflorescence shoot development (Rebocho *et al.*, 2008).

1.3 Petunia floral scent production

Plants, like many sessile organisms, have evolved specific mechanisms to face the environmental challenges. Biotic/abiotic stress responses, communication with pollinators, antagonist and other plants are just few examples. Among the main strategies that plants use to ensure entomophilic reproduction is the emission of scents. The Volatile organic compounds (VOCs) are mixtures of volatile lipophilic molecules of benzenoids/phenylpropanoids and

fatty acid derivatives with low molecular weight and high vapor pressure at ambient temperature, synthesized in all plant organs, from roots to flowers (Knudsen *et al.*, 1993; Pichersky and Gershenzon, 2002).

Over 1,700 volatile compounds have been identified in plants and although some of them are largely widespread among plants, others are exclusive to some specific taxa (Pichersky and Gershenzon, 2002; Pichersky *et al.*, 2006). Petunia emits a wide range of different VOCs during the day, especially in the late evening, making this species an excellent model system for studying the emission and composition of aromas.

Flowers are typically the main organs for the emission of volatile substances in plants, which occurs through the epidermal cells, ensuring rapid release into the atmosphere (Kolosova *et al.*, 2001). Floral VOCs act mainly as signal molecules for pollinators, with a maximal peak of emission when pollinators are seasonally active and flowers are mature. *P. axillaris* for instance, produces fragrant flowers, with an emission peak during the night, featured mainly by methyl benzoate, benzyl alcohol and benzaldehyde (Hoballah *et al.*, 2005). The highest emission coincides with the hawkmoth nocturnal activity. Briefly, different plant species produce different fragrances, reflecting the preferences of their pollinators. This olfactory sensitivity of insects, able to distinguish the different floral fragrances, makes the floral scent a character of fundamental importance for plant-insect interactions (Negre *et al.*, 2003). The species-specificity of the floral fragrance greatly improves the specificity of pollination, reducing the risk of useless interspecific pollination (Huang and Shi, 2013).

On the other hand, in vegetative organs, VOCs are part of the plant's defense system and are mainly synthesized in glandular trichomes (Tissier *et al.*, 2017), single specialized cells (Lewinsohn, 1998) or tubes (Franceschi *et al.*, 2005) from which they can sprout out in case of breakage. They generally act as a deterrent against herbivores and florivores (Klahre *et al.*, 2011), as an attractant for natural enemies of parasites and pests (Schnee *et al.*, 2006; Scala *et al.*, 2013), or directly function as antifeedant or have antimicrobial and antifungal roles (Dudareva *et al.*, 2006).

The availability of carbon, nitrogen, sulfur and energy from the primary metabolism of the plant are essential for the biosynthesis of VOCs (Schuurink *et al.*, 2006; Dudareva *et al.*, 2013), highlighting the high degree of dependence and communication between the secondary and primary metabolism in the plant kingdom (Dudareva *et al.*, 2013).

In Petunia, as in many Angiosperms, the quantity and composition of the VOCs can fluctuate during the day, mainly in relation with the age of the flower. This rhythmic release of scent is also closely related to the flower hormonal regulation, circadian clock, flower and plant development, nutrient availability, temperature, humidity and general environmental conditions (Colquhoun *et al.*, 2010; Cna'Ani *et al.*, 2015; Fenske *et al.*, 2015).

The synthesis and emission of VOCs begin after the opening of the flower bud (anthesis), from the epidermal cells of the corolla limb, following a rhythmic pattern. Thirteen main benzenoids/phenylpropanoids have been identified in Petunia including benzaldehyde, methyl benzoate, benzyl benzoate, benzyl

alcohol, benzyl acetate, phenylacetaldehyde, methyl-salicylate, phenylethyl benzoate, 2-phenylethyl acetate, phenylethyl alcohol, eugenol, isoeugenol and vanillin (Kolosova *et al.*, 2001; Verdonk *et al.*, 2003; Colquhoun *et al.*, 2010).

The plant VOCs are basically classified into different classes according to their biosynthetic origins, such as: terpenoids, benzenoids/phenylpropanoids, fatty acid derivates and amino acid derivates as well as few other genus-specific volatiles (Dudareva *et al.*, 2013). Among the most emitted volatile compounds by *Petunia* flowers there are undoubtedly the benzenoids/phenylpropanoids (Weiss *et al.*, 2016; Amrad *et al.*, 2016; Terry, Pérez-Sanz, *et al.*, 2019) whose emission intensity decreases during the senescence induced after pollination (Negre *et al.*, 2003; van Schie *et al.*, 2006).

The Shikimate pathway converts the carbon of the primary metabolism into chorismate, the precursor of the aromatic amino acids (AAA) phenylalanine (Phe), tyrosine (Tyr) and tryptophan (Trp), through seven enzymatic reactions (Tzin and Galili, 2010; Dudareva *et al.*, 2013), which in turn are precursors of a large number of primary and secondary metabolites (Schuurink *et al.*, 2006). In the shikimate pathway, DAHP synthase is the first enzyme to be activated and is responsible for controlling the amount of carbon that enters in the pathway. Unlike what happens in bacteria, in which DAHP synthase protein is regulated both at transcriptional level and by an inhibition feedback reaction; in plants there is no evidence for an enzyme inhibition (Herrmann and Entus, 2001).

Chorismate is also a precursor of the plant defense hormone salicylic acid and for vitamins K1 and B9 synthesis (Maeda and

Dudareva, 2012). The phosphoenolpyruvate of the glycolysis pathway and the erytrose 4-phosphate of the pentose phosphate pathway, are both the first immediate precursors of this complicated pathway (Widhalm and Dudareva, 2015) (Figure 5).

The first steps for the biosynthesis of the main volatile benzenoid/phenylpropanoid compounds is catalyzed by the action of the enzyme phenylalanine ammonia lyase, that deaminates Phe in *trans*-cinnamic acid, the main intermediate in the VBP biosynthesis (Colquhoun *et al.*, 2010; Dudareva *et al.*, 2013). While the biosynthesis of AAs occurs in plastids, their further conversions to VBP occur outside in the cytosol (Maeda and Dudareva, 2012; Widhalm and Dudareva, 2015).

The synthesis of C_6-C_3 phenylpropanoids, which get their name from the six-carbon aromatic phenyl group and from the three carbons of the propene tail of CA, starts from the formation of para-coumaric acid by the cinnamate-4-hydroxylase enzyme. Among these, the monolignols, monomers used to generate various forms of lignin and suberin, are mainly used as a structural component of plant cell wall.

One of the monolignols is conifer alcohol, which is converted into coniferil acetate before its reduction into eugenol and isoeugenol by eugenol syntase and isogeugenol synthase, respectively (Dexter *et al.*, 2007; Dudareva *et al.*, 2013; Muhlemann *et al.*, 2014) (Figure 5).

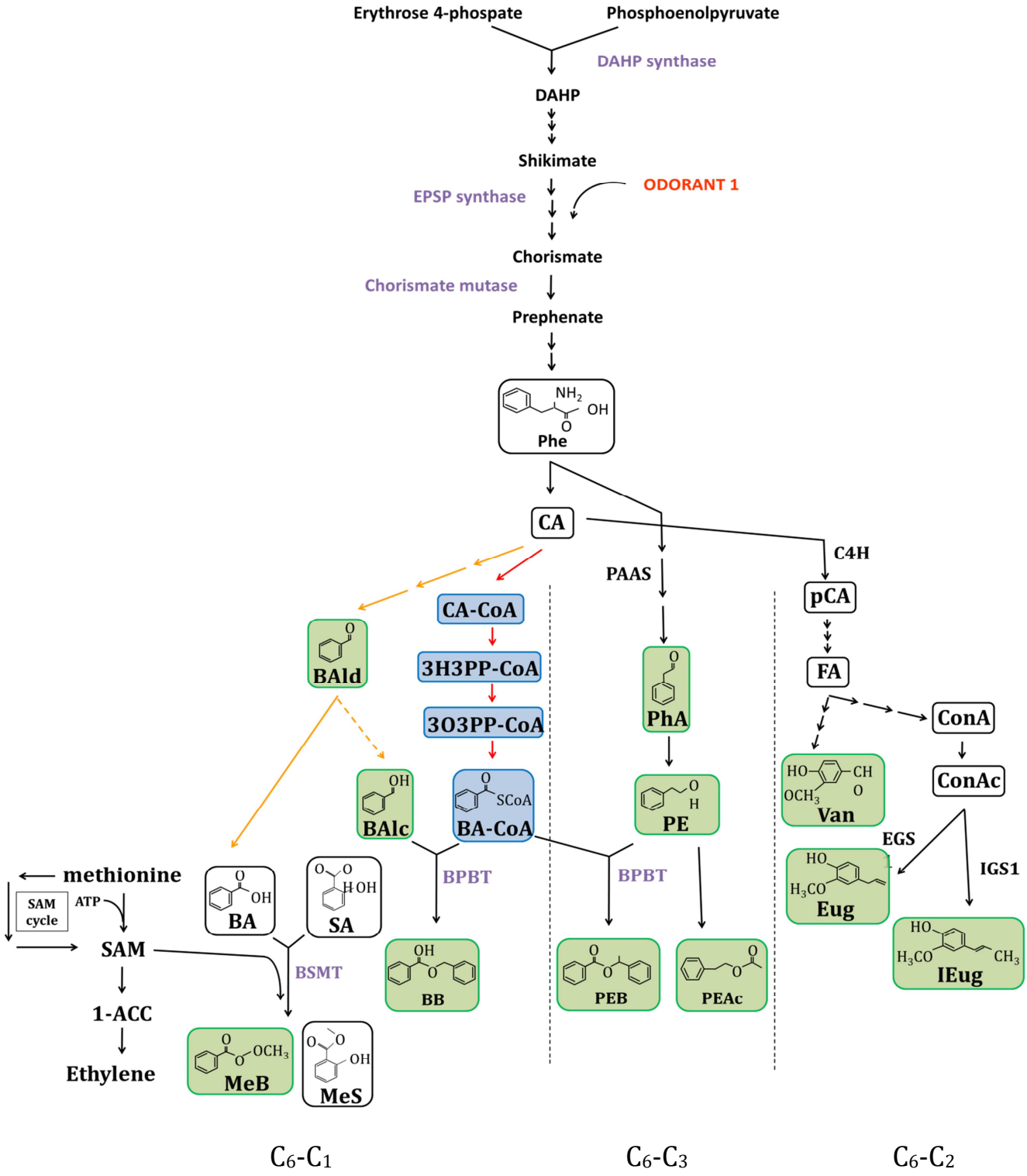

Figure 5| Schematic plant benzenoid/phenylpropanoid VOC synthesis.

Volatile benzenoid/phenylpropanoid C_6-C_1, C_6-C_2 and C_6-C_3 metabolic pathway in Petunia. Volatile compounds are highlighted with a green background. Red and yellow arrows indicate respectively the β-oxidative and non β-oxidative pathway. Plan arrows indicate reactions that are catalyzed by single enzymes. Dashed arrows indicate the involvement of multiple enzymatic reactions. Broken arrows indicate hypothetical

steps not yet described. Abbreviations: **3H3PPA**, 3-hydroxy-3-phenylpropanic acid; **3O3PPA**, 3-oxo-3-phenylpropanoyl acid; **BA**, benzoic acid; **BA-CoA**, benzoyl-Coa; **BAlc**, benzyl alcohol; **Bald**, benzaldehyde; **BALDH**, benzaldehyde dehydrogenase; **BB**, benzyl benzoate; **CA**, trans cinnamic acid; **CA-CoA**, Cinnamoil-CoA; **C4H**, cinnamate-4-hydroxylase; **ConA**, coniferil alcohol; **ConAc**, coniferil acetate; **EGS1**, eugenol synthase1; **Eug**, eugenol; **FA**, ferulic acid; **MB**, methylbenzoate; **PAAS**, phenilacetaldehyde synthase; **PAL**, phenylalanine ammonia lyase; **pCA**, para cumaric acid; **PEAc**, 2-phenylethyl acetate; **PEB**, phenylethylbenzoate; **PhA**, phenylacetaldeyde; **Phe**, phenylalanine; **PhEth**, 2-phenylethanol.

It has been shown that the formation of C_6-C_1 benzenoids proceeds through three routes: a β-oxidative, a non-β-oxidative and a combination of both. The β-oxidative pathway occurs in peroxisomes, in a similar way to the β-oxidation of fatty acids and branched-chains of amino acid (Dudareva *et al.*, 2013). The β-oxidative route starts with CA, which undergoes a series of hydrations and oxidations, leading to the formation of benzoyl-CoA, a key intermediate for the formation of benzylbenzoate and phenylethylbenzoate in the cytosol. Recent experiments, performed on *Nicotiana attenuata* plants, using stable isotope-labeled ($^{2}H_6$, ^{18}O)3-hydroxy-3-phenylpropanic acid, support β-oxidation as one of the possible pathways for the formation of benzoic acid in the cytoplasm. (Jarvis *et al.*, 2000; Widhalm and Dudareva, 2015). Benzaldehyde is the key intermediate for the non-β-oxidative pathway, which is oxidized to benzoic acid. The biochemical steps that lead to the Bald formation are still not entirely clear.

Unlike the C_6-C_1 benzenoids and the C_6-C_3 phenylpropnoids, the remaining VBP C_6-C_2 compounds do not derive directly from CA, but from Phe. The biosynthesis starts with phenylacetaldehyde synthase, that converts Phe to phenylacetaldehyde, this means that it must compete with the PAL enzyme for its use (Kaminaga *et al.*,

2006). 2-phenylethanol and BA-CoA are used by BTBP enzyme to form phenylethylbenzoate (Orlova *et al.*, 2006) (Figure 5). 2-phenylethyl acetate is also produced by PhEth, but the enzyme in Petunia has never been characterized.

2. GIGANTEA

GIGANTEA (GI) is a specific plant nuclear protein, identified for the first time in *Arabidopsis thaliana* as a late flowering mutant (Redei, 1962). Although six decades have passed since its discovery, its precise molecular function has not been clarified yet. Only at the end of the XXth century it was possible to obtain further information describing its chromosomal organization (Fowler *et al.*, 1999). The mapping identified the genomic locus on the chromosome 1, consisting of 14 exons and encoding for a protein of 1,173 amino acids (Park *et al.*, 1999; Fowler *et al.*, 1999).

The *GI* gene, which appeared early in land plants, is present in a single copy in most plants, such as *Arabidopsis thaliana* or rice (Izawa *et al.*, 2011), while in *Solanaceae* it is found in two or three copies (Bombarely *et al.*, 2016). Evolutionary phylogenetic analysis of the gene has shown that *GI* in Petunia and in general in *Solanaceae*, is grouped separately from the clade of *Brassicaceae*, *Rosaceae* and *Fabaceae* (Figure *6*). This indicates an evolutionary departure that appears to be specific to plant families. Further gene duplications have been found in the subclades of tomato, *Nicotiana benthamiana* and *Petunia inflata*.

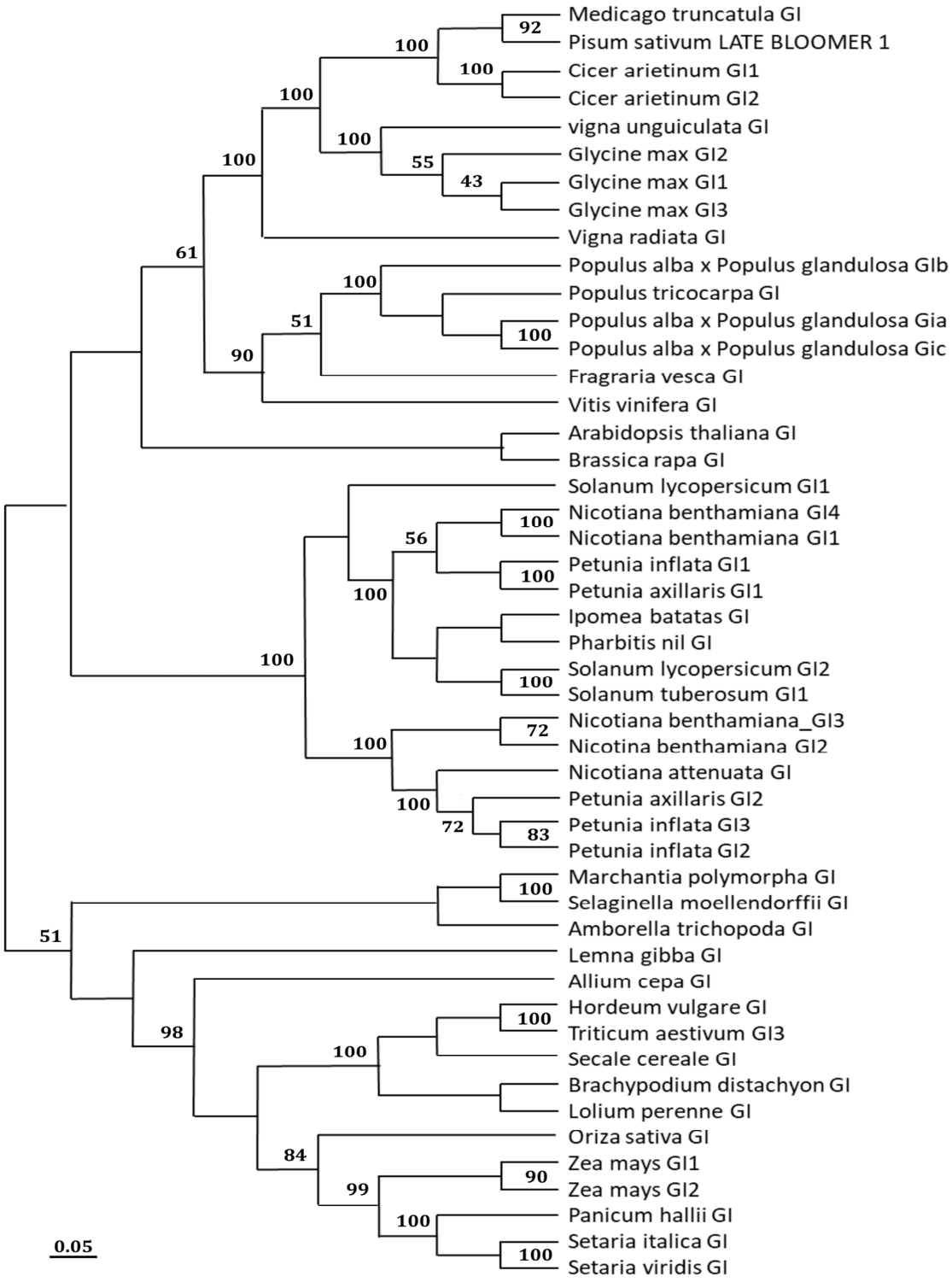

Figure 6| Phylogenetic analysis of GIGANTEA gene.

The phylogenetic tree was performed using MEGA-X software and constructed using the Neighbor-Joining method (NJ). This tree contains 47 sequences from 33 species The accession numbers of the protein sequences used are listed in Table S1.

Recent studies carried out by (Terry, Carrera-Alesina, *et al.*, 2019) supported the hypothesis that the structural evolution of the main circadian clock genes such as *GI*, occurred through changes in the number of paralogs, duplications and subfunctionalizations, changes in the gene structure and in the coding region. The proteins of *Petunia inflata* PinfS6GI1 and *Petunia axillaris* PaxiNGI1 share a conserved N-terminal with the Arabidopsis orthologue AtGI. This N-terminal region is absent in PaxiNGI2. PinfS6GI3 is, on the other hand, much shorter than the other paralogs, with the exception of *Nicotiana benthamiana* NbGI3, which shows the same characteristic. PaxiNGI2 has 41 supplementary amino acids not conserved in PinfS6GI2 or any other GI genes likewise PinfSGI1 that shows an additional C-terminal fragment of 105 amino acids, which is absent in other paralogs (Terry, Carrera-Alesina, *et al.*, 2019).

2.1 Cellular localization of Gigantea

Its sub-cellular localization was identified thanks to the use of the green fluorescent protein (GFP) fused to the GI protein. Fluorescent microscopy analysis on over-expressed GI:GFP transgenic *Arabidopsis* plants revealed that GI protein is predominantly present in the nucleus of some cell types, forming nuclear bodies (Huq *et al.*, 2000; Mizoguchi *et al.*, 2005). To better understand the nature of these formations, specific sub-nuclear marker-proteins of different compartments were used, directed specifically to nucleoli, spliceosomes, heterochromatin beams and Cajal bodies (Kim *et al.*, 2013). GI was not localized in any of the aforementioned nuclear compartments, showing that GI does not

play any role in the processes of protein degradation, pre-mRNA splicing and biogenesis of rRNA and snRNP (Kim *et al.*, 2013).

2.2 Main molecular function of Gigantea

2.2.1 Regulation of photoperiodic flowering

In land plants, the transition from the vegetative phase to flowering is regulated by the diurnal expression of *CONSTANS* (*CO*) (Paula *et al.*, 2001; Imaizumi and Kay, 2006). It has been observed that during LDs, light stabilizes CO protein and the expression of *CO* coincides with the period of light, leading to the activation of *FLOWERING LOCUS T* (*FT*) gene. On the other hand, in SD conditions the peak expression of *CO* occurs after sunset because the *CO* protein is not sufficiently stabilized by light (Valverde *et al.*, 2004). The transcription of *CO* is repressed during sunrise, thanks to the activity of the *CYCLING DOF FACTOR 1* (*CDF1*) transcription repressor bound to the CO promoter.

GIGANTEA plays a key role in growth phase transition. Thanks to a direct protein-protein interaction with FLAVIN-BINDING, KELCH REPEAT, F BOX protein 1 (FKF1), through its FKF1 LOV (Light, Oxygen or Voltage) domain, (Song et al., 2018), it forms an enzymatic complex that mediates the degradation of *CYCLING DOF FACTOR 1* (*CDF1*), a main *CO* repressor. This complex is strictly dependent on light, being the expression of *GI* under the control of the circadian clock. Therefore, towards the middle of the day, when the accumulation of GI along with FKF1 reaches the peak, the *DOF*-degradation complex leads to an increase in the transcription of *CO* and therefore to the transcription of *FT* (Imaizumi *et al.*, 2003; Sawa

et al., 2007). This does not happen in SDs as the GI accumulation peak occurs about three hours earlier than that of FKF1. This prevents the formation of the *DOF*-degradation complex and the consequent reduced abundance of the *CO* transcript.

Additionally, *GI* can regulate the expression of *FT* independently of *CO*. It seizes the *FT* transcriptional repressors such as *SHORT VEGETATIVE PHASE* (*SVP*), *TEMPRANILLO 1* (*TEM1*) and *TEMPRANILLO 2* (*TEM2*). GI alters their stability or neutralizes their repressor effect by blocking their access to the FT promoter region. Likewise, GI binds their specific target regions on the *FT* promoter (Sawa and Kay, 2011) ensuring the abundance of the FT transcript (Figure 7).

Another mechanism through which *GI* regulates *FT* expression independently of *CO* is via its interaction with a microRNA. The *miRNA172* inhibits the expression of the main transcriptional factors of *FT*, such as *TARGET OF EAT 1* (*TOE1*) and *APETALA 2* (*AP2*). (Jung *et al.*, 2007) demonstrated that *miRNA172* is positively regulated in the presence of GI protein through an unclear molecular interaction. Growth of plants under more natural conditions i.e. with photo and thermoperiod, shows that it has a major impact in the coordination of FT suggesting that GI may have a role in temperature and light coordination (Song *et al.*, 2018).

GIGANTEA regulates flowering time through direct protein-protein interaction with SPINDLY (SPY) (Tseng, 2004) a negative regulator of the gibberellic acid (GA) pathways signaling in *Arabidopsis thaliana* (Jacobsen and Olszewski', 1993). SPY has two distinct domains, the C-terminal catalytic domain and the N-terminal

tetratricopeptide repeats that mediates interactions with other proteins (Blatch and Lassle, 1999). GI inhibits SPY, allowing flowering to occur.

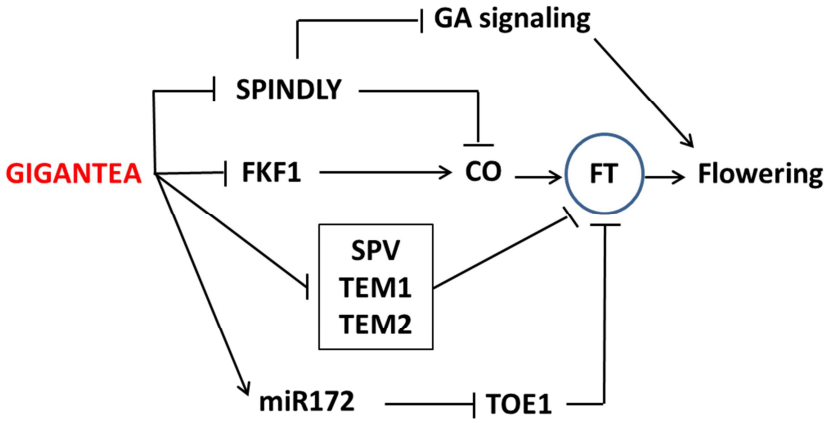

Figure 7| GIGANTEA regulates flowering transition.

Flowering is regulated by GI along with FKF1 with which it forms a complex responsible for the degradation of *CO* repressor, *CDF1.* GI alters the structure of SPV, TEM1 and TEM2 promoting *FT* transcription. The protein-protein interaction with SPINDY allows flowering occur. GI also processes *miR172* preventing it from inhibiting the transcription factors of FT, TOE1 and AP2.

2.2.2 Control of the Circadian Clock

Earth's rotation causes rhythmic changes in environmental conditions that elicit important effects on the physiology, metabolism and behavior of most organisms. The circadian clock has evolved as a molecular timekeeping mechanism that controls many biological processes dependent on that rhythmic oscillations, first of all the length of the day and night cycle (Hsu and Harmer, 2014). The most recent model, based on Arabidopsis, describes the endogenous clock as an intricate system of negative autoregulatory feedback loops interacting with each other via transcriptional and post-translational activation and repression (Pokhilko *et al.*, 2012) (Figure 7).

The circadian clock includes three main loops of regulation. The core-clock loop, consisting of two MYB transcription factors, *CIRCADIAN CLOCK ASSOCIATED 1* (*CCA1*) and *LATE ELONGATED HYPOCOTYL* (*LHY*) as well as the *PSEUDO RESPONSE REGULATOR 1* (*PRR1*), better known as *TIMING OF CAB 1* (*TOC1*). The morning loop, which involves *PSEUDO RESPONSE REGOLULATOR 9* (*PRR9*) and *PSEUDO RESPONSE REGOLULATOR 7* (*PRR7*), which are linked to the *CCA1*/*LHY* core-clock genes. Finally, the evening complex (EC) which includes *EARLY FLOWERING 3* (*ELF3*), *EARLY FLOWERING 4* (*ELF4*) and *LUX ARRHYTMO* (*LUX*). Additional genes that playing a key role are *GI* and *ZEITLUPE* (*ZTL*) which are linked to the core-clock gene *TOC1*.

According to the theory of the repression feedback circuits, the morning elements LHY and CCA1 heterodimerize and repress the expression of *TOC1* and the EC members as *GI, LUX*, *ELF3*, *ELF4*. PRR9, PRR7 and PRR5, which in turn when expressed, repress the expression of *CCA1* and *LHY*. In the evening, *TOC1* represses all of the previously expressed components.

Experiments carried out by (Fowler *et al.*, 1999) in Arabidopsis demonstrated that under both long days (LDs) and short days (SDs), mutation in *GI* locus affects the *CCA1* and *LHY* gene expression. On the other hand, over-expression or mutations of *CCA1* and *LHY* disrupt the *GI* expression. In agreement with these results, the double mutant of *LHY* and *CCA1* show an overabundance of the transcription of *GI* (Mizoguchi *et al.*, 2005). These results led to the conclusion that *GI* operates in a feedback loop for adjusting and maintaining the length of the clock period.

GI contributes to maintain the circadian period length and amplitude, also interacting with ZTL, a F-box protein with a blue light photoreceptor activity which controls TOC1 levels (Kim *et al.*, 2007). GI, with its chaperone activity, facilitates ZTL maturation into an active form, which sustains a normal circadian period through proteasome-dependent degradation of TOC1, a gene of the central loop.

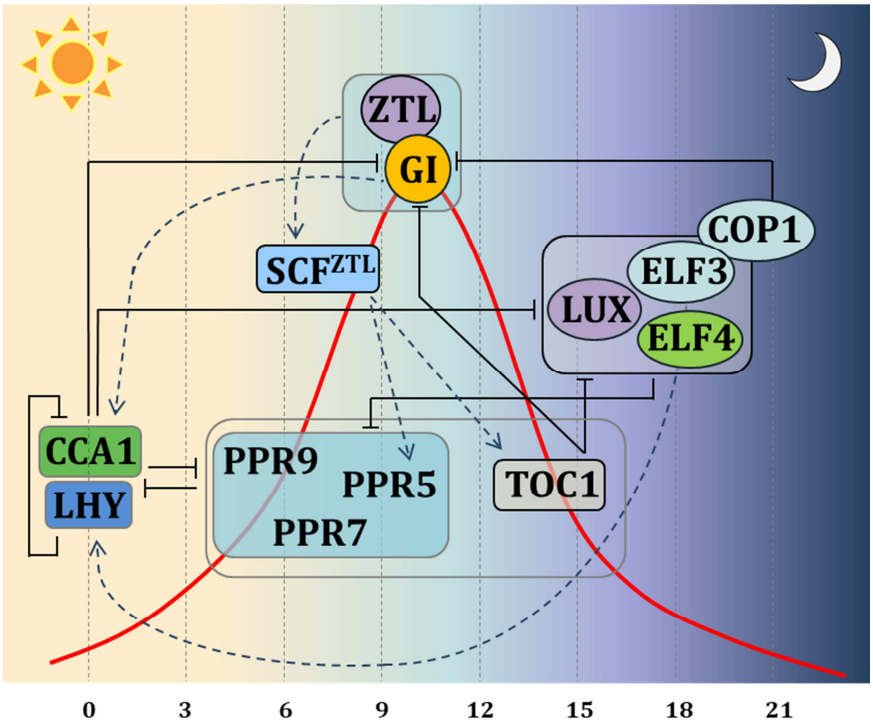

Figure 8| Circadian clock transcriptional and post-transcriptional feedback loops model.

The clock components are depicted according to their peak-time expression from left to right. Black bars indicate repression. Green arrowheads lines indicate activation of transcription. Blue arrowheads lines indicate proteaosome degradation. The red curve represents the expression of GI during the day. TOC1 is protected during the day from ZTL-induced proteasome degradation thanks to the direct protein-protein interaction of GI with ZTL, its interaction with PRR3 which prevents access to ZTL and PRR5. During the evening ELF3 promotes the proteasome degradation of GI through its interaction with COP1, thus promoting the ZTL-dependent TOC degradation.

Kim et al. (2012), also demonstrated in Arabidopsis that *GI* and *ELF4* show an epistatic interaction between each other and have a synergistic effect on endogenous clock regulation.

Another evidence supporting that *GI* plays a central role in maintaining the rhythmicity of the clock, is that *GI* is involved in the temperature compensation processes. It is implicated in maintaining an accurate rhythmicity at high and low temperatures, over a range of ambient temperatures (Cao *et al.*, 2005). It has been recognized indeed, that temperature fluctuations regulate the abundance of *GI* transcription (Gould *et al.*, 2006).

2.2.3 Light signaling

Photoreceptors, such as phytochromes, phototropins, cryptochromes and UV-light photoreceptors, have been well documented in the past two decades, for their pleiotropic control over light-induced plant development (Casal, 2007). Different light cues from the environment, such as intensity and duration of light, are detected by a sophisticated network of photoreceptors that mediate specific wavelength inputs into physiological signals (Casal et al. 2003; Martin-Tryon et al. 2007), a process called photomorphogenesis.

Higher plants, encode a wide shade of photoreceptors. Cryptochromes and phototropins absorb mainly the blue spectrum (B, λ = 400-499 nm) and are involved in the regulation of flowering time, inhibition of the hypocotyl and phototropism (Lin, 2000). On other hand phytochromes (Phy), of which in *A. thaliana* exist five members, from PhyA to PhyE (Huq *et al.*, 2000; Mishra and

Panigrahi, 2015), encode specifically for Red (R, λ=660 nm) and Far-Red (FR, λ=730 nm) photoreceptors which influence many aspects of plant development such as germination, organ orientation, seedling etiolation, vegetative growth and reproductive transition. PhyA is primarily a FR-receptor and mediates two distinct photobiological responses: the very-low-fluence response (VLFR) and the high-irradiance response (HIR) (Casal *et al.*, 2003) while PhyB-E are basically R-light receptors. The discovery of mutants specifically defective in R, FR or in both reactivities, have demonstrated a complex network of signaling in which *PhyA* and *PhyB* have separated but also shared early signaling pathways (Deng and Quail, 1999).

Numerous experiments have been performed on Arabidopsis *gi*-mutants which has shown to be dependent on the light wavelength, acting in the red as well as in the blue light signaling. Arabidopsis *gi*-mutants grown under saturated R light condition, have shown an elongated hypocotyl compared to wild type, and little or no change in responsiveness to continuous FR light (Huq *et al.*, 2000). This led to the conclusion that, as the inhibition of the hypocotyl elongation is mainly mediated by *PhyB* (Reed *et al.*, 1993; Quail *et al.*, 1995), *GI* appears to be a positive regulator of *PhyB* signaling during seedling de-etiolation (Tseng, 2004). Considering also that neither the genes nor the abundance of PhyA-B proteins are affected in *gi*-mutants (Oliverio *et al.*, 2007), it appears clear that *GI* works downstream of PhyA-B, after their migration to the nucleus in response to light, where GI is constitutively localized. Additional data regarding *gi*-mutants grown in FR light condition revealed low VLFR levels, cotyledon unfolding and a low seed germination index. These

phenotypes were rescued through *GI* over-expression, demonstrating that *GI* plays a role in the PhyA signaling (Oliverio *et al.*, 2007). The *gi*-mutant seedlings also exhibited a long hypocotyl phenotype when grown under blue light, proving to have a role also in the signaling of blue light (Martin-Tryon et al. 2007).

In Arabidopsis, it has been shown that GI affects the growth of the hypocotyl through the interaction with SPY in the regulation of gibberellin signaling. SPY is in fact a negative regulator of gibberellin signaling and an inhibitor of hypocotyl lengthening (Tseng, 2004; Kim *et al.*, 2012).

2.2.4 Cold tolerance

Plants cope with the environmental stresses by activating a series of specific metabolic pathways, specifically regarding cold temperatures. They must avoid freezing injury that can occur in both intracellular and extracellular compartments, prevent chilling wounds and cell injuries that could cause tissue death. To do this, they have developed various protection strategies such as sugar accumulation, which reduces the threshold level of freezing within cells. Alternatively, they can stabilize cell membranes producing specific structures that prevent cell disruption. The *Arabidopsis Fatty Acid Desaturase 8* (*FAD8*) gene encodes for a desaturase which alters lipid composition of the membranes by removing two atoms of hydrogen from the fatty acids, creating a double carbon/carbon bond, thus contributing to freezing resistance (Gibson *et al.*, 1994).

Plants have the ability to adapt to low temperatures by increasing their freezing tolerance through the gradual exposure to

low but non-freezing temperatures, a process identified as cold acclimation (Guy, 1990). This process is characterized by complex biochemical and physiological changes, including gene expression (Guy *et al.*, 1985; Thomashow, 1999), enzyme activities (Uemura *et al.*, 2003), lipid membrane composition (Miquel *et al.*, 1993) and leaf ultrastructure modification (Ristic and Ashworth, 1993).

Previous studies in *Arabidopsis,* identified a group of four gene families that are induced mainly during cold acclimation (Thomashow, 1999): I) *COR* (*cold-regulated*) genes, sometimes also called *LTI* (*low temperature-induced*), II) *KIN* (*cold inducible*), III) *RD* (*responsive to desiccation*) and IV) *ERD* (*early dehydration-inducible*). Many members of these families, encode for hydrophilic polypeptides that promote freezing tolerance (Guy *et al.*, 1985; Thomashow, 1999). They are induced in response to many phenomena such as water deficit stress, drought and high salinity.

Cold acclimatization is therefore due to the induction of the COR genes through the activation of a group of DNA regulatory element called dehydration-responsive element/C-repeat (DRE/CRT) (Baker *et al.*, 1994; Yamaguchi-Shinozakiaib and Shinozaki, 1994). The main cold tolerance pathway occurs through the activation of the DRE/CRT binding proteins, commonly defined CBFs (DRE/CRT binding factors), also named DREB (DRE binding factors). These are induced by low temperatures and function as transcriptional activators (Stockinger *et al.*, 1997), specifically binding the DRE/CRT sequences and activating the gene transcription. In *At,* overexpression of *CBF1* and *CBF*3 increases freezing and drought tolerance (Liu *et al.*, 1998). Additional experiments in tomato,

(Zhang et al 2004), rice (Ito et al 2006) or wheat (Sutton et al 2009) indicate a conserved mechanism across plants.

Many scientific evidences indicate the existence of a various CBF-independent pathways in the regulation of the cold stress response. *GI* gene mediates cold stress responses in Arabidopsis without the activation of the CBF pathway. The Arabidopsis *gi-3* mutant showed a reduced acclimation ability and an altered cold tolerance without changes in the *CBF* gene expression levels as well as their target genes (Cao *et al.*, 2005). At the same time, analysis performed on wild type *At* plants subjected to low temperatures showed that *GI* gene was up-regulated in response to the low temperature (Fowler and Thomashow, 2002).

3. Post-transcriptional gene silencing mechanism

The scientific community observed in the '90s that the interaction between RNA and their homologous genomic sequences could cause gene silencing. The breakthrough came in 1998 when, in studies on the nematode *Caenorhabditis elegans*, it was discovered that injection of double stranded RNA (dsRNA) caused gene silencing of sequences, highly homologous to the introduced RNA sequence (Fire *et al.*, 1998).

In the following decades, it was reported that animals (McManus and Sharp, 2002; Scherr and Eder, 2007), plants (Vaucheret *et al.*, 1998) and members of the family of fungi, such as *Neurospora crassa* (Cogoni and Macino, 1999), share the same highly conserved mechanisms for the post-transcriptional gene silencing (PTGS). This characteristic indicates an ancient and common origin (Matzke,

2001; Vance, 2001; Tuschi, 2001) used to protect the genome from the invasion of extraneous mobile genetic elements, such as viruses and transposons that produce, when active, aberrant RNA or dsRNA in the host cell (Vance, 2001).

The PTGS, indeed, is a regulatory process generally mediated by dsRNA. In this case, it is preferable to use the term RNA interference (RNAi). The dsRNA can be produced in different ways: 1) from the activity of the cellular RNA-dependent RNA polymerase (cRdRP), acting on aberrant RNA in the nucleus; 2) by replicating RNA viruses by means of a viral RNA-dependent RNA polymerase (vRdRP); 3) through the transcription of inverted DNA repeats as well as the integration of transposable elements (TEs) alongside promoters of endogenous genes. In all cases, this may lead to the formation of unexpected antisense transcripts that can partially correspond with the sense sequence and form a hairpin-shaped dsRNA. Sometimes the integration of a transgene can induce PTGS, especially if the sense and antisense transcripts are expressed simultaneously (Waterhouse *et al.*, 1998).

The basic processes that govern this complex defense system basically consist on a series of dsRNA degradation reactions by nuclear and cytoplasmic ribonucleases. The dsRNA is processed into small units of about 21-23 nucleotides long, which guide post-transcriptional degradation of the complementary mRNAs in the cytoplasm, causing the subsequent specific inhibition of translation (Matzke, 2001; Zamore, 2001; Van Houdt, 2003).

The first glance of the dsRNA processing, occurred with the biochemical experiments on the cytoplasmic extract of *Drosophila*

melanogaster (Tuschl *et al.*, 1999; Zamore *et al.*, 2000) in which it was possible to identify the specific sequence of the mediator of the PTGS, corresponding to a short sequences of RNAs. Small fragments of 21-23nt long were also identified subsequently in *Drosophila* embryos (Yang *et al.*, 2000), previously subjected to treatment with radiolabeled dsRNA. Molecules of RNA of similar size were also detected in plant tissue that exhibits PTGS (Hamilton, 1999). These results suggested that these fragments were the guide for the target recognition, a theory that was later supported by finding that the target mRNA was cleaved in 21-23-nt intervals (Zamore *et al.*, 2000).

The mechanism of the RNA interference begins with the progressive ATP-dependent cleavage of the long dsRNA into 21-23nt long double-stranded fragments, called small interfering RNA (siRNA) (Hamilton, 1999; Zamore *et al.*, 2000; Elbashir *et al.*, 2001a). It was found that short dsRNAs, less than about 40 bp, are ineffective mediators to activate the PTGS response in comparison with longer dsRNAs (Elbashir *et al.*, 2001a). Those siRNAs are produced by a member of the dsRNA-specific RNase type III endonuclease family, called Dicer. Duplexes of interfering RNA possess fundamental structural characteristics to initiate the RNAi process. They contain a phosphate at the 5' and a terminal hydroxyl at the 3', with the addition of two single-stranded nucleotides on the 3' end (Elbashir, 2001b). It has been demonstrated that siRNAs lacking a phosphate group at the 5' are inefficient triggers for both *in vitro* and *in vivo* RNAi (Elbashir *et al.*, 2001c; Boutla *et al.*, 2001).The length of siRNAs is species-specific and describes the differences in the structure of Dicer's counterparts (Hutvágner and Zamore, 2002). Nevertheless, Dicer contains the typical domains of RNase III ribonucleases such

as: 1) amino-terminal DEAD box RNA helicase domains; 2) a PAZ region, associated with the Argonaute2 protein (AGO2) for cytoplasmic transport; 3) two RNase III domains and 4) a carboxy-terminal region capable of binding dsRNA molecules.

Briefly, while the dsRNA domain maintains the double strand molecule joined to the enzyme, the helicase ATP-dependent domain is used to locally open the dsRNA and perform the enzymatic cutting with its RNAse domain (Ketting, 2001). Once in the cytoplasm, the duplexes of siRNA are incorporated into a protein complex generating an active RNA-induced silencing complex (RISC). The antisense molecule of siRNA guides the protein complex to the endonucleolytic cleavage of homologous mRNA.

Currently, RNAi is one of the most widely used tool for the creation of loss-of-function phenotypes in functional genetic studies. RNAi constructs, introduced in the cytoplasm of a particular cell, trigger efficient PTGS of the target sequence. Therefore, the generation of transgenic intron-hairpin RNA (ihp) type construct provides a powerful tool for functional genomics studies (Musta and Rakosy-Tican, 2014).

4. Genome Editing

Over the years, the induction of mutations has been a common technique applied to increase genetic variability in plant breeding. This can be done through physical mutagenesis techniques, such as ionizing radiation or through exposure to chemical agents such as ethyl methane sulfonate. However, these methodologies produce random mutations.

Targeted genome engineering, known as genome editing, has stand out as a new way to make precise and reliable targeted changes to the genome. Based mainly on the capacity to introduce DNA site-specific double strand breaks (DSBs), it represents an alternative to the classical mutagenesis method and to knockdown experiments performed with RNAi constructs.

4.1 Two distinct pathways to repair DNA double strand break

To deal with DNA damage, all living organisms have developed DSBs repair systems, based on two different mechanisms: the *non-homologous end joining* (NHEJ), called "non-homologous", because it induces the direct union of the break-ends without the need of a homologous template. The *homologous recombination* (HR) repair depends on the presence of homologous sequences to be used as a template (Deriano and Roth, 2013). In higher eukaryotes, the most commonly used path for DSB repair is the NHEJ.

It is important to understand how the repair pathway takes place in the somatic cells of the higher eukaryotes, especially in plant germline cells, that can transmit mutations to the offspring. In the NHEJ, there are two different pathways that can be activated, depending on the type of DNA damage and the presence or absence of homologous micro-sequences nearby the damage. In the classical NHEJ pathway (cNHEJ), the dimeric complex consisting of the Ku70 and Ku80 proteins plays a key role in the reorganization and repair of double strand break, in fact the Ku70/80 heterodimer, highly conserved among eukaryotes, forms a basket-shaped structure that runs along the DNA, acting as a molecular scaffold by recruiting

additional Ku proteins that fit from the free ends and restore the hydroxyl and phospholic groups, protecting the DNA from degradation. (Cary *et al.*, 1997; Walker *et al.*, 2001; Mari *et al.*, 2006). The DNA re-ligation is due to the combined action of the DNA LIGASE 4 (LIG4) with the associated proteins X-Ray Repair Cross-Complementing Protein 4 (XRCC4) (van Attikum *et al.*, 2003; Bennardo *et al.*, 2008). During this phase before the re-ligation, a minimum processing of the free-ends of the DNA can induce random small insertions or deletions (indel) nearby the DSB (Figure 9a). This makes the NHEJ an error-prone process. These indels can interrupt the Open Reading Frame (ORF) causing the knock-out of gene function.

In contrast, in the absence of the Ku-dependent core components, an alternative NHEJ pathway (aNHEJ) may occur (Mansour *et al.*, 2010). Generally, this process exploits the presence of microhomologies on the sides of the DSB to repair the damage. Therefore, it is also called Microhomology Mediated End Joining (MMEJ).

In this case, the X-Ray Repair Cross-Complementing Protein 1 (XRCC1) is activated. Even if this protein does not have any enzymatic activity, it acts as a scaffolding protein, interacting with multiple repair enzymes as PARP1, a POLY (ADP-RIBOSE) POLYMERASE 1 and the MRN complex which subunits initiate the reconstruction of the DNA molecule by spatial juxtaposition of the ends of the broken single-stranded DNA (Lamarche *et al.*, 2010; London, 2015). During this process, the 5'-end breaks are processed into single-stranded DNA by the MRN-complex and the microhomologies within the ssDNA-ends promote strand annealing.

Exonucleases remove the remaining flaps of ssDNAs and ligases combine the terminations with the help of the XRCC1 protein (Figure 9b) (Charbonnel *et al.*, 2010; Sfeir and Symington, 2015; Wang and Xu, 2017). This process may create deletions and for this reason is considered highly mutagenic.

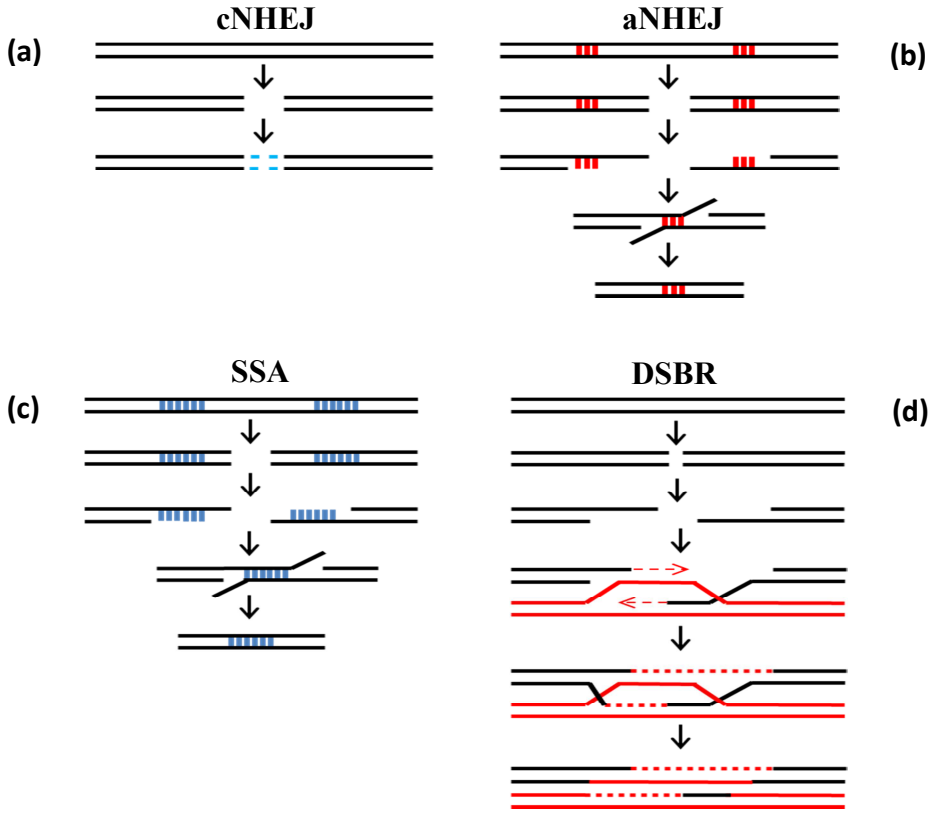

Figure 9| NHEJ and HR pathways in plant somatic cells. Models for double-strand break repair via Non Homologous End joining and Homologous Recombination.

Schematic description of classical Non-Homologous End Joining (cNHEJ) (a). The ends of the break are processed to remove any flaps, then are religated by ligase's action. (b) Representation of alternative Non-Homologous End Joining (aNHEJ). The ends are processed into single-stranded DNA and a short imperfect homology (10 bases average) is sufficient to promote strand annealing. (c) Single-Strand Annealing model (SSA) of Homologous Recombination. After processing the ends into ssDNA, the homologous regions revealed, serve to anneal the ends and promote the ligation. (d) Double-Strand Break Repair model (DSBR). After processing the ends into ssDNA, one single-stranded nucleofilament invades a homologous DNA duplex molecule to use as template to repair the DSB.

Numerous studies have also been performed for homologous recombination (HR), especially in the yeast *S. cerevisiae*, in which most of the proteins involved in this event have been identified (Orr-Weaver *et al.*, 1981; Krogh and Symington, 2004). Genetic studies have shown that there are two main pathways of HR: one completely independent of the presence of the Rad51 protein and another one directly dependent on it. They are generally classified, respectively, as non-conservative and conservative HR (Bleuyard *et al.*, 2006). Both start with the resection of the 5'DNA-ends by the MNR complex, forming long ssDNA 3' overhangs. Then the free-ends are coated by the REPLICATION PROTEIN A (RPA) to prevent DNA degradation and the appearance of secondary structures (Chen and Wold, 2014). If the single-strand sequences present large complementary regions (>30 nucleotides), Rad52 protein binds them promoting the annealing of the 3'overhangs, favoring what is called the Single-Strand Annealing pathway (SSA), (Figure 9c) (Bleuyard *et al.*, 2006).

Alternatively, Rad52 recruits Rad51 protein to form Rad51/ssDNA nucleofilament. This one can invade the homologous DNA double-strand molecule to use as template to repair the DSB by double-strand break repair (DSBR), (Figure 9d) (Sung and Robberson, 1995; Symington, 2002; Dudáš and Chovanec, 2004).

4.2 The CRISPR/Cas system

Recently, a new approach for gene editing has been developed based on the natural defense system that bacteria and archaea use against invading viruses and plasmids (Wiedenheft *et al.*, 2012). This prokaryotic adaptive immunity uses Cas protein, guided by RNA, as

an intercellular defense against foreign genetic material through a process distinct from RNAi.

In response to viral and plasmid infections, bacteria integrate short fragments of that foreign nucleic acid at the end of the sequence known as CRISPR (clustered regularly interspaced short palindromic repeat) in their own genome (Barrangou *et al.*, 2007). This sequence, characterized by repetitive loci, acts as a genetic database of the infections that occurred and behaves like an acquired immune system. The CRISPR loci are then transcribed and the long primary transcription is processed into short RNAs, called CRISPR-derived RNAs (crRNA), each containing a complementary sequence to a nucleic acid resulting from a previous infection. These transcripts can hybridize with an endogenous RNA, termed transactivating CRISPR RNA (tracrRNA), with which it forms a hairpin structure that can structurally join to the Cas endonuclease.

CRISPR sequences were first identified in the *Escherichia coli* genome at the University of Osaka, Japan (Ishino *et al.*, 1987). They found, in the region at the 3'-end of the *apoptosis inhibitor* (*iap*) gene, an unusual sequence of elements consisting of a series of repetitions of 29 nucleotides separated by spatial sequences of 32 nucleotides. In 1993, a group of Dutch researchers discovered the presence of clusters of DNA repeats which they called “direct repeats” (DR) in the genome of *Mycobacterium tuberculosis* (van Soolingen *et al.*, 1993). These different clusters characterized, in a highly specific way, different strains of *M. tuberculosis*. Thanks to this particularity, they elaborated the technique, still used today, called spoligotyping which allows to identify different strains of *M. tubercolosis* on the basis of different DRs. Later, in 2000, at the

University of Alicante (Spain), the presence of clusters of DNA repeats with unidentified functions were found in the archaebacterial *Haloferax* and *Haloarcula* (Mojica *et al.*, 2000). Few years later, Mojica and Rodriguez-Valera proposed to use the acronym CRISPR as a universal term to identify these sequences so far described by different acronyms in the scientific literature (Mojica and Rodriguez-Valera, 2016).

Another fundamental breakthrough came in 2002 from the University of Utrecht, Netherlands. Ruud Jansen observed a set of homologous genes that accompanied the clusters of DNA in prokaryotes, which he named the "CRISPR associated system", or the Cas genes (Jansen *et al.*, 2002). The nature of the transcripts of these genes suggested a hypothetical role in the three-dimensional organization of the CRISPR loci. In fact, the proteins contained helicase and nuclease domains. It was the Mojica group that in 2005 hypothesized for the first time a role of the CRISPR in the adaptive immunity in prokaryotes, following the discovery that some "spacers", present in the CRISPR sequences, were derived from extra-chromosomal DNA (Mojica *et al.*, 2005).

The real involvement of crRNA sequences in CRISPR mediated defense was first highlighted in a study on Cas6e endoribonuclease, CRISPR-specific, in *E. coli* (also known as Cse3 or CasE) (Brouns et al., 2008). This enzyme indeed, specifically binds the long pre-crRNA and cleaves each repeat sequence forming a library of crRNAs. Each fragment contains a unique spacer sequence flanked by fragments of the adjacent repeats. In 2012, an *in vitro* study on *Streptococcus pyogenes* about the CRISPR system, showed that crRNA fused with tracrRNA, were sufficient to activate the Cas transcript and

specifically cleave the DNA sequences corresponding to the crRNA (Jinek *et al.*, 2012). This led to the revolutionary possibility of a new approach for *in vivo* genetic editing.

The CRISPR/Cas system has revolutionized genome editing for its high specificity and efficiency. It is based on the direct recognition of highly specific sequences, coded by DNA and mediated by RNA. At the moment two different classes and six types of CRISPR/Cas systems have been identified (Makarova *et al.*, 2017a; Makarova *et al.*, 2017b). The types I, II and IV belong to the class one meanwhile types II, V and VI belong to the class two. Although type I and II are the most common in nature, type II is the one most used in molecular biology studies, with a unique Cas (Cas9) effector nuclease for both binding and cleavage the dsDNA. The Cas9 type II system from *S. pyogenes* indeed, is undoubtedly the most characterized, becoming the main genetic tool for genome editing in a broad range of organisms.

4.3 CRISPR/Cas Mechanism

The CRISPR/Cas system performs its genome editing function through two main steps: adaptation and defense (Marraffini and Sontheimer, 2010a; Makarova *et al.*, 2011). During adaptation CRISPR loci incorporate additional spacers to quickly adapt to new invaders. Although the molecular mechanism by which spacers are incorporated is not known, Cas1 and Cas2 are believed to play a role in this phase due to the apparent universality of these proteins. Some studies have highlighted that in type I and type II CRISPR/Cas systems, but not in type III, the selection of the proto-spacers

depends on the presence of a very short conserved regions of 2-3 bp flanking the protospacers, that have been named CRISPR motifs or proto-spacer-adjacent motifs (PAM) (Mojica *et al.*, 2009; Marraffini and Sontheimer, 2010b). These sequences provide a specific recognition signal for the selection of target sequences.

The defense phase is based on the expression and processing of the crRNAs, and the interference. The CRISPR locus is expressed producing a long primary pre-crRNA. In this phase, the complex associated with CRISPR for antiviral defense or the Cascade complex, processes the pre-crRNA by forming the crRNA fragment.

Finally, during interference, extra-chromosomal nucleic acid is cleaved. In type I systems, a complex of five Cas proteins, called Cascade (complex associated with CRISPR for antiviral defense), targets complementary invasion sequences. It is guided by the crRNA and the helicase Cas3 subunit, unique to the type I system, which cleaves the DNA (Brouns *et al.*, 2008). In type II systems, Cas9 directly targets DNA, thanks to the presence of the PAM signal sequence (Ran *et al.*, 2013). Unlike other systems, type III systems target either DNA, subtype III-A systems (Makarova and Koonin, 2015), or RNA, subtype III-B systems (Hale *et al.*, 2009; Spilman *et al.*, 2013). In systems of this type, the Cas6 enzyme appears to be responsible for the processing phase, although crRNA appears to join into a distinct Cas complex, called Csm in subtypes III-A and Cmr in subtypes III-B (Hale *et al.*, 2009).

5. Thesis scope

- Genetic analysis of *GIGANTEA* in *Solanaceae* using the *Petunia* model system through two distinct methodologies: creation of knock-down mutants using RNA interference technology and knock-out mutants using CRISPR/Cas9.
- Phenotypic and biochemical analysis of *Petunia*, in order to compare and analyze the mutant phenotype with the respective wild type phenotype.
- To deepen into the knowledge of *GIGANTEA* expression and gene regulation and its role in the control of the circadian rhythm in the *Solanaceae*.

REFERENCES

Almeida, M. de, Graner, É.M., Brondani, G.E., et al. (2015) Plant morphogenesis: theorical bases. , 11.

Amrad, A., Moser, M., Mandel, T., Vries, M. de, Schuurink, R.C., Freitas, L. and Kuhlemeier, C. (2016) Gain and Loss of Floral Scent Production through Changes in Structural Genes during Pollinator-Mediated Speciation. *Curr. Biol.*, **26**, 3303–3312.

Ando, T., NOMURA, M., TSUKAHARA, J., WATANABE, H., KOKUBUN, H., TSUKAMOTO, T., HASHIMOTO, G., MARCHESI, E. and KITCHING, I.J. (2001) Reproductive Isolation in a Native Population of Petunia sensu Jussieu (Solanaceae). *Ann. Bot.*, **88**, 403–413.

Atamian, H.S., Creux, N.M., Brown, E.A., Garner, A.G., Blackman, B.K. and Harmer, S.L. (2016) Circadian regulation of sunflower heliotropism, floral orientation, and pollinator visits. *Science*, **353**, 587–590.

Attikum, H. van, Bundock, P., Overmeer, R.M., Lee, L.-Y., Gelvin, S.B. and Hooykaas, P.J.J. (2003) The Arabidopsis AtLIG4 gene is required for the repair of DNA damage, but not for the integration of Agrobacterium T-DNA. *Nucleic Acids Res.*, **31**, 4247–4255.

Baker, S.S., Wilhelm, K.S. and Thomashow, M.F. (1994) The 5'-region of Arabidopsis thaliana corl5a has cis-acting elements that confer cold-, drought- and ABA-regulated gene expression. , 13.

Bancos, S., Szatmári, A.-M., Castle, J., Kozma-Bognár, L., Shibata, K., Yokota, T., Bishop, G.J., Nagy, F. and Szekeres, M. (2006) Diurnal Regulation of the Brassinosteroid-Biosynthetic *CPD* Gene in Arabidopsis. *Plant Physiol.*, **141**, 299–309.

Barrangou, R., Fremaux, C., Deveau, H., Richards, M., Boyaval, P., Moineau, S., Romero, D.A. and Horvath, P. (2007) CRISPR Provides Acquired Resistance Against Viruses in Prokaryotes. *Science*, **315**, 1709–1712.

Benlloch, R., Berbel, A., Serrano-Mislata, A. and Madueno, F. (2007) Floral Initiation and Inflorescence Architecture: A Comparative View. *Ann. Bot.*, **100**, 659–676.

Bennardo, N., Cheng, A., Huang, N. and Stark, J.M. (2008) Alternative-NHEJ Is a Mechanistically Distinct Pathway of Mammalian Chromosome Break Repair J. E. Haber, ed. *PLoS Genet.*, **4**, e1000110.

Blatch, G.L. and Lassle, M. (1999) The tetratricopeptide repeat: a structural motif mediating protein-protein interactions. , 8.

Blázquez, M.A., Ahn, J.H. and Weigel, D. (2003) A thermosensory pathway controlling flowering time in Arabidopsis thaliana. *Nat. Genet.*, **33**, 168–171.

Blázquez, M.A., Ferrándiz, C., Madueño, F. and Parcy, F. (2006) How Floral Meristems are Built. *Plant Mol. Biol.*, **60**, 855–870.

Blázquez, M.A., Green, R., Nilsson, O., Sussman, M.R. and Weigel, D. (1998) Gibberellins Promote Flowering of Arabidopsis by Activating the LEAFY Promoter. , 11.

Bleuyard, J.-Y., Gallego, M.E. and White, C.I. (2006) Recent advances in understanding of the DNA double-strand break repair machinery of plants. *DNA Repair*, **5**, 1–12.

Bombarely, A., Moser, M., Amrad, A., et al. (2016) Insight into the evolution of the Solanaceae from the parental genomes of Petunia hybrida. *Nat. Plants*, **2**, 16074.

Boutla, A., Delidakis, C., Livadaras, I., Tsagris, M. and Tabler, M. (2001) Short 5′-phosphorylated double-stranded RNAs induce RNA interference in Drosophila. *Curr. Biol.*, **11**, 1776–1780.

Bowman, J.L. (1997) Evolutionary conservation of angiosperm flower development at the molecular and genetic levels. *J. Biosci.*, **22**, 515–527.

Brouns, S.J.J., Jore, M.M., Lundgren, M., et al. (2008) Small CRISPR RNAs Guide Antiviral Defense in Prokaryotes. *Science*, **321**, 960–964.

Cao, S., Ye, M. and Jiang, S. (2005) Involvement of GIGANTEA gene in the regulation of the cold stress response in Arabidopsis. *Plant Cell Rep.*, **24**, 683–690.

Cary, R.B., Peterson, S.R., Wang, J., Bear, D.G., Bradbury, E.M. and Chen, D.J. (1997) DNA looping by Ku and the DNA-dependent protein kinase. *Proc. Natl. Acad. Sci.*, **94**, 4267–4272.

Casal, J.J. (2007) Phytochromes, Cryptochromes, Phototropin: Photoreceptor Interactions in Plants. *Photochem. Photobiol.*, **71**, 1–11.

Casal, J.J., Luccioni, L.G., Oliverio, K.A. and Boccalandro, H.E. (2003) Light, phytochrome signalling and photomorphogenesis in ArabidopsisDedicated to Professor Silvia Braslavsky, to mark her great contribution to photochemistry and photobiology particularly in the field of photothermal methods. *Photochem. Photobiol. Sci.*, **2**, 625.

Charbonnel, C., Gallego, M.E. and White, C.I. (2010) Xrcc1-dependent and Ku-dependent DNA double-strand break repair kinetics in Arabidopsis plants: Double-strand break repair kinetics in Arabidopsis. *Plant J.*, **64**, 280–290.

Chen, R. and Wold, M.S. (2014) Replication protein A: Single-stranded DNA's first responder: Dynamic DNA-interactions allow replication protein A to direct single-strand DNA intermediates into different pathways for synthesis or repair. *BioEssays*, **36**, 1156–1161.

Cna'Ani, A., Mühlemann, J.K., Ravid, J., Masci, T., Klempien, A., Nguyen, T.T.H., Dudareva, N., Pichersky, E. and Vainstein, A. (2015) Petunia × hybrida floral scent production is negatively affected by high-temperature growth conditions: Ambient temperature and floral scent. *Plant Cell Environ.*, **38**, 1333–1346.

Coen, E.S. and Meyerowitz, E.M. (1991) The war of the whorls: genetic interactions controlling flower development. *Nature*, **353**, 31–37.

Cogoni, C. and Macino, G. (1999) Gene silencing in Neurospora crassa requires a protein homologous to RNA-dependent RNA polymerase. *Nature*, **399**, 166–169.

Colquhoun, T.A., Verdonk, J.C., Schimmel, B.C.J., Tieman, D.M., Underwood, B.A. and Clark, D.G. (2010) Petunia floral volatile benzenoid/phenylpropanoid genes are regulated in a similar manner. *Phytochemistry*, **71**, 158–167.

Dell'Olivo, A., Hoballah, M.E., Gübitz, T. and Kuhlemeier, C. (2011) ISOLATION BARRIERS BETWEEN PETUNIA AXILLARIS AND PETUNIA INTEGRIFOLIA (SOLANACEAE): ISOLATION BARRIERS BETWEEN PETUNIA AXILLARIS AND PETUNIA INTEGRIFOLIA. *Evolution*, **65**, 1979–1991.

Deng, X.W. and Quail, P.H. (1999) Signalling in light-controlled development. *Semin. Cell Dev. Biol.*, **10**, 121–129.

Deriano, L. and Roth, D.B. (2013) Modernizing the Nonhomologous End-Joining Repertoire: Alternative and Classical NHEJ Share the Stage. *Annu. Rev. Genet.*, **47**, 433–455.

Dexter, R., Qualley, A., Kish, C.M., Ma, C.J., Koeduka, T., Nagegowda, D.A., Dudareva, N., Pichersky, E. and Clark, D. (2007) Characterization of a petunia acetyltransferase involved in the

biosynthesis of the floral volatile isoeugenol: PhCFAT and Isoeugenol Biosynthesis. *Plant J.*, **49**, 265–275.

Dudareva, N., Klempien, A., Muhlemann, J.K. and Kaplan, I. (2013) Biosynthesis, function and metabolic engineering of plant volatile organic compounds. *New Phytol.*, **198**, 16–32.

Dudareva, N., Negre, F., Nagegowda, D.A. and Orlova, I. (2006) Plant Volatiles: Recent Advances and Future Perspectives. *Crit. Rev. Plant Sci.*, **25**, 417–440.

Dudáš, A. and Chovanec, M. (2004) DNA double-strand break repair by homologous recombination. *Mutat. Res. Mutat. Res.*, **566**, 131–167.

Edwards, K.D., Takata, N., Johansson, M., et al. (2018) Circadian clock components control daily growth activities by modulating cytokinin levels and cell division-associated gene expression in *Populus* trees: Control of growth in Populus. *Plant Cell Environ.*, **41**, 1468–1482.

Elbashir, Sayda M., Harborth, J., Lendeckel, W., Yalcin, A., Weber, K. and Tuschl, T. (2001) Duplexes of 21-nucleotide RNAs mediate RNA interference in cultured mammalian cells. *Nature*, **411**, 494–498.

Elbashir, Sayda M, Martinez, J., Patkaniowska, A., Lendeckel, W. and Tuschl, T. (2001) Functional anatomy of siRNAs for mediating ef®cient RNAi in Drosophila melanogaster embryo lysate. , 12.

Elbashir, S. M., W.Lendeckel and T. Tuschl (2001) RNA interference is mediated by 21- and 22-nucleotide RNAs. *Genes Dev.*, **15**, 188–200.

Endress, P.K. (2006) Angiosperm Floral Evolution: Morphological Developmental Framework. In *Advances in Botanical Research*. Elsevier, pp. 1–61. Available at: https://linkinghub.elsevier.com/retrieve/pii/S0065229606440015 [Accessed September 12, 2019].

Farré, E.M. and Weise, S.E. (2012) The interactions between the circadian clock and primary metabolism. *Curr. Opin. Plant Biol.*, **15**, 293–300.

Fenske, M.P., Hewett Hazelton, K.D., Hempton, A.K., Shim, J.S., Yamamoto, B.M., Riffell, J.A. and Imaizumi, T. (2015) Circadian clock gene *LATE ELONGATED HYPOCOTYL* directly regulates the timing of floral scent emission in *Petunia*. *Proc. Natl. Acad. Sci.*, **112**, 9775–9780.

Fire, A., Xu, S., Montgomery, M.K., Kostas, S.A., Driver, S.E. and Mello, C.C. (1998) Potent and specific genetic interference by double-stranded RNA in. , **391**, 6.

Fowler, S., Lee, K., Onouchi, H., Samach, A., Richardson, K., Morris, B., Coupland, G. and Putterill, J. (1999) GIGANTEA: a circadian clock-controlled gene that regulates photoperiodic flowering in Arabidopsis and encodes a protein with several possible membrane-spanning domains. *EMBO J.*, **18**, 4679–4688.

Fowler, S. and Thomashow, M.F. (2002) Arabidopsis Transcriptome Profiling Indicates That Multiple Regulatory Pathways Are Activated during Cold Acclimation in Addition to the CBF Cold Response Pathway. *Plant Cell*, **14**, 1675–1690.

Franceschi, V.R., Krokene, P., Christiansen, E. and Krekling, T. (2005) Anatomical and chemical defenses of conifer bark against bark beetles and other pests: Tansley review. *New Phytol.*, **167**, 353–376.

Fung-Uceda, J., Lee, K., Seo, P.J., Polyn, S., Veylder, L. De and Mas, P. (2018) The Circadian Clock Sets the Time of DNA Replication Licensing to Regulate Growth in Arabidopsis. *Dev. Cell*, **45**, 101-113.e4.

Gerats, T. and Vandenbussche, M. (2005) A model system for comparative research: Petunia. *Trends Plant Sci.*, **10**, 251–256.

Gibson, S., Arondel, V., Iba, K. and Somerville, C. (1994) Cloning of a Temperature-Regulated Gene Encoding a Chloroplast 0-3 Desaturase from Arabidopsis thaliana'. , **106**, 7.

Gould, P.D., Locke, J.C.W., Larue, C., et al. (2006) The Molecular Basis of Temperature Compensation in the *Arabidopsis* Circadian Clock. *Plant Cell*, **18**, 1177–1187.

Gübitz, T., Hoballah, M.E., Dell'Olivo, A. and Kuhlemeier, C. (2009) Petunia as a Model System for the Genetics and Evolution of Pollination Syndromes. In T. Gerats and J. Strommer, eds. *Petunia*. New York, NY: Springer New York, pp. 29–49. Available at: http://link.springer.com/10.1007/978-0-387-84796-2_2 [Accessed July 26, 2019].

Guy, C.L. (1990) Cold Acclimation and Freezing Stress Tolerance: Role of Protein Metabolism. *Annu. Rev. Plant Physiol. Plant Mol. Biol.*, **41**, 187–223.

Guy, C.L., Niemi, K.J. and Brambl, R. (1985) Altered gene expression during cold acclimation of spinach. *Proc. Natl. Acad. Sci.*, **82**, 3673–3677.

Hale, C.R., Zhao, P., Olson, S., Duff, M.O., Graveley, B.R., Wells, L., Terns, R.M. and Terns, M.P. (2009) RNA-Guided RNA Cleavage by a CRISPR RNA-Cas Protein Complex. *Cell*, **139**, 945–956.

Hamilton, A.J. (1999) A Species of Small Antisense RNA in Posttranscriptional Gene Silencing in Plants. *Science*, **286**, 950–952.

Herrmann, K. and Entus, R. (2001) Shikimate Pathway: Aromatic Amino Acids and Beyond. In John Wiley & Sons, Ltd, ed. *eLS*. Chichester: John Wiley & Sons, Ltd, p. a0001315. Available at: http://doi.wiley.com/10.1038/npg.els.0001315 [Accessed March 15, 2020].

Hoballah, M.E., Stuurman, J., Turlings, T.C.J., Guerin, P.M., Connétable, S. and Kuhlemeier, C. (2005) The composition and timing of flower odour emission by wild Petunia axillaris coincide with the antennal perception and nocturnal activity of the pollinator Manduca sexta. *Planta*, **222**, 141–150.

Hsu, P.Y. and Harmer, S.L. (2014) Wheels within wheels: the plant circadian system. *Trends Plant Sci.*, **19**, 240–249.

Huang, S.-Q. and Shi, X.-Q. (2013) Floral isolation in *Pedicularis* : how do congeners with shared pollinators minimize reproductive interference? *New Phytol.*, **199**, 858–865.

Huq, E., Tepperman, J.M. and Quail, P.H. (2000) GIGANTEA is a nuclear protein involved in phytochrome signaling in Arabidopsis. *Proc. Natl. Acad. Sci.*, **97**, 9789–9794.

Hutvágner, G. and Zamore, P.D. (2002) RNAi: nature abhors a double-strand. *Curr. Opin. Genet. Dev.*, **12**, 225–232.

Imaizumi, T. and Kay, S. (2006) Photoperiodic control of flowering: not only by coincidence. *Trends Plant Sci.*, **11**, 550–558.

Imaizumi, T., Tran, H.G., Swartz, T.E., Briggs, W.R. and Kay, S.A. (2003) FKF1 is essential for photoperiodic-specific light signalling in Arabidopsis. *Nature*, **426**, 302–306.

Immink, R.G., Hannapel, D.J., Ferrario, S., Busscher, M., Franken, J., Lookeren Campagne, M.M. and Angenent, G.C. (1999) A petunia MADS box gene involved in the transition from vegetative to reproductive development. *Dev. Camb. Engl.*, **126**, 5117–5126.

Ishino, Y., Shinagawa, H., Makino, K., Amemura, M. and Nakata, A. (1987) Nucleotide sequence of the iap gene, responsible for alkaline phosphatase isozyme conversion in Escherichia coli, and identification of the gene product. *J. Bacteriol.*, **169**, 5429–5433.

Izawa, T., Mihara, M., Suzuki, Y., et al. (2011) Os- *GIGANTEA* Confers Robust Diurnal Rhythms on the Global Transcriptome of Rice in the Field. *Plant Cell*, **23**, 1741–1755.

Jacobsen, S.E. and Olszewski', N.E. (1993) Mutations at the SPINDLY Locus of Arabidopsis Alter Gibberellin Signal Transduction. , 11.

Jansen, Ruud., Embden, Jan.D.A. van, Gaastra, Wim. and Schouls, Leo.M. (2002) Identification of genes that are associated with DNA repeats in prokaryotes. *Mol. Microbiol.*, **43**, 1565–1575.

Jarvis, A.P., Schaaf, O. and Oldham, N.J. (2000) 3-Hydroxy-3-phenylpropanoic acid is an intermediate in the biosynthesis of benzoic acid and salicylic acid but benzaldehyde is not. *Planta*, **212**, 119–126.

Jinek, M., Chylinski, K., Fonfara, I., Hauer, M., Doudna, J.A. and Charpentier, E. (2012) A Programmable Dual-RNA-Guided DNA Endonuclease in Adaptive Bacterial Immunity. *Science*, **337**, 816–821.

Jung, J.-H., Seo, Y.-H., Seo, P.J., Reyes, J.L., Yun, J., Chua, N.-H. and Park, C.-M. (2007) The GIGANTEA Regulated MicroRNA172 Mediates Photoperiodic Flowering Independent of *CONSTANS* in *Arabidopsis*. *Plant Cell*, **19**, 2736–2748.

Kaminaga, Y., Schnepp, J., Peel, G., et al. (2006) Plant Phenylacetaldehyde Synthase Is a Bifunctional Homotetrameric Enzyme That Catalyzes Phenylalanine Decarboxylation and Oxidation. *J. Biol. Chem.*, **281**, 23357–23366.

Ketting, R.F. (2001) Dicer functions in RNA interference and in synthesis of small RNA involved in developmental timing in C. elegans. *Genes Dev.*, **15**, 2654–2659.

Kim, W.-Y., Fujiwara, S., Suh, S.-S., et al. (2007) ZEITLUPE is a circadian photoreceptor stabilized by GIGANTEA in blue light. *Nature*, **449**, 356–360.

Kim, Y., Lim, J., Yeom, M., Kim, H., Kim, J., Wang, L., Kim, W.Y., Somers, D.E. and Nam, H.G. (2013) ELF4 Regulates GIGANTEA Chromatin Access through Subnuclear Sequestration. *Cell Rep.*, **3**, 671–677.

Kim, Y., Yeom, M., Kim, H., Lim, J., Koo, H.J., Hwang, D., Somers, D. and Nam, H.G. (2012) GIGANTEA and EARLY FLOWERING 4 in Arabidopsis Exhibit Differential Phase-Specific Genetic Influences over a Diurnal Cycle. *Mol. Plant*, **5**, 678–687.

Klahre, U., Gurba, A., Hermann, K., Saxenhofer, M., Bossolini, E., Guerin, P.M. and Kuhlemeier, C. (2011) Pollinator Choice in Petunia Depends on Two Major Genetic Loci for Floral Scent Production. *Curr. Biol.*, **21**, 730–739.

Knudsen, J.T., Tollsten, L. and Bergström, L.G. (1993) Floral scents—a checklist of volatile compounds isolated by head-space techniques. *Phytochemistry*, **33**, 253–280.

Koes, R., Bliek, M., Castel, R., Kusters, E., Procissi, A., Rebocho, A. and Roobeek, I. (2009) Development of the Petunia Inflorescence. In T. Gerats and J. Strommer, eds. *Petunia*. New

York, NY: Springer New York, pp. 179–197. Available at: http://link.springer.com/10.1007/978-0-387-84796-2_9 [Accessed June 7, 2019].

Kolosova, N., Gorenstein, N., Kish, C.M. and Dudareva, N. (2001) Regulation of Circadian Methyl Benzoate Emission in Diurnally and Nocturnally Emitting Plants. , 16.

Krizek, B.A. and Fletcher, J.C. (2005) Molecular mechanisms of flower development: an armchair guide. *Nat. Rev. Genet.*, **6**, 688–698.

Krogh, B.O. and Symington, L.S. (2004) Recombination Proteins in Yeast. *Annu. Rev. Genet.*, **38**, 233–271.

Kulcheski, F.R., Muschner, V.C., Lorenz-Lemke, A.P., Stehmann, J.R., Bonatto, S.L., Salzano, F.M. and Freitas, L.B. (2006) Molecular phylogenetic analysis of Petunia Juss. (Solanaceae). *Genetica*, **126**, 3–14.

Lamarche, B.J., Orazio, N.I. and Weitzman, M.D. (2010) The MRN complex in double-strand break repair and telomere maintenance. *FEBS Lett.*, **584**, 3682–3695.

Lewinsohn, E. (1998) Histochemical Localization of Citral Accumulation in Lemongrass Leaves (Cymbopogon citratus(DC.) Stapf., Poaceae). *Ann. Bot.*, **81**, 35–39.

Lin, C. (2000) Plant blue-light receptors. *Trends Plant Sci.*, 6.

Liu, Q., Kasuga, M., Sakuma, Y., Abe, H., Miura, S., Yamaguchi-Shinozaki, K. and Shinozaki, K. (1998) Two Transcription Factors, DREB1 and DREB2, with an EREBP/AP2 DNA Binding Domain Separate Two Cellular Signal Transduction Pathways in Drought- and Low-Temperature-Responsive Gene Expression, Respectively, in Arabidopsis. , 17.

London, R.E. (2015) The structural basis of XRCC1-mediated DNA repair. *DNA Repair*, **30**, 90–103.

Maeda, H. and Dudareva, N. (2012) The Shikimate Pathway and Aromatic Amino Acid Biosynthesis in Plants. *Annu. Rev. Plant Biol.*, **63**, 73–105.

Makarova, K.S., Haft, D.H., Barrangou, R., et al. (2011) Evolution and classification of the CRISPR–Cas systems. *Nat. Rev. Microbiol.*, **9**, 467–477.

Makarova, K.S. and Koonin, E.V. (2015) Annotation and Classification of CRISPR-Cas Systems. In M. Lundgren, E. Charpentier, and P. C. Fineran, eds. *CRISPR*. Methods in Molecular Biology. New York, NY: Springer New York, pp. 47–75. Available at: http://link.springer.com/10.1007/978-1-4939-2687-9_4 [Accessed February 26, 2020].

Makarova, K.S., Zhang, F. and Koonin, E.V. (2017a) SnapShot: Class 1 CRISPR-Cas Systems. *Cell*, **168**, 946-946.e1.

Makarova, K.S., Zhang, F. and Koonin, E.V. (2017b) SnapShot: Class 2 CRISPR-Cas Systems. *Cell*, **168**, 328-328.e1.

Mansour, W.Y., Rhein, T. and Dahm-Daphi, J. (2010) The alternative end-joining pathway for repair of DNA double-strand breaks requires PARP1 but is not dependent upon microhomologies. *Nucleic Acids Res.*, **38**, 6065–6077.

Marcolino-Gomes, J., Rodrigues, F.A., Fuganti-Pagliarini, R., et al. (2014) Diurnal Oscillations of Soybean Circadian Clock and Drought Responsive Genes N. Cermakian, ed. *PLoS ONE*, **9**, e86402.

Mari, P.-O., Florea, B.I., Persengiev, S.P., et al. (2006) Dynamic assembly of end-joining complexes requires interaction between Ku70/80 and XRCC4. *Proc. Natl. Acad. Sci.*, **103**, 18597–18602.

Marraffini, L.A. and Sontheimer, E.J. (2010a) CRISPR interference: RNA-directed adaptive immunity in bacteria and archaea. *Nat. Rev. Genet.*, **11**, 181–190.

Marraffini, L.A. and Sontheimer, E.J. (2010b) Self versus non-self discrimination during CRISPR RNA-directed immunity. *Nature*, **463**, 568–571.

Martin-Tryon, E.L., Kreps, J.A. and Harmer, S.L. (2007) GIGANTEA Acts in Blue Light Signaling and Has Biochemically Separable Roles in Circadian Clock and Flowering Time Regulation. *Plant Physiol.*, **143**, 473–486.

Matzke, M. (2001) RNA: Guiding Gene Silencing. *Science*, **293**, 1080–1083.

McManus, M.T. and Sharp, P.A. (2002) Gene silencing in mammals by small interfering RNAs. *Nat. Rev. Genet.*, **3**, 737–747.

Miquel, M., James, D., Dooner, H. and Browse, J. (1993) Arabidopsis requires polyunsaturated lipids for low-temperature survival. *Proc. Natl. Acad. Sci.*, **90**, 6208–6212.

Mishra, P. and Panigrahi, K.C. (2015) GIGANTEA an emerging story. *Front. Plant Sci.*, **6**. Available at: http://journal.frontiersin.org/article/10.3389/fpls.2015.00008/abstract [Accessed October 9, 2019].

Mizoguchi, T., Wright, L., Fujiwara, S., et al. (2005) Distinct Roles of *GIGANTEA* in Promoting Flowering and Regulating Circadian Rhythms in Arabidopsis. *Plant Cell*, **17**, 2255–2270.

Mojica, F.J.M., Díez-Villaseñor, C., García-Martínez, J. and Almendros, C. (2009) Short motif sequences determine the targets of the prokaryotic CRISPR defence system. *Microbiology*, **155**, 733–740.

Mojica, F.J.M., Díez-Villaseñor, C., García-Martínez, J. and Soria, E. (2005) Intervening Sequences of Regularly Spaced Prokaryotic Repeats Derive from Foreign Genetic Elements. *J. Mol. Evol.*, **60**, 174–182.

Mojica, F.J.M., Diez-Villasenor, C., Soria, E. and Juez, G. (2000) Biological significance of a family of regularly spaced repeats in the genomes of Archaea, Bacteria and mitochondria. *Mol. Microbiol.*, **36**, 244–246.

Mojica, F.J.M. and Rodriguez-Valera, F. (2016) The discovery of CRISPR in archaea and bacteria. *FEBS J.*, **283**, 3162–3169.

Mouradov, A., Cremer, F. and Coupland, G. (2002) Control of Flowering Time: Interacting Pathways as a Basis for Diversity. *Plant Cell*, **14**, S111–S130.

Muhlemann, J.K., Woodworth, B.D., Morgan, J.A. and Dudareva, N. (2014) The monolignol pathway contributes to the biosynthesis of volatile phenylpropenes in flowers. *New Phytol.*, **204**, 661–670.

Musta, R.-A. and Rakosy-Tican, E. (2014) RNAi AS A TOOL TO OBTAIN POTATO RESISTANT TO VIRUSES. , 8.

Negre, F., Kish, C.M., Boatright, J., Underwood, B., Shibuya, K., Wagner, C., Clark, D.G. and Dudareva, N. (2003) Regulation of Methylbenzoate Emission after Pollination in Snapdragon and Petunia Flowers. *Plant Cell*, **15**, 2992–3006.

Ni, Z., Kim, E.-D., Ha, M., Lackey, E., Liu, J., Zhang, Y., Sun, Q. and Chen, Z.J. (2009) Altered circadian rhythms regulate growth vigour in hybrids and allopolyploids. *Nature*, **457**, 327–331.

Nozue, K., Covington, M.F., Duek, P.D., Lorrain, S., Fankhauser, C., Harmer, S.L. and Maloof, J.N. (2007) Rhythmic growth explained by coincidence between internal and external cues. *Nature*, **448**, 358–361.

Oliverio, K.A., Crepy, M., Martin-Tryon, E.L., Milich, R., Harmer, S.L., Putterill, J., Yanovsky, M.J. and Casal, J.J. (2007) GIGANTEA Regulates Phytochrome A-Mediated Photomorphogenesis Independently of Its Role in the Circadian Clock. *Plant Physiol.*, **144**, 495–502.

Orlova, I., Marshall-Colón, A., Schnepp, J., et al. (2006) Reduction of Benzenoid Synthesis in Petunia Flowers Reveals Multiple Pathways to Benzoic Acid and Enhancement in Auxin Transport. *Plant Cell*, **18**, 3458–3475.

Orr-Weaver, T.L., Szostak, J.W. and Rothstein, R.J. (1981) Yeast transformation: a model system for the study of recombination. *Proc. Natl. Acad. Sci.*, **78**, 6354–6358.

Park, D.H., Somer David E., Kim Yang Suk, Choy Yoon Hi, Lim Hee Kyun, Soh Moon Soo, Kim Hyo Jung, Kay Steve A. and Nam Hong Gil (1999) Control of Circadian Rhythms and Photoperiodic Flowering by the Arabidopsis GIGANTEA Gene. *Science*, **285**, 1579–1582.

Paula, S. rez-LoÂpez, Wheatley, K., Robson, F., Onouchi, H., Valverde, F. and Coupland, G. (2001) CONSTANS mediates between the circadian clock and the control of ¯owering in Arabidopsis. , **410**, 5.

Pichersky, E. and Gershenzon, J. (2002) The formation and function of plant volatiles: perfumes for pollinator attraction and defense. *Curr. Opin. Plant Biol.*, **5**, 237–243.

Pichersky, E., Noel, J.P. and Dudareva, N. (2006) Biosynthesis of Plant Volatiles: Nature's Diversity and Ingenuity. *Science*, **311**, 808–811.

Pokhilko, A., Fernández, A.P., Edwards, K.D., Southern, M.M., Halliday, K.J. and Millar, A.J. (2012) The clock gene circuit in Arabidopsis includes a repressilator with additional feedback loops. *Mol. Syst. Biol.*, **8**. Available at: http://msb.embopress.org/cgi/doi/10.1038/msb.2012.6 [Accessed June 7, 2019].

Quail, P.H., Boylan, M.T., Parks, B.M., Short, T.W., Xu, Y. and Wagner, D. (1995) Phytochromes: Photosensory Perception and Signal Transduction. , **268**, 6.

Quattrocchio, F., Wing, J. and Koes, R. (1999) Molecular Analysis of the anthocyanin2 Gene of Petunia and Its Role in the Evolution of Flower Color. , 12.

Ran, F.A., Hsu, P.D., Wright, J., Agarwala, V., Scott, D.A. and Zhang, F. (2013) Genome engineering using the CRISPR-Cas9 system. *Nat. Protoc.*, **8**, 2281–2308.

Rebocho, A.B., Bliek, M., Kusters, E., Castel, R., Procissi, A., Roobeek, I., Souer, E. and Koes, R. (2008) Role of EVERGREEN in the Development of the Cymose Petunia Inflorescence. *Dev. Cell*, **15**, 437–447.

Redei, G.P. (1962) SUPERVITAL MUTANTS OF ARABIDOPSISl. , 18.

Reed, J.W., Nagpal, P. and Poo, D.S. (1993) Mutations in the Gene for the Red/Far-Red Light Receptor Phytochrome B Alter Cell Elongation and Physiological Responses throughout Arabidopsis Development. , 12.

Rijpkema, A.S., Vandenbussche, M., Koes, R., Heijmans, K. and Gerats, T. (2010) Variations on a theme: Changes in the floral ABCs in angiosperms. *Semin. Cell Dev. Biol.*, **21**, 100–107.

Ristic, Z. and Ashworth, E.N. (1993) Changes in leaf ultrastructure and carbohydrates inArabidopsis thaliana L. (Heyn) cv. Columbia during rapid cold acclimation. *Protoplasma*, **172**, 111–123.

Samach, A., Klenz, J.E., Kohalmi, S.E., Risseeuw, E., Haughn, G.W. and Crosby, W.L. (1999) The UNUSUAL FLORAL ORGANS gene of Arabidopsis thaliana is an F-box protein required for normal patterning and growth in the floral meristem. *Plant J.*, **20**, 433–445.

Sawa, M. and Kay, S.A. (2011) GIGANTEA directly activates Flowering Locus T in Arabidopsis thaliana. *Proc. Natl. Acad. Sci.*, **108**, 11698–11703.

Sawa, M., Nusinow, D.A., Kay, S.A. and Imaizumi, T. (2007) FKF1 and GIGANTEA Complex Formation Is Required for Day-Length Measurement in Arabidopsis. *Science*, **318**, 261–265.

Scala, A., Allmann, S., Mirabella, R., Haring, M. and Schuurink, R. (2013) Green Leaf Volatiles: A Plant's Multifunctional Weapon against Herbivores and Pathogens. *Int. J. Mol. Sci.*, **14**, 17781–17811.

Scherr, M. and Eder, M. (2007) Gene Silencing by Small Regulatory RNAs in Mammalian Cells. *Cell Cycle*, **6**, 444–449.

Schie, C.C. van, Haring, M.A. and Schuurink, R.C. (2006) Regulation of terpenoid and benzenoid production in flowers. *Curr. Opin. Plant Biol.*, **9**, 203–208.

Schnee, C., Kollner, T.G., Held, M., Turlings, T.C.J., Gershenzon, J. and Degenhardt, J. (2006) The products of a single maize sesquiterpene synthase form a volatile defense signal that attracts natural enemies of maize herbivores. *Proc. Natl. Acad. Sci.*, **103**, 1129–1134.

Schuurink, R.C., Haring, M.A. and Clark, D.G. (2006) Regulation of volatile benzenoid biosynthesis in petunia flowers. *Trends Plant Sci.*, **11**, 20–25.

Segatto, A.L.A., Ramos-Fregonezi, A.M.C., Bonatto, S.L. and Freitas, L.B. (2014) Molecular insights into the purple-flowered ancestor of garden petunias. *Am. J. Bot.*, **101**, 119–127.

Sfeir, A. and Symington, L.S. (2015) Microhomology-Mediated End Joining: A Back-up Survival Mechanism or Dedicated Pathway? *Trends Biochem. Sci.*, **40**, 701–714.

Simpson, G.G. (2002) Arabidopsis, the Rosetta Stone of Flowering Time? *Science*, **296**, 285–289.

Song, Y.H., Kubota, A., Kwon, M.S., et al. (2018) Molecular basis of flowering under natural long-day conditions in Arabidopsis. *Nat. Plants*, **4**, 824–835.

Soolingen, D. van, Haas, P.E. de, Hermans, P.W., Groenen, P.M. and Embden, J.D. van (1993) Comparison of various repetitive DNA elements as genetic markers for strain differentiation and epidemiology of Mycobacterium tuberculosis. *J. Clin. Microbiol.*, **31**, 1987–1995.

Souer, E., Krol, A. van der, Kloos, D., Spelt, C., Bliek, M., Mol, J. and Koes, R. (1998) Genetic control of branching pattern and floral identity during Petunia inflorescence development. *Development*, **125**, 733–742.

Souer, E., Rebocho, A.B., Bliek, M., Kusters, E., Bruin, R.A.M. de and Koes, R. (2008) Patterning of Inflorescences and Flowers by the F-Box Protein DOUBLE TOP and the LEAFY Homolog ABERRANT LEAF AND FLOWER of Petunia. *Plant Cell*, **20**, 2033–2048.

Soy, J., Leivar, P., González-Schain, N., Martín, G., Diaz, C., Sentandreu, M., Al-Sady, B., Quail, P.H. and Monte, E. (2016) Molecular convergence of clock and photosensory pathways through PIF3–TOC1 interaction and co-occupancy of target promoters. *Proc. Natl. Acad. Sci.*, 201603745.

Spilman, M., Cocozaki, A., Hale, C., Shao, Y., Ramia, N., Terns, R., Terns, M., Li, H. and Stagg, S. (2013) Structure of an RNA Silencing Complex of the CRISPR-Cas Immune System. *Mol. Cell*, **52**, 146–152.

Stockinger, E.J., Gilmour, S.J. and Thomashow, M.F. (1997) Arabidopsis thaliana CBF1 encodes an AP2 domain-containing transcriptional activator that binds to the C-repeat/DRE, a cis-acting DNA regulatory element that stimulates transcription in response to low temperature and water deficit. *Proc. Natl. Acad. Sci.*, **94**, 1035–1040.

Stuurman, J., Hoballah, M.E., Broger, L., Moore, J., Basten, C. and Kuhlemeier, C. (2004) Dissection of Floral Pollination Syndromes in Petunia. *Genetics*, **168**, 1585–1599.

Sung, P. and Robberson, D.L. (1995) DNA strand exchange mediated by a RAD51-ssDNA nucleoprotein filament with polarity opposite to that of RecA. *Cell*, **82**, 453–461.

Symington, L.S. (2002) Role of RAD52 Epistasis Group Genes in Homologous Recombination and Double-Strand Break Repair. *Microbiol. Mol. Biol. Rev.*, **66**, 630–670.

Terry, M.I., Carrera-Alesina, M., Weiss, J. and Egea-Cortines, M. (2019) *Molecular and transcriptional structure of the petal and leaf circadian clock in Petunia hybrida*, Plant Biology. Available at: http://biorxiv.org/lookup/doi/10.1101/641639 [Accessed July 19, 2019].

Terry, M.I., Pérez-Sanz, F., Díaz-Galián, M.V., Pérez de los Cobos, F., Navarro, P.J., Egea-Cortines, M. and Weiss, J. (2019) The Petunia CHANEL Gene is a ZEITLUPE Ortholog Coordinating Growth and Scent Profiles. *Cells*, **8**, 343.

Thines, B. and Harmon, F.G. (2011) Four easy pieces: mechanisms underlying circadian regulation of growth and development. *Curr. Opin. Plant Biol.*, **14**, 31–37.

Thomashow, M.F. (1999) PLANT COLD ACCLIMATION: Freezing Tolerance Genes and Regulatory Mechanisms. *Annu. Rev. Plant Physiol. Plant Mol. Biol.*, **50**, 571–599.

Tissier, A., Morgan, J.A. and Dudareva, N. (2017) Plant Volatiles: Going 'In' but not 'Out' of Trichome Cavities. *Trends Plant Sci.*, **22**, 930–938.

Tseng, T.-S. (2004) SPINDLY and GIGANTEA Interact and Act in Arabidopsis thaliana Pathways Involved in Light Responses, Flowering, and Rhythms in Cotyledon Movements. *PLANT CELL ONLINE*, **16**, 1550–1563.

Tuschl, T. (2001) RNA Interference and Small Interfering RNAs. *RNA Interf.*, 7.

Tuschl, T., Zamore, P.D., Lehmann, R., Bartel, D.P. and Sharp, P.A. (1999) Targeted mRNA degradation by double-stranded RNA in vitro. *Genes Dev.*, **13**, 3191–3197.

Tzin, V. and Galili, G. (2010) The Biosynthetic Pathways for Shikimate and Aromatic Amino Acids in *Arabidopsis thaliana*. *Arab. Book*, **8**, e0132.

Uemura, M., Warren, G. and Steponkus, P.L. (2003) Freezing Sensitivity in the *sfr4* Mutant of Arabidopsis Is Due to Low Sugar Content and Is Manifested by Loss of Osmotic Responsiveness. *Plant Physiol.*, **131**, 1800–1807.

Valverde, F., Mouradov, A., Soppe, W., Ravenscroft, D., Samach, A. and Coupland, G. (2004) Photoreceptor Regulation of CONSTANS Protein in Photoperiodic Flowering. *Science*, **303**, 1003–1006.

Van Houdt, H. (2003) RNA Target Sequences Promote Spreading of RNA Silencing. *PLANT Physiol.*, **131**, 245–253.

Vance, V. (2001) RNA Silencing in Plants--Defense and Counterdefense. *Science*, **292**, 2277–2280.

Vaucheret, H., Béclin, C., Elmayan, T., Feuerbach, F., Godon, C., Morel, J.-B., Mourrain, P., Palauqui, J.-C. and Vernhettes, S. (1998) Transgene-induced gene silencing in plants: Transgene-induced gene silencing. *Plant J.*, **16**, 651–659.

Verdonk, J.C., Ric de Vos, C.H., Verhoeven, H.A., Haring, M.A., Tunen, A.J. van and Schuurink, R.C. (2003) Regulation of floral scent production in petunia revealed by targeted metabolomics. *Phytochemistry*, **62**, 997–1008.

Walker, J.R., Corpina, R.A. and Goldberg, J. (2001) Structure of the Ku heterodimer bound to DNA and its implications for double-strand break repair. *Nature*, **412**, 607–614.

Wang, H. and Xu, X. (2017) Microhomology-mediated end joining: new players join the team. *Cell Biosci.*, **7**, 6.

Waterhouse, P.M., Graham, M.W. and Wang, M.-B. (1998) Virus resistance and gene silencing in plants can be induced by simultaneous expression of sense and antisense RNA. *Proc. Natl. Acad. Sci.*, **95**, 13959–13964.

Weiss, J., Mühlemann, J.K., Ruiz-Hernández, V., Dudareva, N. and Egea-Cortines, M. (2016) Phenotypic Space and Variation of Floral Scent Profiles during Late Flower Development in Antirrhinum. *Front. Plant Sci.*, **7**. Available at: http://journal.frontiersin.org/article/10.3389/fpls.2016.01903/full [Accessed March 16, 2020].

Widhalm, J.R. and Dudareva, N. (2015) A Familiar Ring to It: Biosynthesis of Plant Benzoic Acids. *Mol. Plant*, **8**, 83–97.

Wiedenheft, B., Sternberg, S.H. and Doudna, J.A. (2012) RNA-guided genetic silencing systems in bacteria and archaea. *Nature*, **482**, 331–338.

Yamaguchi-Shinozakiaib, K. and Shinozaki, K. (1994) A Nove1 cis-Acting Element in an Arabidopsis Gene 1s lnvolved in Responsiveness to Drought, Lowqemperature, or High-Salt Stress. , 15.

Yang, D., Lu, H. and Erickson, J.W. (2000) Evidence that processed small dsRNAs may mediate sequence-specific mRNA degradation during RNAi in Drosophila embryos. *Curr. Biol.*, **10**, 1191–1200.

Yon, F., Joo, Y., Cortés Llorca, L., Rothe, E., Baldwin, I.T. and Kim, S. (2015) Silencing Nicotiana attenuata LHY and ZTL alters circadian rhythms in flowers. *New Phytol.*, **209**, 1058–1066.

Zamore, P.D. (2001) RNA interference: listening to the sound of silence. *Nat. Struct. Biol.*, **8**, 5.

Zamore, P.D., Tuschl, T., Sharp, P.A. and Bartel, D.P. (2000) RNAi: Double-Stranded RNA Directs the ATP-Dependent Cleavage of mRNA at 21 to 23 Nucleotide Intervals. , 9.

CHAPTER 1 - The clock gene *Gigantea 1* from *Petunia hybrida* coordinates vegetative growth and inflorescence architecture.

Abstract

The gene *GIGANTEA* (*GI*) appeared early in land plants. It is a single copy gene in most plants and is found in two to three copies in Solanaceae. We analyzed the silencing of one *GI* copy, *Petunia hybrid GI1* (*PhGI1*), by hairpin RNAs in Petunia in order to gain knowledge about its range of functions. Decreased transcript levels of *PhGI1* were accompanied also by a reduction of *PhGI2*. They were further associated with increased time period between two consecutive peaks for *PhGI1* and *CHANEL (PhCHL)*, the orthologue of the blue light receptor gene *ZEITLUPE* (*ZTL)*, confirming its role in maintaining circadian rhythmicity. Silenced plants were bigger with modified internode length and increased leaf size while flowering time was not altered. We uncovered a new function for *PhGI1* as silenced plants showed reduction of flower bud number and the appearance of two flower buds in the bifurcation point, were normally one flower bud and the inflorescence meristem separate. Furthermore, one of the flower buds consistently showed premature flower abortion. Flowers that developed fully were significantly smaller as a result of decreased cell size. Even so the circadian pattern of volatile emission was unchanged in the silenced lines, flowers emitted 20% less volatiles on fresh weight basis over 24 hours and showed changes in the scent profile. Our results indicate a novel role of *PhGI1* in the development of reproductive organs in Petunia. *PhGI1* therefore represses growth in

vegetative plant parts, maintains the typical cymose inflorescence structure, and inhibits premature flower abortion.

Introduction

The evolution of land plants has included amongst other adaptations the increase in complexity of the circadian clock. Predictable changes in the environment, as light and temperature, are anticipated by the plant circadian clock, which allows them to adjust their developmental and physiological traits. Most detailed studies on plant circadian clock have been performed in *Arabidopsis thaliana* (Staiger *et al.*, 2013). The plant circadian clock is based on a set of genes forming several overlapping loops interacting with each other via transcriptional and post-translational activation and repression (Pokhilko *et al.*, 2012). Based on the time of the day when the mRNA of the gene shows its expression maximum, the genes included in this oscillator have been classified as the morning loop, midday or core loop and evening loop (Más, 2005). In Arabidopsis, *LATE ELONGATED HYPOCOTYL* (*LHY)* and *CIRCADIAN CLOCK ASSOCIATED 1* (*CCA1)*, two MYB transcription factors, form the central circadian oscillator complex, together with *PSEUDO RESPONSE REGULATOR 1* (*PRR1*), better known as *TIMING OF CAB1* (*TOC1*). *PSEUDO-RESPONSE REGULATOR 9* (*PRR9*) and *7* (*PRR7*) form the morning loop genes and the evening complex is formed by the three proteins EARLY FLOWERING 3 and 4 (ELF3 and ELF4) and LUX ARHYTHMO (LUX). These clock genes are interconnected via negative autoregulatory feedback loops, meaning that they reciprocally regulate each other (Kikis *et al.*, 2005; Gendron *et al.*, 2012; Staiger *et al.*, 2013; Adams *et al.*, 2015). Light input is received by *ZEITLUPE (ZTL),* a gene containing

an F-box domain and a blue-light sensing domain, which sustains a normal circadian period through proteasome-dependent degradation of the central clock protein *TOC1* (Más, Kim, *et al.*, 2003). The stabilization of the ZTL protein in turn is obtained through GIGANTEA (GI), a protein with chaperone activity that facilitates ZTL maturation into an active form (Kim *et al.*, 2007, Cha *et al.*, 2017).

Studies in *Arabidopsis thaliana* and other species revealed that the complex wiring of the oscillator network includes an interplay with hormone signaling (Bancos *et al.*, 2006; Nozue *et al.*, 2007; Thines and Harmon, 2011), cell division and expansion (Soy *et al.*, 2016; Fung-Uceda *et al.*, 2018), primary metabolism (Farré and Weise, 2012), abiotic stress response (Marcolino-Gomes *et al.*, 2014), the expression of seed storage proteins (Weiss *et al.*, 2018), biomass (Ni *et al.*, 2009; Atamian *et al.*, 2016; Edwards *et al.*, 2018) flower orientation (Atamian *et al.*, 2016) and flower scent emission (Fenske *et al.*, 2015; Yon *et al.*, 2015; Terry, Pérez-Sanz, Díaz-Galián, *et al.*, 2019; Terry, Pérez-Sanz, Navarro, *et al.*, 2019).

The genetic structure of the circadian clock in the picoeukaryote *Ostreococcus* includes two genes, a *TOC1* and an *LHY* ortholog (Corellou *et al.*, 2009; Morant *et al.*, 2010). A protein comprising a LOV domain and a histidine kinase appears to function as an entry for light cues (Djouani-Tahri *et al.*, 2011). Relative to these two clock genes, other clock genes such as *GI* appear later in evolution and are present in *Marchantia* but not in *Physcomitrella patens* (Linde *et al.*, 2017). The gene *GI* encodes a protein that is not fully characterized. However, it has important functions in plant development including a conserved role in floral transition in *Marchantia* and *Arabidopsis* (Fowler *et al.*, 1999; Kubota *et al.*, 2014) , as well as in Arabidopsis a control of

circadian rhythm (Mizoguchi *et al.*, 2005), both photoperiod-mediated and independent flowering (Jung *et al.*, 2007; Sawa and Kay, 2011) growth cessation (Ding *et al.*, 2018), carbohydrate metabolism (Dalchau *et al.*, 2011), salt tolerance (Park *et al.*, 2013) and cold stress response (Cao *et al.*, 2005). *GI* also affects hypocotyl growth in Arabidopsis (Tseng, 2004; Kim *et al.*, 2007) and this function is related to gibberellin signaling, as SPINDLY (SPY) protein, a negative regulator of gibberellin signaling in Arabidopsis and an inhibitor of hypocotyl elongation, interacts with GI protein (Tseng, 2004). Loss of function of *GI* results in long petioles, tall plant height and many rosette leaves, together with delayed flowering time.

Flower formation in Petunia involves the activity of the flower-meristem-identity genes *PETUNIA FLOWERING GENE* (*PFG*) and *ALF* (*ABERRANT LEAF AND FLOWER)*, the Petunia orthologue of *LEAFY* of Arabidopsis, which induce the floral fate in the lateral shoot meristem (Souer *et al.*, 1998; Immink *et al.*, 1999). The typical determinate inflorescence architecture in Petunia is characterized by a bifurcation of the inflorescence meristem, one terminating into a floral meristem, the other maintaining inflorescence identity and repeating the cymose floral pattern. A few mutants show altered architectures, including *extra petals (exp),* which forms a single terminal flower (Souer *et al.*, 1998) and the mutants *alf* and *double top* (*dot*), a homolog of *UNUSUAL FLORAL ORGANS* (*UFO*) from *Arabidopsis, where* the apical floral meristems convert into inflorescence meristems that do not produce flowers (Souer *et al.*, 1998). Overexpression of *DOT* leads to the production of a solitary flower (Eckardt, 2008). Another gene that determines Petunia inflorescence architecture is *EVERGREEN (EVG)* involved in the activation of *DOT*, the initiation of the floral identity in

the apical meristem as well as lateral inflorescence shoot development (Rebocho *et al.*, 2008). Once the floral program is activated, angiosperm flowers form concentric whorls of organs that include sepals, petals, stamens and carpel and this organ specification relies on the combinatorial genetic function of the organ identity genes according to the Petunia ABCD model (Rijpkema *et al.*, 2010).

GI generally has remained as a single copy gene in most species. Based on the comparison of the Petunia genomes with other Solanaceae, it has been shown that the circadian clock comprises a different set of genes, including *GI*, which in some cases is duplicated or triplicated. The *GI* gene is present in two copies in *P. axillaris* and three in *P. inflata*. It was hypothesized that some duplicated clock genes may have undergone a subfunctionalization or redeployment (Bombarely *et al.*, 2016).

In this work, we have characterized one of the *GI* orthologues from *Petunia hybrida*, *GI1*, by creating loss of function plants, using hairpin RNA constructs of *PhGI1*. Our results demonstrate novel roles of *GI1* during flowering, consisting in the promotion of flower initiation and flower maturation, the maintenance of cymose inflorescence structure as well as a control over the species-specific VOC profile.

Results

Silencing of *PhGI1* has minor effects on clock gene expression and rhythmicity

We have previously shown that *PhGI1* and *PhGI2* have similar expression pattern under a 12:12 Light:Dark photoperiod (12:12 LD) (Terry, Carrera-Alesina, *et al.*, 2019). But we also found that under free running conditions of 12:12 DD, it has a significant change in expression. Thus, we analyzed the expression of *PhGI1* as well as *PhGI2* under long photoperiods of 16:8 LD and continuous darkness.

The expression pattern of *PhGI1* and *PhGI2* in wild type leaves is shown in Figure 10a. Both *PhGI1* and *PhGI2* showed a similar pattern of oscillation with peak expression at 9 hours of light (ZT9). We compared the expression levels of *PhGI1* during 24 hours, measured in 3-hour intervals, and they were inferior to those of *PhGI2* at most time points. Indeed, at ZT9, *PhGI2* expression was double than *PhGI1*. The expression of *PhGI* had been determined previously using an EST from Petunia (Fenske *et al.*, 2015). A DNA alignment of *PhGI1*, *PhGI2* and the previously reported *PhGI* showed that this EST (FN03636) corresponds to *PhGI2* (Figure S1).

We silenced *PhGI1* by hairpin RNAi and obtained several independent transgenic lines. We selected three for further work, *iRNA::PhGI1 3.7, 4.7* and *8.1.* As a result of silencing, all *iRNA::PhGI1* lines lacked the strong increase in *PhGI1* expression at ZT9 shown by wild type plants (Figure 10b) and expression was significantly downregulated at most time points. On average, the peak levels between wild type and iRNA::PhGI lines differed by a factor of 6.

In order to specifically silence only the *PhGI1* without cross-silencing *PhGI2*, we selected a sequence specific for *PhGI*, as indicated by the level of similarity according to the sequence alignment (Figure S2). However, as shown in Figure 10c, *PhGI2* was downregulated to 50% in *iRNA::PhGI1* lines compared to the wild type at peak expression, indicating a certain level of cross-silencing.

Figure 10d-g shows the expression of several circadian genes in the wild type compared to *iRNA::PhGI1* lines. The genes include *CIRCADIAN CLOCK ASSOCIATED1 (LHY) and TIMING OF CAB EXPRESSION1 (TOC1),* belonging to the core midday loop, and *EARLY FLOWERING 4 (ELF4)* and *CHANEL,* the ortholog of *ZTL* in wild type Petunia, belonging to the evening loop. In Arabidopsis, *ZTL* messenger RNA is uniformly expressed, but ZTL protein levels oscillate with a threefold change in amplitude. Even so no rhythmic expression of *ZTL* exists in *Arabidopsis* and *Nicotiana attenuatta* or *PhCHL*, respectively, in *Petunia hybrid* (Somers *et al.*, 2000; Yon *et al.*, 2012; Terry, Pérez-Sanz, Díaz-Galián, *et al.*, 2019) a significant rise at ZT9 was observed in Petunia leaves at a 12:12 LD light regime (Terry, Carrera-Alesina, *et al.*, 2019). Similar to this observation we observed peak expression at midday (ZT6), both in wild type and the silenced lines (Figure 10d).

The expression profile of *PhLHY* (Figure 10e) over 24 hour period (16:8 LD) followed the typical peak at the end of the dark period reported for a wide range of tissues in Arabidopsis and other plants (de Montaigu *et al.*, 2010; Fenske *et al.*, 2015). This pattern was not altered in the silenced lines of *PhGI1.* The expression profile of *TOC1* over a 24 hours period (16:8 LD) was characterized by lowest levels during dark period and until midday, followed by an increase to peak expression at 12 hours of light, corresponding to the late afternoon,

and a sharp decline towards dark period (Figure 10f). Peak expression towards the end of the day was also reported for Arabidopsis (Más, Alabadí, *et al.*, 2003), soybean (Marcolino-Gomes *et al.*, 2014) or cowpea (Weiss *et al.*, 2018). In our case, the expression pattern in *iRNA::PhGI1* lines was similar to wild type plants however, peak expression was advanced by three hours in all three transgenic silenced lines (Figure 10f). The gene *PhELF4*, belonging to the evening loop, showed an identical expression, both concerning pattern and expression level, in wild type and silenced lines, characterized by a peak expression towards the evening (ZT12), followed by a steady decline towards the end of dark period (Figure 10g).

The mathematical analysis for circadian oscillation using the JTK_CYCLE algorithm (Table 1) showed that all analyzed clock genes had a rhythmic gene expression pattern, both in wild type and *iRNA::PhGI1* lines.

In case of *GI2, the ZTL*-orthologue *CHL, and LHY*, a significant shift in phase was observed for one or two of the silenced lines, but lacked consistency over all silenced lines. Concerning changes in the time period between two consecutive peaks, a consistent change in all *iRNA::PhGI1* lines was observed for *GI1* and *ZTL*-orthologue *CHL,* which prolonged from 21 to 24 hours.

	Pval	Per	Phase	Amp
PhGI1 W.T.	6.98E-11	21	10.5	0.63
PhGI1 3.7	7.00E-08	24	10.5	0.13
PhGI1 4.7	1.48E-08	24	10.5	0.11
PhGI1 8.1	1.48E-06	24	10.5	0.14
PhGI2 W.T.	3.23E-11	24	10.5	1.46
PhGI2 3.7	1.45E-10	24	9	0.47
PhGI2 4.7	2.53E-08	24	9	0.48
PhGI2 8.1	7.61E-10	24	10.5	0.64
CHL W.T.	1.55E-02	21	7.5	0.47
CHL 3.7	6.96E-07	24	6	1.06
CHL 4.7	1.71E-04	24	7.5	0.72
CHL 8.1	6.88E-05	24	7.5	0.72
LHY W.T.	9.19E-08	24	22.5	0.26
LHY 3.7	1.07E-05	21	1.5	0.23
LHY 4.7	6.32E-06	21	1.5	0.12
LHY 8.1	1.99E-06	24	22.5	0.30
TOC1 W.T.	2.96E-06	24	13.5	0.44
TOC1 3.7	9.11E-06	24	13.5	0.89
TOC1 4.7	9.11E-06	24	13.5	0.89
TOC1 8.1	1.84E-05	24	13.5	0.68
ELF4 W.T.	1.48E-07	24	13.5	1.29
ELF4 3.7	6.32E-06	24	13.5	0.93
ELF4 4.7	2.96E-06	21	13.5	1.03
ELF4 8.1	1.96E-04	24	13.5	1.50

Table 1| Statistical analysis of rhythmicity of gene expression data.

The P value (Pval) indicates a significative expression rhythm at Pval ≤ 0.05. Period (Per) is defined as the time between two consecutive peaks (expressed in hours). The adjusted phase (Phase), given by JTK_CYCLE and Lomb-Scargle, is considered as the time point with the peak expression (expressed in hours). Amplitude (Amp) is the difference between the peak expression (or minimum expression) and the mean value of the wave.

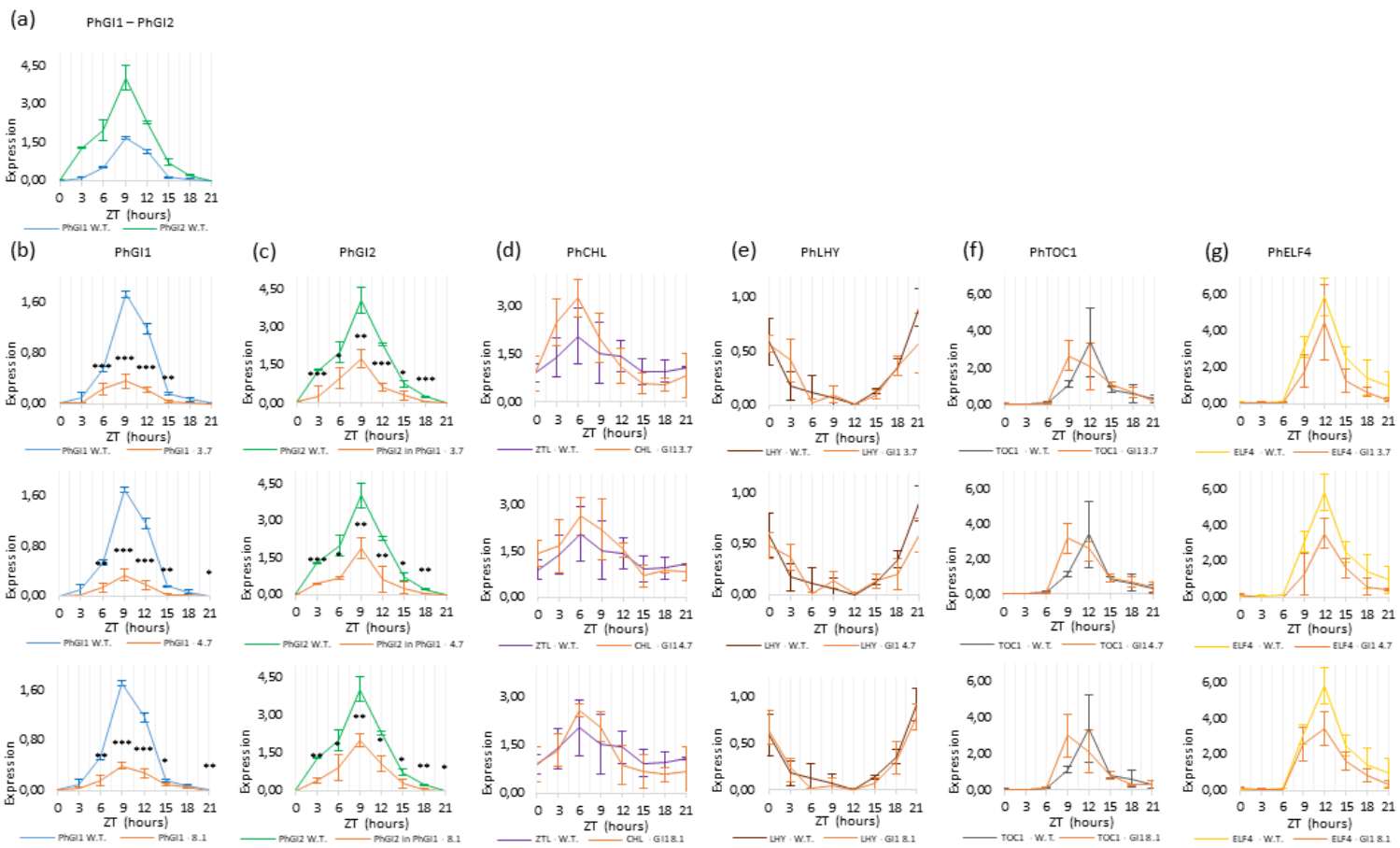

Figure 10| Expression profile during 24 hours.

Expression profile during 24 hours of (a) *PhGI1* and *PhGI2* in wild type plants and (b) PhGI1, (c) *PhGI2, (d) PhCHL, (e) PhLHY, (f) PhTOC* and (g) *PhELF4* in *iRNA::PhGI1* T1 lines 3.7, 4.7, 8.1 compared to expression in the wild type (from ZT 0 to ZT 15 of light and from ZT 15 to ZT 24 of dark). Expression represents the normalized expression NE according to the formula (NE) = 2^-(Ct experimental – Ct normalization). Three samples were analyzed for each time point and error bars indicate the standard deviation. Asterisks indicate statistical significance between wild type and iRNA lines with *P < 0.05; **P < 0.01; ***P < 0.001 according to group-wise comparison with to Student's T-test.

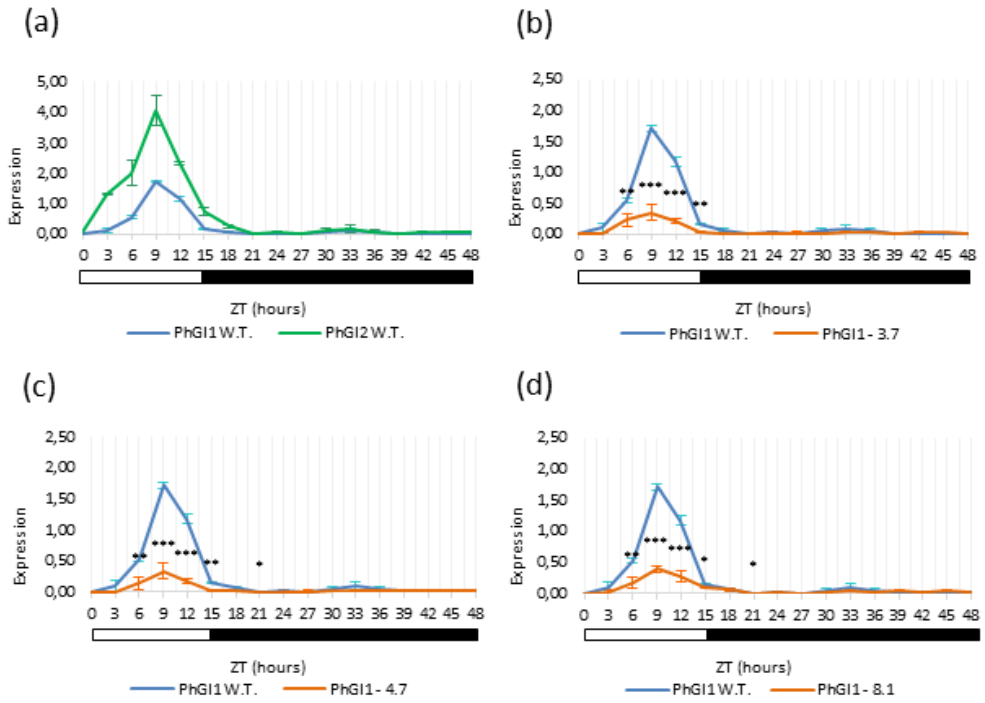

Figure 11|Gene expression profile under light and continuous darkness.

Expression profile in leaves under light and subsequent continuous darkness of (a) *PhGI1* and *PhGI2* in wild type plants and *iRNA::PhGI1* T1 lines 3.7 (b), 4.7 (c) and 8.1 (d). Expression represents the normalized expression NE according to the formula (NE) = 2^-(Ct experimental – Ct normalization). Three samples were analyzed for each time point and error bars indicate the standard deviation. Asterisks indicate statistical significance between wild type and iRNA lines with *P < 0.05; **P < 0.01; ***P < 0.001 according to group-wise comparison with to Student's T-test.

We analyzed the effect of continuous dark conditions on the expression of *PhGI1* in RNA lines. As shown in Figure 11, wild type and silenced lines showed the typical high and reduced peak under light towards the afternoon, respectively, but revealed very low basic expression levels during the subsequent continuous darkness. Wild type and silenced lines lost rhythmicity during continuous darkness.

Altogether we can conclude that a strong silencing of *PhGI1* does not have a major effect on the expression pattern or rhythmicity of other clock genes. As GI function is via protein-protein interactions but

is not known to be part of a transcriptional complex, it could still have major effects on the protein quantities of PhCHL.

PhGI1 is a negative regulator of vegetative growth

We analyzed the effect of downregulating *PhGI1* on vegetative growth. The mean value of the vegetative parameters of transgenic plants from T1 and T2 generation, belonging to 6 independent lines (2, 3, 4, 5, 7 and 8), are given in Table 2. Additionally, the results of three different T1 transgenic plants belonging to the three *iRNA::PhGI1* independent lines (3.7, 4.7 and 8.1), are given in Table S2. For the T2 generation we analyzed at least three plants per line. Both generations, grown under long-day conditions, the T1 lines in the growth chamber, and T2 lines in the greenhouse, had significantly longer and broader basal and apical leaves compared to the wild type. Overall, *GI1* silenced plants of the three independent lines showed a remarkable modification in leaf area and growth habit (Figure 12a and b).

In case of T1 generation, all three lines had a denser apical foliar apparatus, characterized by an apparent increase in the foliar volume. The bushier phenotype may result from an average reduction of the internode length of 37.6% in the median plant region and 33.7% in the apical plant region, while basal internode distance was increased by 34.4%, resulting in overall only slightly taller plants (Table 2). A similar, although minor, significant effect on internode length was observed in the T2 generation, resulting in a plant height identical to wild type. A marked increase in the number of axillary meristems in both generations may also contribute to a bushier phenotype. However, no significant increases in the number of lateral branches or

total leaf number was recorded compared to the wild type (Table 2). Transgenic lines had a greener appearance in the denser apical regions, while basal leaves were more yellowish (Figure 12a). This phenotype coincided with a significant decrease in the relative chlorophyll content in basal leaves and a progressive increase in the median and apical ones compared to the wild type (Table 2).

We can conclude that *PhGI1* plays a role in vegetative development with a clear acropetal gradient, as it has opposite effects during early stages of development and middle to late stages.

Flowering time, expressed as the percentage of plants which fully bloomed after rooted shoots were transferred from *in vitro* jars to pots (in weeks) is given in Figure 13. *iRNA::PhGI1* lines of T1 and T2 generation and wild type plants flowered contemporaneously, indicating that in contrast to Arabidopsis, *PhGI1* does not play a role in floral transition. In general, plants kept in the greenhouse, flowered five to eight weeks earlier than those kept at 16:8 LD in the growth chamber corroborating that fluence accelerates floral transition in Petunia.

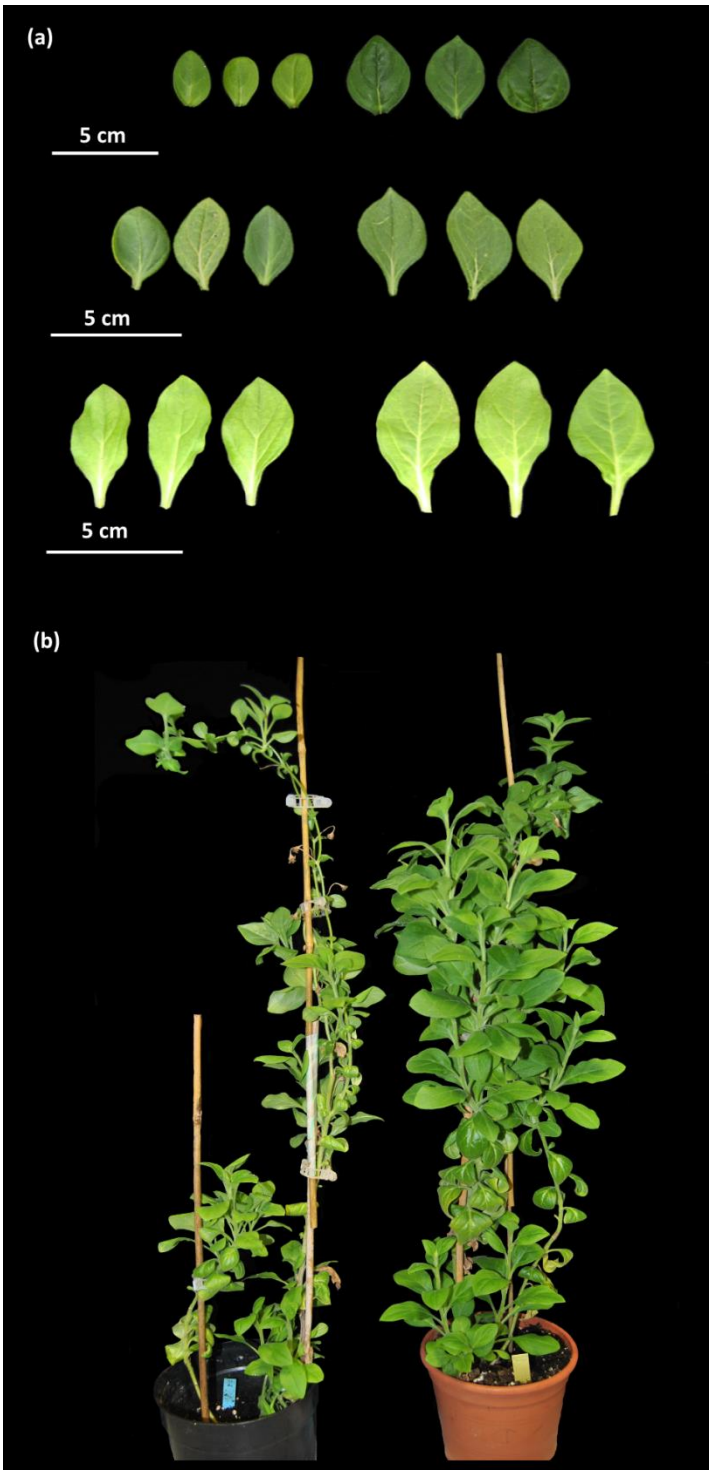

Figure 12|Vegetative growth characteristics in iRNA::PhGI1 T1 lines compared to wild type plants under growth chamber conditions of 16 hours light/ 8 hours darkness.

(**a**) From the bottom to the top, basal, medium and apical leaves of three wild type leaves (left) compared to three leaves of *PhGI1* 3.7, 4.7 and 8.1 lines (right) with the strongest silencing. (**b**) Growth habit of the transgenic lines compared to the wild type. Wild type plant (left) and *iRNA::PhGI1* line 4.7 (right).

Genotype:		W.T.	*iRNA::PhGI1*	% *GI1* versus W.T.	P value
Plant Height (cm)	**T1**	40.9 ± 0.8	44 ± 4.4	+7.6	2.89E-02
	T2	44.7 ± 6.2	44.6 ± 4.9	-0.2	9.93E-01
Basal Internode (mm)	**T1**	12.61 ± 0.91	16.93 ± 0.51	+34.4	2.46E-20
	T2	14.28 ± 1.97	17.16 ± 0.79	+20.3	1.40E-03
Median Internode (mm)	**T1**	16.30 ± 0.56	10.17 ± 0.40	-37.6	3.57E-30
	T2	15.73 ± 1.3	12.44 ± 0.98	-20.8	1.42E-05
Apical Internode (mm)	**T1**	20.5 ± 1.07	13.60 ± 0.31	-33.7	2.51E-23
	T2	27.9 ± 1.63	23.81 ± 0.82	- 14.6	2.77E-05
N° of leaves to the 1° flower	**T1**	37 ± 1.4	36.5 ± 1.2	-1.4	7.62E-01
	T2	28.0 ± 1.0	28.7 ± 1.44	+2.5	3.74E-01
N° of axillary meristems	**T1**	12.5 ± 1.3	27 ± 2.08	+116	3.78E-06
	T2	15.3 ± 1.5	26.6 ± 3.48	+73.9	1.89E-04
N° of branches	**T1**	2 ± 0.0	2.4 ± 0.57	+20	2.73E-01
	T2	6.7 ± 0.55	6.6 ± 0.7	-1.5	7.80E-01
Basal Leaves length (mm)	**T1**	64.57 ± 1.04	91.75 ± 5.24	+42	4.42E-33
	T2	90.99 ± 1.55	112.07 ± 6.05	+23.2	3.31E-30
Basal leaves width (mm)	**T1**	40.93 ± 0.72	50.96 ± 1.53	+24.5	4.97E-30
	T2	49.92 ± 1.6	53.78 ± 1.19	+7.7	4.03E-05
Median Leaves length (mm)	**T1**	72.72 ± 2.84	75.64 ± 1.66	+4.0	8.23E-02
	T2	65.38 ± 1.74	70.25 ± 1.58	+7.4	2.08E-07
Median leaves width (mm)	**T1**	43.82 ± 1.68	48.05 ± 1.39	+9.7	1.13E-08
	T2	36.89 ± 1.45	39.84 ± 1.22	+8.0	1.97E-05
Apical leaves length (mm)	**T1**	38.77 ± 1.31	48 ± 2.91	+24	1.49E-22
	T2	33.15 ± 1.82	36.08 ± 0.81	+8.8	1.36E-03
Apical leaves width (mm)	**T1**	22.54 ± 0.97	30.53 ± 2.54	+35	2.02E-23
	T2	17.86 ± 0.59	21.96 ± 0.64	+23	2.69E-11
Basal leaves Chlorophyll	**T1**	22.38 ± 1.09	14.89 ± 1.14	-33.5	1.05E-23
	T2	17.11 ± 1.08	13.84 ± 0.77	-19.1	7.11E-05
Median leaves Chlorophyll	**T1**	31.04 ± 2.29	37.26 ± 1.07	+20	1.67E-25
	T2	20.14 ±	24.99 ± 0.95	+24.1	2.97E-05
Apical leaves Chlorophyll	**T1**	21.27 ± 0.95	38.19 ± 1.74	+79.5	2.76E-45
	T2	34.47 ± 0.90	43.57 ± 1.03	+26.4	1.96E-14

Table 2| Comparison of vegetative parameters between wild type and the silenced PhGI1 in T1 and T2 generation.

Data are given as averages of at least three biological replicates of all silenced plants. The height was calculated from the base to the first flowering meristem. when the first flowering event occurs. The number of total axillary meristems was calculated between the base and the first apical flowering meristem. P values ≤ 0,05 according to Students T-test were considered as significant.

PhGI1 inhibits ectopic flower formation and premature flower senescence

We analyzed floral development in *iRNA::PHGI1* plants compared to the wild type and observed that even though wild type plants and silenced plants started to flower concurrently (Figure 13), the silenced plants developed new inflorescences at a slower pace so that the total number of flower buds at the end of flowering period was reduced by 58 and 59% in the T1 and T2 generation, respectively, compared to the wild type (Table 3; Table S3). Additionally, we found a striking phenotype that we had not seen previously in wild type plants. We found that at many bifurcation points were the terminal flower and the inflorescence shoot divide, an additional ectopic flower bud appeared (Figure 14). While the normally positioned flower bud tended to develop to full maturity, the ectopic flower bud appeared to undergo early senescence and aborted. Ectopic flower buds accounted for 40% in T1 and 21% in T2 lines. As a consequence of ectopic flower bud abortion (Figures 15 and 16) and slower inflorescence development in the transgenic lines, the final percentage of fully developed flowers diminished to 76 % and 67% in the T1 and T2 generation respectively compared to wild type plants (Table 3).

The differentiation of stamen and carpel tissue could be clearly observed in the aborting flower buds, even so the pale and brownish coloration in *iRNA* lines indicated an abortion in development, chlorophyll loss and necrosis (Figure 16 and Figure S3). This early onset of flower senescence occurred well before flowers achieved the normal size of flower opening in Petunia.

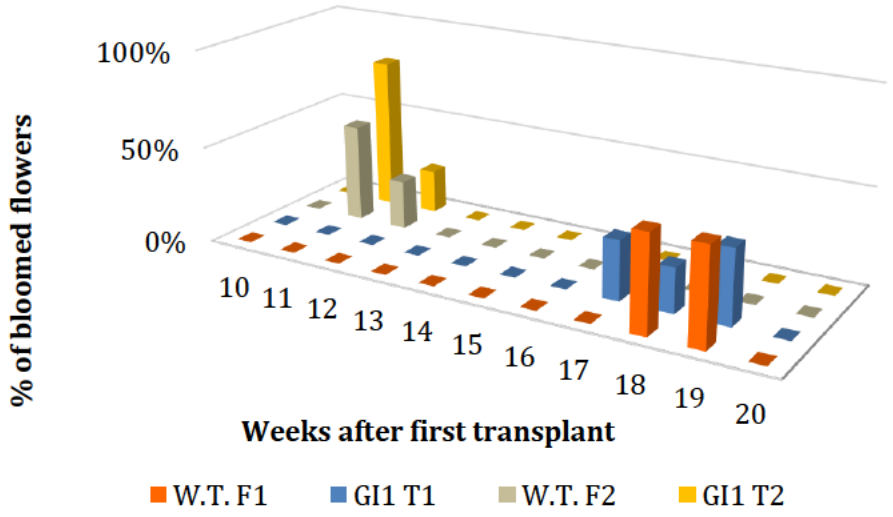

Figure 13| Percentage of fully open flowers in weeks after transplanting from in vitro culture to substrate of T1 and T2 generation of iRNA::PhGI1 lines compared to wild type plant.

T1 lines were grown under growth chamber conditions of 16 hours light/ 8 hours darkness. T2 lines were grown in a greenhouse under natural long-day conditions.

Genotype:		W.T.	*iRNA::PhGI1*	% *GI1* versus W.T.	P value
N° of flower buds	T1	27.8 ± 2.8	11.3 ± 4.1	-59.4	2.21E-05
	T2	29.3 ± 2.3	12.2 ± 5.01	-58.4	2.44E-04
N° of fully developed flowers	T1	27.8 ± 2.8	6.8 ± 2.19	-75.5	1.07E-04
	T2	29.3 ± 2.3	9.6 ± 4.62	-67.2	2.11E-04
% of fully developed flowers	T1	100	60.2	-39.8	1.47E-08
	T2	100	75.0	-25	3.67E-09
Corolla diameter (mm)	T1	46.22 ± 3.41	34.21 ± 2.73	-26.0	4.27E-21
	T2	54.34 ± 3.45	49.66 ± 3.27	-8.6	1.07E-04
Tube length (mm)	T1	40.06 ± 2.10	35.57 ± 2.11	-11.2	2.84E-15
	T2	41.10 ± 1.82	38.79 ± 1.98	-5.6	1.08E-04
Petiole length (mm)	T1	35.96 ± 2.72	35.33 ± 3.20	-1.8	2.67E-01
	T2	47.63 ± 2.51	46.22 ± 3.42	-3.0	5.91E-02

Table 3| Comparison of floral parameters between wild type and silenced PhGI1 in T1 and T2 generation.

Data are given as averages of at least three biological replicates of all silenced plants. P values ≤ 0,05 according to Students T-test were considered as significant.

The flowers of the silenced lines that fully developed appeared to be smaller with a significant reduction both in the corolla diameter as well as the floral tube length (Table 3, Figure 15). The flowers of the silenced lines that fully developed appeared to be smaller with a significant reduction both in the corolla diameter as well as the floral tube length (Table 3, Figure 15). Cell size in the floral tube and two regions of the corolla, the distal outer zone and a proximal zone near the tube, were significantly reduced (Table 4; Figure 17), indicating an effect of *GI1* silencing over petal cell expansion.

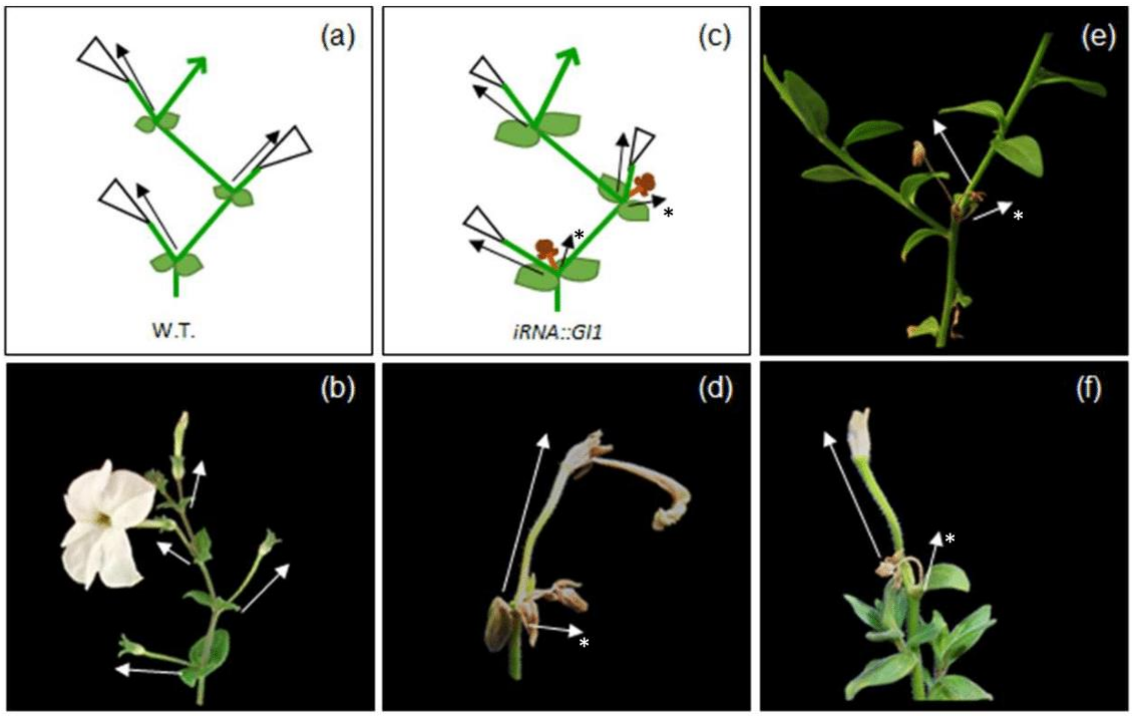

Figure 14|Schematic representation of the petunia inflorescence.

Wild type (**a**) and silenced *iRNA::PhGI1* plants of T1 line (**c**). Side view of a wild type petunia inflorescence (**b**) and *iRNA::PhGI1* plants of T1 line (**d–f**). Arrows indicate the position and direction of the main and aborted (*) floral meristems at each bifurcation.

Figure 15| Flower size and flower appearance in T1 lines of iRNA::PhGI1 compared to the wild type.

Tube length (**a**) of the flowers of the wild type (left) and transgenic lines (right). (**b**) Corolla diameter and the abortive flower appearance (extreme right) in T1 lines of *iRNA::PhGI1* (right) compared to the wild type (left).

Genotype:	W.T.	*iRNA::PhGI1*	% *GI1* versus W.T.	P value
Corolla (µm²)	1132.38 ± 225.13	910.07 ± 171.02	-19.6	8.18E-16
Basal limb (µm²)	345.12 ± 88.85	302.07 ± 74.75	-12.5	1.53E-05
Tube (µm²)	3653.35 ± 794.4	2566.5 ± 647.14	-29.8	8.81E-28

Table 4| Comparison of cellular areas of flowers between wild type and silenced PhGI1 plants of T1 generation.

Values correspond to mean (µm2) ± deviation standard error of at least three flowers belonging to the *iRNA::GI1* lines 3.7, 4.7 and 8.1 and 50 measurements for each flower. P values ≤ 0,05 according to Students T-test were considered as significant.

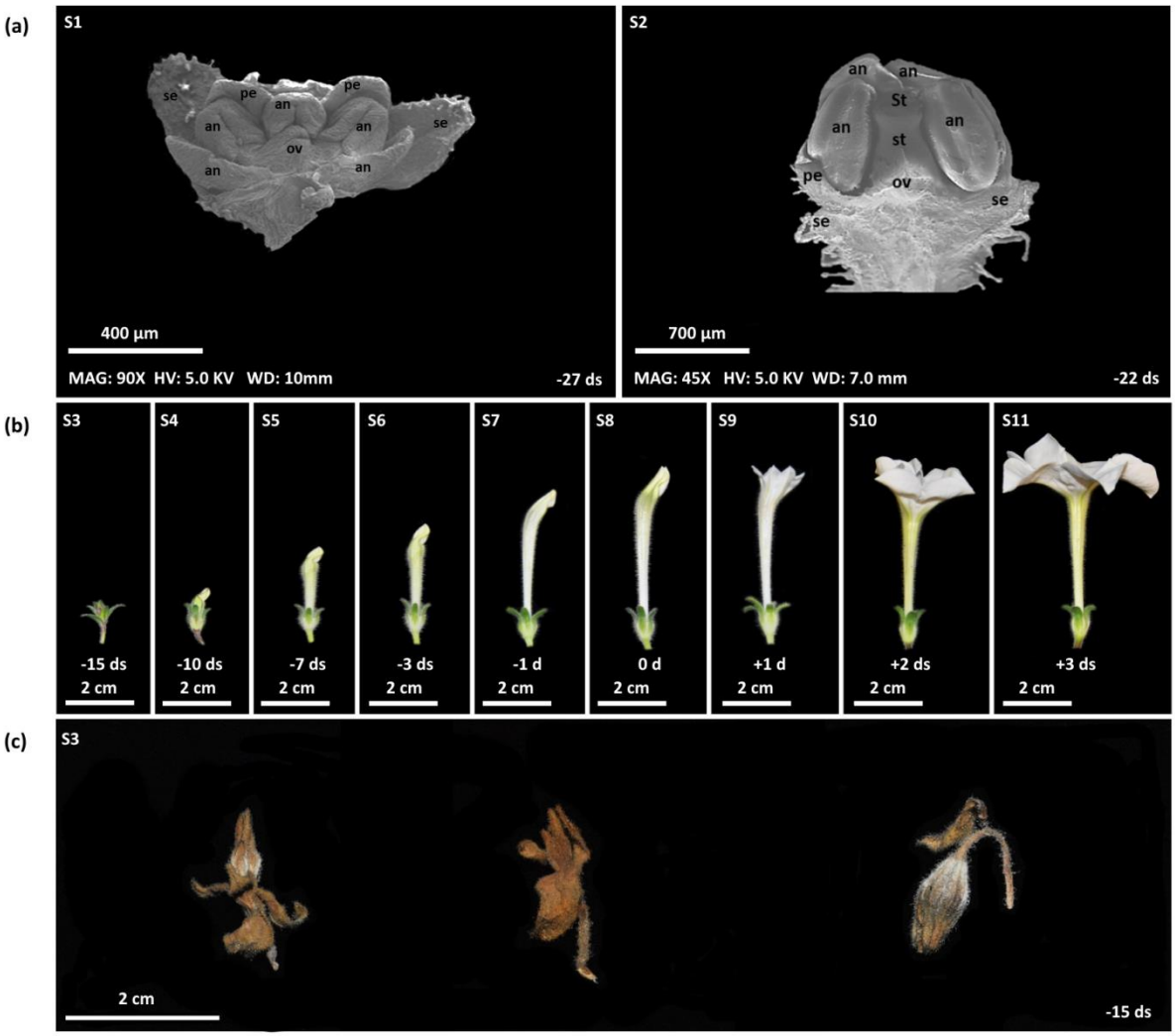

Figure 16| Stages of Petunia flower bud development in wild type and iRNA::PhGI1 T1 lines.

Stages (S) 1–7 represent flower development between 27 to 1 days before anthesis and stages (S) 8–11 represent flowers from 0 to 3 days after anthesis. (**a**) Stages S1 and S2 are given as scanning electron micrographs of the inflorescence apex of Petunia during early stages of development from a wild type plant (S1) and a plant of *iRNA::PhGI1* T1 line (S2). Stigma (St), style (st), ovary (ov), sepal (se), petal (pe), anthers (an). (**b**) Stages S8–11 of flower buds taken from a position within the plant that develops into a normal flower. (**c**) Stage S3 of flower buds taken from a position within the plant that develops into an aborted flower.

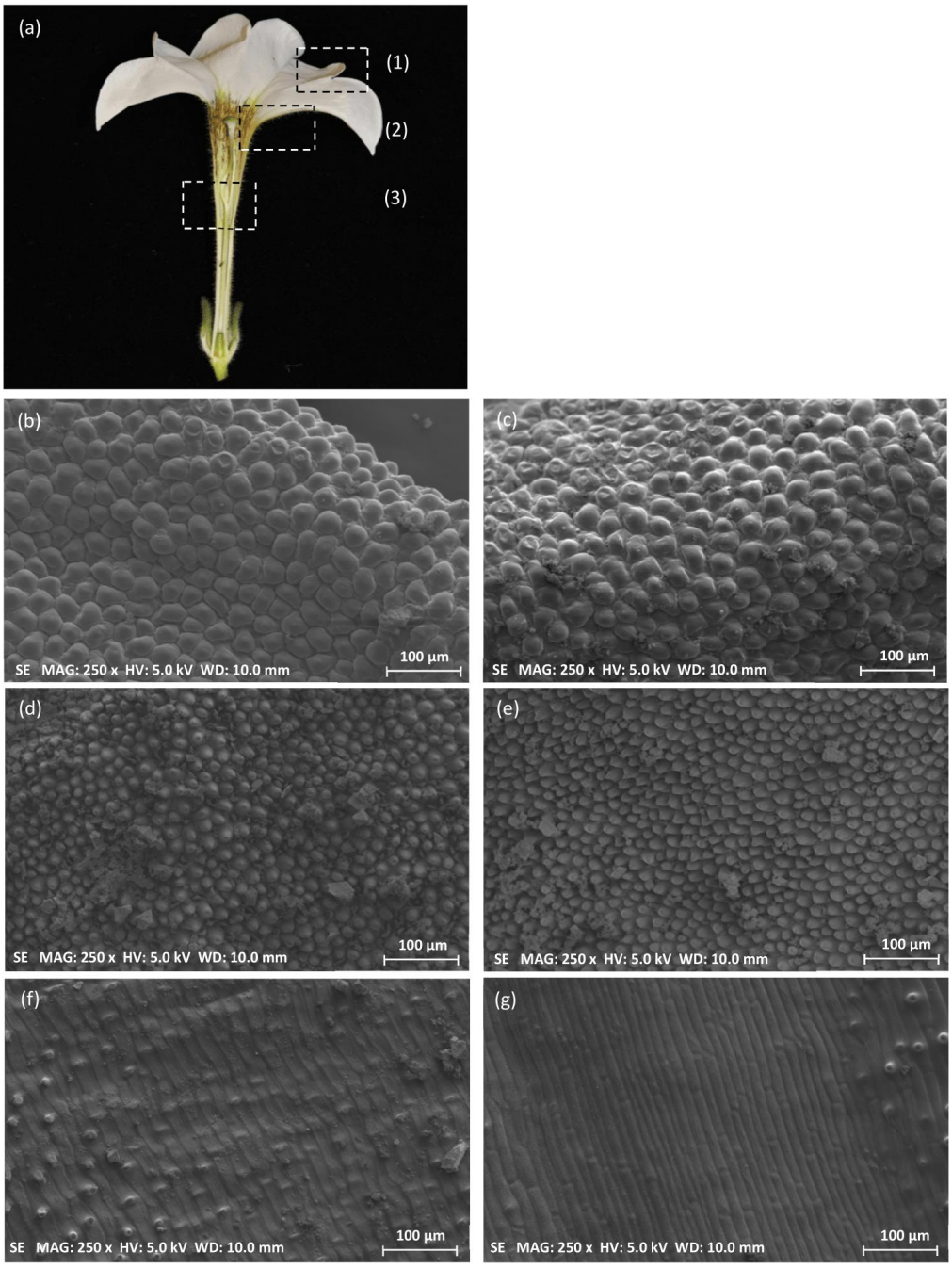

Figure 17| Scanning electron microscopy of petal cell size.

Three petal regions were sampled for scanning electroscopic analysis from T1 lines (**a**). Floral cell size comparison between wild type (left) and *iRNA::PhGI1* (right) of different floral organs: (1)(**b,c**) corolla, (2)(**d,e**) limb and (3)(**f,g**) tube.

PhGI1 regulates the quantity of volatile emission and fine-tuning of volatile profile

The main VOCs were analyzed in the three different plants with the strongest silencing, belonging to three independent *iRNA::PhGI1* lines (3.7, 4.7 and 8.1) and in the wild type. Data are listed in the Table S4. *iRNA::PhGI1* lines showed an average reduction of 20.6% in total VOC emission on the basis of flower fresh weight in grams (Figure 18a). Figure 18b shows the rhythm of VOC emission during 24 hours in 3 hour intervals, which was similar in case of wild type flowers and *iRNA::PhGI1* lines, with lowest emission towards midday at 6 hours of light and increases towards the end of light period with highest emission during the dark phase. We also observed a change in the relative composition (Figures 19a, 19b, 19c and Table S5). In both, wild type plants and *iRNA::PhGI1* lines, methyl benzoate was the major volatile with exception of the beginning of light period in *iRNA::PhGI1* lines, when this compound contributed with only 30% to the VOC profile. Concerning the relative contribution of other compounds, we found remarkable changes among wild type plants and *iRNA::PhGI1* lines, especially with a high contribution of isoeugenol and ethylbenzoate at certain time points (Figure 19b, 19c). Results indicate that even so the pattern of total emission during 24 hours is quite conserved, individual VOC compounds may change their emission pattern.

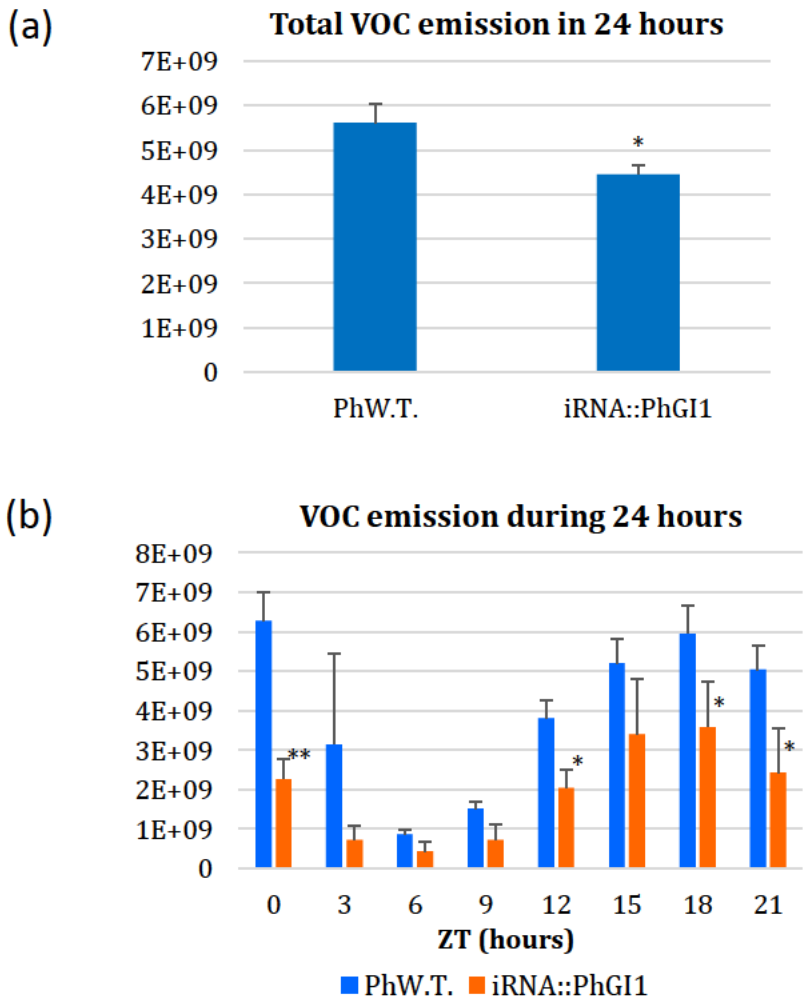

Figure 18| Volatile emission by flowers from wild type and iRNA::PhGI1 T1 lines. Flowers were excised at ZT0.

(a) Total VOC emission in wild type flowers compared to *iRNA::PhGI1* lines in 24 hours and (b) VOCs emission in three hour intervals during 24 hours. Absolute total emission of VOCs per grams of fresh weight is given as sum of integrated peak area. Asterisks indicate statistical significance between wild type and iRNA lines with *P < 0.05; **P < 0.01; ***P < 0.001 according to Student's T-test.

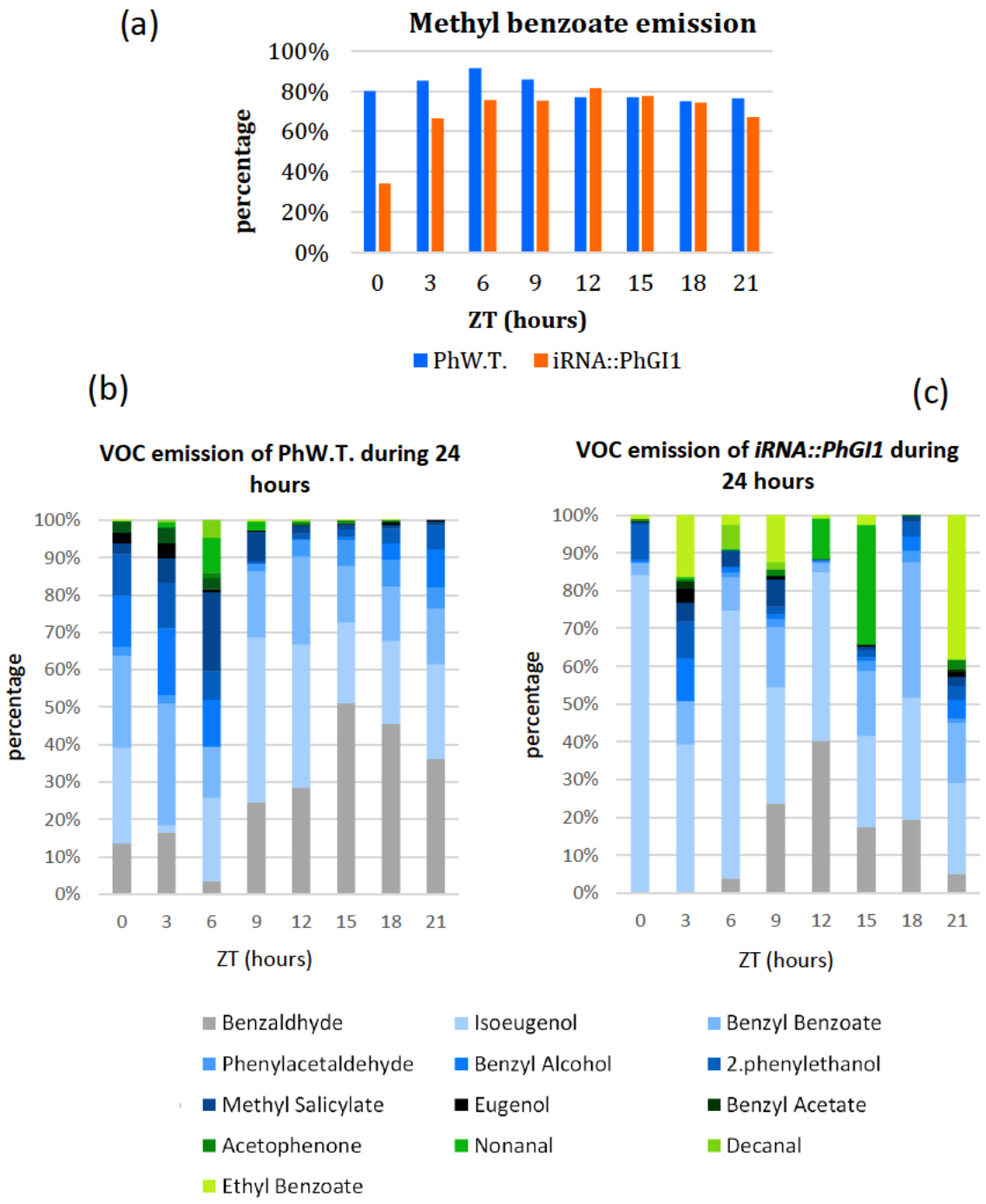

Figure 19| Percent emission of volatile organic compounds (VOCs) from wild type flowers and iRNA::PhGI1 T1 lines 3.7, 4.7 and 8.1

Flowers were excised at ZT0. Methyl benzoate (a) and other main VOCs in wild type flowers (b) and *iRNA::PhGI1* lines (c) in three hour intervals during 24 hours. Percentages were calculated based on the integrated peak area divided by flower fresh weight.

Discussion

In this work we have performed a functional analysis of *GI1* in *Petunia hybrida* by means of loss of function using RNAi lines. There are two paralogs in *Petunia x hybrida* and both *PhGI1* and *PhGI2,* showed a pattern of expression in wild type plants under a 16:8 LD cycle characterized by an increase towards the afternoon at ZT9 followed by a decrease to very low levels during the entire dark period. This pattern is similar to that observed in Arabidopsis, were under long day conditions (16:8 LD), *GI* mRNA peaks at ZT 10 and lowest expression levels occur at ZT 0 (Fowler *et al.*, 1999). Other examples of an evening phased expression pattern for *GI* include cowpea (Weiss *et al.*, 2018; Lonardi *et al.*, 2019) and soybean (Marcolino-Gomes *et al.*, 2014). In Arabidopsis, CCA1 binds to the *G1* promoter and reduces its expression, which only rises towards midday, when *CCA1* expression is repressed by *TOC1* (Lu *et al.*, 2012). We did not observe a robust circadian rhythmicity under continuous darkness for *PhGI1* in the wild type or the transgenic silenced lines. *PhGI1* expression in Petunia therefore diverges from Arabidopsis, were a strong oscillation of *GI* under conditions of continuous darkness can be observed (Park *et al.*, 1999). Observations on *Petunia hybrida* leaves confirm that *PhGI2* does not maintain rhythmicity during continuous darkness (Fenske *et al.*, 2015), indicating the necessity of light for the correct expression signals for oscillation of the *GI* paralogs in Petunia.

The specific silencing of a gene for which several paralogs exist within a plant species is very challenging, as it might be difficult to find regions with a sufficient degree of sequence variation. We selected the 3' untranslated region of *PhGI1* and *PhGI2*, that showed the maximum sequence differences. Even so gene specific sequences were selected

for the silencing of *PhGI1* in order to avoid cross-silencing with *PhGI2*, the selected sequence still contained stretches of identical sequences. As a result, we observed a certain level of silencing of *PhGI2*. While *PhGI1* expression levels were down regulated on average 5.6 fold in *iRNA::PhGI1* lines, the reduction of *PhGI2* in these lines was 2.3 fold compared to wild type. Silencing of non-targeted genes was reported to occur if these targets contain as few as eleven contiguous nucleotides of identity with the siRNA sequence (Jackson *et al.*, 2003), which might explain the observed off-target effects in case of these duplicated *GI* genes. Currently, we cannot determine if the downregulation of *PhGI2* is the result of the *iRNA::PhGI1* construct or if *PhGI1* activates the transcription of *PhGI2* by yet unknown mechanisms, which makes a separation of paralog function difficult.

Expression patterns of the core clock genes *LHY* and *TOC1* were similar in wild type and silenced lines and similar to Arabidopsis, where *LHY* peaks late during the night and is lowest at the onset of the night while *TOC1* expression is counterphased to *LHY*, forming a negative feedback loop (Gendron *et al.*, 2012). This feedback control system therefore was not altered by *PhGI1* silencing. Different from Arabidopsis, were *ZTL* messenger RNA is constitutively expressed, we observed a peak expression towards midday of *PhCHL* both in wild type and silenced lines. A lack of change in *PhCHL* expression in silenced lines can be explained by the fact that in Arabidopsis, interaction of *GI* with *ZTL* occurs at the protein level, consisting in the facilitation of maturation of *ZTL* into a functional protein. *ZTL* targets *TOC1* for proteasomal degradation (Ito *et al.*, 2012), suggesting that changes of TOC1 protein would also be expected. In Arabidopsis, *GI* and *ELF4* have a synergistic effect on endogenous clock regulation,

showing epistatic interactions (Kim *et al.*, 2012). Furthermore, *GI* and *ELF4* proteins interact physically to form discrete nuclear bodies (Kim *et al.*, 2013) but no direct interaction on the expression level is reported, which might explain the similarity in expression pattern between *PhGI1* silenced lines and wild type.

In petal tissue, silencing of *PhLHY* resulted in a phase-advance of *GI* peak expression of 4 hours (Fenske and Imaizumi, 2016), indicating that disturbance of the normal expression pattern of clock genes may alter the rhythmicity of the same and other clock genes. Similarly, the silencing of *GI1* here led to a significant prolongation of rhythmic period of 3 hours for the genes *PhGI1* and *PhCHL* in all silenced lines.

Changes in the vegetative growth of *PhGI1* transgenic lines was characterized by an increased leaf size of basal and apical leaves, and an augmentation in the basal internode length. However, medium and apical internodes were shorter, thus compensating in total plant length, which was not altered. It is well reported that nitrogen concentration diminishes with increasing shoot biomass during plant growth as result of N dilution (Bélanger and Gastal, 2000) and this dilution effect might have contributed to the progressive reduction in internode length in *PhGI1* transgenic lines. Next to the changes in internode length and leaf size, we also observed a structural change in growth characterized by an increased number of axillary meristems as well as a higher chlorophyll level in apical leaves. All changes together led to a bushier phenotype with darker color. In Arabidopsis, *GI* controls the growth of the hypocotyl (Kim *et al.*, 2012) and the loss of function of *GI* results, apart from late flowering, in long petioles, tall plant height and many rosette leaves (Hwang *et al.*, 2011). The findings in Arabidopsis confirm the effect of *GI* on vegetative growth observed

in the silenced Petunia lines. *Gigantea* is known as a key regulator of flowering time. In Arabidopsis, *GI* mutation leads to a late-flowering phenotype in LD conditions (Fowler *et al.*, 1999). The role of *GI* in flowering is conferred through its control over *CO* and *FT* mRNA expression levels under inductive conditions as found in different plant species (Fowler *et al.*, 1999) second pathway involving *GI* is *CONSTANS* (*CO*) independent and involves *GI* regulation of miR172, which than controls *FT* induction and flowering (Jung *et al.*, 2007). We did not observe a switch in inflorescence phase of *iRNA::PhGI1* lines compared to wild type lines, indicating that *PhGI1* does not share a function in controlling flowering time with *AtGI*. Future research will show whether a case of subfunctionalization has occurred in Petunia were only the second copy of *GI* in petunia, *PhGI2*, affects flowering time. However, the relation between late flowering time and increased biomass seen in Arabidopsis is broken in Petunia as the *PhGI1* silenced lines did not flower later than wild type. In fact, mutant combinations of *RVE* genes in Arabidopsis also disrupt the correlation between biomass production and flowering via changes in PIF gene expression (Gray *et al.*, 2017). Altogether our results point out *PhGI1* on plant growth coordination. on coordination of plant growth. Interestingly, the analyzed parameters on vegetative and generative growth in general showed a stronger reduction in T1 lines that T2 lines as compared to the wild type. This might be due to the exposure to lower night temperatures of greenhouse grown T2 lines compared to the growth chamber grown T1 lines, as it known that siRNA generation and silencing is inhibited by low temperatures (Szittya *et al.*, 2003).

PhGI1 silenced lines were characterized by a reduction in the number of flower buds, the appearance of two flower buds at the

bifurcation point of the inflorescence meristem, of which one flower bud aborted, and an increased overall incidence of premature failure in floral development. All these phenomena were not described until now for any other *GI* mutant. The appearance of ectopic flower buds in the bifurcation point of the inflorescence meristem was not described for any other mutant in *Petunia hybrida*. Mutants affecting flower bud appearance described so far are *double top* (*dot)* and *aberrant flower* (*alf),* characterized by a failure to develop flowers and *extra petals (exp)* and *evergreen (evg),* were the inflorescence forms a solitary flower (Souer *et al.*, 2008; Rebocho *et al.*, 2008). Aborted flowers clearly show carpel and stamen tissues indicating that flower abortion occurred following the activation of genes specifying floral organ identity. On the other hand, the overall reduced number of flower buds suggests an effect of *PhGI1* silencing on upstream events, possibly related *the* flower-meristem-identity genes *PETUNIA FLOWERING GENE (PFG)* and *ALF* (*ABERRANT LEAF AND FLOWER)* (Immink *et al.*, 1999; Souer *et al.*, 2008). Mutants showing a developmental arrest in flower bud development all belong to the group of gibberellin deficient mutants, including *gibberellin deficient (ga-2*) (Nester and Zeevaart, 1988) and *gib-1* (Jacobsen and Olszewski, 1991) from tomato or *ga1-1* from Arabidopsis (Goto and Pharis, 1999). The promotion of petal, stamen and anther development in Arabidopsis was proposed to occur by opposing the action of the DELLA proteins RGA, RGL1 and RGL2 (Cheng *et al.*, 2004). As mentioned above, *GI* is a negative regulator of growth, as *GI* loss of function mutants show taller plant height (Hwang *et al.*, 2011) and longer hypocotyls. However, the function of *GI* in flower development seems inverse, as flowers either aborted or showed a reduction in corolla and tube size. The reduced size was accompanied by a significant reduction in cell size, indicating that

flower size changes are, at least in part, due to a reduced cell expansion, even so we cannot rule out a possible effect over cell division. Growth of lateral organs starts with cell division, followed by cell expansion during later stages of development (Reale *et al.*, 2002; Laitinen *et al.*, 2005; Anastasiou *et al.*, 2007; Kazama *et al.*, 2010). Our results indicate that *PhGI1* function on lateral organ growth depends on the acquired meristem identity and that the growth promoting function of *PhGI1* during flower development is restricted rather to developmental stages following organ differentiation, when growth relies on cell expansion.

The floral fragrance in *Petunia hybrida* is dominated by volatile benzenoids, which mostly derive from *trans*-cinnamic acid, whose precursor is phenylalanine. The production of phenylalanine is controlled by *ODORANT1* (*ODO1*), a key volatile regulator and member of the R2R3-type *MYB* family, which controls the synthesis of precursors of the shikimate pathway (Verdonk *et al.*, 2003). The main volatile, methyl benzoate, has its maximum emission at night (Boatright *et al.*, 2004). It is produced from benzoic acid, whose synthesis might be controlled by PAL (Kolosova, Sherman, *et al.*, 2001). Wild type Petunia observed here showed a rhythmic emission pattern with maximal emission during the night and methyl benzoate continuously was the major compound throughout the day. Differences between the wild type and the silenced lines consisted 1) in a lower emission level, 2) in slight changes in the relative abundance of the *trans*-cinnamic acid derivatives benzyl alcohol, ethyl benzoate and benzyl benzoate and 3) a mayor contribution of isoeugenol to the volatile profile in the morning. Isoeugenol also derives from phenylalanine, but its direct precursor was suggested to be ferrulic

acid, produced from *trans*-cinnamic acid through coumaric acid and caffeic acid. Our finding suggest that *GI* interacts in the rhythmic fine tuning of volatile biosynthesis and the daily emission profile of volatiles derived through the phenylalanine pathway. We cannot exclude that some changes in emission quantity and quality shortly after sampling might be related to wounding, as it was shown that stress conditions and membrane damage may affect VOC generation (Loreto *et al.*, 2006).

While the plant circadian clock coordinates environmental inputs into basic processes such as primary and secondary metabolism, cell division or cell expansion, in this work we uncover undescribed functions of *PhGI1* on overall inflorescence architecture. It remains to be determined if the phenotypes found in this study are directly controlled by the clock or are specific functions resulting from neofunctionalization of *GI* genes in Petunia.

Methods

Plant material, growth conditions and sampling

Wild type *Petunia hybrida* plants of the double haploid variety 'Mitchell W115' as well as silenced lines of the T1 generation of *PhGI1* and their non-transgenic siblings were cultured using a commercial substrate (Universal Substrate, Floragard Betriebs GmbH, Oldenburg, Germany) in a growth chamber under conditions of 16 hours light/ 8 hours darkness, a light intensity of 250 µE m^{-2} s^{-1}, and a constant temperature of 26 $\pm$ 1ºC. A T2 generation of *PhG*I1 was grown in a greenhouse under natural long-day conditions. Plants were watered as

required and transplanted to fresh substrate twice during the growth phase.

Phenotyping of vegetative and generative traits, including the size of three leaves and flowers, internode length, flower number, flowering time and relative chlorophyll content was performed. Parameters were evaluated from three wild type plants and 2-3 plants of each *iRNA::PhGI1* line. Of each autopollinated T1 plant, T2 plants were propagated, of which were characterized at least three plants per silenced line, in order to confirm the RNA interference associated phenotypes.

For *PhGI1* expression analysis, as well as other circadian rhythm related genes, three samples of young leaves, from each of the three independent *iRNA::PhGI1* transgenic lines as well as wild type plants, were sampled under the aforementioned growth chamber conditions. Tissue sampling was performed every three hours. For the analysis of the expression under continuous darkness, plants were initially acclimated during 4-5 days to conditions of 16 hours of light / 8 hours of darkness, after which we proceeded to keep the plants in continuous darkness for 24 consecutive hours. The collected tissues were immediately frozen in liquid nitrogen and stored at –80° C until further analysis. To measure the progress of time in hours, we used the ZEITGEBER time scale. The term ZEITGEBER, from the German "time giver", is often used to indicate an external environmental factor capable of synchronizing the biological clock of an organism. We considered ZEITGEBER 0 (ZT0) as the time lights were turned on.

For the analysis of VOC profiles, we sampled three flowers per plant at 2-3 days after flower opening at ZT0. The measurement of VOC

emission was performed as described previously (Manchado-Rojo *et al.*, 2012; Ruíz-Ramón *et al.*, 2014). Briefly, flowers were placed in a glass beaker with a solution of 4% of glucose inside a desiccator and emitted volatiles were collected using the SPME methods from the headspace during 24 hours as well as every three hours during 24 hours under 16h/8h photoperiod, followed by GM/CS. Volatiles were expressed as integrated peak area divided by flower fresh weight (Ruiz-Hernández *et al.*, 2018). VOCs that contribute with at least 2% to the total emission are considered as main VOCs.

Silencing of *PhGI1*: Generation of vector constructs and transformation

For vector construction, we selected a fragment of the 3' untranslated region of *PhGI1* that would discriminate between *PhGI1* and *PhGI2*. The sequence information for the comparison between *PhGI1* and *PhGI2* was obtained from the genomic clones *PhGI1* (Peaxi132Scf1428Ctg026) and *PhGI2* (Peaxi132Scf1428Ctg060) identified in *P. hybrida* W115 (Fig. S1). Based on this comparison, we selected a DNA fragment of 225bp from *PhGI1*, that showed maximal sequence difference with *PhGI2* (Figure S2) and this fragment was PCR-amplified using site-specific primers containing the attB1 and attB2 sites for Gateway® recombination (Helliwell and Waterhouse, 2003). Genomic DNA was used as template for all fragment amplification. Each fragment was first recombined into the entry vector pDONR201 (Invitrogen) and then recombined into the final destination vector pHELLSGATE12 in order to obtain hairpin-like structures. All primers used for plasmids generation are listed in Table S6.

The W115 Mitchell double haploid was transformed as described before (Manchado-Rojo *et al.*, 2014) using *Agrobacterium tumefaciens* strain EHA105. Shoots, developed under selective conditions, were confirmed as transformed through PCR detection of the selection marker gene *nptII* (T0, T1) and DNA blot analysis (T0) with a *npt*II DIG-labeled DNA probe (Figure S4) (Southern, 1975).

Circadian gene expression analysis

Total RNA from leaves was isolated using a phenol:chloroform based protocol (Box *et al.*, 2011). Following spectrophotometric quantification (NanoDrop2000), equal amounts of RNA were used to synthesize cDNA according to the manufacturer's instructions (Maxima First Strand cDNA Synthesis Kit for RT-qPCR, with dsDNase (https://www.thermofischer.com/, catalog number: K1641).

The gene *ACTIN 11 (ACT),* previously selected as valuable housekeeping gene for Petunia leaves and petals under circadian conditions (Terry, Carrera-Alesina, *et al.*, 2019) was used as reference gene for relative expression quantification of clock genes. Primers for *PhGI1*, *PhGI2* and other clock genes (Table S6) were designed using pcrEfficiency software (Mallona *et al.*, 2011). Quantitative PCR and melting point analysis were performed as described previously (Terry, Pérez-Sanz, Díaz-Galián, *et al.*, 2019). Three biological and two technical replicas were analyzed for each sample.

Chlorophyll content

Chlorophyll content was determined in basal, medium and apical leaves of wild type plants and three silenced lines of *PhGI1* from T1 generation kept under 16:8 LD light regime. Relative chlorophyll

content was calculated using a CM-500 Chlorophyll Meter based on measuring light penetration coefficient in a two wavelength range corresponding to red light and IR light.

Scanning electron microscopy analysis

We observed petal cell size in the corolla and the floral tube of silenced lines from T1 generation and non-transgenic siblings. The two areas were separated with a scalpel blade. From the corolla, we prepared two zones for further analysis of cell size, the distal outer zone and a proximal zone near the tube. Petal sections had a size of approximately 0.75 cm^2. Cell size was calculated measuring the area of 50 cells from 3 different flowers of 3 plants by using the program ImageJ (ttps://imagej.nih.gov/ij/download.html).

The floral meristems were sampled from flowers of *GI1* silenced line from both positions, those that develop into mature flowers and those that develop into aborted flowers. Preparation of flower buds for scanning electron microscopy consisted in the removal of the sepals. All tissues were dehydrated as previously described (Delgado-Benarroch *et al.*, 2009), followed by critical point drying.

Data analysis procedures

Expression of circadian genes relative to the reference genes was analyzed applying the comparative CT method (Schmittgen and Livak, 2008) as well as using group-wise comparison with the REST Program (Pfaffl *et al.*, 2002). The JTK Cycle algorithm from the METACYCLE R package (R version 3.3.2) (Hughes *et al.*, 2010; Wu *et al.*, 2016) was applied in order to detect rhythmicity in gene expression. Significance

differences among data were determined based on Fisher´s F-test and Student´s T-Test after testing data for non-normal distributions.

Funding

This research was funded by Fundación Seneca 19398/PI/14, 19895/GERM/15 and MC BFU-2017 88300-C2-1-R and BFU-2017 88300-C2-2-R.

Acknowledgments

We would like to acknowledge María José Roca and Julia Muñoz for technical assistance.

REFERENCES

Adams, S., Manfield, I., Stockley, P. and Carré, I.A. (2015) Revised Morning Loops of the Arabidopsis Circadian Clock Based on Analyses of Direct Regulatory Interactions. *PLoS ONE*, **10**. Available at: https://www.ncbi.nlm.nih.gov/pmc/articles/PMC4666590/ [Accessed February 8, 2019].

Anastasiou, E., Kenz, S., Gerstung, M., MacLean, D., Timmer, J., Fleck, C. and Lenhard, M. (2007) Control of Plant Organ Size by KLUH/CYP78A5-Dependent Intercellular Signaling. *Dev. Cell*, **13**, 843–856.

Atamian, H.S., Creux, N.M., Brown, E.A., Garner, A.G., Blackman, B.K. and Harmer, S.L. (2016) Circadian regulation of sunflower heliotropism, floral orientation, and pollinator visits. *Science*, **353**, 587–590.

Bancos, S., Szatmári, A.-M., Castle, J., Kozma-Bognár, L., Shibata, K., Yokota, T., Bishop, G.J., Nagy, F. and Szekeres, M. (2006) Diurnal Regulation of the Brassinosteroid-Biosynthetic *CPD* Gene in Arabidopsis. *Plant Physiol.*, **141**, 299–309.

Bélanger, G. and Gastal, F. (2000) Nitrogen utilization by forage grasses. *Can. J. Plant Sci.*, **80**, 11–20.

Boatright, J., Negre, F., Chen, X., et al. (2004) Understanding in Vivo Benzenoid Metabolism in Petunia Petal Tissue. *Plant Physiol.*, **135**, 1993–2011.

Bombarely, A., Moser, M., Amrad, A., et al. (2016) Insight into the evolution of the Solanaceae from the parental genomes of Petunia hybrida. *Nat. Plants*, **2**, 16074.

Box, M.S., Coustham, V., Dean, C. and Mylne, J.S. (2011) Protocol: A simple phenol-based method for 96-well extraction of high quality RNA from Arabidopsis. *Plant Methods*, **7**, 7.

Cao, S., Ye, M. and Jiang, S. (2005) Involvement of GIGANTEA gene in the regulation of the cold stress response in Arabidopsis. *Plant Cell Rep.*, **24**, 683–690.

Cha, J.-Y., Kim, J., Kim, T.-S., Zeng, Q., Wang, L., Lee, S.Y., Kim, W.-Y. and Somers, D.E. (2017) GIGANTEA is a co-chaperone which facilitates maturation of ZEITLUPE in the Arabidopsis circadian clock. *Nat. Commun.*, **8**, 3.

Cheng, H., Qin, L., Lee, S., Fu, X., Richards, D.E., Cao, D., Luo, D., Harberd, N.P. and Peng, J. (2004) Gibberellin regulates Arabidopsis floral development via suppression of DELLA protein function. *Development*, **131**, 1055–1064.

Corellou, F., Schwartz, C., Motta, J.P., Djouani-Tahri, E., Sanchez, F. and Bouget, F.Y. (2009) Clocks in the Green Lineage: Comparative Functional Analysis of the Circadian Architecture of the Picoeukaryote Ostreococcus. *Plant Cell*, **21**, 3436–3449.

Dalchau, N., Baek, S.J., Briggs, H.M., et al. (2011) The circadian oscillator gene GIGANTEA mediates a long-term response of the Arabidopsis thaliana circadian clock to sucrose. *Proc. Natl. Acad. Sci. U. S. A.*, **108**, 5104–9.

Delgado-Benarroch, L., Causier, B., Weiss, J. and Egea-Cortines, M. (2009) FORMOSA controls cell division and expansion during floral development in Antirrhinum majus. *Planta*, **229**, 1219–1229.

Ding, J., Böhlenius, H., Rühl, M.G., Chen, P., Sane, S., Zambrano, J.A., Zheng, B., Eriksson, M.E. and Nilsson, O. (2018) GIGANTEA-like genes control seasonal growth cessation in Populus. *New Phytol.*, **218**, 1491–1503.

Djouani-Tahri, E.B., Christie, J.M., Sanchez-Ferandin, S., Sanchez, F., Bouget, F.Y. and Corellou, F. (2011) A eukaryotic LOV-histidine kinase with circadian clock function in the picoalga Ostreococcus. *Plant J.*, **65**, 578–588.

Eckardt, N.A. (2008) DOT/UFO Emerges as a Key Factor in Inflorescence Patterning. *Plant Cell*, **20**, 2003–2005.

Edwards, K.D., Takata, N., Johansson, M., et al. (2018) Circadian clock components control daily growth activities by modulating cytokinin levels and cell division-associated gene expression in *Populus* trees: Control of growth in Populus. *Plant Cell Environ.*, **41**, 1468–1482.

Farré, E.M. and Weise, S.E. (2012) The interactions between the circadian clock and primary metabolism. *Curr. Opin. Plant Biol.*, **15**, 293–300.

Fenske, M.P., Hewett Hazelton, K.D., Hempton, A.K., Shim, J.S., Yamamoto, B.M., Riffell, J.A. and Imaizumi, T. (2015) Circadian clock gene *LATE ELONGATED HYPOCOTYL* directly regulates the timing of floral scent emission in *Petunia*. *Proc. Natl. Acad. Sci.*, **112**, 9775–9780.

Fenske, M.P. and Imaizumi, T. (2016) Circadian Rhythms in Floral Scent Emission. *Front. Plant Sci.*, **7**, 462.

Fowler, S., Lee, K., Onouchi, H., Samach, A., Richardson, K., Morris, B., Coupland, G. and Putterill, J. (1999) GIGANTEA: a circadian clock-controlled gene that regulates photoperiodic flowering in Arabidopsis and encodes a protein with several possible membrane-spanning domains. *EMBO J.*, **18**, 4679–4688.

Fung-Uceda, J., Lee, K., Seo, P.J., Polyn, S., Veylder, L. De and Mas, P. (2018) The Circadian Clock Sets the Time of DNA Replication Licensing to Regulate Growth in Arabidopsis. *Dev. Cell*, **45**, 101-113.e4.

Gendron, J.M., Pruneda-Paz, J.L., Doherty, C.J., Gross, A.M., Kang, S.E. and Kay, S.A. (2012) Arabidopsis circadian clock protein, TOC1, is a DNA-binding transcription factor. *Proc. Natl. Acad. Sci. U. S. A.*, **109**, 3167–72.

Goto, N. and Pharis, R.P. (1999) Role of gibberellins in the development of floral organs of the gibberellin-deficient mutant, ga1-1, of Arabidopsis thaliana. *Can. J. Bot.*, **77**, 944–954.

Gray, J.A., Shalit-Kaneh, A., Chu, D.N., Hsu, P.Y. and Harmer, S.L. (2017) The REVEILLE Clock Genes Inhibit Growth of Juvenile and Adult Plants by Control of Cell Size. *Plant Physiol.*, **173**, 2308–2322.

Helliwell, C. and Waterhouse, P. (2003) Constructs and methods for high-throughput gene silencing in plants. *Methods San Diego Calif*, **30**, 289–95.

Hughes, M.E., Hogenesch, J.B. and Kornacker, K. (2010) JTK_CYCLE: an efficient nonparametric algorithm for detecting rhythmic components in genome-scale data sets. *J. Biol. Rhythms*, **25**, 372–380.

Hwang, I., Park, J., Lee, B. and Cheong, H. (2011) Loss of Function in GIGANTEA Gene is Involved in Brassinosteroid Signaling. , **4**, 8.

Immink, R.G., Hannapel, D.J., Ferrario, S., Busscher, M., Franken, J., Lookeren Campagne, M.M. and Angenent, G.C. (1999) A petunia MADS box gene involved in the transition from vegetative to reproductive development. *Dev. Camb. Engl.*, **126**, 5117–5126.

Ito, S., Song, Y.H. and Imaizumi, T. (2012) LOV Domain-Containing F-Box Proteins: Light-Dependent Protein Degradation Modules in Arabidopsis. *Mol. Plant*, **5**, 573–582.

Jackson, A.L., Bartz, S.R., Schelter, J., Kobayashi, S. V, Burchard, J., Mao, M., Li, B., Cavet, G. and Linsley, P.S. (2003) Expression profiling reveals off-target gene regulation by RNAi. *Nat. Biotechnol.*, **21**, 635–637.

Jacobsen, S.E. and Olszewski, N.E. (1991) Characterization of the Arrest in Anther Development Associated with Gibberellin Deficiency of the gib-1 Mutant of Tomato. *Plant Physiol.*, **97**, 409–414.

Jung, J.-H., Seo, Y.-H., Seo, P.J., Reyes, J.L., Yun, J., Chua, N.-H. and Park, C.-M. (2007) The GIGANTEA Regulated MicroRNA172 Mediates Photoperiodic Flowering Independent of *CONSTANS* in *Arabidopsis*. *Plant Cell*, **19**, 2736–2748.

Kazama, T., Ichihashi, Y., Murata, S. and Tsukaya, H. (2010) The Mechanism of Cell Cycle Arrest Front Progression Explained by a KLUH/CYP78A5-dependent Mobile Growth Factor in Developing Leaves of Arabidopsis thaliana. *Plant Cell Physiol.*, **51**, 1046–1054.

Kikis, E.A., Khanna, R. and Quail, P.H. (2005) ELF4 is a phytochrome-regulated component of a negative-feedback loop involving the central oscillator components CCA1 and LHY. *Plant J.*, **44**, 300–313.

Kim, W.-Y., Fujiwara, S., Suh, S.-S., et al. (2007) ZEITLUPE is a circadian photoreceptor stabilized by GIGANTEA in blue light. *Nature*, **449**, 356–360.

Kim, Y., Lim, J., Yeom, M., Kim, H., Kim, J., Wang, L., Kim, W.Y., Somers, D.E. and Nam, H.G. (2013) ELF4 Regulates GIGANTEA Chromatin Access through Subnuclear Sequestration. *Cell Rep.*, **3**, 671–677.

Kim, Y., Yeom, M., Kim, H., Lim, J., Koo, H.J., Hwang, D., Somers, D. and Nam, H.G. (2012) GIGANTEA and EARLY FLOWERING 4 in Arabidopsis Exhibit Differential Phase-Specific Genetic Influences over a Diurnal Cycle. *Mol. Plant*, **5**, 678–687.

Kolosova, N., Sherman, D., Karlson, D. and Dudareva, N. (2001) Cellular and Subcellular Localization of *S* -Adenosyl-l-Methionine:Benzoic Acid Carboxyl Methyltransferase, the Enzyme Responsible for Biosynthesis of the Volatile Ester Methylbenzoate in Snapdragon Flowers. *Plant Physiol.*, **126**, 956–964.

Kubota, A., Kita, S., Ishizaki, K., Nishihama, R., Yamato, K.T. and Kohchi, T. (2014) Co-option of a photoperiodic growth-phase transition system during land plant evolution. *Nat. Commun.*, **5**, 3668.

Laitinen, R.A.E., Immanen, J., Auvinen, P., et al. (2005) Analysis of the floral transcriptome uncovers new regulators of organ determination and gene families related to flower organ differentiation in Gerbera hybrida (Asteraceae). *Genome Res.*, **15**, 475–486.

Linde, A., Eklund, D.M., Kubota, A., et al. (2017) Early evolution of the land plant circadian clock. *New Phytol.*

Lonardi, S., Muñoz-Amatriaín, M., Liang, Q., et al. (2019) The genome of cowpea (Vigna unguiculata [L.] Walp.). *Plant J.*, **98**, 767–782.

Loreto, F., Barta, C., Brilli, F. and Nogues, I. (2006) On the induction of volatile organic compound emissions by plants as consequence of wounding or fluctuations of light and temperature. *Plant Cell Environ.*, **29**, 1820–1828.

Lu, S.X., Webb, C.J., Knowles, S.M., Kim, S.H.J., Wang, Z. and Tobin, E.M. (2012) CCA1 and ELF3 Interact in the control of hypocotyl length and flowering time in Arabidopsis. *Plant Physiol.*, **158**, 1079–88.

Mallona, I., Weiss, J. and Egea-Cortines, M. (2011) pcrEfficiency: a Web tool for PCR amplification efficiency prediction. *BMC Bioinformatics*, **12**, 404.

Manchado-Rojo, M., Delgado-Benarroch, L., Roca, M.J., Weiss, J. and Egea-Cortines, M. (2012) Quantitative levels of Deficiens and Globosa during late petal development show a complex transcriptional network topology of B function. *Plant J. Cell Mol. Biol.*, **72**, 294–307.

Manchado-Rojo, M., Weiss, J. and Egea-Cortines, M. (2014) Validation of Aintegumenta as a gene to modify floral size in ornamental plants. *Plant Biotechnol. J.*, **12**.

Marcolino-Gomes, J., Rodrigues, F.A., Fuganti-Pagliarini, R., et al. (2014) Diurnal Oscillations of Soybean Circadian Clock and Drought Responsive Genes N. Cermakian, ed. *PLoS ONE*, **9**, e86402.

Más, P. (2005) Circadian clock signaling in Arabidopsis thaliana: from gene expression to physiology and development. *Int. J. Dev. Biol.*, **49**, 491–500.

Más, P., Alabadí, D., Yanovsky, M.J., Oyama, T. and Kay, S.A. (2003) Dual Role of TOC1 in the Control of Circadian and Photomorphogenic Responses in Arabidopsis. *Plant Cell*, **15**, 223–236.

Más, P., Kim, W.-Y., Somers, D.E. and Kay, S.A. (2003) Targeted degradation of TOC1 by ZTL modulates circadian function in Arabidopsis thaliana. *Nature*, **426**, 567–570.

Mizoguchi, T., Wright, L., Fujiwara, S., et al. (2005) Distinct Roles of *GIGANTEA* in Promoting Flowering and Regulating Circadian Rhythms in Arabidopsis. *Plant Cell*, **17**, 2255–2270.

Montaigu, A. de, Tóth, R. and Coupland, G. (2010) Plant development goes like clockwork. *Trends Genet.*, **26**, 296–306.

Morant, P.E., Thommen, Q., Pfeuty, B., Vandermoere, C., Corellou, F., Bouget, F.Y. and Lefranc, M. (2010) A robust two-gene oscillator at the core of Ostreococcus tauri circadian clock. *Chaos*, **20**.

Nester, J.E. and Zeevaart, J.A.D. (1988) FLOWER DEVELOPMENT IN NORMAL TOMATO AND A GIBBERELLIN-DEFICIENT (ga-2) MUTANT. *Am. J. Bot.*, **75**, 45–55.

Ni, Z., Kim, E.-D., Ha, M., Lackey, E., Liu, J., Zhang, Y., Sun, Q. and Chen, Z.J. (2009) Altered circadian rhythms regulate growth vigour in hybrids and allopolyploids. *Nature*, **457**, 327–331.

Nozue, K., Covington, M.F., Duek, P.D., Lorrain, S., Fankhauser, C., Harmer, S.L. and Maloof, J.N. (2007) Rhythmic growth explained by coincidence between internal and external cues. *Nature*, **448**, 358–361.

Park, D.H., Somer David E., Kim Yang Suk, Choy Yoon Hi, Lim Hee Kyun, Soh Moon Soo, Kim Hyo Jung, Kay Steve A. and Nam Hong Gil (1999) Control of Circadian Rhythms and Photoperiodic Flowering by the Arabidopsis GIGANTEA Gene. *Science*, **285**, 1579–1582.

Park, H.J., Kim, W.-Y. and Yun, D.-J. (2013) A role for GIGANTEA: Keeping the balance between flowering and salinity stress tolerance. *Plant Signal. Behav.*, **8**, e24820.

Pfaffl, M.W., Horgan, G.W. and Dempfle, L. (2002) Relative expression software tool (REST©) for group-wise comparison and statistical analysis of relative expression results in real-time PCR. *Nucleic Acids Res.*, **30**, 10.

Pokhilko, A., Fernández, A.P., Edwards, K.D., Southern, M.M., Halliday, K.J. and Millar, A.J. (2012) The clock gene circuit in Arabidopsis includes a repressilator with additional feedback loops. *Mol. Syst. Biol.*, **8**. Available at: http://msb.embopress.org/cgi/doi/10.1038/msb.2012.6 [Accessed June 7, 2019].

Reale, L., Porceddu, A., Lanfaloni, L., Moretti, C., Zenoni, S., Pezzotti, M., Romano, B. and Ferranti, F. (2002) Patterns of cell division and expansion in developing petals of Petunia hybrida. *Sex. Plant Reprod.*, **15**, 123–132.

Rebocho, A.B., Bliek, M., Kusters, E., Castel, R., Procissi, A., Roobeek, I., Souer, E. and Koes, R. (2008) Role of EVERGREEN in the Development of the Cymose Petunia Inflorescence. *Dev. Cell*, **15**, 437–447.

Rijpkema, A.S., Vandenbussche, M., Koes, R., Heijmans, K. and Gerats, T. (2010) Variations on a theme: Changes in the floral ABCs in angiosperms. *Semin. Cell Dev. Biol.*, **21**, 100–107.

Ruiz-Hernández, V., Roca, M.J., Egea-Cortines, M. and Weiss, J. (2018) A comparison of semi-quantitative methods suitable for establishing volatile profiles. *Plant Methods*, **14**, 67.

Ruíz-Ramón, F., Águila, D.J., Egea-Cortines, M. and Weiss, J. (2014) Optimization of fragrance extraction: Daytime and flower age affect scent emission in simple and double narcissi. *Ind. Crops Prod.*, **52**.

Sawa, M. and Kay, S.A. (2011) GIGANTEA directly activates Flowering Locus T in Arabidopsis thaliana. *Proc. Natl. Acad. Sci.*, **108**, 11698–11703.

Schmittgen, T.D. and Livak, K.J. (2008) Analyzing real-time PCR data by the comparative CT method. *Nat. Protoc.*, **3**, 1101–1108.

Somers, D.E., Schultz, T.F., Milnamow, M. and Kay, S.A. (2000) ZEITLUPE Encodes a Novel Clock-Associated PAS Protein from Arabidopsis. *Cell*, **101**, 319–329.

Souer, E., Krol, A. van der, Kloos, D., Spelt, C., Bliek, M., Mol, J. and Koes, R. (1998) Genetic control of branching pattern and floral identity during Petunia inflorescence development. *Development*, **125**, 733–742.

Souer, E., Rebocho, A.B., Bliek, M., Kusters, E., Bruin, R.A.M. de and Koes, R. (2008) Patterning of Inflorescences and Flowers by the F-Box Protein DOUBLE TOP and the LEAFY Homolog ABERRANT LEAF AND FLOWER of Petunia. *Plant Cell*, **20**, 2033–2048.

Southern, E.M. (1975) Detection of specific sequences among DNA fragments separated by gel electrophoresis. *J. Mol. Biol.*, **98**, 503–517.

Soy, J., Leivar, P., González-Schain, N., Martín, G., Diaz, C., Sentandreu, M., Al-Sady, B., Quail, P.H. and Monte, E. (2016) Molecular convergence of clock and photosensory pathways through PIF3–TOC1 interaction and co-occupancy of target promoters. *Proc. Natl. Acad. Sci.*, 201603745.

Staiger, D., Shin, J., Johansson, M. and Davis, S.J. (2013) The circadian clock goes genomic. *Genome Biol.*, **14**, 208.

Szittya, G., Silhavy, D., Molnár, A., Havelda, Z., Lovas, Á., Lakatos, L., Bánfalvi, Z. and Burgyán, J. (2003) Low temperature inhibits RNA silencing-mediated defence by the control of siRNA generation. *EMBO J.*, **22**, 633–640.

Terry, M.I., Carrera-Alesina, M., Weiss, J. and Egea-Cortines, M. (2019) *Molecular and transcriptional structure of the petal and leaf circadian clock in Petunia hybrida*, Plant Biology. Available at: http://biorxiv.org/lookup/doi/10.1101/641639 [Accessed July 19, 2019].

Terry, M.I., Pérez-Sanz, F., Díaz-Galián, M.V., Pérez de los Cobos, F., Navarro, P.J., Egea-Cortines, M. and Weiss, J. (2019) The Petunia CHANEL Gene is a ZEITLUPE Ortholog Coordinating Growth and Scent Profiles. *Cells*, **8**, 343.

Terry, M.I., Pérez-Sanz, F., Navarro, P.J., Weiss, J. and Egea-Cortines, M. (2019) The Snapdragon LATE ELONGATED HYPOCOTYL Plays A Dual Role in Activating Floral Growth and Scent Emission. *Cells*, **8**, 920.

Thines, B. and Harmon, F.G. (2011) Four easy pieces: mechanisms underlying circadian regulation of growth and development. *Curr. Opin. Plant Biol.*, **14**, 31–37.

Tseng, T.-S. (2004) SPINDLY and GIGANTEA Interact and Act in Arabidopsis thaliana Pathways Involved in Light Responses, Flowering, and Rhythms in Cotyledon Movements. *PLANT CELL ONLINE*, **16**, 1550–1563.

Verdonk, J.C., Ric de Vos, C.H., Verhoeven, H.A., Haring, M.A., Tunen, A.J. van and Schuurink, R.C. (2003) Regulation of floral scent production in petunia revealed by targeted metabolomics. *Phytochemistry*, **62**, 997–1008.

Weiss, Julia., Terry, M.Isabel., Martos-Fuentes, M., et al. (2018) Diel pattern of circadian clock and storage protein gene expression in leaves and during seed filling in cowpea (Vigna unguiculata). *BMC Plant Biol.*, **18**, 33–53.

Wu, G., Anafi, R.C., Hughes, M.E., Kornacker, K. and Hogenesch, J.B. (2016) MetaCycle: an integrated R package to evaluate periodicity in large scale data. *Bioinformatics*, **32**, 3351–3353.

Yon, F., Joo, Y., Cortés Llorca, L., Rothe, E., Baldwin, I.T. and Kim, S. (2015) Silencing Nicotiana attenuata LHY and ZTL alters circadian rhythms in flowers. *New Phytol.*, **209**, 1058–1066.

Yon, F., Seo, P.-J., Ryu, J., Park, C.-M., Baldwin, I.T. and Kim, S.-G. (2012) Identification and characterization of circadian clock genes in a native tobacco, Nicotiana attenuata. *BMC Plant Biol.*, **12**, 172.

CHAPTER 2 - Phenotypic- and expression analysis of *GIGANTEA* paralog *GI2* in *iRNA::PhGI2* silenced *Petunia x hybrida* plants reveals both sub- and neofunctionalizations with respect to paralog *GI1*

Abstract

The gene *GIGANTEA* is duplicated in *Petunia x hybrida*. We analyzed the effect of silencing *PhGI2* by hairpin RNAs in Petunia. Decreased levels of *PhGI2* did not affect the rhythmicity parameters: amplitude, phase and period for the clock genes *PhGI1, PhGI2, PhCHL, PhELF4.* However, it caused delayed time period between two consecutive peaks for *PhTOC1*, confirming its role in maintaining circadian rhythmicity. Silencing of *PhGI2* led to a modified branching pattern as well as internode length and leaf size. Depending on growth conditions, branch type and position within the plant, were either promoted or reduced, indicating that the regulation over vegetative growth by *PhGI2* depends on ontogeny and environmental context. In accordance to *GI* function reported for other plants, silencing of *PhGI2* resulted in delayed flowering. We also observed a reduced flower bud number and the appearance of prematurely aborting ectopic flower buds. Additionally, silencing of *PhGI2* caused growth inhibition in floral corolla and tube as a result of decreased cell size. The smaller flowers emitted 19% less volatiles over 24 hours on fresh weight basis. While methyl benzoate consistently formed the major VOC compound, VOC profiles differed especially concerning the relative contribution of isoeugenol and nonanal at specific time points. On the light of previous

results of *PhGI1* function, we can conclude that the *PhGI* paralogs experienced both sub- and neofunctionalizations. Common features consist in the repression of growth of vegetative plant organs, maintenance of the typical cymose inflorescence structure, inhibition of premature flower abortion and promotion of petal growth by cell expansion. A divergent function consists in the promotion of transition to flowering and an environmentally dependent growth habit that appears to be controlled by *PhGI2* and not *PhGI1.*

Introduction

The coordination of plant development with the environment occurs via the plant circadian clock. A common set of genes found in the picoeukariote *Ostreococcus* all the way to higher plants include a MYB transcription factor like *LATE ELONGATED HYPOCOTYL (LHY*), a *PSEUDO RESPOSE REGULATOR (TOC1)*, and a blue light receptor similar to ZEITLUPE (ZTL) (Corellou *et al.*, 2009; Bouget *et al.*, 2011). Early in the evolution of land plants, the genetic structure of the plant circadian clock became more complex. The clock components are interlocked by multiple feedback loops (McClung, 2006; Staiger *et al.*, 2013). The central feedback loop is formed of two MYB domain transcription factors, *CIRCADIAN CLOCK ASSOCIATED 1 (CCA1)* and *LHY* together with *TOC1.* The expression of *CCA1*, *LHY* and *TOC*1 is coordinated by mutual negative regulation through binding to its corresponding promoters (Alabadi *et al.*, 2001). Another negative feedback loop exists between *CCA1* and *LHY* and the *PSEUDO-RESPONSE REGULATORs* (*PRRs*) 9,7 and 5 (Adams *et al.*, 2015). The

feedback loops ensure expression peaks of the different clock genes at specific times of the day.

The evening loop is composed of *EARLY FLOWERING 3 and 4 (ELF3 and ELF4)* and *LUX ARHYTHMO (LUX).* The protein ZTL, which receives light input through its blue-light sensing domain, interacts with the circadian clock by degrading the central clock protein TOC1 (Más, Kim, *et al.*, 2003), a process that requires stabilization of the ZTL protein through GIGANTEA (GI) (Cha *et al.*, 2017).

Whole genome sequencing and assembly of the *Petunia x hybrida* parents, *P. axillaris* and *P. inflata,* allowed a comprehensive comparison of the *Solanaceae* clock structure to Arabidopsis. Genome analysis revealed that two hexaploidization events had occurred in the solanaceous species and while the general configuration of the circadian clock is conserved compared to Arabidopsis, a certain level of restructuring and a change of clock gene copy number was observed (Bombarely *et al.*, 2016). Clock gene functions have been analyzed in many plants other than Arabidopsis, including related *Brassica* species, legumes and CAM plants (Brachi *et al.*, 2010; Mallona *et al.*, 2011; Lou *et al.*, 2012; Weller *et al.*, 2012; Zakhrabekova *et al.*, 2012; Marcolino-Gomes *et al.*, 2014; Müller *et al.*, 2016) and results indicate that modifications within the clock might be responsible for the adaption to differing environmental conditions.

Gene duplication and gene neofunctionalization are suggested to be related events, when a gene copy assumes a new function as a consequence of an adaptive evolutionary process but without negatively affecting the fitness of the organism since the ancestral function is maintained in the other copy (Rastogi and Liberles, 2005).

Indeed, despite the paleohexaploidy shared by all Solanaceae, gene duplication is not uniform for all clock genes and species, indicating that maintenance of copy mutants depends on the specific species and the ecological niche that it occupies (Bombarely *et al.*, 2016).

Duplicated clock genes in Petunia include *GI, ELF3, ELF4* as well as *TOC1, PRR7and PRR5* (Bombarely *et al.*, 2016). The gene *GI* (Park *et al.*, 1999) is involved in the control of circadian rhythm, taking part in the post-translational processes comprising the circadian oscillator. GI stabilizes the F-box protein ZTL, a key regulator of the circadian clock. Its protein chaperone activity facilitates ZTL maturation into an active form. ZTL specifies an evening-phased E3 ubiquitin ligase (SCF^{ZTL}) that targets TOC1 for proteasomal degradation. ZTL possesses a blue-light sensing LOV (LIGHT, OXYGEN, VOLTAGE) domain at the N-terminus and GI interacts with this domain to post-translationally stabilize ZTL under blue light (Ito *et al.*, 2012).

The biological functions of *GI* include other aspects of plant development and plant physiology, including hypocotyl elongation (Tseng, 2004) stem length and leave growth (Hwang *et al.*, 2011), the control over photoperiod-mediated flowering (Sawa and Kay, 2011), and *miRNA* processing (Jung *et al.*, 2007). Thus, mutants of *GI*, show very diverse phenotypes, one of them being late flowering (Mishra and Panigrahi, 2015).

The control of *GI* over flowering was intensively analyzed in Arabidopsis, where certain mutants are late flowering (Mishra and Panigrahi, 2015) while over-expression of *AtGI* promotes flowering (Fowler *et al.*, 1999). The photoperiodic control functions through the

GI interaction with the regulatory module comprising the genes *CONSTANS (CO)* and *FLOWERING LOCUS T (FT).* CO is the key regulator of photoperiodic flowering and induces the expression of the floral *integrator FLOWERING LOCUS T* (*FT*) gene in a light-dependent manner. In the late afternoon under long days, GI forms a complex with FLAVIN-BINDING, KELCH REPEAT, F-BOX 1 (FKF1) and this interaction is induced by blue light absorbed by the LOV domain of FKF1. This complex interacts with a *CO* repressor, *CYCLING DOF FACTOR 1 (CDF1),* leading to lowest CDF1 protein levels at late afternoon, a rise in *CO* expression and finally light induced *FT* expression. GIGANTEA complex formation is therefore required for day-length measurement in Arabidopsis (Sawa *et al.*, 2007). Another *CO* independent control over flowering involving *GI* is related to *miRNA* processing. The control system consists in the upregulation of *FT by* miR172, whose abundance in turn is regulated via *GI*-mediated miRNA processing (Jung *et al.*, 2007).

The function of *GI* in controlling flowering time observed in Arabidopsis is conserved over a number of species. Transition from vegetative to reproductive growth requires *MpGI* in the basal angiosperm *Marchantia polymorpha* (Kubota *et al.*, 2014). In soybean, the *GIGANTEA* ortholog *GmGIa,* controls flowering time by inducing the expression of the soybean florigen gene ortholog*, GmFT2a*. In rice (*Oryza sativa*), a quantitative short day species, over-expression of the *GIGANTEA* gene (*OsGI*) inhibits flowering and this is consistent with the fact that in rice, *FT* is repressed by the *CO* ortholog *Hd1* (Hayama *et al.*, 2003). In barley, an upregulation of *HvGI* observed in *HvELF3* mutants resulted in an early flowering phenotype (Zakhrabekova *et al.*, 2012). In *Zea mays*, which has two circadian regulated *GI* paralogs (Khan *et al.*,

2010), *ZmGI1* is higher expressed in leaves than *ZmGI2*. *ZmGI1* mutants are characterized by early flowering, increased plant height and altered timing of the vegetative phase (Bendix *et al.*, 2013) while no information on *GI2* function exists. Similar to *GI* in Maize, the expression of one paralog, *PhGI1*, is double that of *PhGI2* in leaves from Petunia (Brandoli *et al.*, 2020). Silencing of *GI1* conferred several typical *gi* mutant phenotypes observed in other species, including increased internode length and leaf size. However, plants were not early flowering and showed a novel flower phenotype, consisting in reduced flower number, ectopic flower bud development, increased premature flower abortion and reduced flower size.

In this chapter, we have characterized the *Petunia x hybrida GI* paralog *PhGI2*, creating loss of function plants using hairpin RNA constructs of *PhGI2.* These data were compared to findings obtained from silencing the other *GI* paralog, *PhGI1,* following a similar approach (Brandoli *et al.*, 2020), in order to establish the level of re-functionalization among the two homologs. Our results indicate that *PhGI2* shares functions with *PhGI1*, including the promotion of vegetative and flower growth, the prevention of ectopic flower bud production and premature flower abortion as well as a control over floral scent composition. In contrast to *PhGI1*, *PhGI2* also controls lateral branching, flowering time as well as the rhythmicity of volatile emission.

Methods

Design of the RNAi construct and silencing

We obtained the *PhGI2* coding region from the genome sequence of *Petunia x hybrida* W115 (Bombarely *et al.*, 2016). The coding gene model corresponds to Peaxi162Scf00160g01744.1. We developed a hairpin construct that would discriminate *PhGI2* from *PhGI1* for the vector construction. Site-specific primers (Table S7) with the attB1 and attB2 sites for Gateway® recombination, were used to PCR-amplify a DNA fragment of 208 bp (Helliwell and Waterhouse, 2003).

To obtain an RNA hairpin structure, the *PhGI2* fragment was first recombined into the entry vector pDONR201 (Invitrogen) and then into the final destination vector pHELLSGATE 12. Integrity of the construct was confirmed through PCR amplification and visualization on 1% agarose gel.

Plant material, transformation and sampling

Seeds of *Petunia x hybrida* of the double haploid variety 'Mitchell W115' were collected. *In vitro* germinated plants were used as the wild type controls and as the source of explants for plant transformation. The disarmed *Agrobacterium tumefaciens* strain EHA105 was used for transformation as previously described (Manchado-Rojo *et al.*, 2014). Plant stable transformation was confirmed through PCR detection of the *nptII* selection marker gene on the shoots of T0, T1 and T2 generations, as well as DNA blot analysis (T0) (Figure S4) (Southern, 1975).

Three independent T0 lines RNAi::*PhGI2* were selected for further studies. The T1 generation of wild type plants as well as silenced lines

of the *PhGI2*, were cultured in a growth chamber under controlled conditions of 16 hours of light/8 hours of darkness (16:8 LD), luminous intensity of 250 μE m^{-2} s^{-1} and a constant temperature of 26 ± 1° C. Each selected T1 line was autopollinated and T2 plants were cultured in a greenhouse under natural long-day conditions.

Phenotypic analysis

At least three T1 and T2 plants were characterized for each line to analyze the phenotypes associated with *GI2* RNA interference.

The analysis of volatile organic emission compounds (VOCs) were performed analyzing three flowers from wild type plants and 2 plants of 2 silenced lines after 2-3 days after anthesis. The study was performed as described in (Manchado-Rojo *et al.*, 2012; Ruíz-Ramón *et al.*, 2014).

Analysis of the circadian gene expression

A phenol:chloroform based protocol was used to isolate total RNA from leaves (Box *et al.*, 2011) followed by spectrophotometric quantification (NanoDrop2000). Equal amounts of RNA were used to synthesize cDNA according to the manufacturer's instructions (Maxima First Strand cDNA Synthesis Kit for RT-qPCR, with dsDNase, https://www.thermofischer.com/, catalog number: K1641). Three biological and two technical replicas were analyzed for each sample in quantitative PCR analysis. The qPCR and melting point analysis were performed as described in (Terry, Pérez-Sanz, Díaz-Galián, *et al.*, 2019). The gene *ACTIN* 11 (*ACT*), was used as the endogenous reference gene for relative expression quantification, after confirmation as a reliable housekeeping gene for Petunia leaves and petals under circadian

conditions (Terry, Pérez-Sanz, Díaz-Galián, *et al.*, 2019). All the primers used for RT-qPCR (Table S7) were designed using pcrEfficiency software (Mallona *et al.*, 2011).

One or two plants of each of the three independent iRNA::*PhGI2* T1 lines, as well as wild type plants, were cultured and sampled under the conditions of the aforementioned growth chamber. ZEITGEBER Time 0 (ZT0) was considered as the time when the light was turned on. For the analysis of the *PhGI2* and *PhGI1* gene expression, and other circadian rhythm genes, at least three young leaves per plant were sampled every three hours during 24 hours. For the analysis of gene expression under continuous darkness, three wild type plants and 2 plants from 2 silenced lines were cultured during 4-5 days under a 16:8 LD photoperiod, and after that plants were cultured in continuous darkness for consecutive 24 hours.

The collected tissues were immediately frozen in liquid nitrogen and stored at –80°C until further analysis.

Analysis of the chlorophyll content

Relative chlorophyll content was determined on at least three biological replicates in basal, median and apical leaves of wild type plants, non-transgenic sibling and the silenced lines of *PhGI2* from T1 generation, cultured under 16:8 LD condition. The CM-500 Chlorophyll Meter was used to calculate the relative chlorophyll content, based on the light penetration coefficient in a 2-wavelength range corresponding to red light and IR light.

Scanning electron microscopy analysis

The size of the cells of the petals of the floral tube and of two regions of the corolla, the distal external area and a proximal area near the tube, of the wild type and silenced lines of T1 generation were analyzed. Areas of about 0.75 cm^2 were selected and the cell size was calculated by measuring the area of 50 cells per analyzed area belonging to 3 different flowers of 3 different plant, using the ImageJ program (https: //imagej.nih.gov /ij/download.html).

The floral meristems were sampled from both flowers, those that develop into mature ones and those that develop into aborted ones. The preparation of flower buds for scanning electron microscopy was performed as described in (Delgado-Benarroch *et al.*, 2009) through dehydration in alcohol, followed by critical point drying.

Data analysis

The relative gene expression of the circadian genes, relative to the reference gene *ACT*, was calculated applying the comparative CT method (Schmittgen and Livak, 2008) as well as using group-wise comparison with the REST Program (Pfaffl *et al.*, 2002).

To detect rhythmicity in gene expression, we applied the JTK Cycle algorithm from the METACYCLE R package (R version 3.3.2) (Hughes *et al.*, 2010; Wu *et al.*, 2016). Significance differences among data were determined based on Fisher´s F-test and Student´s T-Test after data transformation to fit to a normal distribution.

Results

Hairpin construct targeting PhGI2 caused a reduction on the *PhGI*2 and *PhGI*1 relative expression.

In order to evaluate the effect of *PhGI2* knock-down on the expression pattern and rhythmicity of the two *GI* orthologues, *PhGI1* and *PhGI2*, as well as the other clock related genes, we performed a time series analysis of gene expression pattern at 3-hours intervals under long photoperiods (16:8 LD). We also analyzed the genes relative expression under free running conditions of continuous darkness. The *PhGI2* construct for the gene knock-down was designed here in a manner that would prevent cross silencing with *PhGI1* (chapter 1 - Brandoli *et al.*, 2020). The paralog *PhGI*2 corresponds to the published *PhGI* and analyzed previously under free running conditions in Petunia (Fenske *et al.*, 2015) (see alignment Figure S1 Chapter 1). Figure 20a and b show the expression pattern of *PhGI2* and *PhGI1* for wild type plants as well as three T0 iRNA::*PhGI*2 silenced lines 4, 6 and 7, including (T1) plants 4.2, 4.4, 6.1, 6.3 and 7.6. In wild type plants, *PhGI2* and *PhGI1* showed their peak expression at 9 hours of light (ZT9). The adjusted peak phase based on the mathematical analysis for circadian oscillation using the JTK_CYCLE algorithm coincided with ZT 10.5 (Table 5). *PhGI2* silenced lines maintained this expression pattern, but the expression level was significantly reduced both for *PhGI1* and *PhGI2*. This reduction was especially pronounced in case of *PhGI2* with an up to 8-fold expression difference, while *PhGI1* expression was reduced by about 50%. The down regulation of *PhGI1* may be the result of cross-silencing by the *iRNA::PhGI2* construct or *PhGI2* gene might function as activator of *PhGI1* transcription. Under conditions of

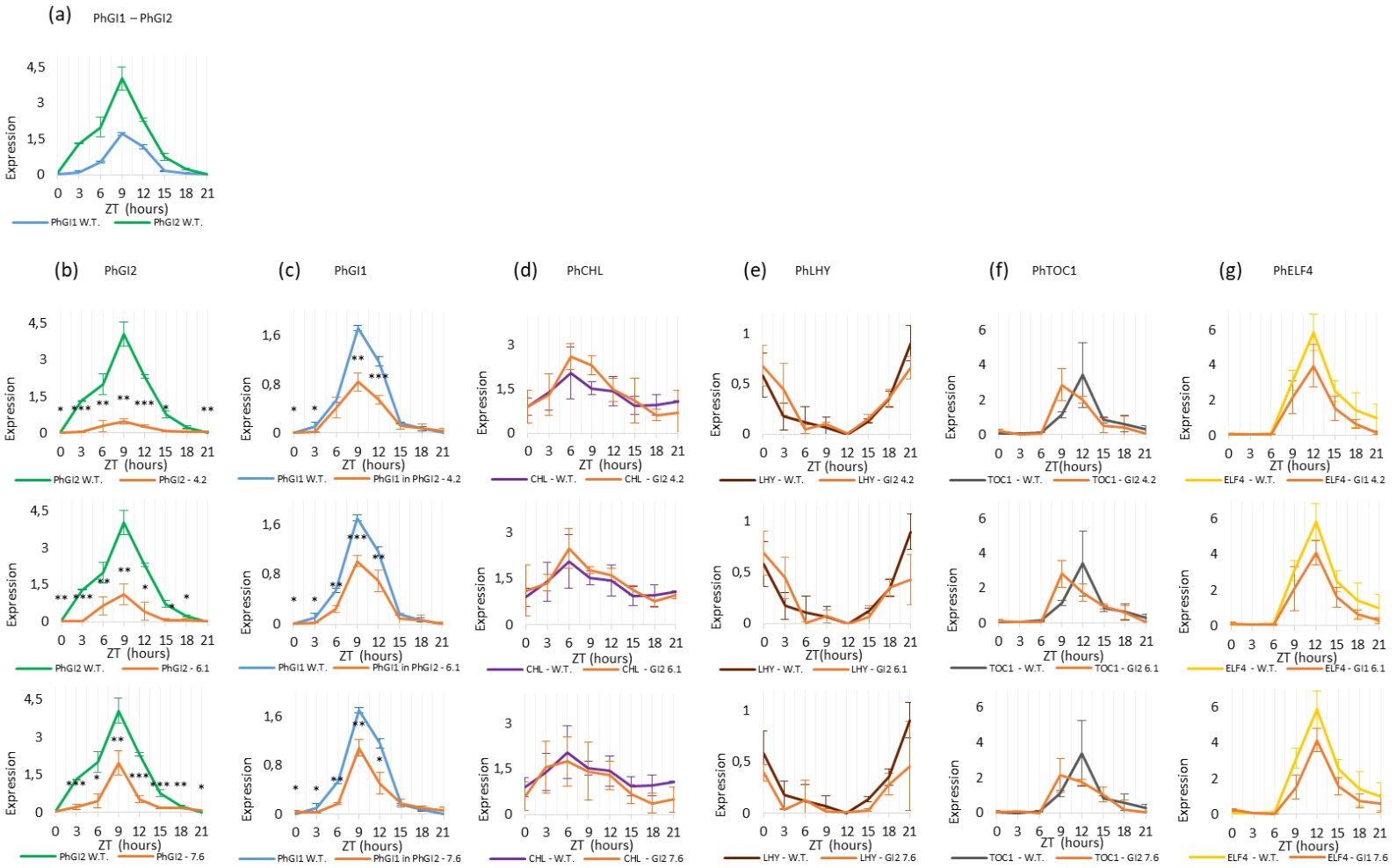
(a) PhGI1 – PhGI2
(b) PhGI2
(c) PhGI1
(d) PhCHL
(e) PhLHY
(f) PhTOC1
(g) PhELF4
Expression
ZT (hours)
PhGI1 W.T.
PhGI2 W.T.
PhGI2 - 4.2
PhGI2 - 6.1
PhGI2 - 7.6
PhGI1 in PhGI2 - 4.2
PhGI1 in PhGI2 - 6.1
PhGI1 in PhGI2 - 7.6
CHL - W.T.
CHL - GI2 4.2
CHL - GI2 6.1
CHL - GI2 7.6
LHY - W.T.
LHY - GI2 4.2
LHY - GI2 6.1
LHY - GI2 7.6
TOC1 - W.T.
TOC1 - GI2 4.2
TOC1 - GI2 6.1
TOC1 - GI2 7.6
ELF4 - W.T.
ELF4 - GI1 4.2
ELF4 - GI1 6.1
ELF4 - GI1 7.6

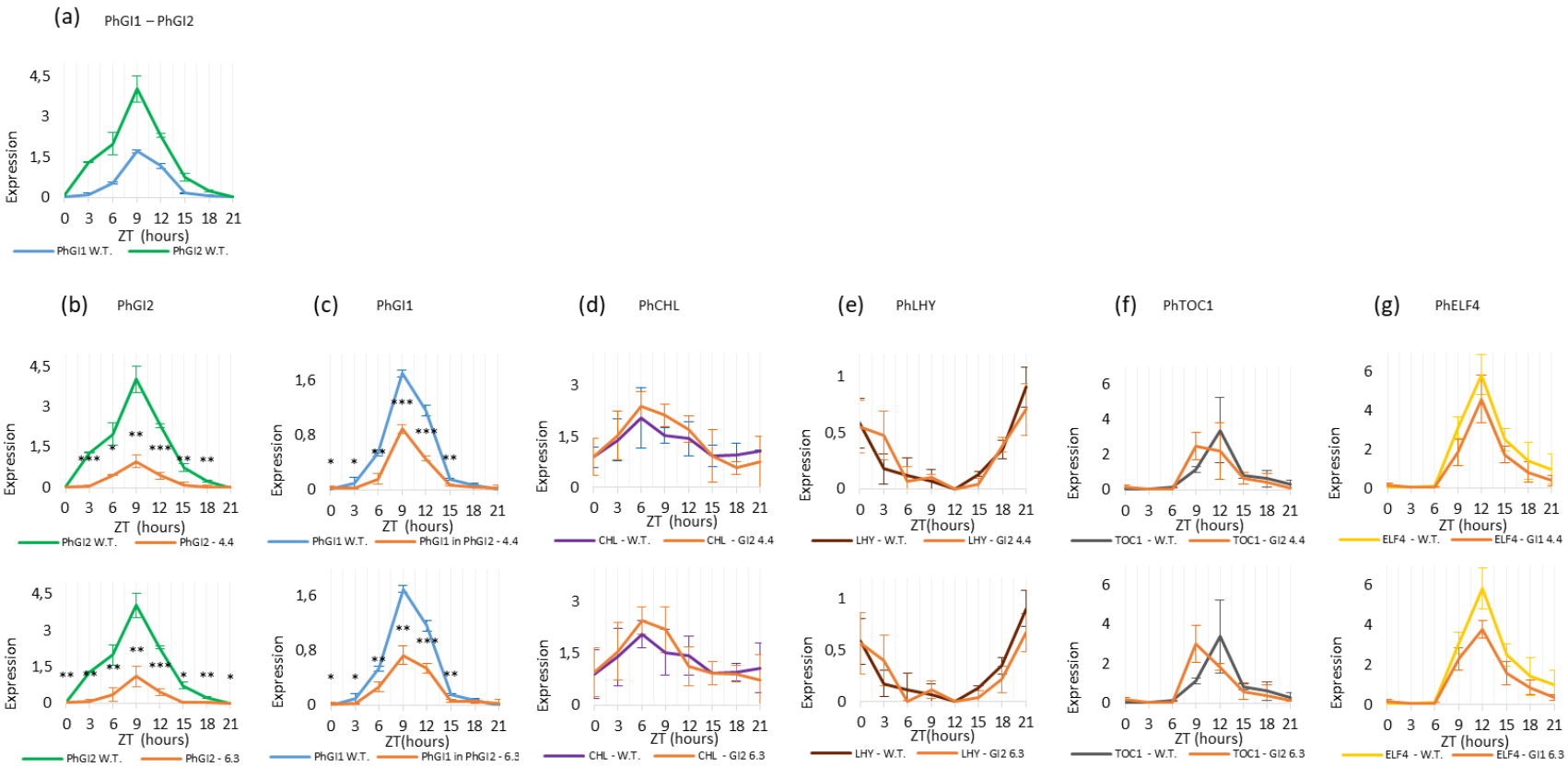

Figure 20| Expression profile during 24 hours.

Expression profile during 24 hours of (a) *PhGI2* and *PhGI1* in wild type plants and (b) *PhGI2*, (c) *PhGI1, (d) PhCHL, (e) PhLHY, (f) PhTOC* and (g) *PhELF4* in *iRNA::PhGI2* T1 lines 4.2, 4.4, 6.1, 6.3 and 7.3 compared to expression in the wild type (from ZT 0 to ZT 15 of light and from ZT 15 to ZT 24 of dark). Expression represents the normalized expression NE according to the formula (NE) = 2^-(Ct experimental – Ct normalization). Three samples were analyzed for each time point and error bars indicate the standard deviation. Asterisks indicate statistical significance between wild type and iRNA lines with *P < 0.05; **P < 0.01; ***P < 0.001 according to group-wise comparison with to Student's T-test.

continuous dark, *PhGI2* lost its rhythmicity after 24 hours in both, wild type and silenced lines (Figure 21).

PhGI2 affects the peak expression of *PhTOC1*

The expression of the Petunia circadian clock genes *PhCHL, PhLHY, PhTOC1* and *PhELF4* is given in Figure 20 c-f, for wild type and *iRNA::PhGI2* lines. Table 5 indicates rhythmicity, period, phase and amplitude of the expression pattern. All genes showed a significant circadian rhythmicity, both in wild type and silenced lines.

The period, phase or expression amplitude of *PhCHL,* the orthologue *ZTL* in Arabidopsis, was not affected by *iRNA::PhGI2* (Table 5). As observed in wild type lines, the expression peak occurred at ZT 7.5 at early afternoon. Similarly, *PhLHY and PhELF4* all maintained an expression level and rhythmicity similar to wild type plants. In case of *PhTOC1*, the rhythmicity parameter "phase" was not significantly different. However, peak expression seemed to be advanced (Fig.1f) but with an expression level similar to wild type plants. Furthermore, *PhTOC1* period, the time between two consecutive peaks, was consistently shortened from 24 to 21 hours in all *iRNA::PhGI2* lines compared to wild type plants (Table 5).

A change in *iRNA::PhGI2* lines concerning the period between two consecutive peaks was also observed for *ZTL,* which prolonged from 21 to 24 hours, even so this phenomenon did not occur in all silenced lines.

Our data indicate that silencing of PhGI2 does not have a major effect on the expression pattern or rhythmicity of other clock genes with the exception of TOC1, which clearly showed a shorter time period between two consecutive peaks of 3 hours.

	Pval	Per	Phase	Amp
PhGI2 W.T.	3.23E-11	24	10.5	1.46
PhGI2 4.2	2.36E-07	21	10.5	0.16
PhGI2 4.4	1.48E-07	21	10.5	0.31
PhGI2 6.1	5.62E-08	24	10.5	0.35
PhGI2 6.3	1.06E-06	24	9	0.27
PhGI2 7.6	1.44E-09	21	10.5	0.24
PhGI1 W.T.	6.98E-11	21	10.5	0.63
PhGI1 4.2	2.36E-07	21	10.5	0.34
PhGI1 4.4	2.89E-07	21	10.5	0.21
PhGI1 6.1	4.24E-08	24	10.5	0.21
PhGI1 6.3	1.33E-06	24	10.5	0.22
PhGI1 7.6	4.34E-06	21	10.5	0.21
ZTL W.T.	1.55E-02	21	7.5	0.47
ZTL 4.2	2.39E-06	24	7.5	0.77
ZTL 4.4	2.00E-08	21	9	0.73
ZTL 6.1	5.16E-06	24	7.5	0.52
ZTL 6.3	3.53E-06	24	9	0.55
ZTL 7.6	3.02E-05	24	7.5	0.62
LHY W.T.	9.19E-08	24	22.5	0.26
LHY 4.2	7.00E-08	21	1.5	0.22
LHY 4.4	1.60E-06	21	1.5	0.25
LHY 6.1	1.53E-05	24	0	0.30
LHY 6.3	7.47E-06	21	1.5	0.16
LHY 7.6	4.34E-06	21	1.5	0.12
TOC1 W.T.	2.96E-06	24	13.5	0.44
TOC1 4.2	2.29E-04	21	13.5	1.04
TOC1 4.4	7.95E-05	21	13.5	0.93
TOC1 6.1	6.32E-06	21	13.5	0.90
TOC1 6.3	6.05E-03	21	13.5	0.98
TOC1 7.6	5.28E-04	21	12	0.81
ELF4 W.T.	1.48E-07	24	13.5	1.29
ELF4 4.2	6.96E-07	24	13.5	1.06
ELF4 4.4	4.20E-05	21	13.5	1.21
ELF4 6.1	1.53E-05	21	15	1.05
ELF4 6.3	2.59E-05	21	13.5	1.50
ELF4 7.6	1.27E-04	21	13.5	1.07

Table 5| Statistical analysis of rhythmicity of gene expression data.

The P value (Pval) indicates a significative expression rhythm at Pval ≤ 0.05. Period (Per) is defined as the time between two consecutive peaks (expressed in hours). The adjusted phase (Phase), given by JTK_CYCLE and Lomb-Scargle, is considered as the time point with the peak expression (expressed in hours). Amplitude (Amp) is the difference between the peak expression (or minimum expression) and the mean value of the wave.

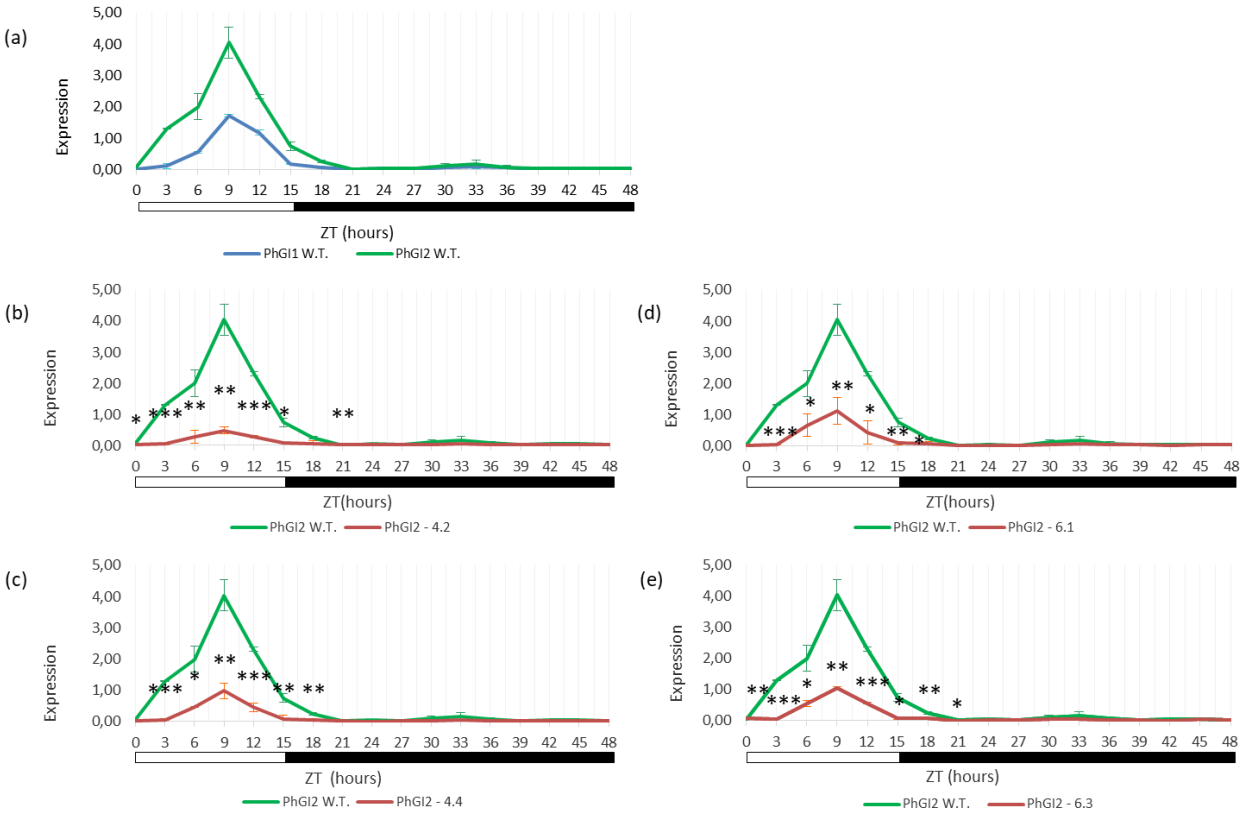

Figure 21| Expression profile in leaves in continuous dark.

(a) *PhGI2* and *PhGI1* in wild type plants and *iRNA::PhGI2* lines 4.2 (b), 4.4 (c) 6.1 (d) and 6.3 (e). Expression represents the normalized expression NE according to the formula (NE) = 2^-(Ct experimental – Ctn). Three samples were analyzed for each time point and error bars indicate the standard deviation. Asterisks indicate statistical significance between wild type and iRNA lines with *P < 0,05; **P < 0,01; ***P < 0,001 according to group-wise comparison with to Students T-test.

PhGI2 negatively regulates vegetative growth and controls plant structure

The vegetative parameters of three independent transgenic lines with the strongest *iRNA::PhGI2* expression reduction, compared to wild type, are given for T1 and T2 generation (Table 6, Table S8). In the T1 generation, all leaves exhibited a significant increase in length and width, with the exception of median leaf length (Table 6, Table S8 and Figure 22). As shown in Figure 22, the transgenic lines had undergone

structural changes in the growth habit. Even so, plants of the T1 generation did not differ in total leaf number from wild type plants, the foliar apparatus seemed denser especially in the apical plant region, coinciding with a reduction in median and apical internode length of 32,5% and 34,5%. However, total plant length was not significantly different as basal internodes were longer in wild type plants than in the silenced clones. The denser growing habit might also be related to a duplication in the number of axillary meristems and branches. In the T2 generation, lateral branches overgrew the main branch leading to a candelabra like growth habit. Main and lateral branches differed strongly in phenotype, and vegetative parameters are therefore given separately for the two branch types (Table 6). Leaf size in the median and apical plant area was inversely affected on the main branch, with significantly smaller and slimmer leaves, and the lateral branches, with longer and broader leaves. Basal, median and apical internode length was significantly reduced both in the main and lateral branches, resulting in a significant reduction in height of main and lateral branches (Figure S5). The total number of branches was not significantly altered and while the main stem showed a significant reduction in axillary meristem number, this factor was not changed in lateral branches.

All transgenic lines of both generations (T1 and T2) had a greener appearance towards the apical region, coinciding with a significant increase in chlorophyll levels in the median and apical leaves of both branch types, while the yellowish basal leaves showed lower chlorophyll levels in comparison to the wild type (Table 6, Table S8).

Genotype:			W.T.	*iRNA::PhGI2*	% GI2 versus W.T.	P value
Plant Height (cm)	T1	Main Stem	40.9 ± 0.8	49.0 ± 5.4	+19.8	6.03E-01
	T2	Main Stem	44.7 ± 6.2	20.3 ± 8.2	-54.7	5.93E-03
		Lateral branches	36.2 ± 0.8	37.8 ± 3.9	+4.4	1.46E-03
Basal Internode (mm)	T1	Main Stem	12.6 ± 0.9	17.2 ± 0.8	+36.5	3.91E-19
	T2	Main Stem	14.3 ± 1.9	9.3 ± 1.3	-34.6	7.74E-06
		Lateral branches	49.8 ± 1.45	31.8 ± 1.4	-36.2	3.81E-12
Median Internode (mm)	T1	Main Stem	16.3 ± 0.56	11.0 ± 0.9	-32.5	3.31E-22
	T2	Main Stem	15.7 ± 1.3	12.3 ± 1.2	-22.1	1.80E-06
		Lateral branches	26.7 ± 1.88	17.8 ± 1.3	-33.5	4.51E-08
Apical Internode (mm)	T1	Main Stem	20.5 ± 1.07	13.4 ± 0.7	-34.5	8.50E-25
	T2	Main Stem	27.9 ± 1.6	16.7 ± 1.4	-40.1	1.41E-16
		Lateral branches	17.8 ± 1.5	12.7 ± 1.4	-28.7	9.60E-07
N° of leaves to the 1° flower	T1	Main Stem	37 ± 1.4	43.8 ± 1.6	+18.4	5.60E-01
	T2	Main Stem	28.0 ± 1.0	14.9 ± 2.1	-46.7	1.63E-06
		Lateral branches	28.3 ± 1.2	28.0 ± 1.3	-1.1	6.85E-01
N° of axillary meristems	T1	Main Stem	12.5 ± 1.3	30.0 ± 4.6	+140	1.48E-04
	T2	Main Stem	15.3 ± 1.5	11.9 ± 2.0	-22	3.48E-02
		Lateral branches	4.7 ± 1.5	6.0 ± 1.5	+27.7	2.65E-01
N° of branches	T1	Main Stem	2 ± 0.0	4.8 ± 0.4	+140	5.53E-06
	T2		6.7 ± 0.55	7.6 ± 1.2	+13.4	8.34E-02
Basal Leaves length (mm)	T1	Main Stem	64.6 ± 1.04	89.2 ± 1.2	+38.1	6.51E-18
	T2		90.9 ± 1.6	91.3 ± 1.2	+0.3	6.64E-01
Basal leaves width (mm)	T1	Main Stem	40.9 ± 0.7	49.8 ± 3.4	+21.7	3.03E-12
	T2		49.9 ± 1.6	49.7 ± 0.98	-0.4	7.11E-01
Median leaves length (mm)	T1	Main Stem	72.7 ± 2.8	759 ± 1.4	+4.3	2.81E-02
	T2	Main Stem	65.4 ± 1.74	58.1 ± 1.7	-11.2	3.65E-08
		Lateral branches	49.1 ± 1.7	51.4 ± 1.1	+4.5	1.39E-03
Median leaves width (mm)	T1	Main Stem	43.8 ± 1.7	48.8 ± 1.2	+11.1	9.44E-08
	T2	Main Stem	36.9 ± 1.5	30.7 ± 1.2	-16.7	3.68E-09
		Lateral branches	29.8 ± 1.09	31.8 ± 0.8	+6.4	3.25E-04
Apical leaves length (mm)	T1	Main Stem	38.8 ± 1.3	45.6 ± 0.99	+17.6	4.61E-14
	T2	Main Stem	33.2 ± 1.8	30.9 ± 0.9	-6.7	6.86E-03
		Lateral branches	32.8 ± 1.5	36.60 ± 0.97	+11.6	8.89E-06

Apical leaves width (mm)	**T1**	**Main Stem**	22.5 ± 0.97	26.1 ± 0.8	+15.6	4.69E-08
	T2	**Main Stem**	17.86 ± 0.59	16.8 ± 0.7	-6.0	5.60E-03
		Lateral branches	17.8 ± 0.9	21.5 ± 0.8	+21.1	1.33E-09
Basal leaves Chlorophyll	**T1**	**Main Stem**	22.4 ± 1.09	15.8 ± 1.3	-29.6	9.45E-19
	T2	**Main Stem**	17.1 ± 1.08	13.8 ± 0.7	-19.6	4.76E-05
		Lateral branches	14.6 ± 1.1	12.4 ± 0.9	-15.0	8.11E-04
Median leaves Chlorophyll	**T1**	**Main Stem**	31.04 ± 2.3	35.7 ± 1.2	+15.0	2.05E-11
	T2	**Main Stem**	20.1 ± 0.7	26.1 ± 0.9	+29.5	6.17E-06
		Lateral branches	18.5 ± 1.02	22.7 ± 1.05	+22.7	2.49E-06
Apical leaves Chlorophyll	**T1**	**Main Stem**	21.3 ± 0.9	35.6 ± 1.1	+67.2	4.68E-17
	T2	**Main Stem**	34.5 ± 0.9	44.2 ± 1.02	+28.2	4.36E-15
		Lateral branches	30.4 ± 1.7	39.9 ± 1.05	+31.6	9.75E-10

Table 6| Comparison of vegetative parameters between wild type and the silenced PhGI1 in T1 and T2 generation

Data are given as averages ± standard error of at least three biological replicates of all silenced plants. The height was calculated from the base to the first flowering meristem, when the first flowering event occurs. The number of total axillary meristems was calculated between the base and the first apical flowering meristem. P values ≤ 0.05 according to Students T-test were considered as significant.

Figure 22| Vegetative growth characteristics in iRNA::PhGI2 T1 lines compared to wild type plants under growth chamber conditions of 16 hours light/8 hours darkness.

Growth habit of the transgenic lines compared to the wild type. Wild type plant (left) and *iRNA::PhGI2* line 6.1 (right).

PhGI2 is involved in flowering time and flower tissue expansion and prevents ectopic flower development

iRNA::PhGI2 plants showed marked differences in the flowering time, flower number and flower size compared to wild type plants. Flowering time, characterized as the percentage of plants with fully opened flowers in each week after transplantation from *in vitro* culture to substrate, is shown in Figure 23. A clear delay in flowering time of two to three weeks in case of T1 and of one to four weeks in case of T2 was observed for *iRNA::PhGI2* lines. Late flowering was accompanied by a reduction in the total number of flower buds at the end of flowering period of 33.5% and 58.4%, respectively, in T1 and T2 generation (Table 7, Table S9). Additionally, 38.5% in T1 and 21.4% in T2 of these flower buds emerged ectopically as a third lateral organ next to the terminal flower and the inflorescence shoot (Figure 24). All the ectopic flowers aborted prematurely, leading to a final reduction in fully developing flowers of 35% in T1 and 38% in T2 generation, compared to wild type plants. Premature abortion of the ectopic flowers occurred after differentiation of floral organs, as stamen and carpel tissue could be clearly distinguished under the scanning electron microscope. The corolla diameter, as well as the floral tube length of fully developed flowers, were significantly reduced (Table 8; Figure 25). This reduction was more pronounced in the T1 generation. The corolla diameter was 31% smaller in the *iRNA::PhGI2* silenced plants than in wild type flowers in T1 and only 8.3% smaller in the T2 with a similar trend in tube length. The changes in flower size coincided with a reduction in cell expansion as cell size, both in the floral tube as well as the corolla in regions close to the tube and in the distal outer zone, were reduced (Table 8; Figure 25).

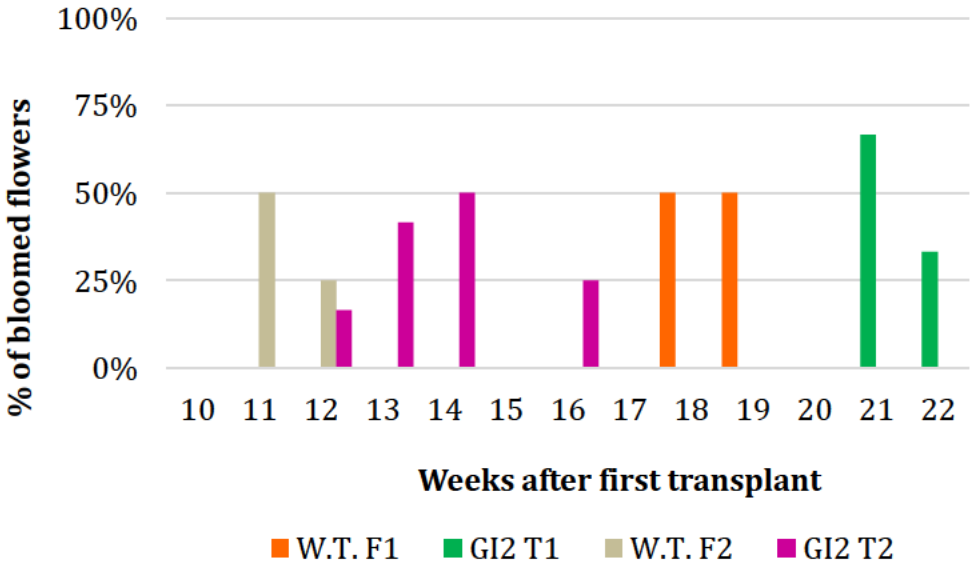

Figure 23| Percentage of fully open flowers in weeks after transplanting from in vitro culture to substrate of T1 and T2 generation of iRNA::PhGI2 lines compared to wild type plant.

T1 lines were grown under growth chamber conditions of 16 hours light/8 hours darkness. T2 lines were grown in a greenhouse under natural long-day conditions.

Genotype:		W.T.	*iRNA::PhGI2*	% GI2 versus W.T.	P value
N° of flower buds	T1	27.8 ± 2.8	18.5 ± 5.67	-33.5	1.19E-03
	T2	29.3 ± 2.3	8.8 ± 5.4	-58.4	7.70E-06
N° of fully developed flowers	T1	27.8 ± 2.8	10.7 ± 4.56	-61.5	1.58E-05
	T2	29.3 ± 2.3	6.27 ± 4.54	-78.6	1.62E-05
% of fully developed flowers	T1	100	65	-35	1.35E-04
	T2	100	62	-38	1.31E-05
Corolla diameter (mm)	T1	46.22 ± 3.41	31.91 ± 2.56	-31	1.22E-24
	T2	54.34 ± 3.45	49.85 ± 2.98	-8.3	3.16E-03
Tube length (mm)	T1	40.06 ± 2.10	34.74 ± 2.04	-13.3	1.13E-14
	T2	41.10 ± 1.82	38.30 ± 1.87	-6.8	4.49E-04
Petiole length (mm)	T1	35.96 ± 2.72	35.86 ± 4.32	-0.3	8.19E-01
	T2	47.63 ± 2.51	45.35 ± 3.56	-4.8	1.03E-01

Table 7| Comparison of floral parameters between wild type and silenced PhGI1 in T1 and T2 generation.

Data are given as averages ± standard error of at least three biological replicates of all silenced plants. P values ≤ 0.05 according to Students T-test were considered as significant.

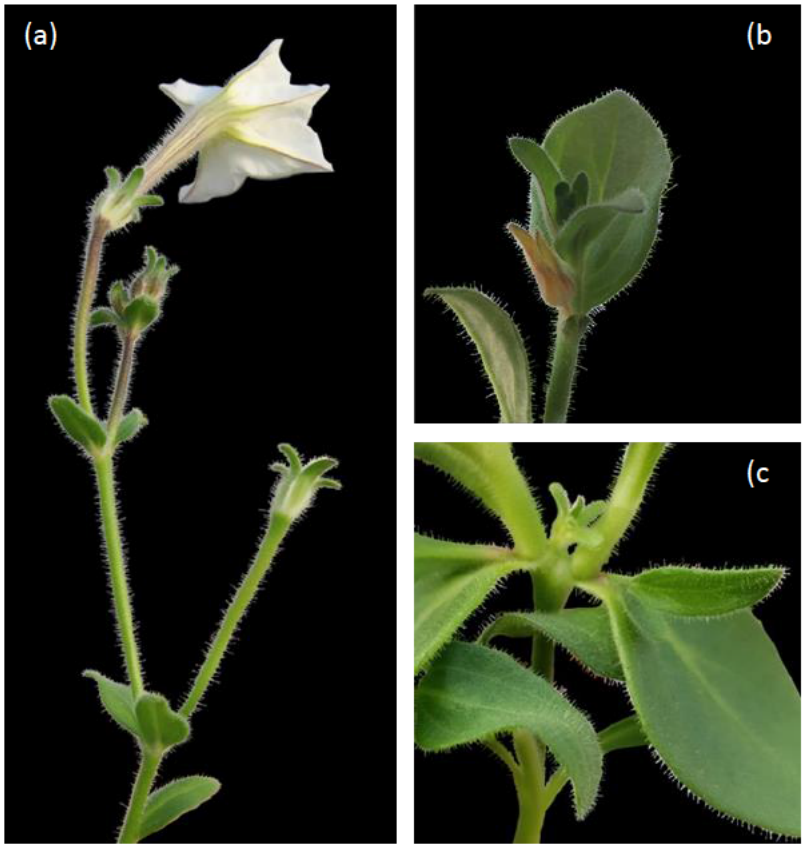

Figure 24| Schematic representation of the petunia inflorescence.

Wild type (a) and silenced *iRNA::PhGI2* plants of T1 line (b-c).

Genotype:	W.T.	*iRNA::PhGI2*	% GI2 versus W.T.	P value
Corolla (µm²)	1132.38 ± 225.13	756.00 ± 235.60	-33.24	6.75E-10
Basal limb (µm²)	345.12 ± 88.85	309.62 ± 73.33	-10.29	3.37E-04
Tube (µm²)	3653.35 ± 794.38	2683.51 ± 706.08	-26.55	8.95E-22

Table 8| Comparison of cellular areas of flowers between wild type and silenced PhGI1 plants of T1 generation.

Values correspond to mean (µm²) ± standard error of at least three flowers belonging to the *iRNA::GI2* lines 4.2. 4.4. 6.1 and 6.3 and 50 measurements for each flower. P values ≤ 0.05 according to Students T-test were considered as significant.

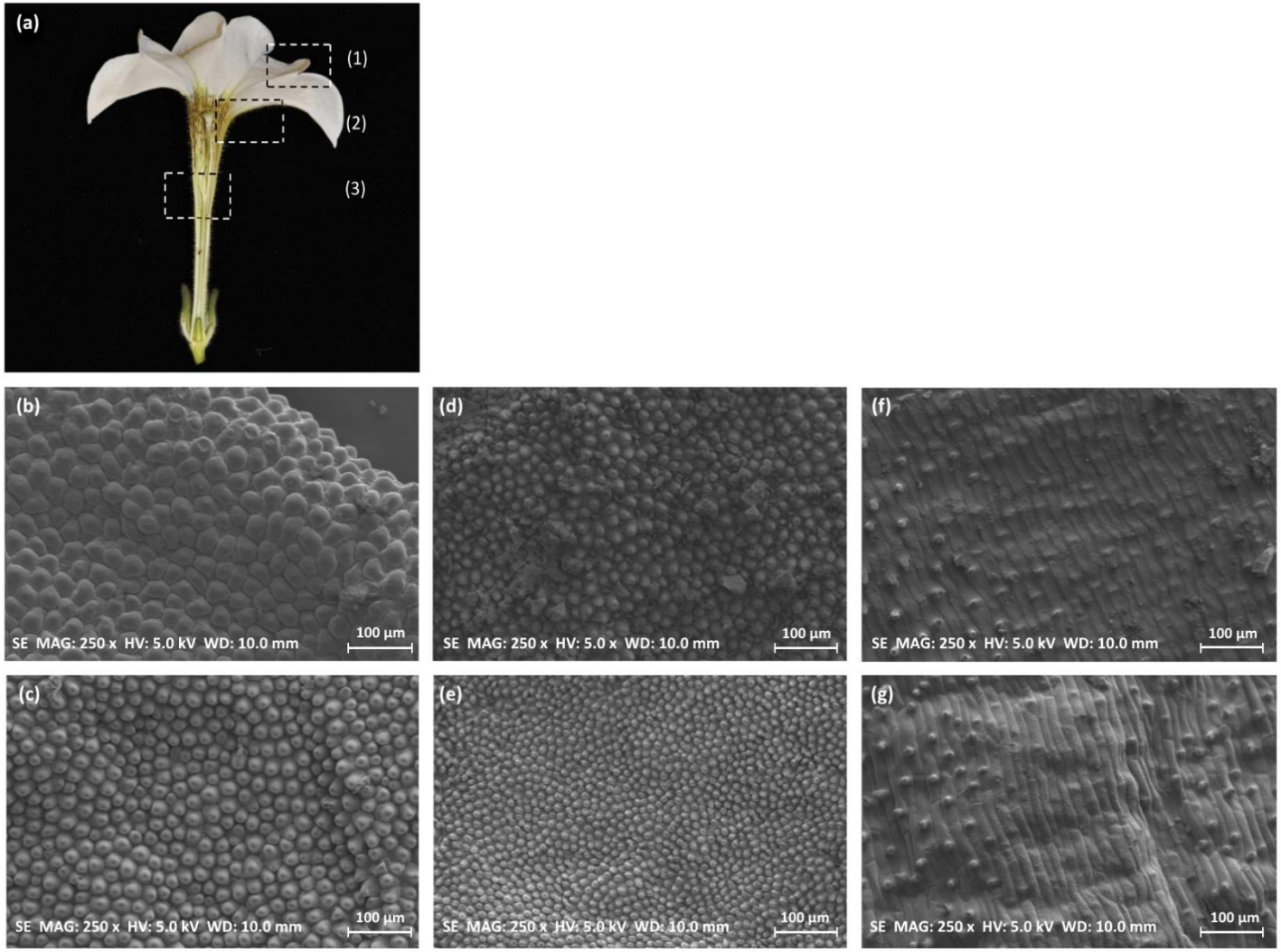

Figure 25| Scanning electron microscopy of petal cell size.

Three petal regions were sampled for scanning electroscopic analysis from T1 lines (a). Floral cell size comparison between wild type (top) and *iRNA::PhGI2* (bottom) of different floral organs: (1)(b,c) corolla, (2)(d,e) limb and (3)(f,g) tube.

PhGI2 regulates the quantity, profile and rhythmicity of VOC emission

We analyzed the emission of VOCs from the flowers of four plants of the *iRNA::PhGI*2 lines 4 and 6 and wild type plants. We distinguished into main VOCs, characterized by a threshold level of 2% of total VOCs (Table S10), and minor VOCs. Plants of both *iRNA::PhG2* lines showed a reduction, on average, of 19.42% in total VOC emission (Figure 26a). The rhythm of VOC emission during 24 hours in 3 hour intervals is shown in Figure 26b. In silenced lines, lowest emission was recorded at ZT9, three hours later than in wild type flowers. Both wild type and silenced lines showed peak emission during the dark phase at ZT18.

In order to evaluate changes in the VOC pattern, we analyzed the relative contribution of VOCs to the scent profile (Figure 27a, b and c and Table S11). Methyl benzoate was the major volatile compound in both wild type plants and *iRNA::PhGI2* lines. The relative contribution of emission of this mayor compound was similar to the wild type at most time points except at ZT3, when it contributed with less than 50% to the total VOCs compared to 85% in wild type flowers. However, the relative contribution of other compounds varied markedly in *iRNA::PhGI2* lines from wild type plants at specific time points. We can highlight the relative higher emission of isoeugenol at ZT3 and nonanal at ZT9 in the *PhGi2* silenced lines compared to wild type plants. Also, a general reduction in the relative contribution of benzaldehyde is observable.

In summary, our results indicate that *PhGI2* controls the quantity, rhythmicity as well as the fine-tuning of VOC emission. However, methyl benzoate as major VOC throughout the day was maintained.

(a)

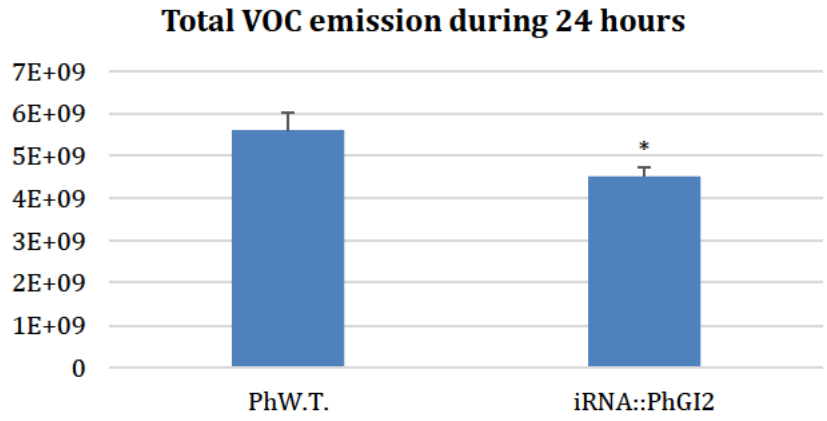

(b)

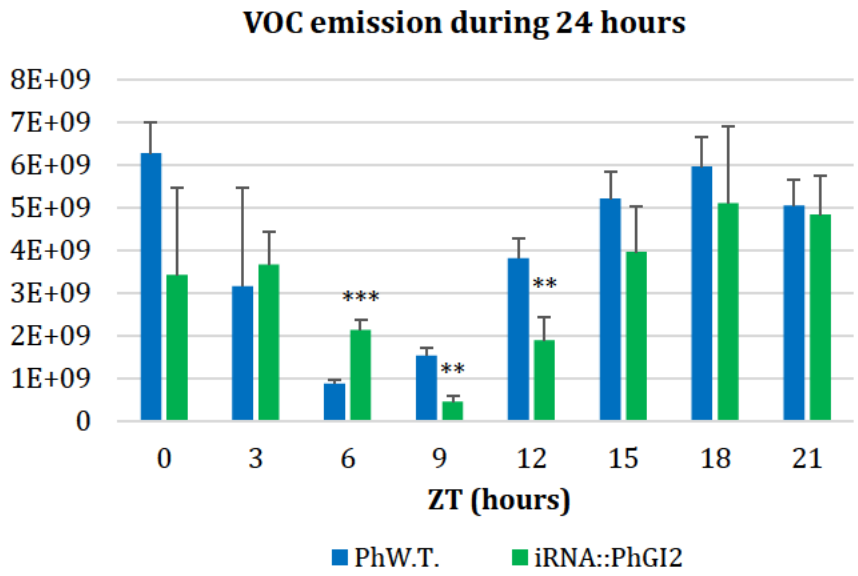

Figure 26| Volatile emission by flowers from wild type and iRNA::PhGI2 T1 lines. Flowers were excised at ZT0.

(**a**) Total VOC emission in wild type flowers compared to *iRNA::PhGI2* lines in 24 hours and (**b**) VOCs emission in three hour intervals during 24 hours. Absolute total emission of VOCs per grams of fresh weight is given as sum of integrated peak area. Asterisks indicate statistical significance between wild type and iRNA lines with *P < 0.05; **P < 0.01; ***P < 0.001 according to Student's T-test.

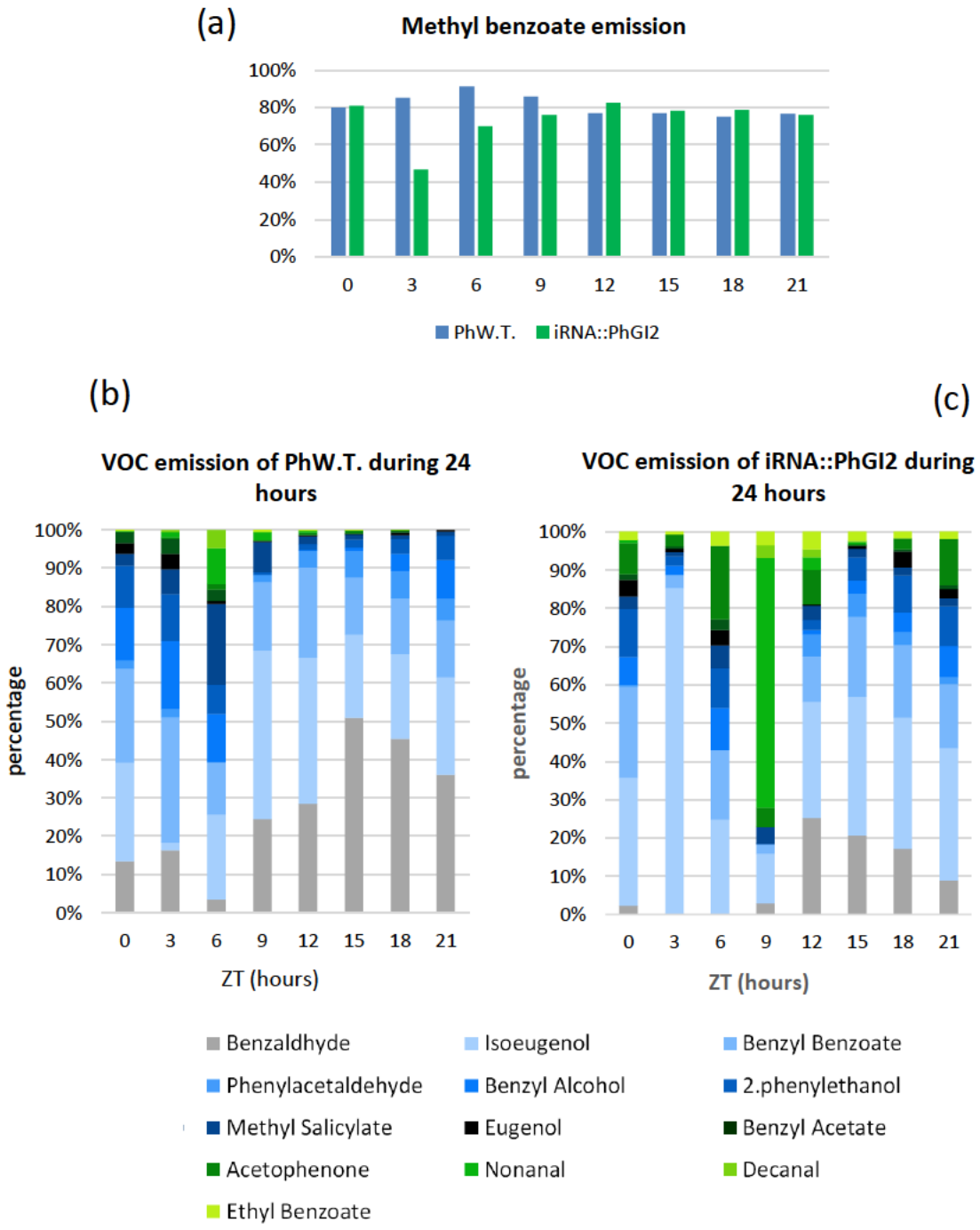

Figure 27| Percent emission of volatile organic compounds (VOCs) from wild type flowers and iRNA::PhGI2 T1 lines 4.2, 4.4, 6.1 and 6.3.

Flowers were excised at ZT0. Methyl benzoate (a) and other main VOCs in wild type flowers (b) and *iRNA::PhGI2* (b) lines in three hour intervals during 24 hours. Percentages were calculated based on the integrated peak area divided by flower fresh weight.

Discussion

The *GI* gene appeared early in the land plants lineage but, in contrast to other genes, it has remained at a low copy number in most genomes. Due to the lack of homology to other proteins, and despite extensive studies, the molecular functions of *GI* are not fully understood. Studies in Arabidopsis, Marchantia or rice, all plants with a single copy of *GI,* show that at least part of the biological functions of *GI* are conserved. In this work we have characterized *PhGI2*, one of the paralogs of *GI* present in *Petunia x hybrida*.

In wild type plants, the expression pattern of *PhGI2* was characterized by a peak expression at ZT9, which coincides with *PhGI1* expression (Chapter 1) and similar to the evening phased expression observed for *GI* orthologs in other species, including Arabidopsis (Fowler *et al.*, 1999), or soybean (Marcolino-Gomes *et al.*, 2014). Similar to previous observations on *PhGI2* expression in Petunia leaves (Fenske *et al.*, 2015) and identical to *PhGI1* (chapter 1), but different from Arabidopsis, where a strong free-running oscillation of *GI* under conditions of continuous darkness can be observed (Park *et al.*, 1999), no robust expression rhythmicity occurred under continuous darkness. Our results indicate that light input is required for the maintenance of expression levels of the *GI* paralogs in Petunia.

As already observed for *PhGI1* (Brandoli *et al.*, 2020) expression of *PhGI2* was rhythmic. While silencing of *PhGI1* led to a significant prolongation of rhythmic period of 3 hours for *PhGI1,* silencing of *PhGI2* did not alter the rhythmic period of *PhGI2*, indicating different functions of the two homologs within the clock gene network. Identical to *PhGI1* silenced lines, the *iRNA::PhGI2* lines maintained the

expression amplitude of the core clock genes *PhLHY, PhTOC1, PhELF4* and *PhCHL.* Furthermore, the rhythmicity was not affected with exception of a shortening of the period between consecutive peaks of three hours in case of *PhTOC1*. In contrast, silencing of *PhGI1* led to a significant prolongation of rhythmic period of 3 hours for the genes *PhGI1* and *PhCHL* (Brandoli *et al.*, 2020). The observed difference suggests a divergence in the clock network interaction of the two *GI* paralogs in Petunia. The expression level of *GI* is controlled by *CCA1* in Arabidopsis, which binds to the *G1* promoter and reduces its expression (Lu *et al.*, 2012). In Arabidopsis, GI functions as stabilizer of ZTL, which in the evening targets TOC1 for proteasomal degradation. Reduced *PhGI2* expression levels might cause a disequilibrium in protein-protein interaction and finally a feedback on expression rhythmicity of *PhTOC1*.

Concerning the effect on vegetative parameters, *PhGI2* silenced lines showed both common and divergent effects depending on the growth condition of the two observed generations, T1 in growth chamber and T2 in the greenhouse, although in both cases plants were cultivated under long day conditions. The growth habit of T1 plants, characterized by apical dominance, a bushier phenotype, an increase in the number of axillary meristems, longer, broader and darker green median and apical leaves as well as a reduction in median and apical internode length but with a conserved overall plant height coincide with those observed for *PhGI1* silenced plants. Furthermore, a function of *GI* as negative regulator of vegetative parameters seems conserved as this gene controls petiole length, plant height and leave growth in Arabidopsis. While the above mentioned phenotype was maintained in the T2 of *PhGI1* under greenhouse conditions, *PhGI2* silenced lines

showed a mixed phenotype which included both inhibition and promotion of vegetative growth. While lateral branches were similar to the T1 plants concerning the promotion of leaf size, stronger growth reductions occurred on the main branch in stem length and leaf dimensions, leading to a candelabra like phenotype. Our results indicate common and divergent functions of the two paralogs *PhGI1* and *PhGI2* concerning vegetative growth and subfunctionalization depending on the specific environmental inputs.

Silencing of *PhGI1* and *PhGI2* revealed both common and divergent functions concerning flowering time and flower development. While flowering of *PhGI1* silenced lines coincided with that of wild type plants, we observed a delay in the onset of flowering of up to five weeks in case of *PhGI2* silenced lines. This function is in agreement with observations in many other species including Arabidopsis (Mishra and Panigrahi, 2015), soybean (Watanabe *et al.*, 2011), barley (Zakhrabekova *et al.*, 2012) or maize (Khan *et al.*, 2010). On the other hand, and coinciding with *PhGI1* (Brandoli *et al.*, 2020), we observed *PhGI2* functions not reported yet for any other *GI* ortholog in any other species, including the control of flower bud production, prevention of ectopic flower bud formation and premature flower abortion as well as petal growth promotion. The reduced petal size in *PhGI1* and *PhGI2* silenced lines, coincided with a reduction in cell expansion, which follows cell division during organ development (Reale *et al.*, 2002; Laitinen *et al.*, 2005; Anastasiou *et al.*, 2007; Kazama *et al.*, 2010). These results, as well as the fact that flower abortion occurs after floral organ differentiation, indicates that in Petunia the *GIGANTEA* gene paralogs control flower growth in later developmental stages after organ differentiation is completed.

In *Petunia x hybrida*, the emission of floral fragrance is dominated by volatile benzenoids. Similar to wild type flowers and flowers of *iRNA::PhGI1* lines (Brandoli *et al.*, 2020) the flowers of *PhGI2* silenced line emitted mostly methyl benzoate and even though the total amount of VOCs emitted during 24 hours was significantly reduced, the relative contribution of emission of this mayor compound was similar to the wild type at most time points except at ZT3, when it contributed with less than 50% to the total VOCs compared to 85% in wild type flowers. Interestingly, in *iRNA::PhGI1* lines, lowest relative methyl benzoate contribution to the VOC profile occurred 3 hours earlier, at ZT0 (Brandoli *et al.*, 2020). Our data indicate that changes in the fine tuning of the VOC profile must be mostly attributed to other compounds than methyl benzoid, including nonanal and isoeugenol. VOC emission is rhythmic in Petunia (Schuurink *et al.*, 2006) and this rhythmicity is maintained in both *PhGI* paralogs. However, different from *PhGI1*, *PhGI2* silenced lines showed a three-hours phase delay in the lowest emission point during the day. Our observations indicate that disturbances in the normal expression of clock genes may lead to changes in the rhythmicity of clock gated processes and that the *PhGI* paralogs differ in their control over timing of VOC emission.

The duplication of genes may result in genes with complete functional redundancy. However, often times the newly formed paralogs diverge in functions. Neofunctionalization occur were one paralog acquires a function not present in the orthologous gene before duplication. A third scenario occurs via subfunctionalization, where both paralogs maintain the ancestral functions in a non-overlapping way. A gene duplication model proposes that subfunctionalization is a transition step towards neofunctionalization (Rastogi and Liberles,

2005). Our data on the function of *PhGI1* and *PhGI2* are in agreement with the proposed model, as these two paralogs show both shared and divergent functions. Clock genes control many target genes, gating clock outputs such as response to cold, flowering time, starch accumulation or scent emission (de Montaigu *et al.*, 2010; Graf and Smith, 2011; Kolosova, Gorenstein, *et al.*, 2001) and neofunctionalization and fine-tuning of clock paralogs within a species might therefore contribute to adaptation to environmental signals (Zakhrabekova *et al.*, 2012). The control of *GI* over flowering time and vegetative growth is common to many *GI* orthologs in other species and can be considered an ancestral function. While the regulation of flowering time was lost after duplication in *PhGI1,* both paralogs maintained a negative control over vegetative growth. The shared control of *PhGI* over flower size, flower bud production and flower maturation can be considered a Petunia specific adaptive neofunctionalization of the ancestral Petunia ortholog that occurred before gene duplication and maintained redundant in both paralogs. Analysis of Arabidopsis ecotypes and *Oryza* subspecies showed that duplicated genes not necessarily are more free to amino acid changes compared to single genes and it is hypothesized that the maintenance of especially crucial functions can also provide buffer capacity (Chapman *et al.*, 2006) and genetic robustness (Gu *et al.*, 2003). The existence of both functional redundancy and redeployment was also reported for other clock genes with high sequence similarity. Arabidopsis mutants of the morning phase MYB transcription factors *CCA1* and *LHY* both have a short period phenotype, but this phenotype is even more pronounced in double mutants *cca1 lhy*, indicating both redundancy and a proper clock function of each gene (Alabadi *et al.*, 2001; Mizoguchi *et al.*, 2005). Both redundant and synergistic

functions within the Arabidopsis clock mechanism was also reported for the *PRR* paralogs *9, 7* and *5*, which are all negative regulators of *CCA1* and *LHY*, but each one acts at a specific time between early daytime to midnight (Nakamichi *et al.*, 2005).

The silencing of *PhGI2* in this work confirms the function of circadian clock genes in the coordination of environmental inputs into various processes including vegetative growth, flowering time, VOC emission and flower tissue growth based on changes in cell expansion. We also present an unknown function of *PhGI* consisting in the organization of overall inflorescence architecture. The comparison with previously obtained information on functions of the Petunia paralog *PhGI1*, uncovers three events: loss of function, neofunctionalization and subfunctionalization among the *GI* paralogs in Petunia.

Funding

This research was funded by Fundación Seneca 19398/PI/14, 19895/GERM/15 and MC BFU-2017 88300-C2-1-R and BFU-2017 88300-C2-2-R.

Acknowledgments

We would like to acknowledge María José Roca and Julia Muñoz for technical assistance.

REFERENCES

Adams, S., Manfield, I., Stockley, P. and Carré, I.A. (2015) Revised Morning Loops of the Arabidopsis Circadian Clock Based on Analyses of Direct Regulatory Interactions. *PLoS ONE*, **10**. Available at: https://www.ncbi.nlm.nih.gov/pmc/articles/PMC4666590/ [Accessed February 8, 2019].

Alabadi, D., Oyama, T., Yanovsky, M.J., Harmon, F.G., Ma«s, P. and Kay, S.A. (2001) Reciprocal Regulation Between TOC1 and LHY/CCA1 Within the Arabidopsis Circadian Clock. *Science*, **293**, 880–883.

Anastasiou, E., Kenz, S., Gerstung, M., MacLean, D., Timmer, J., Fleck, C. and Lenhard, M. (2007) Control of Plant Organ Size by KLUH/CYP78A5-Dependent Intercellular Signaling. *Dev. Cell*, **13**, 843–856.

Bendix, C., Mendoza, J.M., Stanley, D.N., Meeley, R. and Harmon, F.G. (2013) The circadian clock-associated gene gigantea1 affects maize developmental transitions. *Plant Cell Environ.*, **36**, 1379–1390.

Bombarely, A., Moser, M., Amrad, A., et al. (2016) Insight into the evolution of the Solanaceae from the parental genomes of Petunia hybrida. *Nat. Plants*, **2**, 16074.

Bouget, F.Y., Troein, C., Corellou, F., Dixon, L.E., Ooijen, G. van, O'Neill, J.S. and Millar, A.J. (2011) Multiple light inputs to a simple clock circuit allow complex biological rhythms. *Plant J.*, **66**, 375–385.

Box, M.S., Coustham, V., Dean, C. and Mylne, J.S. (2011) Protocol: A simple phenol-based method for 96-well extraction of high quality RNA from Arabidopsis. *Plant Methods*, **7**, 7.

Brachi, B., Faure, N., Horton, M., Flahauw, E., Vazquez, A., Nordborg, M., Bergelson, J., Cuguen, J. and Roux, F. (2010) Linkage and Association Mapping of Arabidopsis thaliana Flowering Time in Nature T. F. C. Mackay, ed. *PLoS Genet.*, **6**, e1000940.

Brandoli, C., Petri, C., Egea-Cortines, M. and Weiss, J. (2020) The clock gene Gigantea 1 from Petunia hybrida coordinates vegetative growth and inflorescence architecture. *Sci. Rep.*, **10**, 275.

Cha, J.-Y., Kim, J., Kim, T.-S., Zeng, Q., Wang, L., Lee, S.Y., Kim, W.-Y. and Somers, D.E. (2017) GIGANTEA is a co-chaperone which facilitates maturation of ZEITLUPE in the Arabidopsis circadian clock. *Nat. Commun.*, **8**, 3.

Chapman, B.A., Bowers, J.E., Feltus, F.A. and Paterson, A.H. (2006) Buffering of crucial functions by paleologous duplicated genes may contribute cyclicality to angiosperm genome duplication. *Proc. Natl. Acad. Sci.*, **103**, 2730–2735.

Corellou, F., Schwartz, C., Motta, J.P., Djouani-Tahri, E., Sanchez, F. and Bouget, F.Y. (2009) Clocks in the Green Lineage: Comparative Functional Analysis of the Circadian Architecture of the Picoeukaryote Ostreococcus. *Plant Cell*, **21**, 3436–3449.

Delgado-Benarroch, L., Causier, B., Weiss, J. and Egea-Cortines, M. (2009) FORMOSA controls cell division and expansion during floral development in Antirrhinum majus. *Planta*, **229**, 1219–1229.

Fenske, M.P., Hewett Hazelton, K.D., Hempton, A.K., Shim, J.S., Yamamoto, B.M., Riffell, J.A. and Imaizumi, T. (2015) Circadian clock gene *LATE ELONGATED HYPOCOTYL* directly regulates the timing of floral scent emission in *Petunia*. *Proc. Natl. Acad. Sci.*, **112**, 9775–9780.

Fowler, S., Lee, K., Onouchi, H., Samach, A., Richardson, K., Morris, B., Coupland, G. and Putterill, J. (1999) GIGANTEA: a circadian clock-controlled gene that regulates photoperiodic flowering in Arabidopsis and encodes a protein with several possible membrane-spanning domains. *EMBO J.*, **18**, 4679–4688.

Graf, A. and Smith, A.M. (2011) Starch and the clock: the dark side of plant productivity. *Trends Plant Sci.*, **16**, 169–175.

Gu, Z., Steinmetz, L.M., Gu, X., Scharfe, C., Davis, R.W. and Li, W.-H. (2003) Role of duplicate genes in genetic robustness against null mutations. *Nature*, **421**, 63.

Hayama, R., Yokoi, S., Tamaki, S., Yano, M. and Shimamoto, K. (2003) Adaptation of photoperiodic control pathways produces short-day flowering in rice. *Nature*, **422**, 719–722.

Helliwell, C. and Waterhouse, P. (2003) Constructs and methods for high-throughput gene silencing in plants. *Methods San Diego Calif*, **30**, 289–95.

Hughes, M.E., Hogenesch, J.B. and Kornacker, K. (2010) JTK_CYCLE: an efficient nonparametric algorithm for detecting rhythmic components in genome-scale data sets. *J. Biol. Rhythms*, **25**, 372–380.

Hwang, I., Park, J., Lee, B. and Cheong, H. (2011) Loss of Function in GIGANTEA Gene is Involved in Brassinosteroid Signaling. , **4**, 8.

Ito, S., Song, Y.H. and Imaizumi, T. (2012) LOV Domain-Containing F-Box Proteins: Light-Dependent Protein Degradation Modules in Arabidopsis. *Mol. Plant*, **5**, 573–582.

Jung, J.-H., Seo, Y.-H., Seo, P.J., Reyes, J.L., Yun, J., Chua, N.-H. and Park, C.-M. (2007) The GIGANTEA Regulated MicroRNA172 Mediates Photoperiodic Flowering Independent of *CONSTANS* in *Arabidopsis*. *Plant Cell*, **19**, 2736–2748.

Kazama, T., Ichihashi, Y., Murata, S. and Tsukaya, H. (2010) The Mechanism of Cell Cycle Arrest Front Progression Explained by a KLUH/CYP78A5-dependent Mobile Growth Factor in Developing Leaves of Arabidopsis thaliana. *Plant Cell Physiol.*, **51**, 1046–1054.

Kolosova, N., Gorenstein, N., Kish, C.M. and Dudareva, N. (2001) Regulation of Circadian Methyl Benzoate Emission in Diurnally and Nocturnally Emitting Plants. , 16.

Kubota, A., Kita, S., Ishizaki, K., Nishihama, R., Yamato, K.T. and Kohchi, T. (2014) Co-option of a photoperiodic growth-phase transition system during land plant evolution. *Nat. Commun.*, **5**, 3668.

Laitinen, R.A.E., Immanen, J., Auvinen, P., et al. (2005) Analysis of the floral transcriptome uncovers new regulators of organ determination and gene families related to flower organ differentiation in Gerbera hybrida (Asteraceae). *Genome Res.*, **15**, 475–486.

Lou, P., Wu, J., Cheng, F., Cressman, L.G., Wang, X. and McClung, C.R. (2012) Preferential Retention of Circadian Clock Genes during Diploidization following Whole Genome Triplication in *Brassica rapa*. *Plant Cell*, **24**, 2415–2426.

Lu, S.X., Webb, C.J., Knowles, S.M., Kim, S.H.J., Wang, Z. and Tobin, E.M. (2012) CCA1 and ELF3 Interact in the control of hypocotyl length and flowering time in Arabidopsis. *Plant Physiol.*, **158**, 1079–88.

Mallona, I., Weiss, J. and Egea-Cortines, M. (2011) pcrEfficiency: a Web tool for PCR amplification efficiency prediction. *BMC Bioinformatics*, **12**, 404.

Manchado-Rojo, M., Delgado-Benarroch, L., Roca, M.J., Weiss, J. and Egea-Cortines, M. (2012) Quantitative levels of Deficiens and Globosa during late petal development show a complex transcriptional network topology of B function. *Plant J. Cell Mol. Biol.*, **72**, 294–307.

Manchado-Rojo, M., Weiss, J. and Egea-Cortines, M. (2014) Validation of Aintegumenta as a gene to modify floral size in ornamental plants. *Plant Biotechnol. J.*, **12**.

Marcolino-Gomes, J., Rodrigues, F.A., Fuganti-Pagliarini, R., et al. (2014) Diurnal Oscillations of Soybean Circadian Clock and Drought Responsive Genes N. Cermakian, ed. *PLoS ONE*, **9**, e86402.

Más, P., Kim, W.-Y., Somers, D.E. and Kay, S.A. (2003) Targeted degradation of TOC1 by ZTL modulates circadian function in Arabidopsis thaliana. *Nature*, **426**, 567–570.

McClung, C.R. (2006) Plant circadian rhythms. *Plant Cell*, **18**, 792–803.

Mishra, P. and Panigrahi, K.C. (2015) GIGANTEA an emerging story. *Front. Plant Sci.*, **6**. Available at: http://journal.frontiersin.org/article/10.3389/fpls.2015.00008/abstract [Accessed October 9, 2019].

Mizoguchi, T., Wright, L., Fujiwara, S., et al. (2005) Distinct Roles of *GIGANTEA* in Promoting Flowering and Regulating Circadian Rhythms in Arabidopsis. *Plant Cell*, **17**, 2255–2270.

Montaigu, A. de, Tóth, R. and Coupland, G. (2010) Plant development goes like clockwork. *Trends Genet.*, **26**, 296–306.

Müller, N.A., Wijnen, C.L., Srinivasan, A., et al. (2016) Domestication selected for deceleration of the circadian clock in cultivated tomato. *Nat. Genet.*, **48**, 89–93.

Nakamichi, N., Kita, M., Ito, S., Sato, E., Yamashino, T. and Mizuno, T. (2005) PSEUDO-RESPONSE REGULATORS, PRR9, PRR7 and PRR5, together play essential roles close to the circadian clock of Arabidopsis thaliana. *Plant Cell Physiol*, **46**, S135–S135.

Park, D.H., Somer David E., Kim Yang Suk, Choy Yoon Hi, Lim Hee Kyun, Soh Moon Soo, Kim Hyo Jung, Kay Steve A. and Nam Hong Gil (1999) Control of Circadian Rhythms and Photoperiodic Flowering by the Arabidopsis GIGANTEA Gene. *Science*, **285**, 1579–1582.

Pfaffl, M.W., Horgan, G.W. and Dempfle, L. (2002) Relative expression software tool (REST©) for group-wise comparison and statistical analysis of relative expression results in real-time PCR. *Nucleic Acids Res.*, **30**, 10.

Rastogi, S. and Liberles, D.A. (2005) Subfunctionalization of duplicated genes as a transition state to neofunctionalization. *BMC Evol. Biol.*, **5**, 28.

Reale, L., Porceddu, A., Lanfaloni, L., Moretti, C., Zenoni, S., Pezzotti, M., Romano, B. and Ferranti, F. (2002) Patterns of cell division and expansion in developing petals of Petunia hybrida. *Sex. Plant Reprod.*, **15**, 123–132.

Ruíz-Ramón, F., Águila, D.J., Egea-Cortines, M. and Weiss, J. (2014) Optimization of fragrance extraction: Daytime and flower age affect scent emission in simple and double narcissi. *Ind. Crops Prod.*, **52**.

Sawa, M. and Kay, S.A. (2011) GIGANTEA directly activates Flowering Locus T in Arabidopsis thaliana. *Proc. Natl. Acad. Sci.*, **108**, 11698–11703.

Sawa, M., Nusinow, D.A., Kay, S.A. and Imaizumi, T. (2007) FKF1 and GIGANTEA Complex Formation Is Required for Day-Length Measurement in Arabidopsis. *Science*, **318**, 261–265.

Schmittgen, T.D. and Livak, K.J. (2008) Analyzing real-time PCR data by the comparative CT method. *Nat. Protoc.*, **3**, 1101–1108.

Schuurink, R.C., Haring, M.A. and Clark, D.G. (2006) Regulation of volatile benzenoid biosynthesis in petunia flowers. *Trends Plant Sci.*, **11**, 20–25.

Southern, E.M. (1975) Detection of specific sequences among DNA fragments separated by gel electrophoresis. *J. Mol. Biol.*, **98**, 503–517.

Staiger, D., Shin, J., Johansson, M. and Davis, S.J. (2013) The circadian clock goes genomic. *Genome Biol.*, **14**, 208.

Terry, M.I., Pérez-Sanz, F., Díaz-Galián, M.V., Pérez de los Cobos, F., Navarro, P.J., Egea-Cortines, M. and Weiss, J. (2019) The Petunia CHANEL Gene is a ZEITLUPE Ortholog Coordinating Growth and Scent Profiles. *Cells*, **8**, 343.

Tseng, T.-S. (2004) SPINDLY and GIGANTEA Interact and Act in Arabidopsis thaliana Pathways Involved in Light Responses, Flowering, and Rhythms in Cotyledon Movements. *PLANT CELL ONLINE*, **16**, 1550–1563.

Watanabe, S., Xia, Z., Hideshima, R., et al. (2011) A Map-Based Cloning Strategy Employing a Residual Heterozygous Line Reveals that the *GIGANTEA* Gene Is Involved in Soybean Maturity and Flowering. *Genetics*, **188**, 395–407.

Weller, J.L., Liew, L.C., Hecht, V.F.G., et al. (2012) A conserved molecular basis for photoperiod adaptation in two temperate legumes. *Proc. Natl. Acad. Sci.*, **109**, 21158–21163.

Wu, G., Anafi, R.C., Hughes, M.E., Kornacker, K. and Hogenesch, J.B. (2016) MetaCycle: an integrated R package to evaluate periodicity in large scale data. *Bioinformatics*, **32**, 3351–3353.

Zakhrabekova, S., Gough, S.P., Braumann, I., et al. (2012) Induced mutations in circadian clock regulator Mat-a facilitated short-season adaptation and range extension in cultivated barley. *Proc. Natl. Acad. Sci.*, **109**, 4326–4331.

CHAPTER 3 – Phenotypic characterization of *Petunia x hybrida* plants transformed with a CRISPR/*Cas*9 construct targeting both GIGANTEA paralogs *PhGI1* and *PhGI2*.

Abstract

The gene *GIGANTEA* codes for a large protein with several biological functions including control of growth transition, abiotic stress and flower senescence. There are two paralogs in *Petunia* x *hybrida*, *PhGI1* and *PhGI*2. We have used a CRISPR/Cas9 approach to knockout both genes using a highly conserved region as target for mutation. In agreement with observations on *PhGI*1 and *PhGI*2 iRNA-silenced *P. hybrida* plants, *Cas*9/gRNA*PhGI1/2* lines confirmed *PhGI1* and *PhGI2* function as a negative regulator of vegetative growth, with a denser median-apical growth habit. Similar to iRNA lines, the *Cas*9/gRNA*PhGI* transformed lines showed a reduction in floral bud number, early flower bud senescence and abortion as well as a reduced flower size. The present analysis confirms the functions of the *PhGI1* and *PhGI2* paralogs as positive regulators of generative growth and negative regulators of vegetative growth. However, we cannot rule out if a synergistic action among both the paralogs occurred. Previous phenotyping of iRNA lines indicated that while *PhGI1* does not affect flowering time, *PhGI2* has a conserved function in flowering time promotion. However, *Cas*9/gRNA*PhGI* transformed lines showed advanced flowering time and this opposite phenotype might be related to day-length experimental conditions or a dosage effect.

Introduction

The CRISPR (regularly interspaced, short palindromic repeat) Cas9 (CRISPR associated endonuclease 9) technology has recently shown to be an efficient system for targeted mutagenesis in many plant species, including Arabidopsis, tomato, potato or wheat (Upadhyay *et al.*, 2013; Li *et al.*, 2013; Jiang *et al.*, 2013; Ito *et al.*, 2015; Wang *et al.*, 2015). The system is composed of the Cas9 nuclease and a guide RNA (gRNA), which determines the sequence specificity where the nuclease will cut. The system derives from a microbial immune system, where the gRNA guides the nuclease which cleaves the invader DNA of viruses or plasmids (F Ann Ran *et al.*, 2013). The resulting double strand breaks (DSB) lead to repair pathways, consisting in non-homologous end joining (NHEJ) or homologous recombination (HR). Both mechanisms lead to genome modifications (Jinek *et al.*, 2012). The CRISPR/Cas9 technology has also shown to be feasible for gene knockout modifications in *Petunia hybrida* (Zhang *et al.*, 2016). In the first application of this technology in *P. hybrida*, the gene *Phytoene desaturase* (*PDS*), a key enzyme in carotenoid biosynthesis, was efficiently knocked-out, leading to albino phenotypes. Another example from Petunia is the knockout of ethylene biosynthesis enzyme 1-aminocyclopropane-1-carboxylate oxidase, an enzyme involved on flower senescence, which successfully led to an enhanced flower longevity (Xu *et al.*, 2020).

P. hybrida is an ornamental bedding plant species as well as a model plant for comparative and developmental genetics (Gerats and Vandenbussche, 2005). It also serves as a model for studying the function of genes belonging to the circadian clock gene network (Bombarely *et al.*, 2016; Terry, Carrera-Alesina, *et al.*, 2019; Terry,

Pérez-Sanz, Díaz-Galián, *et al.*, 2019; Brandoli *et al.*, 2020). The genome sequencing and assembly of the *P. hybrida* parents, *P. axillaris and P. inflata,* revealed the Petunia clock structure. The analysis identified a generally conserved configuration of the clock gene network, but with changes in gene copy number of certain genes, including the genes *PRR7*, *PRR5* and *GIGANTEA* (Bombarely et al., 2016). In case of the *PRR* genes, a detailed analysis of these paralogs indicated the occurrence of changes in intron-exon structure as well as of certain protein domains during evolution. While *P. hybrida,* like the parental *P. axillaris,* has only two paralogs of *GIGANTEA* (*PhGI1* and *PhGI2*), the other parent, *P. inflata,* has three *GI* paralogs. *PaxiGI2* shows a deletion at the N-terminus compared to the other Petunia *GI* paralogs and *AtGI*, as well as a 41 amino acid insertion (Terry, Carrera-Alesina, *et al.*, 2019). The differences in the coding region between *PhGI1* and *PhGI2* may hint to a possible functional diversification between the two paralogs.

The role of *GI* as a circadian clock gene results from its interaction with the gene *CHANEL*, the *ZEITLUPE (ZTL)* orthologue in Petunia, one of the three clock genes belonging to the evening loop. ZTL protein controls the proteasome-dependent degradation of *TIMING OF CAB EXPRESSION 1 (TOC1),* the central clock protein. Thus, GI is essential for ZTL protein oscillation through direct protein-protein interaction. *GI* transcription is clock-controlled and the resulting rhythmicity in GI protein abundance consequently confers a post-translational rhythm on ZTL protein. Therefore, both genes are necessary to maintain a normal circadian period (Kim *et al.*, 2007).

GI functions were identified analyzing it in different species. A relatively conserved function consists in a control over flowering, as observed in Arabidopsis (Fowler *et al.*, 1999), soybean (Watanabe *et*

al., 2011), rice (Hayama *et al.*, 2003), *Marchantia* (Kubota *et al.*, 2014), barley (Zakhrabekova *et al.*, 2012) and Petunia (chapter 2). Additionally, *GI* has been shown to be involved in diverse functions such as control of the vegetative growth phase length (Ding *et al.*, 2018), salt and cold stress tolerance (Cao *et al.*, 2005; Park *et al.*, 2013), gibberellin signaling (Tseng, 2004) and sugar sensing (Dalchau *et al.*, 2011). The latter function is related to its involvement in maintaining circadian oscillation, as *GI* is required for the full response of the circadian clock to sucrose, which is characterized by a particular sensitivity in the dark (Dalchau *et al.*, 2011).

Silencing of the two GI paralogs in Petunia by interference RNA (iRNA) revealed both subfunctionalization and neofunctionalization (Brandoli *et al.*, 2020; Chapter 2). Functions common to both paralogs include an effect on the emission of volatile organic compounds (VOCs), which follows a circadian rhythm with a higher emission at night and a lower one at midday in *Petunia x hybrida*. Reduced *PhGI*1 and *PhGI*2 expression, through iRNA, led to generally lower emission rates and changes in the relative contribution of the different compounds (Brandoli *et al.*, 2020; Chapter 2). Apart from the effect on floral volatile emission, the two paralogs also coincide in controlling specific parameters of vegetative growth and flower production. The vegetative growth effects upon silencing by iRNA consisted in a reduction of median and apical internode length and leaf size. Concerning flower bud production, iRNA lines of both paralogs showed a reduction in flower bud number, flower size and a premature abortion of flower buds. The effect on inflorescence architecture, floral size and floral volatile emission are *GI* functions undescribed until now in any other plant. In addition to the common functions, some subfunctionalization occurred between the two paralogs including the

control over flowering time, coordinated by *PhGI2*, the control over the rhythmic expression period of the clock genes *PhGI1* and *PhCHL* by *PhGI1*, and the control over the rhythmic period of expression of the clock gene *PhTOC1* and the rhythmic pattern of VOCs emission by *PhGI2* (Brandoli *et al.*, 2020; Chapter 2).

In this work, we have characterized both *GI* paralogs from *Petunia hybrida*, *PhGI1* and *PhGI2*, by creating transgenic Cas9/gRNAPhGI lines using the CRISPR/Cas9 technique with the objective to confirm the functions previously described by using iRNA constructs of *PhGI*1 and *PhGI*2 (Brandoli *et al.*, 2020; Chapter 2). Our results confirm the role of *GIGANTEA* as a negative regulator of vegetative growth, as well as a regulator of flowering by controlling floral bud formation and inhibiting early senescence of flowers.

Methods

Plant Growth Conditions and Sampling

Petunia x hybrida plants of the double haploid variety 'Mitchell W115' were used in all experiments. Seeds were surface-sterilized with 95% ethanol for one minute, followed by washing under stirring for 25 minutes in a mix of 25% bleach and 20% tween. Finally, seeds were rinsed three times with sterile distillated water and germinated in half-strength MS (Murashige and Skoog, 1962) with MS vitamins in a growth chamber under long-day conditions (16h light/8h dark), a light intensity of 250 μE m^{-2} s^{-1}, and a constant temperature of 26 ± 1ºC. All transgenic lines were cultured *in vitro* under the aforementioned growth conditions before being acclimatized and grown in a greenhouse under natural short-day conditions. Plants were cultured using a commercial substrate (Universal Substrate, Floragard Betriebs

GmbH, Oldenburg, Germany), watered as required and transplanted to fresh substrate twice during the growth phase.

Young leaves for each transgenic *hCas9* plant were collected, frozen in liquid nitrogen and stored at -80° C until further analyses. Total RNA was isolated using a phenol:chloroform based protocol (Box *et al.*, 2011). Genomic DNA from the double-transformed *Cas9/gRNAPhGI* plants was extracted using a standard CTAB method.

The phenotypic analysis of the vegetative traits was performed by analyzing the basal, median and apical areas of the plants, considering the size and the relative level of chlorophyll of, at least, three leaves for each area as well as the length of the internodes. Regarding the generative traits, the number and size of flowers, and the flowering time from the moment of the first transplant in the ground to the appearance of the first flower bud, were taken into consideration.

Constructs design and plant transformation.

For the gRNA design, we carried out a pyramid screening of the genomic sequences of the two paralogs. The sequences information for the comparison were obtained from the genomic clones *PhGI1* (Peaxi132Scf1428Ctg026) and *PhGI2* (Peaxi132Scf1428Ctg060) identified in *P. hybrida* 'W115 Mitchell' (Bombarely *et al.*, 2016). Firstly, the areas with the highest levels of homology were identified by aligning the sequences of *GI* and its alleles, using the online software "Tcoffee" (http://tcoffee.crg.cat/) (Figure S6). Subsequently the PAM (5'-NGG-3') sequences were identified in the areas of homology and finally, the target site was selected based on several characteristics. These included the GC content, between 40% and 80% (Bortesi *et al.*, 2016; Bruegmann *et al.*, 2019), location in the gene (Doench *et al.*,

2014), number of consecutive base pairing (CBPs) between the guide sequence and the other sequences (crRNA and tracrRNA) (Liang *et al.*, 2016), off-target possibilities and the absence of the stop codon for the U6 Promoter (Gao *et al.*, 2018). We used the online software "CCTop - CRISPR/Cas9 target online predictor" (https://crispr.cos.uni-heidelberg.de/) and "CRISPR Efficiency Prediction Tool" (https://www.flyrnai.org/evaluateCrispr/help.jsp).

The 'W115 Mitchell' double haploid was transformed as described before (Manchado-Rojo *et al.*, 2014). We performed a two-step plant *Agrobacterium*-mediated transformation strategy as previously described (Jinek *et al.*, 2012). The plasmid pK7WGF2::hCas9 (Addgene ID 46965), was firstly transformed into Petunia wild type plants. Subsequently, the *hCas*9 transgenic plants were re-transformed with gRNA constructs.

The *hCas*9 plants of the T0 generation were grown under selective conditions and the *hCas*9 expression was confirmed by reverse transcription-PCR amplification (RT-PCR) using specific primers (Table S12). Following self-pollination of the *hCas*9 T0 transgenic plants, T1generation was used for the second transformation with the gRNA constructs. None of the T0 *hCas*9 Petunia plants showed morphological or developmental changes compared to the wild type and their non-transgenic siblings.

Analysis of the chlorophyll content

The CM-500 Chlorophyll Meter was used to calculate the relative chlorophyll content in basal, median and apical leaves of the transgenic lines of *PhGI* from T0 generation as well as in wild type plants. The relative chlorophyll content was determined on at least three

biological replicates, based on the light penetration coefficient in a 2-wavelength range corresponding to red light and IR light.

Data analysis procedures.

The statistical analysis of the vegetative traits was carried out on at least three samples per plant. Significance differences among data were determined based on the T-test analysis. All the P values ≤ 5.00E-02 were considered significant.

Results

CRISPR/Cas9 targeting of the *PhGI1/2 loci* in Petunia

RNAi silencing of both *RNAiPhGI1* (Brandoli *et al.*, 2020) and *RNAiPhGI2* (Chapter 2) showed modified volatile profiles, floral abortion and ectopic flower inibition. However, in both sets of RNAi-silenced lines, clear differences could be found in the phenotypes suggesting a possible subfunctionalization of floral transition and coordination of the clock. We attempted to knock down simultaneously both *PhGI* paralogs via CRISPR/Cas9, exploiting some regions with sufficient DNA homology (Figure 28). Eight independent double-transformed h*Cas9/gRNAPhGI* lines (1, 6, 7, 8, 9, 11, 17 and 18) resulted positive according to the molecular analysis for both the *hCas*9 sequence (Figure 29a) and the fragment of the U6 promoter-guide-gRNA scaffold (Figure 29b). Three wild type plants were included as controls for further studies.

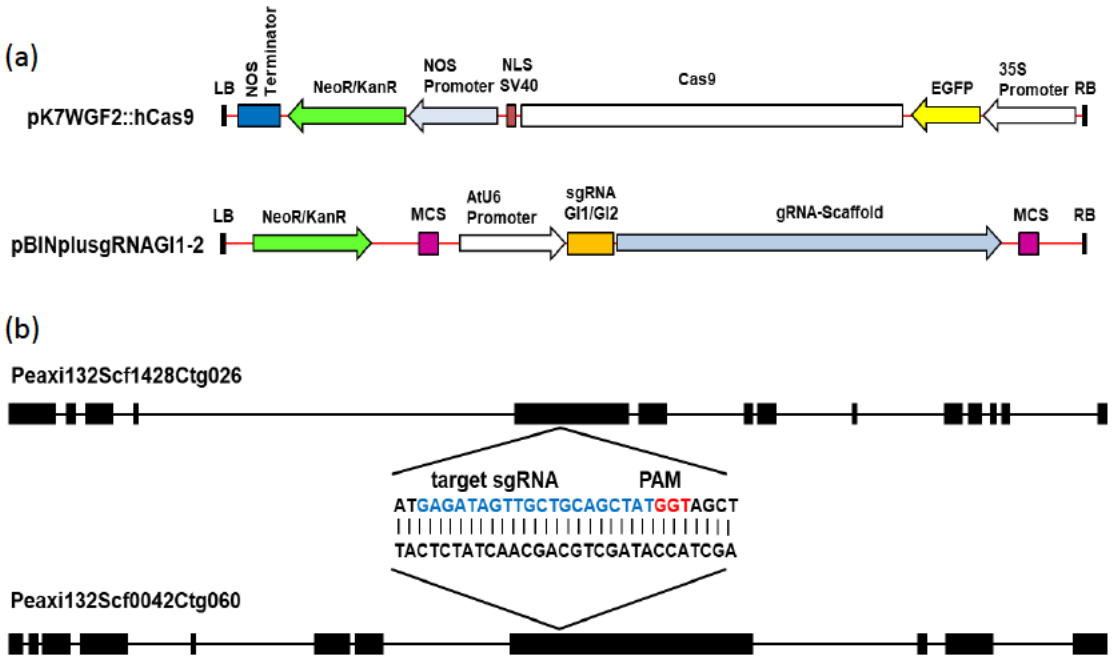

Figure 28| Diagram of the CRISPR/Cas9 constructs used in this study.

(a) The binary plasmids for targeted genome mutagenesis used. (b) Schematic representation of the petunia *GI1* and *GI2* genes indicating the gRNA target sites and sequences. Lines in bold indicate exons, thin lines indicate introns. **Neo/KanR**, Neomycin/kanamycin resistance; **PAM**, proto-spacer adjacent motif; **LB**, left border; **RB**, right border; **MCS**, multiple cloning site; **EGFP**. Enhanced green fluorescent protein.

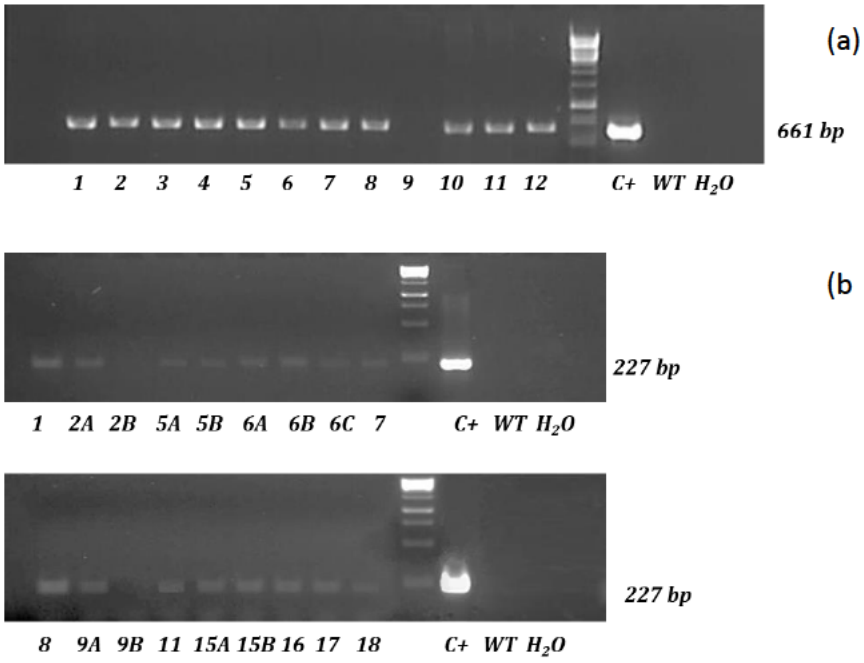

Figure 29| Agarose gel 2% (w/v) analysis of CRISPR/Cas9 components.

(a) RT-PCR amplification of the *hCas*9 sequence after the first transformation with the plasmid pK7WGF2::hCas9. A DNA miniprep of the binary plasmid pK7WGF2::hCas9 was used as positive control, water and wild type Petunia genomic DNA as negative controls. (b) PCR with genomic DNA for the identification of the fragment containing the "AtU6 promoter-guide RNA-gRNA scaffold" after the second transformation. The binary plasmid pBINplusgRNA GI1-2 was used as positive control, water and wild type Petunia genomic DNA as negative controls. GeneRuler 1 kb DNA Ladder (Thermo Fisher Scientific) was used as a molecular weight ladder (catalog number: SM0312, https://www.thermofisher.com).

PhGI1/2 regulate vegetative growth and development

The vegetative parameters of the transgenic plants compared to the wild type plants are given in Table 9. Additional information about the individual independent lines are given in Table S13. The basal and apical leaves of the transformed plants stood out for a significant increase ($P \leq 5.00E-02$) in width of 8.15% and 11.6% respectively. The basal leaves did not show appreciable variations in length, while the apical ones were characterized by an increase of 6.2%. On the contrary,

the leaves of the central area showed a reduction both in length and in width (Figure 30).

Genotype:	W.T.	*PhGI*	% GI versus W.T.	P value
Plant Height (cm)	39.7 ± 1.0	39.8 ± 1.14	+0.25	9.55E-01
N° of leaves to the 1° flower	37.3 ± 1.5	38.1 ± 1.24	+2.14	4.79E-01
Basal Leaves length (mm)	68.9 ± 1.5	69.9 ± 1.8	+1.48	1.50E-01
Basal leaves width (mm)	40.9 ± 1.3	44.1 ± 1.4	+8.15	1.74E-05
Median Leaves length (mm)	51.8 ± 1.4	50.1 ± 1.2	-3.22	2.93E-03
Median leaves width (mm)	28.3 ± 1.1	26.7 ± 1.2	-5.97	1.25E-03
Apical leaves length (mm)	31.6 ± 1.3	33.4 ± 1.00	+6.2	1.82E-03
Apical leaves width (mm)	18.37 ± 0.8	20.5 ± 1.7	+11.6	4.64E-04
Basal leaves Chlorophyll	25.8 ± 1.5	23.9 ± 1.1	-7.2	7.23E-03
Median leaves Chlorophyll	30.15 ± 1.3	35.8 ± 1.4	+18.9	1.77E-08
Apical leaves Chlorophyll	26.8 ± 1.7	36.1 ± 1.2	+34.7	4.82E-10

Table 9| Comparison of vegetative parameters between wild type plants and the Cas9/gRNAPhGI lines.

Data are given as the average ± standard error, based on at least three biological replicates of all transgenic plants. The height was calculated from the base to the first flowering meristem, when the first flowering event occurred. P values ≤ 5.00E-02, according to Student's T-test, were considered as significant.

Although the *Cas*9/gRNA*PhGI* plants did not differ both in height and in the total number of leaves from the wild type plants, the foliar apparatus generally seemed denser, particularly in the apical region, probably due to an increased number of axillary meristems in the median-apical portions (data not shown), with a darker green color (Table 9). The plants of all eight transformed lines indeed showed a common greener appearance than the wild type phenotype, due to a significant increase in chlorophyll levels, especially in the median and

apical leaves of 18,9 and 34,7% respectively (Figure 30). The basal leaves showed less differences than the middle and apical ones even so they stood out for a lower level of chlorophyll than the wild type (Table 9).

Figure 30| PhG1 T0 lines compared to wild type plants in greenhouse under natural long-day conditions.

Wild type plant (left) and transformed *PhG1* lines (right).

PhGI1/2 controls ectopic flower formation and premature flower senescence.

All the plants analized showed an average reduction of 12.78% in the total number of fully developed flowers compared to wild type plants (Table 10). Many of these flowers were characterized by reduced dimensions both in terms of corolla diameter and tube length

(Figure 31), respectively, of 4.8 and 4.6%, while no changes in the length of the petiole were detected (Table 10).

Genotype:	W.T.	*PhGI*	% GI versus W.T.	P value
N° of flower buds	22.7 ± 1.5	20.1 ± 3.8	-11.45	1.20E-01
N° of fully developed flowers	22.7 ± 1.5	17.4 ± 4.7	-23.35	1.66E-02
% of fully developed flowers	100	85	-15	1.58E-02
Corolla diameter (mm)	50.9 ± 1.08	48.5 ± 2.19	-4.8	2.84E-05
Tube length (mm)	32.5 ± 3.8	30.9 ± 1.8	-4.65	4.34E-02
Petiole length (mm)	35.6 ± 3.7	34.7 ± 3.7	-2.67	3.82E-01

Table 10| Comparison of floral parameters between wild type plants and Cas9/gRNAPhGI transformed lines.

Data are given as average ± standard errors of at least three biological replicates of all transgenic plants. P values ≤ 5.00E-02, according to Student's T-test, were considered as significant.

Additional information about the individual independent lines are given in Table S14. Many plants showed the presence of aborted ectopic flowers, which appeared prematurely during the *in vitro* cultivation phase, in a growth chamber under controlled conditions, and then continued throughout the greenhouse growth phase under short day natural conditions, excluding the possibility of legitimizing environmental causes for this phenomenon (Figure 31b, 31c**)**. These flowers appeared at the bifurcation points where the mature flower separates from the new floral meristem, characterized by a premature senescence of the tissues that led them to developmental arrest, without therefore reaching the size of a mature flower.

Figure 31| Flower size in T0 Cas9/gRNAPhGI lines compared to the wild type.

(a) Corolla diameter and tube length of the wild type (left) and transgenic lines (right). (b) Aborted ectopic flower appeared *in vitro* under controlled conditions in growth chamber phase. (c) Aborted ectopic flower in plants grown in greenhouse under short day natural conditions.

Transformed *Cas*9/gRNA*PhGI1/2* plants showed an altered flowering time profile compared with the wild type phenotypes (Figure 32). Flowering began 3 weeks earlier than the wild type plants and continued gradually but with increasing incidence, in the following 4 weeks until flowering of the control plants occurred. Flowering time was calculated as the percentage of fully open flowers in weeks after transplanting from *in vitro* culture to the soil substrate.

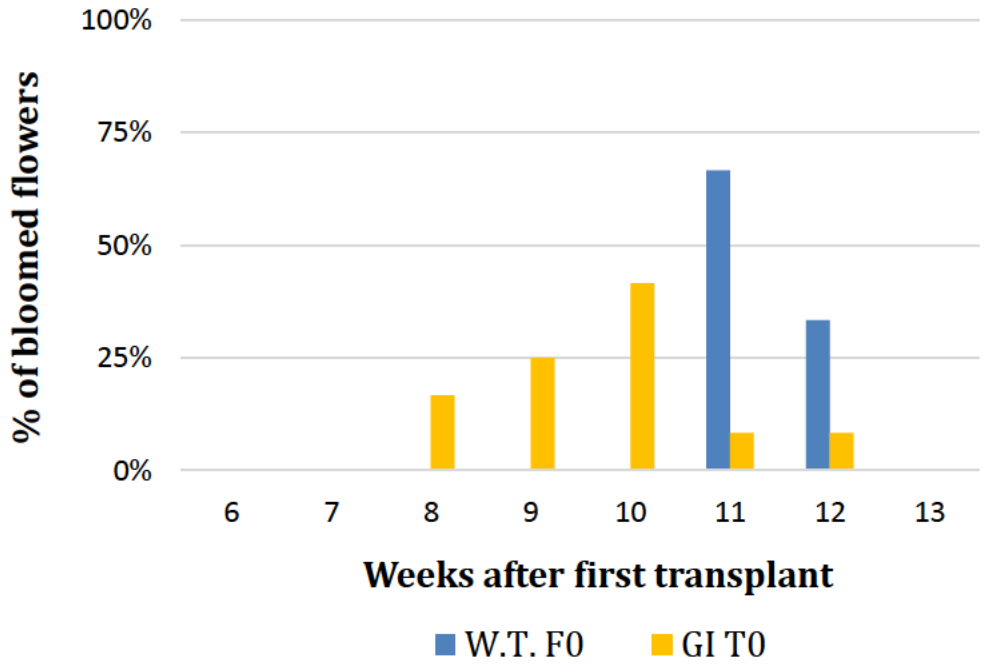

Figure 32| Percentage of fully open flowers in weeks after transplanting from in vitro culture to substrate of transformed Cas9/gRNAPhGI lines compared to wild type plants.

Plants were cultured in a greenhouse under natural long-day conditions.

Discussion

In this work we performed a functional analysis in *Petunia x hybrida* by knocking out simultaneously its two paralogs, *PhGI1* and *PhGI2,* using the CRISPR/Cas9 technique. We have identified two regions with a high degree of homology as the nuclease target sequence. We also carried out a thorough analysis, thanks to various informatics tools, to exclude possible unwanted off-targets in the genome. Even though the specific gene sequence has been carefully selected for the editing of *PhGI1* and *PhGI2*, we cannot exclude the possibility of undetectable off-target cleavage in other parts of the genome (Cho *et al.*, 2014).

Overall, the double-transformed *Cas*9/gRNA*PhG*I lines were characterized by a strong modification in the growth habit and vegetative parameters, resembling the *RNAiPhGI1* and *RNAiPHGI2* lines. This indicated that the CRISPR/Cas was able to render plants with multiple gene knockouts. Previous studies in rice and Arabidopsis have shown that most plants are edited in both wild type copies, thus homozygous knockouts can be obtained already in T0 plants (Miao *et al.*, 2014). The actual allelic combinations obtained for the different transgenic lines remains to be determined.

All transgenic plants stood out for a greater dimension in length and width in the apical leaves while in the basal ones, this was observed only in leaf width. We also observed a structural change in plant growth mainly due to an increase in relative levels of chlorophyll in the central and apical leaves with a darker green color. These phenomena had already been described in an earlier study (Brandoli *et al.*, 2020), in which these characteristics were attributed to the *PhGI1* gene. Our results using CRISPR/Cas9 technology confirmed the role of *PhGI*1/2 as a negative regulator of the vegetative growth as already observed in Arabidopsis, were *GI* was shown to control the growth of the hypocotyl (Kim *et al.*, 2012) and its loss of function results in taller plants with an increased number of leaves in the rosettes (Hwang *et al.*, 2011).

The parameters analyzed have highlighted some morphological characteristics among the transformed plants compared to the wild type phenotypes, which agree with previously described findings in *GI* iRNA-silenced *P. hybrida* plants (Brandoli *et al.*, 2020). In the current study, the *Cas*9/gRNA*PhGI* transgenic lines displayed notable changes such as the general reduction in the number of floral buds, mature

flowers of a reduced size and the appearance of a further meristematic flower buds at the bifurcation point, marked by a premature senescence tissue and abortion. All these characteristics agree with previously described findings in *GI* iRNA-silenced *P. hybrida* plants (Brandoli *et al.*, 2020). Therefore, we can add *GI* to the list of genes involved in controlling flower development described in Petunia. These include *double top* (*dot*) and *aberrant flower* (*alf*) (Souer *et al.*, 1998), which cause a failure of flower formation; *extra petals* (*exp*), that cause an increase in petal number above four, chimeric floral organs and unfused carpel tips, as well as *evergreen* (*evg*), which causes a solitary flower formation in the meristematic inflorescence (Rebocho *et al.*, 2008).

The reduced number of flowers in *Cas*9/gRNA*PhG*I confirms the hypothesis of an upstream involvement of *PhGI1/2* in the regulation of flower-meristem-identity genes *PETUNIA FLOWERING GENE* (*PFG*) (R., G., H., Immink *et al.*, 1999) and *ABERRANT LEAF AND FLOWER* (*ALF*) (Souer *et al.*, 1998). Currently, we are not able to define if this role is due to a synergistic action of both paralogs or only one of the two and which one. On the other hand, the aborted flowers clearly indicate its role on the origins of the reproductive organs, indicating that the senescence of the tissues occurred after the activation of the genes that define the identity of the floral organs. This aspect leaves the possibility of further and more detailed studies in this regard.

Almost all transformed plants showed a different flowering time compared to the control wild type plants. This phenomenon can be attributed to the fact that *GI* is known to be a key regulator of photoperiodic flowering processes in many different species. It indirectly controls the activation of *CONSTANS* (*CO)* and therefore of

FLOWERING LOCUS T (*FT*), through its protein-protein interaction with FLAVIN-BINDING, KELCH REPEAT, F BOX protein 1 (FKF1) (Sawa *et al.*, 2007). This enzyme complex mediates the degradation of *CYCLING DOF FACTOR 1* (*CDF1*), the main repressor of *CO*. Alternatively, it can induce flowering by altering the stability of the *FT* transcriptional repressors such as *TEMPRANILLO 1* (*TEM1*), *TEMPRANILLO 2* (*TEM2*) and *SHORT VEGETATIVE PHASE* (*SVP*) (Sawa and Kay, 2011). An additional pathway by which *GI* regulates flowering independently of *CO* is through the interaction with miR172, which controls the induction of *FT* and therefore flowering (Jung *et al.*, 2007).

Our results show that *PhGI* is undoubtedly involved in the regulation of flowering, as happens in many other plant species including Arabidopsis (Mishra and Panigrahi, 2015), soybeans (Watanabe *et al.*, 2011), barley (Zakhrabekova *et al.*, 2012), wheat (Zhao *et al.*, 2005) and maize (Bendix *et al.*, 2013). While silencing of *PhGI1* did not affect flowering time (Brandoli *et al.*, 2020) and silencing of *PhGI2* resulted in late flowering under long-day conditions (Chapter 2), here we observed an advanced flowering time. GI promotion of flowering time is day length dependent in Arabidopsis and *GI* promotes flowering under long days by promoting the expression of flowering time genes, but has minor effects under short days (Fowler *et al.*, 1999). Similarly, Petunia, a facultative long day plant, seems to show flower promotion through GI only under long day conditions, while this effect does not exist under short day conditions. Based on the present data we cannot determine whether the change in flowering time compared to wild type plants depends exclusively on the action of one of the two paralogs or on the action of both. A possible neofunctionalization of one of the two paralogs as a response to

evolutionary needs has already been hypothesized (Chapter 2), leaving wide and interesting research perspectives open in this direction.

REFERENCES

Bendix, C., Mendoza, J.M., Stanley, D.N., Meeley, R. and Harmon, F.G. (2013) The circadian clock-associated gene gigantea1 affects maize developmental transitions. *Plant Cell Environ.*, **36**, 1379–1390.

Bombarely, A., Moser, M., Amrad, A., et al. (2016) Insight into the evolution of the Solanaceae from the parental genomes of Petunia hybrida. *Nat. Plants*, **2**, 16074.

Bortesi, L., Zhu, C., Zischewski, J., et al. (2016) Patterns of CRISPR/Cas9 activity in plants, animals and microbes. *Plant Biotechnol. J.*, **14**, 2203–2216.

Box, M.S., Coustham, V., Dean, C. and Mylne, J.S. (2011) Protocol: A simple phenol-based method for 96-well extraction of high quality RNA from Arabidopsis. *Plant Methods*, **7**, 7.

Brandoli, C., Petri, C., Egea-Cortines, M. and Weiss, J. (2020) The clock gene Gigantea 1 from Petunia hybrida coordinates vegetative growth and inflorescence architecture. *Sci. Rep.*, **10**, 275.

Bruegmann, T., Deecke, K. and Fladung, M. (2019) Evaluating the Efficiency of gRNAs in CRISPR/Cas9 Mediated Genome Editing in Poplars. *Int. J. Mol. Sci.*, **20**, 3623.

Cao, S., Ye, M. and Jiang, S. (2005) Involvement of GIGANTEA gene in the regulation of the cold stress response in Arabidopsis. *Plant Cell Rep.*, **24**, 683–690.

Cho, S.W., Kim, S., Kim, Y., Kweon, J., Kim, H.S., Bae, S. and Kim, J.-S. (2014) Analysis of off-target effects of CRISPR/Cas-derived RNA-guided endonucleases and nickases. *Genome Res.*, **24**, 132–141.

Dalchau, N., Baek, S.J., Briggs, H.M., et al. (2011) The circadian oscillator gene GIGANTEA mediates a long-term response of the Arabidopsis thaliana circadian clock to sucrose. *Proc. Natl. Acad. Sci. U. S. A.*, **108**, 5104–9.

Ding, J., Böhlenius, H., Rühl, M.G., Chen, P., Sane, S., Zambrano, J.A., Zheng, B., Eriksson, M.E. and Nilsson, O. (2018) GIGANTEA-like genes control seasonal growth cessation in Populus. *New Phytol.*, **218**, 1491–1503.

Doench, J.G., Hartenian, E., Graham, D.B., et al. (2014) Rational design of highly active sgRNAs for CRISPR-Cas9–mediated gene inactivation. *Nat. Biotechnol.*, **32**, 1262–1267.

Fowler, S., Lee, K., Onouchi, H., Samach, A., Richardson, K., Morris, B., Coupland, G. and Putterill, J. (1999) GIGANTEA: a circadian clock-controlled gene that regulates photoperiodic flowering in Arabidopsis and encodes a protein with several possible membrane-spanning domains. *EMBO J.*, **18**, 4679–4688.

Gao, Z., Herrera-Carrillo, E. and Berkhout, B. (2018) Delineation of the Exact Transcription Termination Signal for Type 3 Polymerase III. *Mol. Ther. - Nucleic Acids*, **10**, 36–44.

Gerats, T. and Vandenbussche, M. (2005) A model system for comparative research: Petunia. *Trends Plant Sci.*, **10**, 251–256.

Hayama, R., Yokoi, S., Tamaki, S., Yano, M. and Shimamoto, K. (2003) Adaptation of photoperiodic control pathways produces short-day flowering in rice. *Nature*, **422**, 719–722.

Hwang, I., Park, J., Lee, B. and Cheong, H. (2011) Loss of Function in GIGANTEA Gene is Involved in Brassinosteroid Signaling. , **4**, 8.

Immink, R.G.H., Hannapel, D.J., Ferrario, S., Busscher, M., Franken, J., Lookeren Campagne, M.M. and Angenent, G.C. (1999) A MADS box gene involved in flowering. , 10.

Ito, Y., Nishizawa-Yokoi, A., Endo, M., Mikami, M. and Toki, S. (2015) CRISPR/Cas9-mediated mutagenesis of the RIN locus that regulates tomato fruit ripening. *Biochem. Biophys. Res. Commun.*, **467**, 76–82.

Jinek, M., Chylinski, K., Fonfara, I., Hauer, M., Doudna, J.A. and Charpentier, E. (2012) A Programmable Dual-RNA-Guided DNA Endonuclease in Adaptive Bacterial Immunity. *Science*, **337**, 816–821.

Jung, J.-H., Seo, Y.-H., Seo, P.J., Reyes, J.L., Yun, J., Chua, N.-H. and Park, C.-M. (2007) The GIGANTEA Regulated MicroRNA172 Mediates Photoperiodic Flowering Independent of *CONSTANS* in *Arabidopsis*. *Plant Cell*, **19**, 2736–2748.

Kim, W.-Y., Fujiwara, S., Suh, S.-S., et al. (2007) ZEITLUPE is a circadian photoreceptor stabilized by GIGANTEA in blue light. *Nature*, **449**, 356–360.

Kim, Y., Yeom, M., Kim, H., Lim, J., Koo, H.J., Hwang, D., Somers, D. and Nam, H.G. (2012) GIGANTEA and EARLY FLOWERING 4 in Arabidopsis Exhibit Differential Phase-Specific Genetic Influences over a Diurnal Cycle. *Mol. Plant*, **5**, 678–687.

Kubota, A., Kita, S., Ishizaki, K., Nishihama, R., Yamato, K.T. and Kohchi, T. (2014) Co-option of a photoperiodic growth-phase transition system during land plant evolution. *Nat. Commun.*, **5**, 3668.

Liang, G., Zhang, H., Lou, D. and Yu, D. (2016) Selection of highly efficient sgRNAs for CRISPR/Cas9-based plant genome editing. *Sci. Rep.*, **6**, 21451.

Manchado-Rojo, M., Weiss, J. and Egea-Cortines, M. (2014) Validation of Aintegumenta as a gene to modify floral size in ornamental plants. *Plant Biotechnol. J.*, **12**.

Mishra, P. and Panigrahi, K.C. (2015) GIGANTEA an emerging story. *Front. Plant Sci.*, **6**. Available at: http://journal.frontiersin.org/article/10.3389/fpls.2015.00008/abstract [Accessed October 9, 2019].

Murashige, T. and Skoog, F. (1962) Murashige T & Skoog F. A revised medium for rapid growth and bioassays with tobacco tissue cultures. Physiol. Plant. 15:473-97, 1962. , 1.

Park, H.J., Kim, W.-Y. and Yun, D.-J. (2013) A role for GIGANTEA: Keeping the balance between flowering and salinity stress tolerance. *Plant Signal. Behav.*, **8**, e24820.

Ran, F. Ann, Hsu, P.D., Wright, J., Agarwala, V., Scott, D.A. and Zhang, F. (2013) Genome engineering using the CRISPR-Cas9 system. *Nat. Protoc.*, **8**, 2281–2308.

Ran, F Ann, Hsu, P.D., Wright, J., Agarwala, V., Scott, D.A. and Zhang, F. (2013) Genome engineering using the CRISPR-Cas9 system. *Nat. Protoc.*, **8**, 2281–2308.

Rebocho, A.B., Bliek, M., Kusters, E., Castel, R., Procissi, A., Roobeek, I., Souer, E. and Koes, R. (2008) Role of EVERGREEN in the Development of the Cymose Petunia Inflorescence. *Dev. Cell*, **15**, 437–447.

Sawa, M. and Kay, S.A. (2011) GIGANTEA directly activates Flowering Locus T in Arabidopsis thaliana. *Proc. Natl. Acad. Sci.*, **108**, 11698–11703.

Sawa, M., Nusinow, D.A., Kay, S.A. and Imaizumi, T. (2007) FKF1 and GIGANTEA Complex Formation Is Required for Day-Length Measurement in Arabidopsis. *Science*, **318**, 261–265.

Souer, E., Krol, A. van der, Kloos, D., Spelt, C., Bliek, M., Mol, J. and Koes, R. (1998) Genetic control of branching pattern and floral identity during Petunia inflorescence development. *Development*, **125**, 733–742.

Terry, M.I., Carrera-Alesina, M., Weiss, J. and Egea-Cortines, M. (2019) *Molecular and transcriptional structure of the petal and leaf circadian clock in Petunia hybrida*, Plant Biology. Available at: http://biorxiv.org/lookup/doi/10.1101/641639 [Accessed July 19, 2019].

Terry, M.I., Pérez-Sanz, F., Díaz-Galián, M.V., Pérez de los Cobos, F., Navarro, P.J., Egea-Cortines, M. and Weiss, J. (2019) The Petunia CHANEL Gene is a ZEITLUPE Ortholog Coordinating Growth and Scent Profiles. *Cells*, **8**, 343.

Tseng, T.-S. (2004) SPINDLY and GIGANTEA Interact and Act in Arabidopsis thaliana Pathways Involved in Light Responses, Flowering, and Rhythms in Cotyledon Movements. *PLANT CELL ONLINE*, **16**, 1550–1563.

Wang, S., Zhang, S., Wang, W., Xiong, X., Meng, F. and Cui, X. (2015) Efficient targeted mutagenesis in potato by the CRISPR/Cas9 system. *Plant Cell Rep.*, **34**, 1473–1476.

Watanabe, S., Xia, Z., Hideshima, R., et al. (2011) A Map-Based Cloning Strategy Employing a Residual Heterozygous Line Reveals that the *GIGANTEA* Gene Is Involved in Soybean Maturity and Flowering. *Genetics*, **188**, 395–407.

Xu, J., Kang, B.-C., Naing, A.H., Bae, S.-J., Kim, J.-S., Kim, H. and Kim, C.K. (2020) CRISPR/Cas9-mediated editing of 1-aminocyclopropane-1-carboxylate oxidase1 enhances Petunia flower longevity. *Plant Biotechnol. J.*, **18**, 287–297.

Zakhrabekova, S., Gough, S.P., Braumann, I., et al. (2012) Induced mutations in circadian clock regulator Mat-a facilitated short-season adaptation and range extension in cultivated barley. *Proc. Natl. Acad. Sci.*, **109**, 4326–4331.

Zhang, B., Yang, X., Yang, C., Li, M. and Guo, Y. (2016) Exploiting the CRISPR/Cas9 System for Targeted Genome Mutagenesis in Petunia. *Sci. Rep.*, **6**, 20315–20315.

Zhao, X.Y., Liu, M.S., Li, J.R., Guan, C.M. and Zhang, X.S. (2005) The wheat TaGI1, involved in photoperiodic flowering, encodesan Arabidopsis GI ortholog. *Plant Mol. Biol.*, **58**, 53–64.

GENERAL CONCLUSIONS

In this PhD thesis we performed a functional analysis of the gene *GIGANEA* (*GI*) in *Petunia x hybrida* by means of independent knock down of its two paralogues *PhGI1* and *PhGI2* by RNA interference technique and on the other hand by the contemporary knock out of both paralogues using the CRISPR/Cas9 method.

The silencing of *GIGANTEA* paralogues via iRNA, revealed both common and divergent functions between the two paralogues, confirming overall the characteristics of *GI* previously described in Arabidopsis as well as in other species.

Concerning vegetative growth, our results confirm the activity of *GI* as a negative growth regulator. *PhGI1* loss of function plants are characterized by apical dominance, bushier phenotype, increase in the number of axillary meristems, longer, broader and darker green median and apical leaves as well as longer basal internodes. In contrast, median and apical internode length was reduced, resulting in a conserved overall plant height compared to wild type. In the same way, the activity of *PhGI2* as a negative regulator of vegetative development appears to be conserved with similar phenotypes to the *iRNA::PhGI1* lines but only in the T1 generation grown under controlled growth-chamber conditions. Differently, the T2 generation, grown under greenhouse conditions, showed a more complex model of inhibition and promotion of vegetative growth. The promotion of leaf size was restricted to lateral branches, while both the length of the stem and the area of the leaf were reduced on the main branch.

Both results indicate an acropetal gradient, as it has opposite effects during early stages of development and middle to late stages.

In addition and regarding generative characters, we uncovered functions of *GI* that have not been identified so far in any other *GI* mutant of any other species. Both paralogs seemed to control the number of flower buds and the final flower size and they acted preventing the premature senescence of the flowers. In contrast to *PhGI1*, *PhGI2* silenced lines maintained the classical late flowering phenotype already described in *Arabidopsis thaliana* and other species. The observed common and divergent functions of the two paralogs concerning vegetative growth, inflorescence architecture and flowering time uncovers a series of events consisting in loss of function, neofunctionalisation and subfunctionalisation among the *GI* homologs in Petunia. Furthermore, we found that *PhGI1* and *PhGI2* are involved in the control over flower VOCs emission, as both iRNA lines were characterized by a general reduction in the relative quantity of volatile compounds emitted during 24 hours as well as by an altered aromatic profile in comparison to the wild type. It remains to be analyzed if the flower phenotypes observed are functions gated by the circadian clock or are specific functions resulting from neofunctionalization of *GI* genes in Petunia.

The double transformed hCas9/gRNAPhGI T0 lines obtained by CRISPR/Cas9 technique displayed strong modifications in both growth habit and vegetative parameters, similar to those observed in the *RNAiPhGI1* and *RNAiPHGI2* lines.

In the hCas9/gRNAPhGI T0 lines, structural changes in plant growth were characterized by apical dominance and a bushier

phenotype mainly due to a greater dimension in length and width in the apical leaves and a darker green aspect in median and apical leaves caused by increased levels of chlorophyll compared to wild type plants. On the other hand, the basal leaves were characterized by a greater width while the median ones by a general reduced size. Our results using CRISPR/Cas9 technology confirmed the role of PhGI1/2 as a negative regulator of the vegetative growth as already observed in Arabidopsis.

Concerning the generative characters, the analyzed parameters highlighted some morphological characteristics which agree with the previously described findings. All the h*Cas*9/gRNA*PhGI* transgenic lines showed a general reduction in flower number, premature senescence of flower buds as well as a reduced petal size confirming the hypothesis of an upstream involvement of *PhGI1/2* in the regulation of flower-meristem-identity genes. Our findings, at the moment, are not sufficient to define if this role is due to a synergistic action of both paralogs or only one of the two and which one but leave the possibility of further studies regarding this aspect. considering that the aborted flowers clearly showed the origins of the reproductive organs, indicating that the senescence of the tissues occurred after the activation of the flower-meristem-identity genes.

Most of the h*Cas*9/gRNA*PhGI* plants showed a different flowering time period than wild type plants, mainly characterized by an early flowering time. These data, although divergent from those observed in the two previous works, undoubtedly indicate that *GI* affects flowering in Petunia. Currently, we are not able to define whether the change in flowering time is due to the different exposure to light or whether the observed effect is due to a synergistic action of both paralogs or to the

action of only one and which one. Further studies will be performed for clarification of these results.

Supplementary Material

Species	Protein	Accession
Arabidopsis thaliana	AtGI	GI AAT80910.1
Allium cepa	AcGI	ACT22764.1
Amborella trichopoda	GI	XP_020521566.1
Brachypodium distachyon	BdGI	XP_024314292.1
Cicer arietinum	GI1	XP_004496435.1
	GI2	XP_027189172.1
Fragaria vesca	FvGI	XP_004290483.1
Glycine max	GmGI1	BAJ22595.1
	GmGI2	BAN82589.1
	GmGI3	ACA24490.1
Hordeum vulgare	HvGI	AAW66945.1
Lemna gibba	LgGI	BAD97869.1
Lolium perenne	LpGI	CAY26028.1
Marchantia polymorpha	GI	Mapoly0019s0145.1
Medicago truncatula	MtGI	XP_003592048.2
Nicotiana attenuata	GI	OIS97362.1
Nicotiana benthamiana	NbGI1	Niben101Scf01453g02010.1
	NbGI2	Niben101Scf04641g03006.1
	NbGI3	Niben101Scf09649g01002.1
	NbGI4	NbS00010805g0006.1
Oryza sativa	OsGI	XP_015649578.1
Panicum hallii	GI	XP_025816791.1
Petunia axillaris	GI1	Peaxi162Scf00360g00418.1
	GI2	Peaxi162Scf00160g01744.1
Petunia inflata	GI1	Peinf101Scf00386g02019.1
	GI2	Peinf101Scf02877g01057.1
	GI3	Peinf101Scf02877g01057.1
Pharbitis nil	PnGI	BAK19067.1
Pisum sativum	PsGI	ABP81863.1
Populus alba x Populus glandulosa	PagGIa	AOX13585.1
	PagGIb	AOX13586.1
	PagGIc	AOX13587.1
Populus trichocarpa	PtGI	XP_002307516.2
Secale cereal	ScGI	ADR51711.1
Selaginella moellendorffii	SmoeGI	XP_024528715.1
Setaria italica	SiGI1	XP_004968438.1
	SiGI2	XP_022682651.1
Setara viridis	SvGI	Sevir.5G127000.1
Solanum lycopersicum	SlGI1	Solyc04g071990.3.1
	SlGI2	Solyc12g056650.2.1
Solanum tuberosum	StGI	XP_006359039.1
Triticum aestivum	TaGI3	AAT79487.1
Vigna radiata	GI	XP_014514153.1
Vigna unguiculata	VunGI	Vun_T01130.1_6
Vitis vinifera	VvGI	XP_010665061.1
Zea mays	ZmGI1	GRMZM2G107101_T03
	ZmGI2	GRMZM5G844173_T01

Table S1| Accession numbers of the protein sequences used.

Genotype:	W.T.	*iRNA::PhGI 1*	*iRNA::PhGI 1 (3.7)*	*iRNA::PhGI 1 (4.7)*	*iRNA::PhGI 1 (8.1)*	% GI1 versus W.T.	P value	% GI1 (3.7) versus W.T.	P value	% GI1 (4.7) versus W.T.	P value	% GI1 (8.1) versus W.T.	P value
Plant Height (cm)	40.9 ± 0.8	44 ± 3.5	50	46	43	+7.6	2.89E-02	+22.2		+12.5		+5.1	
N° of leaves to the 1° flower	37 ± 1.4	36.5 ± 1.2	30	32	32	-1.4	7.62E-01	-18.9		-13.5		13.5	
Basal Internode (mm)	12.6 ± 0.9	16.9 ± 0.5	17.4 ± 0.5	16.7 ± 1.2	16.9 ± 0.7	+34.4	2.46E-20	+38.1	7.64E-05	+40.5	2.55E-02	+34.1	2.31E-03
Median Internode (mm)	16.3 ± 0.6	10.2 ± 0.4	9.6 ± 0.5	9.9 ± 0.2	9.8 ± 0.6	-37.6	3.57E-30	-41.1	2.22E-04	-39.3	4.94E-18	-39.9	7.31E-04
Apical Internode (mm)	20.5 ± 1.1	13.6 ± 0.3	13.8 ± 0.8	13.8 ± 0.8	13.4 ± 0.9	-33.7	2.51E-23	-32.7	1.23E-03	-34.1	9.79E-05	-34.6	1.96E-03
N° of axillary meristems	12.5 ± 1.3	27 ± 2.08	28	29	25	+116.0	4.08E-07	+124		+132		+100	
N° of branches	2 ± 0.0	2.4 ± 0.57	2	3	2	+20	2,73E-01	+0		+50		+0	
Basal Leaves length (mm)	64.57	91.75	88.2 ± 0.9	92.5 ± 1.5	88.3 ± 1.27	+42.1	4.42E-33	+36.6	1.02E-05	+43.3	2.17E-04	+36.8	1.17E-04
Basal leaves width (mm)	40.93	50.96	50.1 ± 0.7	53.8 ± 1.3	44.6 ± 0.5	+24.5	4.97E-30	+22.4	1.98E-05	+31.4	9.49E-04	+9.0	5.61E-07
Median Leaves length (mm)	72.7 ± 2.8	75.6 ± 1.6	70.3 ± 1.2	82 ± 1.6	73.4 ± 1.8	+4	8.23E-02	-3.3	5.71E-02	+12.8	2.95E-04	+0.9	6.55E-04
Median leaves width (mm)	43.8 ± 1.7	48.1 ± 1.4	45.4 ± 0.1	50.7 ± 1.7	49.4 ± 0.7	+9.7	1.13E-08	+3.6	1.40E-01	+5.5	8.70E-03	+2.1	4.94E-05
Apical leaves length (mm)	38.8 ± 1.3	48 ± 2.91	44.9 ± 1.3	49.5 ± 1.5	45.6 ± 1.8	+24	1.49E-22	+16	1.08E-02	+28	1.65E-03	+17.6	1.66E-02
Apical leaves width (mm)	22.5 ± 0.9	30.5 ± 2.5	30.1 ± 0.8	28.6 ± 1.6	31.1 ± 1.03	+35	2.02E-23	+34	3.60E-04	+27	1.60E-02	+38	1.65E-03

Basal leaves Chlorophyll	22.4 ± 1.1	14.9 ± 1.1	12.00 ± 1.1	13.97 ± 1.6	15.30 ± 0.8	-33.5	1.05E-23	-46.38	7.96E-04	-37.58	1.31E-02	-31.64	1.79E-04
Median leaves Chlorophyll	31.04 ± 2.3	37.26 ± 1.1	36.30 ± 0.6	35.97 ± 1.3	39.47 ± 1.4	+20	1.67E-25	+16.95	4.57E-04	+15.88	4.85E-03	+27.16	1.18E-02
Apical leaves Chlorophyll	21.27 ± 0.9	38.19 ± 1.7	35.33 ± 1.3	36.17 ± 1.5	38.97 ± 0.9	+79.5	2.76E-45	+66.1	1.26E-03	+70.05	1.29E-03	+83.22	1.58E-04

Table S2| Comparison of vegetative parameters between wild type and the silenced lines 3.7. 4.7 and 8.1 of PhGI1 in the T1 generation. Data are given as averages. based on at least three biological replicates. The height was calculated from the base to the first flowering meristem. when the first flowering event occurs. The number of total axillary meristems was calculated between the base and the first apical flowering meristem. P values ≤ 0.05 according to Students T-test were considered as significant.

Genotype:	W.T.	*iRNA::PhGI 1*	*iRNA::PhGI 1 (3.7)*	*iRNA::PhGI 1 (4.7)*	*iRNA::PhGI 1 (8.1)*	% GI1 versus W.T	P value	% GI1 (3.7) versus W.T.	P value	% GI1 (4.7) versus W.T.	P value	% GI1 (8.1) versus W.T.	P value
N° of flower buds	27.8 ± 2.8	11.3 ± 4.1	18	13	16	-42		-59.4		-35		-53	
N° of fully developed flowers	27.8 ± 2.8	6.8 ± 2.2	8	6	9	-68		-75.5		-71		-78	
% of fully developed flowers	100	60.2	44	46	56	-44		-39.8		-56		-54	
Corolla diameter (mm)	46.22 ± 3.4	34.21 ± 2.7	34.18 ± 2.7	34.38 ± 2.3	35.54 ± 0.7	-23.1	4.27E-21	-26.0	1.14E-04	-26.0	2.24E-05	-25.6	2.36E-15
Tube length (mm)	40.06 ± 2.1	35.57 ± 2.1	35.38 ± 2.4	35.86 ± 1.5	35.70 ± 1.9	-10.9	2.84E-15	-11.2	1.59E-03	-11.7	1.09E-03	-10.5	3.53E-03
Petiole length (mm)	35.96 ± 2.7	35.33 ± 3.2	36.99 ± 2.9	36.04 ± 2.7	33.83 ± 4.2	-5.9	2.67E-01	-1.8	6.67E-01	-2.9	8.03E-01	-0.2	3.04E-01

Table S3| Comparison of floral parameters between wild type and silenced *PhGI1* in T1 generation. Data are given as averages. based on at least three biological replicates. P values ≤ 0.05 according to Students T-test were considered as significant.

RT (min)	Hit Name	CAS Number
7.318	*Methyl Benzoate*	93-58-3
4.82	*Benzaldehyde*	100-52-7
13.311	*Isoeugenol* (isomers)	97-45-1; 5932-68-3
17.44	*Benzyl Benzoate*	120-51-4
6.711	*Phenylacetaldehyde*	122-78-1
6.511	*Benzyl Alcohol*	100-51-6
8.111	*2.phenylethanol*	60-12-8
9.615	*Methyl Salicylate*	119-36-8
12.211	*Eugenol*	97-53-0
9.077	*Benzyl Acetate*	140-11-4
7.063	*Acetophenone*	98-86-2
7.797	*Nonanal*	124-19-6
9.639	*Decanal*	112-31-2
9.063	*Ethyl Benzoate*	93-89-0

Table S4| Main Volatile Organic Compounds analyzed. Data are given as percentage based on at least three biological replicates. (RT) Retention time.

VOCs:	ZT 0			ZT 3			ZT 6			ZT 9			ZT 12			ZT 15			ZT 18			ZT 21		
	W.T.	GI1	P value	W.T.	GI1	P value	W.T.	GI1	P value	W.T.	GI1	P value .	W.T.	GI1	P value	W.T.	GI1	P value	W.T.	GI1	P value	W.T.	GI1	P value
Methyl Benzoate	79.9	34.3	1.65E-04	85.8	66.3	3.02E-02	91.3	75.5	1.50E-01	85.7	75.2	1.82E-01	76.8	81.2	2.26E-01	77	77.5	3.01E-01	75.1	74.4	2.64E-01	76.4	67.0	4.13E-01
Benzaldehyde	2.6	0.00	1.18E-06	2.3	0.00	6.85E-04	0.3	0.8	8.77E-01	3.4	3.4	1.96E-01	6.5	8.5	2.66E-01	11.7	5.7	1.94E-01	11.3	4.9	1.97E-01	8.5	1.7	3.97E-02
Isoeugenol	5.0	54.3	7.03E-01	0.3	12.7	1.52E-03	1.7	15.7	1.35E-01	6.1	4.4	1.42E-01	8.7	9.4	2.29E-01	5.0	7.9	4.58E-01	5.7	8.3	3.69E-01	6.0	7.9	8.49E-01
Benzyl Benzoate	4.8	2.1	4.74E-02	4.7	3.7	1.12E-01	1.1	2.0	3.48E-02	2.5	2.3	1.68E-01	5.4	0.5	1.97E-01	3.4	5.6	4.61E-01	3.6	9.2	6.76E-01	3.5	5.2	7.01E-01
Phenylacetaldehyde	0.4	0.00	2.13E-08	0.3	0.00	8.18E-02	0.00	0.3	1.72E-02	0.3	0.3	2.22E-01	1.0	0.1	2.16E-01	1.6	0.9	2.10E-01	1.8	0.8	1.95E-01	1.3	0.4	4.15E-02
Benzyl Alcohol	2.7	0.6	1.41E-04	2.6	3.6	1.46E-01	0.9	0.3	8.95E-02	0.00	0.2	1.74E-02	0.1	0.01	2.29E-01	0.2	0.3	4.56E-01	1.1	1.0	2.47E-01	2.4	1.6	2.87E-01
2.phenylethanol	2.2	6.1	3.43E-05	1.8	3.2	1.83E-02	0.5	0.00	9.03E-02	0.1	0.3	8.32E-01	0.3	0.04	2.59E-01	0.5	0.6	3.63E-01	0.9	1.00	2.59E-01	1.5	1.3	3.90E-01
Methyl Salicylate	0.6	0.2	1.41E-02	0.9	1.6	2.54E-02	1.6	0.9	1.21E-01	1.09	1.05	1.93E-01	0.5	0.06	2.37E-01	0.3	0.3	3.19E-01	0.2	0.4	4.18E-01	0.2	0.8	1.07E-03
Eugenol	2.5	0.07	3.47E-06	0.6	1.3	1.05E-02	0.06	0.00	8.07E-02	0.05	0.12	6.10E-01	0.06	0.00	1.15E-01	0.04	0.1	9.81E-01	0.1	0.00	1.20E-01	0.1	0.4	1.55E-01
Benzyl Acetate	0.6	0.1	2.79E-04	0.6	0.5	9.94E-02	0.2	0.00	6.46E-02	0.00	0.00	1.00E+00	0.00	0.00	3.47E-01	0.03	0.02	2.37E-01	0.1	0.02	2.46E-01	0.00	0.3	9.52E-01
Acetophenone	0.03	0.4	5.00E-02	0.06	0.3	8.13E-01	0.1	0.00	1.39E-01	0.00	0.3	4.69E-02	0.1	0.01	1.85E-01	0.2	0.07	2.14E-01	0.06	0.00	1.39E-01	0.00	0.8	9.23E-02
Nonanal	0.04	0.10	4.34E-01	0.2	0.00	5.36E-03	0.7	2.3	7.75E-02	0.31	10.3	9.31E-01	0.07	0.02	6.94E-01	0.00	0.06	8.62E-02	0.00	0.00	1.00E+00	0.00	0.1	5.74E-02
Decanal	0.00	0.00	1.77E-01	0.08	0.00	8.47E-03	0.4	1.4	9.05E-02	0.00	0.3	3.67E-02	0.04	0.01	7.26E-01	0.00	0.00	1.00E+00	0.00	0.00	1.00E+00	0.00	0.01	3.47E-01
Ethyl Benzoate	0.05	0.6	3.58E-01	0.00	5.3	3.30E-04	0.00	0.6	2.73E-01	0.07	1.8	3.16E-02	0.04	0.2	3.55E-01	0.02	0.9	3.37E-01	0.00	0.00	1.00E+00	0.00	12.6	3.14E-01

Table S5| Percentage of the main Volatile Organic Compounds analyzed during 24 hours between wild type and the silenced *PhGI1* flowers of T1 generation. P values ≤ 0.05 according to Students T-test were considered as significant.

PhGi1 For	TGGAGAAAGGGCAGAGACAT
PhGi1 Rev	GTGGAGCCACCCTTACGTT
PhGi1attb1 For	GGGGACAAGTTTGTACAAAAAAGCAGGCTTGGAGAAAGGGCAGAGACAT
PhGi1attb2 Rev	GGGGACCACTTTGTACAAGAAAGCTGGGTAGTGGAGCCACCCTTACGTT
SecpDON201 For	TCGCGTTAACGCTAGCATGGATCTC
SecpDON201 Rev	GTAACATCAGAGATTTTGAGACAC
nptII For	CCTGCTTGCCGAATATCATGGTGG
nptII Rev	CGAAATCTCGTGATGGCAGGTTGG
Agri 51	CAACCACGTCTTCAAAGCAA
Agri 56	CTGGGGTACCGAATTCCTC
Agri 64	CTTGCGCTGCAGTTATCATC
Agri 69	AGGCGTCTCGCATATCTCAT
PhAct For	TGCACTCCCACATGCTATCCT
PhAct Rev	TCAGCCGAAGTGGTGAAAGAG
PaxilGI1 For	TTGTACGTGCACTCAGCACA
PaxilGI1 Rev	CCATTTTTGATTCGGCTGTT
PhGi2 For	TTTAGAGTCCTTTCACTCATCCATC
PhGi2 Rev	AATACAGCATTTGTTACATGGAGGT
PhZTL For	TGCATCTGTTGGCTCTGTTT
PhZTL Rev	CCCCAACCCAATCTCTTAGC
PhLHY For	CGACGTGGTAGGAATTGCATC
PhLHY Rev	GACCGAAATGGTCATCAAAGGAC
PhTOC1 For	TGATGGTAAGGGGAGCAAAG
PhTOC1 Rev	CTGAAGCAGGATGCCCATTA
PhELF4 For	GCCACCACCAAACCCTAAC
PhELF4 Rev	AGGCTTCAAAGGCAGTGCT

Table S6| List of primers used.

PhGI2 3UTR For	TTTAGAGTCCTTTCACTCATCCATC
PhGI2 3UTR Rev	AATACAGCATTTGTTACATGGAGGT
PhGI2 3UTR attb1 For	TACAAAAAAGCAGGCTCATTTAGAGTCCTTTCACTCATCCATC
PhGI2 3UTR attb2 Rev	CAAGAAAGCTGGGTAAATACAGCATTTGTTACATGGAGGT
SecpDON201 For	TCGCGTTAACGCTAGCATGGATCTC
SecpDON201 Rer	GTAACATCAGAGATTTTGAGACAC
nptII For	CCTGCTTGCCGAATATCATGGTGG
nptII Rev	CGAAATCTCGTGATGGCAGGTTGG
Agri 51	CAACCACGTCTTCAAAGCAA
Agri 56	CTGGGGTACCGAATTCCTC
Agri 64	CTTGCGCTGCAGTTATCATC
Agri 69	AGGCGTCTCGCATATCTCAT
PhAct For	TGCACTCCCACATGCTATCCT
PhAct Rev	TCAGCCGAAGTGGTGAAAGAG
PaxilGI1 For	TTGTACGTGCACTCAGCACA
PaxilGI1 Rev	CCATTTTTGATTCGGCTGTT
PhGI2 3UTR For	TTTAGAGTCCTTTCACTCATCCATC
PhGI2 3UTR Rev	AATACAGCATTTGTTACATGGAGGT
PhZTL For	TGCATCTGTTGGCTCTGTTT
PhZTL Rev	CCCCAACCCAATCTCTTAGC
PhLHY For	CGACGTGGTAGGAATTGCATC
PhLHY Rev	GACCGAAATGGTCATCAAAGGAC
PhTOC1 For	TGATGGTAAGGGGAGCAAAG
PhTOC1 Rev	CTGAAGCAGGATGCCCATTA
PhELF4 For	GCCACCACCAAACCCTAAC
PhELF4 Rev	AGGCTTCAAAGGCAGTGCT

Table S7| List of primers used

Genotype:	W.T.	*iRNA::PhGI2*	*iRNA::PhGI2* (4.2)	*iRNA::PhGI2* (4.4)	*iRNA::PhGI2* (6.1)	*iRNA::PhGI2* (6.3)	*iRNA::PhGI2* (7.6)	% GI2 versus W.T.	P value	% GI2 (4.2) versus W.T.	P value	% GI2 (4.4) versus W.T.	P value	% GI2 (6.1) versus W.T.	P value	% GI2 (6.3) versus W.T	P value	% GI2 (7.6) versus W.T	P value
Plant Height (cm)	40.9 ± 0.8	49 ± 5.4	44	48	35	45	45	+19.8	6.03E-01	+7.6		+17.4		-14.4		+10.0		+10.0	
N° of leaves to the 1° flower	37 ± 1.4	43.8 ± 1.6	40	39	38	37	37	+18.4	5.60E-01	+8.1		+5.4		+2.7		+0.0		+0.0	
Basal Internode (mm)	12.6 ± 0.9	17.2 ± 0.8	18 ± 0.76	16.74 ± 1.24	17.4 ± 0.76	17.83 ± 0.44	17.25 ± 0.65	+36.5	3.91E-19	+42.9	2 31E-03	+32.9	2.33E-02	+38.1	3.07E-03	+41.5	3.81E-05	+36.9	1.49E-03
Median Internode (mm)	16.3 ± 0.6	11 ± 0.9	11.37 ±	10.54 ± 0.49	11.31 ±	10.7 ± 0.34	10.8 ±	-32.5	3.31E-22	-30.2	2 51E-02	-35.3	3.37E-04	-30.6	2.00E-02	-34.4	1.16E-05	-33.8	3.18E-04
Apical Internode (mm)	20.5 ± 1.1	13.4 ± 0.7	13.1 ± 0.65	12.98 ±0.6	13.9 ± 0.72	13.3 ± 0.68	13.6 ± 1.18	-34.5	8.50E-25	-36.2	2.41E-04	-36.7	1.44E-04	-32.4	7.41E-04	-35.1	3.71E-04	-33.6	5.99E-03
N° of axillary meristems	12.5 ± 1.3	30 ± 4.6	26	30	26	19	28	+140	1.48E-04	+108		+140		+108		+52		+124	
N° of branches	2 ± 0.0	4.8 ± 0.4	4	4	4	4	4	+140	5.53E-06	+100		+100		+100		+100		+100	
Basal Leaves length (mm)	64.57	89.2 ± 1.1	91.8 ± 0.5	83.73 ± 1.72	96.03 ± 1.36	82 ± 0.95	89.7 ± 1.81	+38.1	6.51E-18	+42.2	1.15E-12	+29.7	1.08E-03	+48.7	8.75E-05	+27	2.66E-05	+38.9	6.83E-04
Basal leaves width (mm)	40.93	49.8 ± 1.3	53.6 ± 1.9	47.43 ±2.26	53.7 ± 0.64	50.1 ± 0.7	50.03 ± 1.51	+21.7	3.03E-12	+31	4 87E-03	+15.9	3.01E-02	+31.2	2.10E-06	+22.4	2.83E-05	+22.2	4.77E-03
Median Leaves length (mm)	72.7 ± 2.8	75.9 ± 1.4	74.9 ± 0.42	70.6 ± 0.79	80.7 ± 1.27	76.87 ± 1.61	77.43 ± 1.7	+4.3	2.81E-02	+3	1 05E-02	+2.9	8.19E-03	+11	3.00E-04	+5.7	2.61E-02	+6.5	2.48E-02
Median leaves width (mm)	43.8 ± 1.7	48.7 ± 1.2	46.03 ± 0.61	44.87 ± 1.4	50.63 ± 0.7	50.7 ± 1.87	49.7 ± 0.45	+11.1	9.44E-08	+5	1 09E-03	+2.4	2.13E-01	+15.5	1.11E-05	+15.7	1.37E-02	+13.4	7.87E-09
Apical leaves length (mm)	38.7 ± 1.3	45.6 ± 0.9	45.53 ± 0.8	45.5 ± 0.26	45.8 ± 0.23	46.47 ± 1.21	41.4 ± 0.95	+17.6	4.61E-14	+17.4	3 39E-04	+17.4	2.35E-13	+18.1	1.26E-14	+19.9	2.94E-03	+6.8	2.02E-02
Apical leaves width (mm)	22.5 ± 0.9	26.1 ± 0.8	25.33 ± 0.81	27.27 ± 0.15	25.33 ± 0.67	26.7 ± 1.04	24.5 ± 1	+15.6	4.69E-08	+12.4	1 00E-02	+21	2.47E-14	+12.4	3.63E-03	+18.5	1.00E-02	+8.7	4.63E-02
Basal leaves Chlorophyll	22.4 ± 1.1	15.8 ± 1.3	13.3 ± 1.11	16.3 ±1.06	15.93 ± 1.35	15.47 ± 2.1	16.8 ± 1.1	-29.6	9.45E-19	-40.6	3 06E-03	-27.2	3.70E-03	-28.8	8.57E-03	-30.9	2.62E-02	-24.9	5.62E-03
Median leaves Chlorophyll	31.0 ± 2.3	35.7 ± 1.2	37.83 ± 1.31	34.43 ± 1.35	35.57 ±1.39	34.13 ± 0.87	34.57 ± 0.95	+15.0	2.05E-11	+21.	7 94E-03	+10.9	3.89E-02	+14.6	2.28E-02	+10	1.31E-02	+11.4	1.29E-02
Apical leaves Chlorophyll	21.3 ± 0.9	35.6 ± 1.1	37.2 ± 1.14	37.7 ± 1.14	36.0 ± 1.51	35.57 ± 1.1	29.7 ± 1.69	+67.2	4.68E-17	+74.9	6.41E-04	+77.2	5.95E-04	+69.3	2.18E-03	+67.2	7.14E-04	+39.6	9.91E-03

Table S8| Comparison of vegetative parameters between wild type and the silenced *PhGI2* lines in the T1 generation. Data are given as averages, based on at least three biological replicates. The height was calculated from the base to the first flowering meristem, when the first flowering event occurs. The number of total axillary meristems was calculated between the base and the first apical flowering meristem. P Values ≤ 5.00E-02 according to Students T-test were considered as significant.

Genotype:	W.T.	*iRNA::PhGI2*	*iRNA::PhGI2* (4.2)	*iRNA::PhGI2* (4.4)	*iRNA::PhGI2* (6.1)	*iRNA::PhGI2* (6.3)	*iRNA::PhGI2* (7.6)	% GI2 versus W.T	P value	% GI2 (4.2) versus W.T.	P value	% GI2 (4.4) versus W.T.	P value	% GI2 (6.1) versus W.T.	P value	% GI2 (6.3) versus W.T.	P value	% GI2 (7.6) versus W.T.	P value
N° of flower buds	27.8 ± 2.8	18.5 ± 5.6	10	9	19	15	24	-33.5	1.19E-03	-64		-67.6		-31.7		46		-13.7	
N° of fully developed flowers	27.8 ± 2.8	10.7 ± 4.5	5	4	10	6	17	-61.5	1.58E-05	-82		-85.6		-64		-78.4		-38.8	
% of fully developed flowers	100	65	50	44	53	40	71	-35	1.35E-04	-50		-56		-47		-60		-29	
Corolla diameter (mm)	46.2 ± 3.4	31.9 ± 2.5	30.9 ± 2.9	33.1 ± 2.4	31.6 ± 2.3	32.4 ± 3.8	29.8 ± 1.8	-31	1.22E-24	-33.1	4.82E-05	-28.3	2.23E-05	-31.7	5.21E-06	-30	6.97E-04	-35.5	4.81E-08
Tube length (mm)	40.1 ± 2.1	34.7 ± 2.04	35.2 ± 1.6	35.1 ± 0.8	34.7 ± 1.8	32.4 ± 1.3	34.5 ± 1.5	-13.3	1.13E-14	-12.2	7.44E-04	-12.4	3.31E-08	-13.4	1.18E-03	-19	5.82E-06	-13.9	1.47E-04
Petiol length (mm)	35.9 ± 2.7	35.9 ± 4.3	36.5 ±3.7	35.3 ± 7.0	33.6 ±2.8	36.7 ± 1.9	36.1 ± 3.6	-0.3	8.19E-01	+1.4	8.20E-01	-1.8	8.22E-01	-6.5	1.27E-01	+2.2	4.97E-01	+0.3	9.95E-01

Table S9| Comparison of floral parameters between wild type and silenced *PhGI2* in T1 generation. Data are given as averages based on at least three biological replicates. P Values ≤ 5.00E-02 according to Students T-test were considered as significant.

RT (min)	Hit Name	CAS Number
7.318	*Methyl Benzoate*	93-58-3
4.82	*Benzaldhyde*	100-52-7
13.311	*Isoeugenol* (isomers)	97-45-1; 5932-68-3
17.44	*Benzyl Benzoate*	120-51-4
6.711	*Phenylacetaldehyde*	122-78-1
6.511	*Benzyl Alcohol*	100-51-6
8.111	*2.phenylethanol*	60-12-8
9.615	*Methyl Salicylate*	119-36-8
12.211	*Eugenol*	97-53-0
9.077	*Benzyl Acetate*	140-11-4
7.063	*Acetophenone*	98-86-2
7.797	*Nonanal*	124-19-6
9.639	*Decanal*	112-31-2
9.063	*Ethyl Benzoate*	93-89-0

Table S10| Main Volatile Organic Compounds analyzed.

VOCs:	ZT 0			ZT 3			ZT 6			ZT 9			ZT 12			ZT 15			ZT 18			ZT 21		
	W.T.	GI2	P value	W.T.	GI2	P value	W.T.	GI2	P value	W.T.	GI2	P value	W.T.	GI2	P value	W.T.	GI2	P value	W.T.	GI2	P value	W.T.	GI2	P value
Methyl Benzoate	79.9	80.8	2.40E-01	85.8	46.6	6.51E-01	91.3	69.9	4.19E-01	85.8	76.1	8.67E-02	76.8	82.5	2.17E-01	77.0	78.0	3.41E-01	75.1	78.9	6.55E-01	76.5	76.1	5.91E-01
Benzaldheyde	2.65	0.43	1.22E-01	2.36	0.04	2.21E-01	0.27	0.00	4.02E-03	3.39	0.69	7.01E-02	6.51	4. 40	1.54E-01	11.7	4.54	2.24E-01	11.4	3.62	1.38E-06	8.48	2.11	3.23E-03
Isoeugenol	5.02	6.44	3.38E-01	0.30	45.6	2.74E-04	1.72	7.46	5.82E-01	6.09	3.09	6.90E-02	8.76	5.29	2.48E-01	4.99	7.98	4.34E-01	5.56	7.24	9.65E-02	5.98	8.28	2.79E-01
Benzyl Benzoate	4.83	4.56	2.30E-01	4.72	1.77	4.60E-01	1.05	5.45	4.30E-02	2.46	0.60	6.25E-02	5.39	2.09	1.63E-02	3.42	4.57	3.80E-01	3.62	4.02	6.99E-01	3.52	3.95	9.57E-01
Phenylacetaldehyde	0.42	0.10	1.30E-01	0.31	0.00	2.22E-01	0.00	0.00	4.20E-03	0.27	0.00	6.92E-02	0.97	1.02	1.81E-01	1.57	1.36	3.10E-01	1.79	0.72	1.30E-09	1.32	0.49	3.86E-03
Benzyl Alcohol	2.68	1.40	1.63E-01	2.59	1.30	5.66E-01	0.98	3.31	3.79E-04	0.00	0.00	6.48E-02	0.09	0.18	1.81E-02	0.21	0.73	1.34E-01	1.12	1.07	7.79E-01	2.39	1.89	2.93E-01
2-phenylethanol	2.16	2.40	2.53E-01	1.76	1.37	8.69E-01	0.59	3.12	9.33E-06	0.10	0.01	6.66E-02	0.33	0.46	2.02E-01	0.47	1.36	3.54E-01	0.96	2.04	2.64E-05	1.49	2.49	2.34E-02
Methyl Salicylate	0.60	0.64	2.48E-01	0.93	0.50	5.16E-01	1.63	1.78	8.26E-02	1.09	1.8	1.17E-01	0.50	0.65	3.71E-01	0.29	0.49	6.74E-01	0.24	0.42	2.50E-05	0.24	0.50	3.86E-04
Eugenol	2.54	0.82	3.49E-01	0.59	0.53	9.61E-01	0.06	1.20	9.37E-05	0.05	0.00	8.78E-02	0.06	0.03	1.72E-01	0.04	0.15	3.62E-01	0.15	0.90	2.35E-01	0.11	0.56	4.66E-03
Benzyl Acetate	0.57	0.29	1.61E-01	0.58	0.30	5.83E-01	0.22	0.86	1.49E-03	0.00	0.00	1.00E+00	0.00	0.00	1.13E-01	0.03	0.03	1.12E-01	0.13	0.12	7.36E-01	0.00	0.28	7.76E-01
Acetophenone	0.01	1.56	8.35E-03	0.06	1.67	9.61E-05	0.12	5.78	4.72E-06	0.00	1.20	4.82E-01	0.14	1.60	4.44E-01	0.19	0.08	3.47E-01	0.06	0.59	6.87E-05	0.00	2.87	1.53E-01
Nonanal	0.04	0.15	9.12E-01	0.19	0.00	1.12E-01	0.73	0.00	1.32E-03	0.31	15.6	2.85E-01	0.07	0.58	1.35E-03	0.00	0.11	5.82E-05	0.00	0.00	1.00E+00	0.00	0.00	1.00E+00
Decanal	0.00	0.01	1.71E-01	0.08	0.00	1.14E-01	0.36	0.00	3.56E-01	0.00	0.78	3.87E-01	0.04	0.37	4.61E-03	0.00	0.08	2.60E-04	0.00	0.00	1.00E+00	0.00	0.00	1.00E+00
Ethyl Benzoate	0.05	0.42	1.66E-01	0.00	0.38	2.36E-02	0.00	1.12	1.76E-02	0.07	0.86	3.33E-01	0.04	0.79	7.25E-03	0.02	0.52	9.08E-04	0.00	0.38	2.71E-03	0.00	0.44	4.30E-03

Table S11| Percentage of the main Volatile Organic Compounds analyzed during 24 hours between wild type and the silenced *PhGI1* flowers of T1 generation. P values ≤ 5.00E-02, according to Students T-test, were considered as significant.

hCas9_For	TGAGATGGCTAAGGTGGATGACTCTT
hCas9_Rev	CACTCGCAGAATATCACTCAGCAGAA
AtU6_For	CTTGAGAAGGAAGCGAGGGA
gRNA_Scaffold_Rev	CGACTCGGTGCCACTTTT
GI1_gRNA_For	TCTGTTGGAACTTCATGGAGC
GI1_gRNA_Rev	CGAAGATGCTCTGGAGTGAATT
GI2_gRNA_For	CATCATCTGTTGGAACCTCATG
GI2_gRNA_Rev	AGGTTATAGAGTGAAGATGCCCT
nptII_For	CCTGCTTGCCGAATATCATGGTGG
nptII _Rev	CGAAATCTCGTGATGGCAGGTTGG
M13_FOR	TGTAAAACGACGGCCAGT
M13_Rev	CAGGAAACAGCTATGAC

Table S12| List of primers used

Genotype:	Plant Height (cm)	N° of leaves to the 1° flower	Basal Leaves length (mm)	Basal leaves width (mm)	Median Leaves length (mm)	Median leaves width (mm)	Apical leaves length (mm)	Apical leaves width (mm)	Basal leaves Chlorophyll	Median leaves Chlorophyll	Apical leaves Chlorophyll
W.T.	39.7 ± 1.0	37.3 ± 1.5	68.9 ± 1.5	40.9 ± 1.3	51.8 ± 1.4	28.3 ± 1.1	31.6 ± 1.3	18.4 ± 0.8	25.8 ± 1.5	30.2 ± 1.3	26.8 ± 1.7
PhGI	39.8 ± 1.1	38.1 ± 1.2	69.9 ± 1.8	44.1 ± 1.4	50.1 ± 1.2	26.7 ± 1.2	33.4 ± 1.0	20.5 ± 1.7	23.9 ± 1.1	35.8 ± 1.4	36.1 ± 1.2
***PhG*I (1)	39.5	39	68.8 ± 1.6	43.7 ± 1.8	50.3 ± 0.9	26.6 ± 0.5	33.7 ± 0.8	21.4 ± 1.3	24.1 ± 0.6	36.2 ± 1.3	35.2 ± 1.3
PhGI (6A)	41	40	68.3 ± 1.6	43.9 ± 0.7	50.5 ± 1.7	26.1 ± 1.3	33.2 ± 0.6	18.6 ± 0.7	23.5 ± 1.2	35.5 ± 1.0	36.6 ± 2.0
PhGI (6B)	39	37	71.2 ± 1.8	45.3 ± 1.2	49.7 ± 1.6	27.6 ± 1.1	31.9 ± 0.4	18.6 ± 1.2	24.3 ± 1.4	36.3 ± 1.6	36.2 ± 0.5
PhGI (6C)	38.5	39	71.1 ± 3.4	43.1 ± 0.3	50.1 ± 0.9	25.7 ± 2.0	33.8 ± 1.1	20.4 ± 1.1	23.4 ±0.9	35.8 ± 1.0	36.5 ± 0.9
PhGI (7)	41	37	69.9 ± 2.1	44.1 ± 1.6	50 ± 1.5	26.1 ± 2.0	33.6 ± 0.4	21.9 ± 1.5	24.1 ± 1.7	36.8 ± 1.0	37.3 ± 0.4
PhGI (8)	40	38	72.5 ± 1.3	44.6 ± 1.5	49.8 ± 1.4	27.4 ± 1.4	32.7 ± 1.3	21.6 ± 1.8	24.2 ± 1.3	34.9 ± 1.6	36.9 ± 1.6
PhGI (9)	41.5	38	68.2 ± 0.2	43.3 ± 2.1	51.2 ± 0.8	27.8 ± 0.5	33.9 ± 2.1	22.3 ± 2.4	23.3 ± 1.1	36.1 ± 1.3	33.2 ± 1.3
PhGI (11)	39	40	71.4 ± 2.3	44.6 ± 1.7	49.5 ± 1.0	25.6 ± 1.1	34.2 ± 1.5	21.3 ± 2.8	24.3 ± 0.4	35.0 ± 1.7	35.8 ± 1.3
PhGI (17)	39.5	37	69.4 ± 2.4	43.4 ± 0.9	49.6 ± 0.7	27.4 ± 0.9	32.2 ± 1.1	20.8 ± 2.6	24.7 ± 0.9	35.8 ± 2.0	36.7 ± 1.9
PhGI (18)	40	38	68.4 ± 1.1	45.1 ± 2.7	50.3 ± 1.5	26.9 ± 0.7	35.2 ± 0.9	18.4 ± 1.1	23.9 ± 1.5	36.0 ±1.6	36.9 ± 1.4
% GI versus W.T	+0.25	+2.14	+1.39	+7.95	-3.32	-5.72	+5.73	+11.7	-6.83	+18.9	+35.0
P value	9.55E-01	4.79E-01	1.50E-01	1.74E-05	2.93E-03	1.25E-03	1.82E-03	4.64E-04	7.23E-03	1.77E-08	4.82E-10
% GI (1) versus W.T.	-0.005	+0.05	-0.3	+6.8	-3.0	-6.0	+6.6	+16.4	-6.4	+20.1	+31.4
P value			8.76E-01	9.88E-02	6.87E-02	3.91E-03	1.68E-02	3.92E-02	2.22E-02	3.15E-03	4.78E-04
% GI (6A) versus W.T.	+0.03	+0.07	-0.9	+7.5	-2.6	-8.0	+5.0	+1.6	-8.7	+17.6	+36.8
P value			5.94E-01	1.19E-03	2.90E-01	7.82E-02	1.71E-02	6.21E-01	4.83E-02	1.59E-03	4.95E-03
% GI (6B) versus W.T.	-0.02	-0.008	+3.3	+11	-4.0	-2.5	+0.8	+1.2	-5.6	+20.4	+35.3
P value			1.49E-01	5.18E-03	1.29E-01	4.02E-01	5.92E-01	7.97E-01	2.16E-01	9.21E-03	2.44E-08
% GI (6C) versus W.T.	-0.03	+0.05	+3.1	+5.5	-3.4	-9.5	+6.9	+10.8	-9.1	+18.6	+36.4
P value			3.90E-01	8.09E-04	5.44E-02	1.40E-01	4.40E-02	5.52E-02	1.98E-02	1.12E-03	4.22E-06
% GI (7) versus W.T.	+0.03	-0.008	+1.5	+7.9	-3.4	-7.9	+6.3	+19.0	-6.3	+22.0	+39.5
P value			5.07E-01	4.61E-02	1.61E-01	1.87E-01	1.58E-03	4.12E-02	2.40E-01	5.85E-04	5.42E-09
% GI (8) versus W.T.	+0.008	+0.02	+5.1	+9	-3.9	-3.3	+3.5	+17.8	-6.1	+16.0	+37.9
P value			1.65E-02	2.84E-02	1.05E-01	3.74E-01	2.75E-01	7.30E-02	1.45E-01	2.08E-02	1.49E-03

% GI (9) versus W.T.	+0.05	+0.02	-1.1	+6.1	-1.1	-2.0	+7.1	+21.5	-9.6	+19.6	+24.0
P value			1.65E-01	1.62E-01	3.78E-01	2.40E-01	1.91E-01	9.73E-02	3.04E-02	4.95E-03	2.23E-03
% GI (11) versus W.T.	-0.02	+0.07	+3.6	+9.2	-4.5	-9.7	+8.0	+16.0	-5.6	+16.2	+33.8
P value			2.00E-01	4.41E-02	3.05E-02	3.01E-02	7.98E-02	2.02E-01	2.36E-02	2.29E-02	5.34E-04
% GI (17) versus W.T.	-0.005	-0.008	+0.6	+6.3	-4.3	-3.5	+1.9	+13.1	-4.3	+18.8	+37.1
P value			7.87E-01	1.18E-02	6.50E-03	1.92E-01	4.69E-01	2.43E-01	1.64E-01	2.60E-02	3.44E-03
% GI (18) versus W.T.	+0.008	+0.02	-0.8	+10.3	-3.0	-5.1	+11.2	+0.0	-6.9	+19.6	+37.8
P value			5.09E-01	1.03E-01	2.12E-01	4.61E-02	3.36E-03	9.95E-01	1.60E-01	1.06E-02	4.67E-04

Table S13| Comparison of vegetative parameters between wild type and the transformed plants 1, 6A, 6B, 6C, 7, 8, 9, 11, 17 and 18 of *PhGI* in the T0 generation. Data are given as averages based on at least three biological replicates. The height was calculated from the base to the first flowering meristem when the first flowering event occurs. P values ≤ 5.00E-02 according to Students T-test were considered as significant.

Genotype:	N° of flower buds	N° of fully developed flowers	% of fully developed flowers	Corolla diameter (mm)	Tube length (mm)	Petiole length (mm)
W.T.	22.7 ± 1.5	22.7 ± 1.5	100	50.9 ± 1.08	32.5 ± 3.8	35.6 ± 3.7
PhGI	20.1 ± 3.8	17.4 ± 4.7	85	48.5 ± 2.19	30.9 ± 1.8	34.7 ± 3.7
***PhGI* (1)**	13	6	46	48.7 ± 1.9	30.8 ± 1.2	35.3 ± 2.8
***PhGI* (6A)**	21	19	90	49.8 ± 1.2	29.1 ± 1.8	32.5 ± 5.7
PhGI (6B)	18	18	100	48.8 ± 1.4	29.3 ± 1.6	33.9 ± 3.4
PhGI (6C)	23	21	91	47.4 ± 2.4	30.5 ± 1.7	34.8 ± 2.4
PhGI (7)	17	12	71	48.2 ± 1.4	33.8 ± 1.5	35.3 ± 2.0
PhGI (8)	19	15	79	48.9 ± 3.5	32.3 ± 2.0	33.6 ± 1.6
PhGI (9)	23	21	91	48.1 ± 3.1	30.9 ± 2.4	34.2 ± 3.1
PhGI (11)	19	19	100	48.3 ± 2.3	31.3 ± 1.8	36.5 ± 7.5
PhGI (17)	27	24	89	48.4 ± 2.5	30.8 ± 2.3	33.9 ± 5.2
PhGI (18)	21	19	90	48.1 ± 2.6	30.8 ± 1.2	36.5 ± 2.7
% GI versus W.T	-11.45	-23.35	-15	-4.8	-4.65	-2.67
P value	1,20E-01	1,66E-02	1,58E-02	2,84E-05	4,34E-02	3,82E-01
% GI (1) versus W.T.	-43	-74	-54	-4.3	-5.2	-0.8
P value				6,29E-02	6,43E-02	8,56E-01
% GI (6A) versus W.T.	-7	-16	-10	-2.2	-10.5	-8.6
P value				1,21E-01	7,17E-03	3,07E-01
% GI (6B) versus W.T.	-21	-21	-0.0	-4.1	-9.8	-4.7
P value				2,13E-02	7,08E-03	3,76E-01
% GI (6C) versus W.T.	+1	-7	-9	-7.0	-6.0	-2.3
P value				2,72E-02	7,98E-02	5,72E-01
% GI (7) versus W.T.	-25	-47	-29	-5.4	-4.0	-0.9
P value				7,28E-03	1,88E-01	8,08E-01
% GI (8) versus W.T.	-16	-34	-21	-3.9	-0.5	-5.6
P value				2,70E-01	8,90E-01	1,03E-01
% GI (9) versus W.T.	+1	-7	-9	-5.6	-4.6	-4.0
P value				1,08E-01	2,67E-01	4,24E-01
% GI (11) versus W.T.	-16	-16	-0.0	-5.2	-3.6	+2.6
P value				5,56E-02	2,73E-01	8,04E-01
% GI (17) versus W.T.	+19	+6	-11	-5.0	-5.1	-4.8
P value				8,26E-02	2,13E-01	5,24E-01
% GI (18) versus W.T.	-7	-16	-10	-5.5	-5.2	+2.4
P value				7,17E-02	6,49E-02	5,82E-01

Table S14| Comparison of floral parameters between wild type and transformed plants 1, 6A, 6B, 6C, 7, 8, 9, 11, 17 and 18 of *PhGI* in the T0 generation. Data are given as averages of at least three biological replicates of all transgenic plants. P values ≤ 5.00E-02 according to Students T-test were considered as significant.

```
PhGI1          GAAAGCAGAAAGGCAAAGGATCTAAGAAAGTGAAAAAACAAGGACCTGTTTCAGCGTTTG      60
PhGI2          AAAAACCGAAACAGCTGGGAAGTAAAAAGGTGAAGAAACAAGGGCCCGTTGCAGCATTTG      60
FN036363       ------------------------------------------------------------      0


PhGI1          ATTCTTATGTTCTTGCTGCTGTCTGTGCTCTTTCATGTGAACTTCAACTCTTTCCTTTGA      120
PhGI2          ATTCTTACGTACTTGCTGCTGTGTGTGCTCTTTCTTGTGAACTTCAGCTCTTCACTTTAA      120
FN036363       ------------TTGCTGCTGTGTGTGCTCTTTCTTGTGAACTTCAGCTCTTCACTTTAA      48
                           ********** ***********:***********.***** .****.*

PhGI1          TTTCAAGAGGGACTAATTATTCAGATCCAAAAACCATCCCCGATGCTGCAAAGCATGCAA      180
PhGI2          TTTCAAGAGGGACTAATCATCCAGATCCAAAAATCATCATGGATGAAGCAAAGCCCGCAA      180
FN036363       TTTCAAGAGGGACTAATCATTCAGATCCAAAAATCATCATGGATGAAGCAAAGCCCGCAA      108
               ***************** ** ************ ****.  ****.:*******. ****

PhGI1          ATGATTCGTCTATTGAGTTAAAAAATGGGATGCATTCTGCTATCTATCATACTCGGAGGA      240
PhGI2          ATGATTCGTCGATTGAGTTACGAAACGGGATTCATTCTGCAGTCTGTCATACTCGGAGAA      240
FN036363       ATGATTCGTCGATTGAGTTACGAAACGGGATTCATTCTGCCGTCCGTCATACTCGGAGAA      168
               ********** *********..*** ***** ******** .** .************.*

PhGI1          TATTGGCAATTCTGGAGGCTCTTTTCTCTTTGAAACCATCATCTGTTGGAACTTCATGGA      300
PhGI2          TATTAGCAATTTTAGAGGCTCTTTTTTCTTTGAAACCATCATCTGTTGGAACCTCATGGA      300
FN036363       TATTAGCAATTTTAGAGGCTCTTTTTTCTTTGAAACCATCATCTGTTGGAACCTCATGGA      228
               ****.****** *.*********** ************************ *******

PhGI1          GCTACAGCTCAAATGAGATAGTTGCTGCAGCTATGGTAGCTGCTCATATATCTGATTTGT      360
PhGI2          GCTACAGCTCAAATGAGATAGTTGCTGCAGCTATGGTAGCTGCTCATATTTCTGATCTGT      360
FN036363       GCTACAGCTCAAATGAGATAGTTGCTGCAGCTATGGTAGCTGCTCATATTTCTGATCTGT      288
               ************************************************:****** ***

PhGI1          TTAGATGCTCCAAGGCTTGCATGCATTCTCTTTCAATCTTAATAAGGTGTAAGTGGGATA      420
PhGI2          TTAGACGCTCCAAGGCTTGCATGCAGGGTCTTGCTATCTTGATACGGTGTAAGTGGGATA      420
FN036363       TTAGACGCTCCAAGGCTTGCATGCAGGGTCTTGCTATCTTGATACGGTGTAAGTGGGATA      348
               ***** ******************   **** *:*****.***.***************

PhGI1          ATGAAATTCACTCCAGAGCATCTTCGCTGTATAACCTCATTGACATTCATAGCAAAGTTG      480
PhGI2          ATGAAATTCATTCAAGGGCATCTTCACTCTATAACCTAATTGATATTCATAGTAAGACTG      480
FN036363       ATGAAATTCATTCAAGGGCATCTTCACTCTATAACCTAATTGATATTCATAGTAAGACTG      408
               ********** **.**.********.** ********.***** ******** **.. **

PhGI1          TTGCATCAATTGTTGACAAGGCCGAACCATTGGAAGCACACCTAATACCTGCACCTGTTC      540
PhGI2          TTGCATCAATTGTCAACAAGGCTGAACCATTGGAAGCTTATTTAATACATGCACCAATTC      540
FN036363       TTGCATCAATTGTCAACAAGGCTGAACCATTGGAAGCTTATTTAATACATGCACCAATTC      468
               ************* .******* **************: *  ******.******:.***

PhGI1          TTAATAAAAGAAGCATGTGCGTGAATGGGAGAAAACGTAATAAATATAGCACTTGTAGCT      600
PhGI2          TGAAGGAGCGGCCCAGGTGCTTAAATGGGAAGAAACATTATAAATATACCAATCGTAACT      600
FN036363       TGAAGGAGCGGCCCAGGTGCTTAAATGGGAAGAAACATTATAAATATACCAATCGTAACT      528
               * ** .*..*.. ** **** *.*******..****.*:********* **.* ***.**

PhGI1          GCTTAACTGCAGAACAATCATCGTTGCTCGAGTGCAACTCAACTGATTGTAAAAGTTTAA      660
PhGI2          GCTTAACAGCAGAAGAGCCATCAGTGTCACAGTGTAAAGATTC------------CTCTA      648
FN036363       GCTTAACAGCAGAAGAGCCATCAGTGTCTCAGTGTAAAGAT-------------------      569
               *******:****** *. ****. **    **** **. .:

PhGI1          TTATGAGTGAGAAAGTTTTACACTCAAGTGAGGTTTCACAGTGCGCCACTGGTAAAGGGA      720
PhGI2          ATTGGTGCGACAAAGCTTCACACCCAAGTGAGGTTGCTGGAGGCACCATCAGCAAAGTGT      708
FN036363       ------------------------------------------------------------      569
```

Figure S1| DNA alignment of *PhGI1* (Peaxi132Scf1428Ctg026), *PhGI2* (Peaxi132Scf1428Ctg060) from *Petunia hybrida* and the *PhGI* sequence FN03636 reported by Fenske *et al.*, (2015), using Clustal Omega (https://www.ebi.ac.uk/Tools/msa/clustalo/).

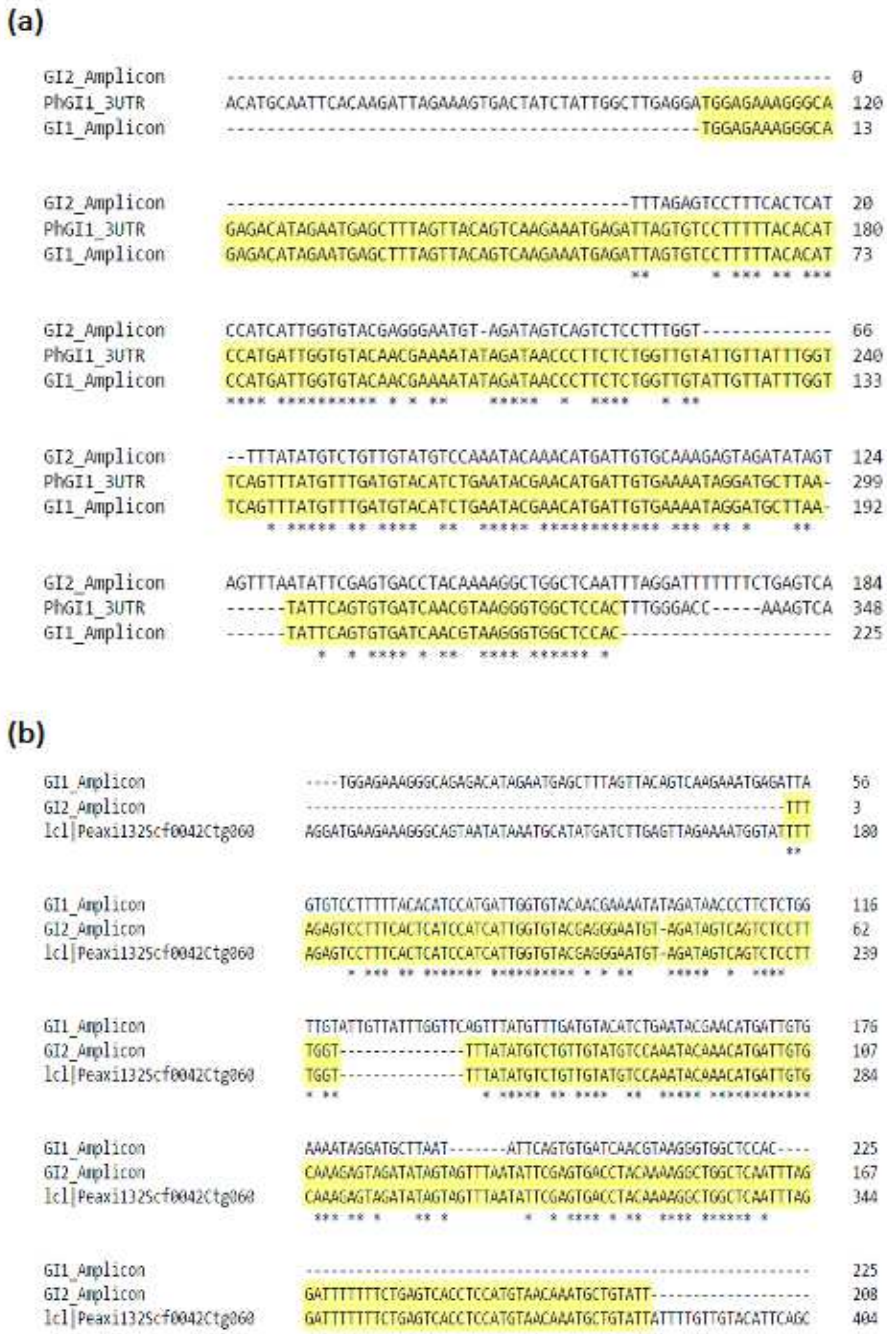

Figure S2| Alignment between (a) amplified regions of *PhGI1* and *PhGI2 (GI1_Amplicon and GI2_Amplicon)* and the 3'UTR region of *PhGI1* sequence from *Petunia hybrida (PhGI1_3'UTR)* and (b) amplified regions of *PhGI1* and *PhGI2 (GI1_Amplicon and GI2_Amplicon)* and *PhGi2* sequence from *Petunia axillaris* (Peaxi132Scf1428Ctg060) using Clustal Omega (https://www.ebi.ac.uk/Tools/msa/clustalo/). Regions marked in color emphasize on sequence similarity between amplicons and genomic clones.

Figure S3| Fully developed flower bud (left) of a wild type line compared to aborted flower bud (right) of *iRNA::PhGI1* T1 line 3.7 as observed in all *iRNA::PhGI* lines.

(a)

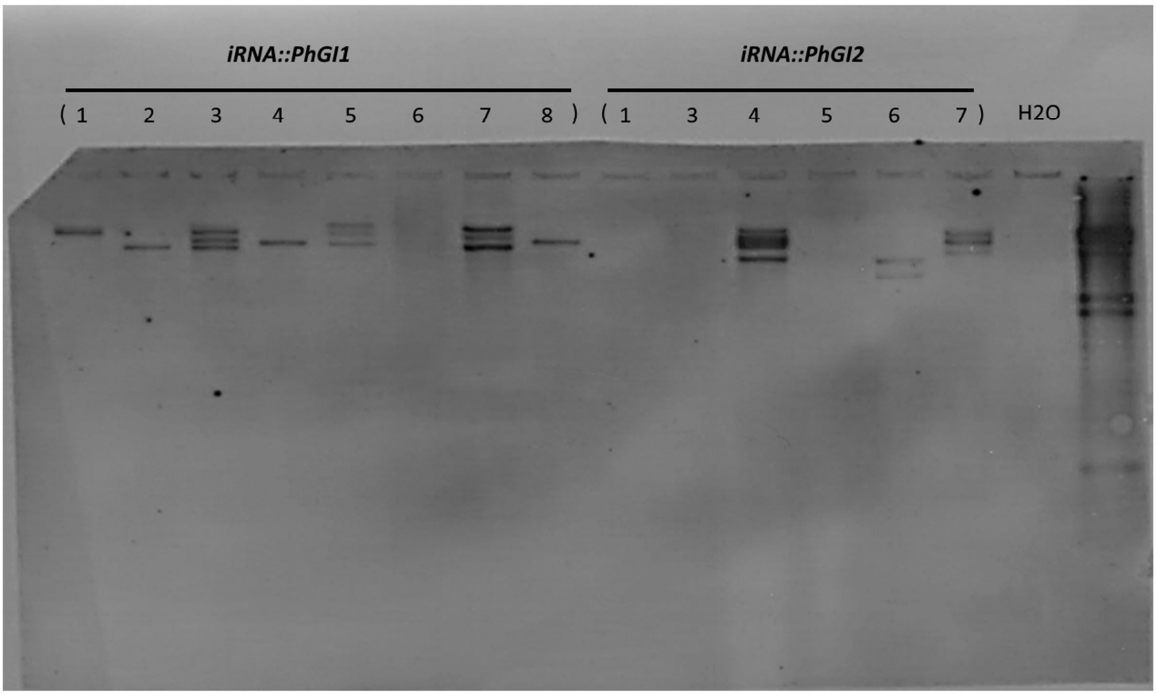

(b)

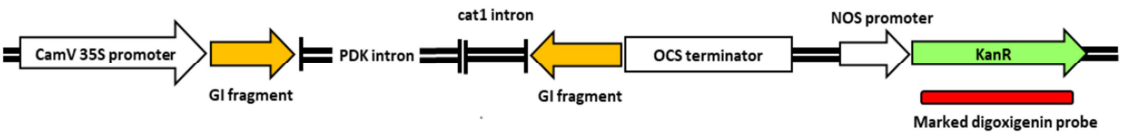

Figure S4| Southern Blot analysis of the T0 generation. (a) Result of T0 lines of *iRNA::PhGI1* on the left and *iRNA::PhGI2* on the right. (b) Schematic representation of the localization of the marked digoxigenin probe used.

Figure S5| Vegetative growth characteristics in *iRNA::PhGI2* T2 *lines* compared to wild type plants under natural greenhouse condition of long days. Growth habit of the transgenic lines compared to the wild type. Wild type plant (left) and *iRNA::PhGI2* line 4.2 (right).

Figure S6| DNA alignment of *PhGI1* (Peaxi132Scf1428Ctg026), *PhGI2* (Peaxi132Scf1428Ctg060) from *Petunia hybrida* using the online software "Tcoffee" (http://tcoffee.crg.cat/).

Congresses and Posters

The GIGANTEA1 iRNA-silencing effects in Petunia, show new surprising floral buds growth and scent emission habits.

C. Brandoli[1], M. Egea-Cortines[1], C. Petri[2], J. Weiss[1]

[1] Instituto de Biotecnología Vegetal – Universidad Politécnica de Cartagena, 30203, Cartagena, Spain

[2] Instituto de Hortofruticultura Subtropical y Mediterránea – CSIC, Avenida Dr. Wienberg, s/n, 29750, Málaga, España.

Universidad Politécnica de Cartagena

Genetics Tecnical University of Cartagena

Instituto de Biotecnología Vegetal, Universidad Politécnica de Cartagena

Introduction:

The clock gene Gigantea (GI), a gene belonging to the evening loop, affects various aspects of plant development and plant physiology including control of circadian rhythm (Fowler et al., 1999), photoperiod-mediated flowering (Sawa & Kay, 2011), growth cessation (Ding et al., 2018), hypocotyl elongation (Tseng et al., 2004), carbohydrate metabolism (Dalchau et al., 2011), salt tolerance (Park et al., 2013) as well as *miRNA* processing (Jung et al., 2007) are controlled by this gene.
The overall objective has been to analyze the function of the GI gene as a circadian rhythm gene, with respect to vegetative and generative development with special emphasis on flowering time and volatile emission.

Design Of Binary Vector And Plant Transformation:

A fragment of the GI coding region was selected by PCR. The sequence information were obtained from the genomic clones *PhGI1* identified in *P. hybrida* W115 (Bombarely, et al., 2016). The fragment was first recombined into the entry vector pDONR201 (Invitrogen) and then recombined into the final destination vector pHellsGate12 in order to obtain hairpin-like structures.

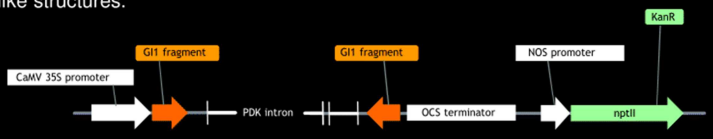

The unarmed strain of Agrobacterium tumefaciens EHA105 was used to transform the W115 Mitchell double haploid plant, following standard procedure (M. Manchado-Rojo, Weiss, & Egea-Cortines, 2014).

Results Concerning Flower Development:

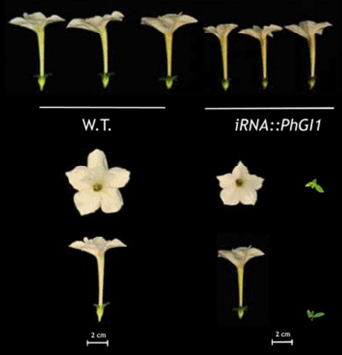

1. The diameter of the corolla and the length of the floral tube, of fully developed flowers, were significantly smaller.
2. The number of flower buds is drastically reduced by 59% compared to wildtype.
3. Most buds do not develop, although the differentiation of stamens and carpels can be clearly observed in all buds.
4. Considering the floral abortion in transgenic lines, the final percentage of fully developed flowers is reduced to 75%.

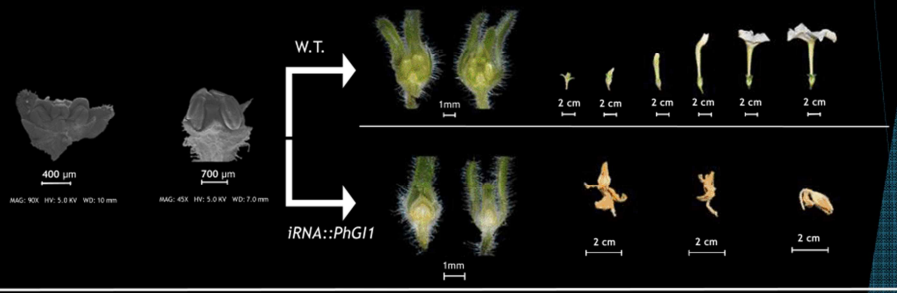

Results Concerning Floral Scent Emission:

1. Total VOC emission was reduced of 20,6% in the *iRNA::PhGI1* lines compared to the Wild-Type.
2. For both, W.T. and iRNA::PhGI1, VOC emission increased towards the end of the light period, stayed high during the dark phase and decreased towards midday at 6 hours of light.
3. The relative composition has changed, while the METHYL BENZOATE is the main compound and only presents slight variations; marked changes have occurred in the relative contribution of ISOEUGENOL, BENZYL BENZOATE and ETHYL BENZOATE

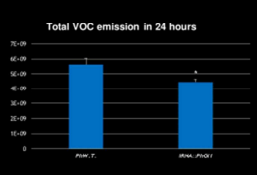

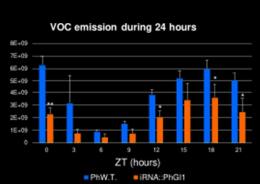

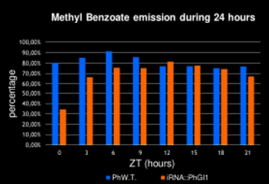

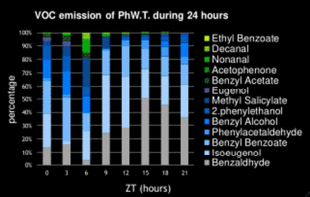

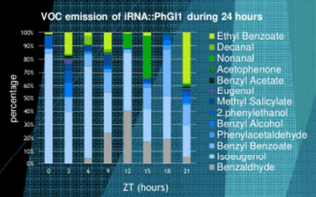

Conclusion:

The strong reduction in the number of flower buds and the high percentage of flower abortion, a phenomenon not described until now for any other *GI* mutant, suggests the existence of a new function in flower bud development. The aborted flowers clearly show the carpel and stamen tissue, indicating that the abortion of the flowers occurred after the activation of the floral identity genes. By other side, the reduced number of flower buds development suggests an effect of genetic silenicng following events related to organ identity. Regarding the floral scent emission our findings suggests that GI interacts with the rhythmic regulation of the biosynthesis of volatile compounds and in the emission of phenylalanine during the day.

References:

Bombarely, A., Moser, M., Amrad, A., Bao, M., Bapaume, L., Barry, C. C. S., Kuhlemeier, C. (2016a). Insight into the evolution of the Solanaceae from the parental genomes of Petunia hybrida. *Nature Plants*, *2*(May), 1–9. http://doi.org/10.1038/nplants.2016.74

Dalchau, N., Baek, S. J., Briggs, H. M., Robertson, F. C., Dodd, A. N., Gardner, M. J., … Webb, A. A. R. (2011). The circadian oscillator gene GIGANTEA mediates a long-term response of the Arabidopsis thaliana circadian clock to sucrose. *Proceedings of the National Academy of Sciences of the United States of America*, *108*(12), 5104–9. http://doi.org/10.1073/pnas.1015452108

Ding, J., Böhlenius, H., Rühl, M. G., Chen, P., Sane, S., Zambrano, J. A., … Nilsson, O. (2018). *GIGANTEA*-like genes control seasonal growth cessation in *Populus*. *New Phytologist*, *218*(4), 1491–1503. http://doi.org/10.1111/nph.15087

Fowler, S., Lee, K., Onouchi, H., Samach, A., Richardson, K., Morris, B., … Putterill, J. (1999). GIGANTEA: a circadian clock-controlled gene that regulates photoperiodic flowering in Arabidopsis and encodes a protein with several possible membrane-spanning domains. *The EMBO Journal*, *18*(17), 4679–4688. http://doi.org/10.1093/emboj/18.17.4679

Jung, J.-H., Seo, Y.-H., Seo, P. J., Reyes, J. L., Yun, J., Chua, N.-H., & Park, C.-M. (2007). The GIGANTEA-Regulated MicroRNA172 Mediates Photoperiodic Flowering Independent of CONSTANS in Arabidopsis. *THE PLANT CELL ONLINE*, *19*(9), 2736–2748. http://doi.org/10.1105/tpc.107.054528

Manchado-Rojo, M., Weiss, J., & Egea-Cortines, M. (2014). Validation of Aintegumenta as a gene to modify floral size in ornamental plants. *Plant Biotechnology Journal*, *12*(8). http://doi.org/10.1111/pbi.12212

Park, H. J., Kim, W.-Y., & Yun, D.-J. (2013). A role for GIGANTEA: keeping the balance between flowering and salinity stress tolerance. *Plant Signaling & Behavior*, *8*(7), e24820. http://doi.org/10.4161/psb.24820

Sawa, M., & Kay, S. A. (2011). GIGANTEA directly activates Flowering Locus T in Arabidopsis thaliana. *Proceedings of the National Academy of Sciences*, *108*(28), 11698–11703. http://doi.org/10.1073/pnas.1106771108

Tseng, T.-S., Salomé, P. A., McClung, C. R., & Olszewski, N. E. (2004). SPINDLY and GIGANTEA interact and act in Arabidopsis thaliana pathways involved in light responses, flowering, and rhythms in cotyledon movements. *The Plant Cell*, *16*(6), 1550–63. http://doi.org/10.1105/tpc.019224

The GIGANTEA1 iRNA-silencing effects in Petunia, show new surprising floral buds growth and scent emission habits.

C. Brandoli[1], M. Egea-Cortines[2], C. Petri[3], J. Weiss[4]

1 - *Instituto de Biotecnología Vegetal, Universidad Politécnica de Cartagena, calle linterna s/n, 30203, Cartagena, Spain.*
2, 4 - Instituto de Biotecnología Vegetal, Universidad Politécnica de Cartagena, calle linterna s/n, 30203, Cartagena, Spain.
3 - *Instituto de Hortofruticultura Subtropical y Mediterránea – CSIC, Avenida Dr. Wienberg, s/n, 29750, Málaga, Spain.*

Introduction: The clock gene Gigantea (GI), a gene belonging to the evening loop, affects various aspects of plant development and physiology including control of circadian rhythm (Fowler et al., 1999), photoperiod-mediated flowering (Sawa & Kay, 2011), hypocotyl elongation (Tseng et al., 2004), as well as *miRNA* processing (Jung et al., 2007) are controlled by this gene. The overall objective has been to analyze the function of the GI gene as a circadian rhythm gene, with respect to vegetative and generative development with special emphasis on flowering time and volatile emission.

Material and methods: A fragment of the GI coding region was selected by PCR. The sequence information were obtained from the genomic clones *PhGI1* identified in *P. hybrida* W115 (Bombarely, 2016). The fragment was first recombined into the entry vector pDONR201 (Invitrogen) and then recombined into the final destination vector pHellsGate12 in order to obtain hairpin-like structures. The unarmed strain of Agrobacterium tumefaciens EHA105 was used to transform the W115 Mitchell double haploid plant, following standard procedure (M. Manchado-Rojo, Weiss, & Egea-Cortines, 2014).

Results concerning flower development: The diameter of the corolla and the length of the floral tube, of fully developed flowers, were significantly smaller. The number of flower buds is drastically reduced by 59% compared to wild type. Most buds do not develop, although the differentiation of stamens and carpels can be clearly observed in all buds. Considering the floral abortion in transgenic lines, the final percentage of fully developed flowers is reduced to 75%.

Results concerning floral scent emission: Total VOC emission was reduced of 20,6% in the *iRNA::PhGI1* lines compared to the wild type. For both, W.T. and iRNA::PhGI1, VOC emission increased towards the end of the light period, stayed high during the dark phase and decreased towards midday at 6 hours of light. The relative composition has changed, while the methyl benzoate is the main compound and only presents slight variations; marked changes have occurred in the relative contribution of isoeugenol, benzyl benzoate and ethyl benzoate

Conclusion: The strong reduction in the number of flower buds and the high percentage of flower abortion, a phenomenon not described until now for any other *GI* mutant, suggests the existence of a new function in flower bud development. The aborted flowers clearly show the carpel and stamen tissue, indicating that the abortion of the flowers occurred after the activation of the floral identity genes. By other side, the reduced number of flower buds development suggests an effect of genetic silencing following events related to organ identity. Regarding the floral scent emission our findings suggests that GI interacts with the rhythmic regulation of the biosynthesis of volatile compounds and in the emission of phenylalanine during the day.

References:

Bombarely, A., Moser, M., Amrad, A., Bao, M., Bapaume, L., Barry, C. C. S., Kuhlemeier, C. (2016). Insight into the evolution of the Solanaceae from the parental genomes of Petunia hybrida. *Nature Plants*.

Fowler, S., Lee, K., Onouchi, H., (1999). GIGANTEA: a circadian clock-controlled gene that regulates photoperiodic flowering in Arabidopsis and encodes a protein with several possible membrane-spanning domains. *The EMBO Journal*.

Jung, J.-H., Seo, Y.-H., Seo, P. J., Reyes, J. L., Yun, J., Chua, N.-H., & Park, C.-M. (2007). The GIGANTEA-Regulated MicroRNA172 Mediates Photoperiodic Flowering Independent of CONSTANS in Arabidopsis. *THE PLANT CELL*.

Manchado-Rojo, M., Weiss, J., & Egea-Cortines, M. (2014). Validation of Aintegumenta as a gene to modify floral size in ornamental plants. *Plant Biotechnology Journal*.

Sawa, M., & Kay, S. A. (2011). GIGANTEA directly activates Flowering Locus T in Arabidopsis thaliana. *Proceedings of the National Academy of Sciences*.

Tseng, T.-S., Salomé, P. A., McClung, C. R., & Olszewski, N. E. (2004). SPINDLY and GIGANTEA interact and act in Arabidopsis thaliana pathways involved in light responses, flowering, and rhythms in cotyledon movements. *The Plant Cell.*

The GIGANTEA iRNA-silencing effects in Petunia, show new surprising vegetative and floral growth habits.

C. Brandoli[1], M. Egea-Cortines[1], C. Petri[2], J. Weiss[1]

[1] Instituto de Biotecnología Vegetal – Universidad Politécnica de Cartagena, 30203, Cartagen, Spain

[2] Departamento de Fruticultura IHSM - CSIC

Universidad Politécnica de Cartagena

Genetics Tecnical University of Cartagena

Instituto de Biotecnologia Vegetal
Universidad Politécnica de Cartagena

Introduction:

The clock gene Gigantea (GI), a gene belonging to the evening loop, affects various aspects of plant development and plant physiology including control of circadian rhythm (Fowler et al., 1999), photoperiod-mediated flowering (Sawa & Kay, 2011), growth cessation (Ding et al., 2018), hypocotyl elongation (Tseng et al., 2004), carbohydrate metabolism (Dalchau et al., 2011), salt tolerance (Park et al., 2013) as well as *miRNA* processing (Jung et al., 2007) are controlled by this gene.

Design Of Binary Vector And Plant Transformation:

A fragment of the GI coding region, that would discriminate between both paralogous, GI1 and GI2, was selected. The sequences information were obtained from the genomic clones *PhGI1* and *PhG2* identified in *P. hybrida* W115 (Bombarely, et al., 2016). Each fragment was first recombined into the entry vector pDONR201 (Invitrogen) and then recombined into the final destination vector pHellsGate12 in order to obtain hairpin-like structures.

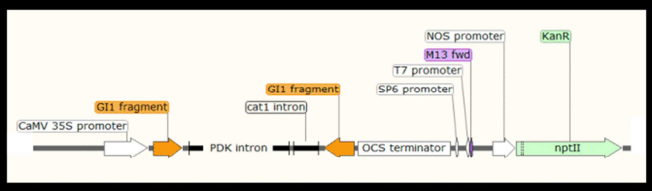

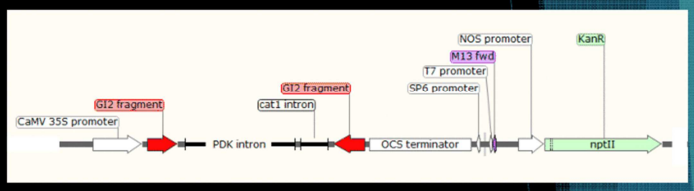

The unarmed strain of Agrobacterium tumefaciens EHA105 was used to transform the W115 Mitchell double haploid plant, following standard procedure (M. Manchado-Rojo, Weiss, & Egea-Cortines, 2014).

Results Concerning Vegetative Growth:

1. For both the transgenic lines PhGI1 and PhGI2, basal and apical leaves, appeared significantly longer and broader compared to wildtype as well as non-transgenic siblings.
2. Apical and median internodes length decreased, conferring a more bushy phenotype, while basal internode distance was increased, resulting in overall slightly taller plants, for both the transgenic lines *PhGI1* and *PhGI2*.
3. Transgenic lines had a greener appearance thanks to an evident difference in the levels of chlorophyll, showing a progressive increase in the median and apical leaves in comparison to the wildtype and non-transgenic siblings.
4. The number of axillary meristems increased markedly in t both in for *iRNA::PhGI1* and *iRNA::PhGI2* lines contributing to the more bushy phenotype.
5. Only *iRNA::PhGI2* lines showed a consistent increase in the number of branches compared to the wildtype and non-transgenic siblings.

Results Concerning Flower Development:

1. A strong delay in flowering time of 2-3 weeks, was observed only for the *iRNA::PhGI2* lines, while the plants of *iRNA::PhGI1* and wildtype both have the same flowering time, from 17 to 18 weeks after transplantation.
2. The number of flower buds result dramatically reduced by 59% and 48%, respectively in *iRNA::PhGI1* and *iRNA::PhGI2*, compared to the wildtype.
3. The corolla diameter as well as the floral tube length, of fully developed flowers, was significantly smaller for both GI-silenced constructs.

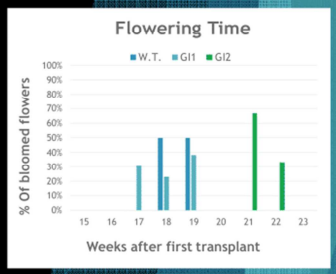

Conclusion:

A differential role between GI1 and GI2 exists in Petunia concerning flower development, while the effect on vegetative growth seems to be redundant..

References:

Bombarely, A., Moser, M., Amrad, A., Bao, M., Bapaume, L., Barry, C. C. S., … Kuhlemeier, C. (2016a). Insight into the evolution of the Solanaceae from the parental genomes of Petunia hybrida. *Nature Plants*, *2*(May), 1–9. http://doi.org/10.1038/nplants.2016.74

Dalchau, N., Baek, S. J., Briggs, H. M., Robertson, F. C., Dodd, A. N., Gardner, M. J., … Webb, A. A. R. (2011). The circadian oscillator gene GIGANTEA mediates a long-term response of the Arabidopsis thaliana circadian clock to sucrose. *Proceedings of the National Academy of Sciences of the United States of America*, *108*(12), 5104–9. http://doi.org/10.1073/pnas.1015452108

Ding, J., Böhlenius, H., Rühl, M. G., Chen, P., Sane, S., Zambrano, J. A., … Nilsson, O. (2018). *GIGANTEA*-like genes control seasonal growth cessation in *Populus*. *New Phytologist*, *218*(4), 1491–1503. http://doi.org/10.1111/nph.15087

Fowler, S., Lee, K., Onouchi, H., Samach, A., Richardson, K., Morris, B., … Putterill, J. (1999). GIGANTEA: a circadian clock-controlled gene that regulates photoperiodic flowering in Arabidopsis and encodes a protein with several possible membrane-spanning domains. *The EMBO Journal*, *18*(17), 4679–4688. http://doi.org/10.1093/emboj/18.17.4679

Jung, J.-H., Seo, Y.-H., Seo, P. J., Reyes, J. L., Yun, J., Chua, N.-H., & Park, C.-M. (2007). The GIGANTEA-Regulated MicroRNA172 Mediates Photoperiodic Flowering Independent of CONSTANS in Arabidopsis. *THE PLANT CELL ONLINE*, *19*(9), 2736–2748. http://doi.org/10.1105/tpc.107.054528

Manchado-Rojo, M., Weiss, J., & Egea-Cortines, M. (2014). Validation of Aintegumenta as a gene to modify floral size in ornamental plants. *Plant Biotechnology Journal*, *12*(8). http://doi.org/10.1111/pbi.12212

Park, H. J., Kim, W.-Y., & Yun, D.-J. (2013). A role for GIGANTEA: keeping the balance between flowering and salinity stress tolerance. *Plant Signaling & Behavior*, *8*(7), e24820. http://doi.org/10.4161/psb.24820

Sawa, M., & Kay, S. A. (2011). GIGANTEA directly activates Flowering Locus T in Arabidopsis thaliana. *Proceedings of the National Academy of Sciences*, *108*(28), 11698–11703. http://doi.org/10.1073/pnas.1106771108

Tseng, T.-S., Salomé, P. A., McClung, C. R., & Olszewski, N. E. (2004). SPINDLY and GIGANTEA interact and act in Arabidopsis thaliana pathways involved in light responses, flowering, and rhythms in cotyledon movements. *The Plant Cell*, *16*(6), 1550–63. http://doi.org/10.1105/tpc.019224

The GIGANTEA iRNA-silencing effects in petunia, show new surprising vegetative and floral growth habits

CLAUDIO BRANDOLI / INSTITUTO DE BIOTECNOLOGÍA VEGETAL, UNIVERSIDAD POLITÉCNICA DE CARTAGENA

DR.EGEA CORTINES, MARCOS; DR.PETRI SERRANO, CÉSAR; DR.WEISS, JULIA

Introducción: El gen GIGANTEA (GI), pertenece al ciclo de la tarde y afecta al desarrollo de las plantas y a su fisiología, incluso el control del ritmo circadiano.
Métodos y materiales: Se obtuvo de los clones genómicos PhGI1 y PhGI2 un fragmento de la región codificante de GI, que discriminara entre los parálogos GI1 y GI2. Cada fragmento se recombinó en el vector de clonación pDONR201 y luego en el vector de destino pHellsGate12 para obtener estructuras en forma de horquilla. Se utilizó la cepa desarmada de Agrobacterium tumefaciens EHA105 para la transformación, siguiendo un procedimiento estándar.
Resultados sobre el crecimiento vegetativo:
- En ambas las líneas transgénicas, las hojas basales y apicales aparecieron significativamente más largas y amplias en com- paración con los de tipo salvaje.
- La longitud de los entrenudos apicales y medianos disminuyó, mientras el número de meristemas axilares aumentó notablemente, confiriendo un fenotipo más espeso.
- Las líneas transgénicas tenían un aspecto más verde gracias a una diferencia evidente en los niveles declorofila.
Resultados sobre el desarrollo floral:
- El tiempo de floración retrasó considerablemente, de 2 a 3 semanas, solo para las líneas iRNA::PhGI2.
- El número de brotes florales se redujo drásticamente en ambas las líneas.
- El diámetro de la corola y longitud del tubo floral, fue significativamente menor en ambas las construcciones.
Conclusiones: Existe un diferente papel entre GI1 y GI2 en Petunia con respecto al desarrollo de las flores, mientras que el efecto sobre el crecimiento vegetativo parece ser redundante.

Introduction: The GIGANTEA (GI) gene belongs to the evening loop and affects the development of the plants and their physiology, including the control of the circadian rhythm.
Methods and materials: A fragment of the GI coding region, which discriminates between the GI1 and GI2 paralogs, was obtained from the genomic clones PhGI1 and PhGI2. Each fragment was recombined in the cloning vector pDONR201 and then in the target vector pHellsGate12 to obtain hairpin structures. The unarmed strain of Agrobacterium tumefaciens EHA105 was used for the transformation, following a standard procedure.
Results on vegetative growth:
- In both the transgenic lines, the basal and apical leaves appeared significantly longer and wider compared to the wild type.
- The length of the apical and median internodes decreased, while the number of axillary meristems increased markedly, conferring a bushy phenotype.
- The transgenic lines had a greener appearance thanks to an evident difference in chlorophyll levels.
Results on floral development:
- The flowering time delayed considerably, from 2 to 3 weeks, only for the lines iRNA::PhGI2.
- The number of flower buds was drastically reduced in both lines.
- The diameter of the corolla and length of the floral tube was significantly lower in both constructions.
Conclusions: There is a different role between GI1 and GI2 in Petunia with respect to the development of flowers, while the effect on vegetative growth seems to be redundant.

Genetic and molecular analysis of Gigantea, a gene involved in adaptation to climate via regulation of the circadian clock in Solanaceae

C.Brandoli[1], M. Egea-Cortines[1], J. Weiss[1]
Instituto de Biotecnología Vegetal –Universidad Politécnica de Cartagena, 30203, Cartagen, Spain

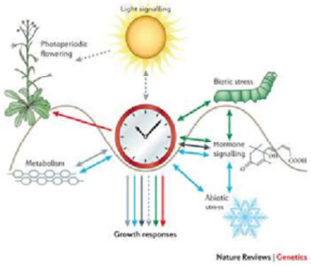

Introduction

In the plant kingdom, the circadian clock has the function to regulate many of the physiological and metabolic processes, essential to the survival of the plants. One of the genes involved in this regulation is GIGANTEA (GI)

Although discovered in the past century, some of its functions, at the molecular level, are unclear and still a source of intense scientific research.

Objectives

The following thesis project has different objectives related to the genetic regulation of Gigantea gene in plant crops, as:

- Phenotypic and biochemical analysis of Petunia, bearing the transposon in homozygous form in comparison with the wild type phenotype;
- Gene silencing and phenotypic- biochemical comparison between the mutant form and the wild type phenotype.

Figure 1.

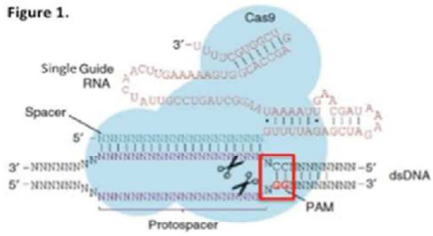

Mali P et al. *Nature Methods* 10, 2013

Method

- Characterization and genetic selection
- RNA interference technique
- The CRISPR/Cas9 system

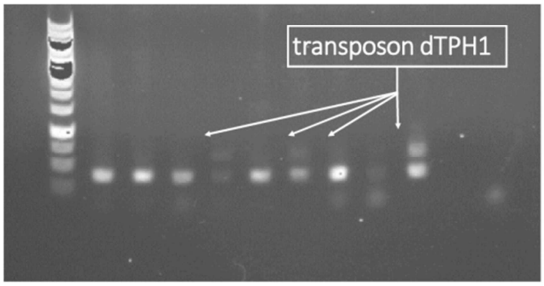

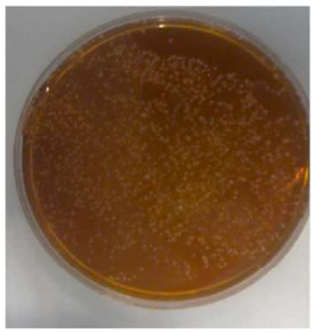

Many thanks to Dr Julia Rosl Weiss and Dr. Marcos Egea Gutierrez Cortines for their valuable advice and constant support

Genetic and molecular analysis of *Gigantea*, a gene involved in adaptation to climate via regulation of the circadian clock in *Solanaceae*

Análisis genético y molecular de *Gigantea*, un gen involucrado en la adaptación al clima a través de la regulación del reloj circadiano en *Solanaceae*

C. Brandoli[1*], Dr. J. Weiss[2], Dr. M. Egea Gutierrez Cortines[3]

[1] IBV, Institudo de Biotecnología Vegetal, Universidad Politecnica de Cartagena, Campus Muralla del Mar, Murcia, Spain, e-mail: claudio.brandoli@gmail.com

[2, 3] ETSIA, Universidad Politécnica de Cartagena, Paseo Alfonso XIII, 48, 30203 Cartagena, Murcia, Spain

Abstract

The metabolism, physiology, and also the behavior of most living beings, profoundly changes between day and night. These biological oscillations happen due to the circadian rhythm, an endogenous clock that regulates most of biological events. In the plant kingdom, one of the genes involved in this important regulation is *Gigantea*. Although discovered in the past century, some of its functions, at the molecular level, are unclear and still a source of intense scientific research. In this thesis project we'll try to analyze phenotypic and biochemical changes induced by gene silencing in Solanaceae with the aim to better understand the function of Gigantea.

Keyword: Gigantea, recombinant plasmid, gene silencing, RNA interference, CRISPR/Cas9 System.

Resumen

El metabolismo, fisiología y comportamiento de los organismos vivos cambia entre el día y la noche. Estas oscilaciones biológicas se deben al reloj circadiano, un sistema endógeno que regula la mayoría de los procesos biológicos. En el reino vegetal, uno de los genes involucrados en esta regulación es Gigantea. Aunque fue descubierto en los años 50, sus funciones biológicas y moleculares no se conocen con detalle y son objeto de intenso trabajo debido a su importancia en la adaptación. En este proyecto de tesis pretendemos analizar cambios fenotípicos y bioquímicos relacionados con el silenciamiento de Gigantea en Solanáceas.

Palabras clave: Indique 3 a 5 palabras clave separadas por punto y coma relacionadas con su trabajo (ninguna deberá estar en el título).